

Registration No.

22248



Diagnostic Health Monitoring System Development for Army Vehicle Reliability

DISTRIBUTION STATEMENT A. Approved for public release; distribution is unlimited.

Disclaimer: Reference herein to any specific commercial company, product, process, or service by trade name, trademark, manufacturer, or otherwise, does not necessarily constitute or imply its endorsement, recommendation, or favoring by the United States Government or the Department of the Army (DoA). The opinions of the authors expressed herein do not necessarily state or reflect those of the United States Government or the DoA, and shall not be used for advertising or product endorsement purposes.

July 2011

U.S. Army Tank Automotive Research,
Development, and Engineering Center
Detroit Arsenal
Warren, Michigan 48397-5000

Report Documentation Page		<i>Form Approved OMB No. 0704-0188</i>
Public reporting burden for the collection of information is estimated to average 1 hour per response, including the time for reviewing instructions, searching existing data sources, gathering and maintaining the data needed, and completing and reviewing the collection of information. Send comments regarding this burden estimate or any other aspect of this collection of information, including suggestions for reducing this burden, to Washington Headquarters Services, Directorate for Information Operations and Reports, 1215 Jefferson Davis Highway, Suite 1204, Arlington VA 22202-4302. Respondents should be aware that notwithstanding any other provision of law, no person shall be subject to a penalty for failing to comply with a collection of information if it does not display a currently valid OMB control number.		
1. REPORT DATE 30 JUN 2011	2. REPORT TYPE N/A	3. DATES COVERED 01 JUL 2010 - 30 JUN 2011
4. TITLE AND SUBTITLE Diagnostic Health Monitoring System Development for Army Vehicle Reliability		5a. CONTRACT NUMBER TCN 10009
		5b. GRANT NUMBER
		5c. PROGRAM ELEMENT NUMBER
6. AUTHOR(S) Douglas Adams Kenninger; Tiffany DiPetta; David Loester		5d. PROJECT NUMBER
		5e. TASK NUMBER
		5f. WORK UNIT NUMBER
7. PERFORMING ORGANIZATION NAME(S) AND ADDRESS(ES) Purdue Center for Systems Integrity 1500 Kepner Road, , Lafayette, IN 47905, USA.		8. PERFORMING ORGANIZATION REPORT NUMBER 22248RC
9. SPONSORING/MONITORING AGENCY NAME(S) AND ADDRESS(ES) TARDEC VEA Group Attn: RDTA-RS (MS-264) 6501 E.11 Mile Road Bldg 200C Warren, MI 48397-5000		10. SPONSOR/MONITOR'S ACRONYM(S)
		11. SPONSOR/MONITOR'S REPORT NUMBER(S) 22248RC
12. DISTRIBUTION/AVAILABILITY STATEMENT Approved for public release, distribution unlimited		
13. SUPPLEMENTARY NOTES Reference herein to any specific commercial company, product, process, or service by trade name, trademark, manufacturer, or otherwise, does not necessarily constitute or imply its endorsement, recommendation, or favoring by the United States Government or the Department of the Army (DoA). The opinions of the authors expressed herein do not necessarily state or reflect those of the United States Government or the DoA, and shall not be used for advertising or product endorsement purposes., The original document contains color images.		

14. ABSTRACT

Current maintenance schedules for ground vehicles are determined largely based on reliability predictions of a population of vehicles under anticipated operational loads. This approach leads to unnecessary maintenance and, in some cases, in-eld failures depending on differences in the usage of individual vehicles. Condition-based maintenance is scheduled instead according to the condition of each vehicle to reduce the risk of failure and maintenance costs. However, on-board instrumentation for acquiring, processing, and storing operational data is expensive, and this data is also difficult to analyze due to variations in loading. An instrumented diagnostic cleat for diagnosing mechanical faults in ground vehicle wheel ends and suspensions is studied in this paper. The cleat excites the vehicles dynamic response through an impulse delivered to the vehicles front and back tires. The response of the instrumented segment of the cleat is then recorded while in contact with the vehicles tires using accelerometers. The measured dynamic response is compared to a reference response, and anomalies that correspond to vehicle faults are then detected. This paper demonstrates that the measured response spectrum from the instrumented diagnostic cleat can be attributed to vehicle chassis modes of vibration in the frequency range below 10 Hz and natural frequencies in the free dynamic response of the cleat above 10 Hz. Tire and suspension faults are simulated in a high mobility multi-purpose wheeled vehicle and the faults are detected. Tire faults are simulated by decreasing the pressure within each tire below the manufacturer recommended level, whereas suspension faults are simulated by disconnecting each damper to mimic the effects of broken damper. The data indicates that the faults and locations of the faults are identified with 90% confidence in 7 out of 8 fault cases. Errors in the measurements are modeled to compensate for changes in vehicle speed.

15. SUBJECT TERMS

16. SECURITY CLASSIFICATION OF:			17. LIMITATION OF ABSTRACT SAR	18. NUMBER OF PAGES 176	19a. NAME OF RESPONSIBLE PERSON
a. REPORT unclassified	b. ABSTRACT unclassified	c. THIS PAGE unclassified			

REPORT DOCUMENTATION PAGE

*Form Approved
OMB No. 0704-0188*

Public reporting burden for this collection of information is estimated to average 1 hour per response, including the time for reviewing instructions, searching existing data sources, gathering and maintaining the data needed, and completing and reviewing this collection of information. Send comments regarding this burden estimate or any other aspect of this collection of information, including suggestions for reducing this burden to Department of Defense, Washington Headquarters Services, Directorate for Information Operations and Reports (0704-0188), 1215 Jefferson Davis Highway, Suite 1204, Arlington, VA 22202-4302. Respondents should be aware that notwithstanding any other provision of law, no person shall be subject to any penalty for failing to comply with a collection of information if it does not display a currently valid OMB control number. **PLEASE DO NOT RETURN YOUR FORM TO THE ABOVE ADDRESS.**

1. REPORT DATE (DD-MM-YYYY) June 30, 2011	2. REPORT TYPE Final Report and Presentation	3. DATES COVERED (From - To) July 1, 2010 – June 30, 2011 4. TITLE AND SUBTITLE Diagnostic health monitoring system development for Army vehicle reliability 6. AUTHOR(S) Douglas Adams Kenninger Professor of Mechanical Engineering Purdue University Tiffany DiPetta Student Purdue University David Koester Student Purdue University 7. PERFORMING ORGANIZATION NAME(S) AND ADDRESS(ES) Purdue Center for Systems Integrity 1500 Kepner Road, , Lafayette, IN 47905, USA.		
			5a. CONTRACT NUMBER TCN 10009	5b. GRANT NUMBER 5c. PROGRAM ELEMENT NUMBER 5d. PROJECT NUMBER 5e. TASK NUMBER 5f. WORK UNIT NUMBER
			8. PERFORMING ORGANIZATION REPORT NUMBER	
			10. SPONSOR/MONITOR'S ACRONYM(S)	11. SPONSOR/MONITOR'S REPORT NUMBER(S) #22248
12. DISTRIBUTION / AVAILABILITY STATEMENT DISTRIBUTION STATEMENT A. Approved for public release; distribution is unlimited. Disclaimer: Reference herein to any specific commercial company, product, process, or service by trade name, trademark, manufacturer, or otherwise, does not necessarily constitute or imply its endorsement, recommendation, or favoring by the United States Government or the Department of the Army (DoA). The opinions of the authors expressed herein do not necessarily state or reflect those of the United States Government or the DoA, and shall not be used for advertising or product endorsement purposes.				
13. SUPPLEMENTARY NOTES				
14. ABSTRACT <p>Current maintenance schedules for ground vehicles are determined largely based on reliability predictions of a population of vehicles under anticipated operational loads. This approach leads to unnecessary maintenance and, in some cases, in-field failures depending on differences in the usage of individual vehicles. Condition-based maintenance is scheduled instead according to the condition of each vehicle to reduce the risk of failure and maintenance costs. However, on-board instrumentation for acquiring, processing, and storing operational data is expensive, and this data is also difficult to analyze due to variations in loading. An instrumented diagnostic cleat for diagnosing mechanical faults in ground vehicle wheel ends and suspensions is studied in this paper. The cleat excites the vehicle's dynamic response through an impulse delivered to the vehicle's front and back tires. The response of the instrumented segment of the cleat is then recorded while in contact with the vehicle's tires using accelerometers. The measured dynamic response is compared to a reference response, and anomalies that correspond to vehicle faults are then detected. This paper demonstrates that the measured response spectrum from the instrumented diagnostic cleat can be attributed to vehicle chassis modes of vibration in the frequency range below 10 Hz and natural frequencies in the free dynamic response of the cleat above 10 Hz. Tire and suspension faults are simulated in a high mobility multi-purpose wheeled vehicle and the faults are detected. Tire faults are simulated by decreasing the pressure within each tire below the manufacturer recommended level, whereas suspension faults are simulated by disconnecting each damper to mimic the effects of broken damper. The data indicates that the faults and locations of the faults are identified with 90% confidence in 7 out of 8 fault cases. Errors in the measurements are modeled to compensate for changes in vehicle speed.</p>				
15. SUBJECT TERMS				
16. SECURITY CLASSIFICATION OF: UNCLAS		17. LIMITATION OF ABSTRACT SAR	18. NUMBER OF PAGES	19a. NAME OF RESPONSIBLE PERSON 19b. TELEPHONE NUMBER (include area code) 586.282.5377
a. REPORT UNCLAS	b. ABSTRACT UNCLAS	c. THIS PAGE UNCLAS		

Final Report
SUBCONTRACT AGREEMENT - TCN 10009

Diagnostic health monitoring system development for Army vehicle reliability

Prepared by
Douglas Adams
Kenninger Professor of Mechanical Engineering
Purdue University

Prepared for
Philip Doherty
VEA Condition-Based Maintenance
US Army TARDEC

Describing work accomplished in the period
July 1, 2010 – June 30, 2011

DISTRIBUTION STATEMENT A. Approved for public release; distribution is unlimited.

Disclaimer: Reference herein to any specific commercial company, product, process, or service by trade name, trademark, manufacturer, or otherwise, does not necessarily constitute or imply its endorsement, recommendation, or favoring by the United States Government or the Department of the Army (DoA). The opinions of the authors expressed herein do not necessarily state or reflect those of the United States Government or the DoA, and shall not be used for advertising or product endorsement purposes.

Executive Summary

Current maintenance schedules for ground vehicles are determined largely based on reliability predictions of a population of vehicles under anticipated operational loads. This approach leads to unnecessary maintenance and, in some cases, in-field failures depending on differences in the usage of individual vehicles. Condition-based maintenance is scheduled instead according to the condition of each vehicle to reduce the risk of failure and maintenance costs. However, on-board instrumentation for acquiring, processing, and storing operational data is expensive, and this data is also difficult to analyze due to variations in loading.

A diagnostic speed bump for diagnosing mechanical faults in ground vehicle wheel ends and suspensions is investigated in this project. The speed bump excites the vehicle's dynamic response through an impulse delivered to the vehicle's front and back tires. The response of the instrumented segment of the diagnostic speed bump is then recorded while in contact with the vehicle's tires using accelerometers. The measured dynamic response is compared to a reference response, and anomalies that correspond to vehicle faults are then detected. This report demonstrates that the measured response spectrum from the instrumented diagnostic cleat can be attributed to vehicle chassis modes of vibration in the frequency range below 10 Hz and natural frequencies in the free dynamic response of the cleat above 10 Hz. Tire and suspension faults are simulated in a high mobility multi-purpose wheeled vehicle and the faults are detected. Tire faults are simulated by decreasing the pressure within each tire below the manufacturer recommended level, whereas suspension faults are simulated by disconnecting each damper to mimic the effects of broken damper. Using a reference-based algorithm, the data indicates that the faults and locations of the faults are identified with 90% confidence in 7 out of 8 fault cases. Errors in the measurements are modeled to compensate for changes in vehicle speed. It is also demonstrated that a reference-free algorithm can be utilized to detect these faults by calculating the cross-correlation between measurement channels to identify when the vehicle is "limping" due to a fault. This algorithm demonstrates much higher levels of detection approaching 99%.

On June 21 2011, a summary demonstration documenting the products of this research program was performed at U.S. Army TARDEC in Warren, MI. A briefing was also provided and is attached to this final report along with a journal paper that was cleared for public release through OPSEC and has been submitted for review. Both the briefing and the demonstration were well received. Tire faults were detected and located during the demonstration despite poor weather on the day of the demonstration in the form of precipitation. A graphical user interface was used to present the results of these demonstrations. Recommendations were made by several individuals who attended the demonstration about how the technology could be further developed.

Table of contents

1. Objectives.....	4
2. Approach.....	5-7
3. Results.....	8-21
3.1 Baseline data analysis.....	8-15
3.2 Variation with speed.....	16-18
3.3 Tire fault data analysis	19-24
3.4 Receiver Operator Characteristics for fault detection	24-28
3.5 Extended diagnostic speed bump modal data analysis	28-36
3.6 Kinematic analysis of tracking wheels	36-45
3.7 Dynamic analysis of diagnostic speed bump	45-49
3.8 Modeling of extended diagnostic speed bump	49-54
3.9 Simulation of extended diagnostic speed bump	55-62
3.10 Simulation of faults in quarter car using extended cleat model	63-65
3.11 Simulation of changes in wheel crossing location using extended cleat model..	66-69
3.12 Analysis of vehicle response measured using extended cleat	70-75
3.13 Final demonstration of diagnostic speed bump	76-80

1. Objectives

The objectives of the project this quarter were to address Tasks (a) and (c) of the Statement of Work, which are listed below:

- a. The Contractor shall select the necessary sensors and fixtures, implement a diagnostic speed-bump sensor and data acquisition system that places sensors in a speed-bump over which the HMMWV drives over to acquire data, and study the ability to identify faults due to fatigue, misassembly, and other types of physical anomalies in mechanical components. The diagnostic speed bump shall be no larger than a traditional speed bump found on a public roadway.
- c. The Contractor shall study the effects of variability in speed, angle of approach, temperature, and other variables on the ability of the speed bump to diagnose vehicle subsystem condition. Models will be modified to account for variation that is introduced by these factors where the factors are found to have a statistically significant effect on the system response.

The focus of Task (a) was to select a diagnostic speed bump configuration that provided measurements that were sensitive to the faults of interest in the wheels and suspensions. It was also desirable to provide response time histories with varying time periods so the effects of this period on diagnostic capabilities could be quantified when selecting the diagnostic speed bump configuration.

The focus of Task (c) was to develop an understanding of how sources of variability in the measurements affected the ability to detect the faults of interest using the diagnostic speed bump sensor data. The ultimate goal of these two tasks was to develop a robust demonstration that could be conducted at the end of this year's program. The word "robust" in this context is used to indicate that it is desirable for the diagnostic performance to be insensitive to variability in the dynamic measurements that are acquired using the diagnostic speed bump.

Approach

The previous year's effort focused on the modeling and testing of a rubberized diagnostic speed bump, which is pictured in Figure 1. The speed bump was 108 inches long, 2.5 inches tall, and 18 inches wide. It was instrumented with two triaxial accelerometers beneath the left and right wheels of an approaching vehicle as shown in Figure 1. As discussed by DiPetta et al.¹, the use of the instrumented speed bump enabled some faults to be detected; however, the inherent variability in diagnostic testing using this narrow speed bump required that several datasets (at least 5) be acquired from multiple runs for averaging to develop a reliable fault index that detected faults. The reason that this narrow speed bump required measurement averaging to reliably detect faults was because of the short period response time history that was acquired as the vehicle traversed the bump. When the vehicle traversed this narrow speed bump at 5 mph, a measurement that was approximately 0.2 second was acquired. Rayleigh's criterion states that the frequency resolution, Δf , in a dynamic measurement was equal to $1/T$, where T was the time over which the measurement was made. Shorter measurements (i.e., smaller values of T) resulted in more coarse frequency resolution (i.e., larger values of Δf). In the case of the narrow speed bump, the frequency resolution was 5 Hz. Because a typical military ground vehicle has many vehicle modes of vibration below 5 Hz, this measurement lumped the energy in all of these modes of vibration into a single frequency component at 5 Hz. This type of leakage error was not conducive for providing sensitive or repeatable diagnostic measurements².

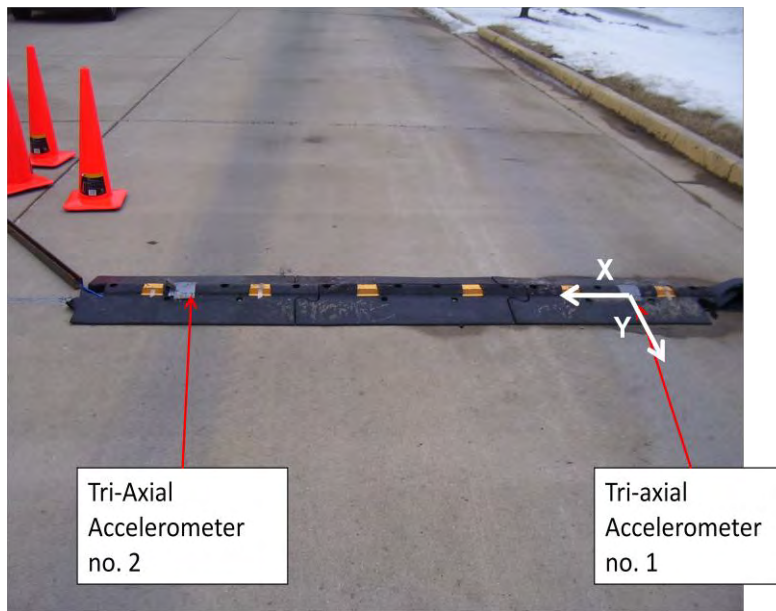


Figure 1. Diagnostic speed bump configuration tested in previous year's work.

¹ DiPetta, T., Adams, D. E., Koester, D., Gotham, J., Decker, P., and Lamb, D., "Health Monitoring for Condition-Based Maintenance of a HMMWV using an Instrumented Diagnostic Cleat," 2009, *Proceedings of the 2009 Congress of the Society for Automotive Engineers*.

² Adams, D. E., "Health Monitoring of Structural Materials and Components: Methods with Applications," 2007, John Wiley & Sons, Chichester, UK.

In order to realize a more robust measurement approach that does not require averaging in the form of multiple runs to conduct diagnostic testing on ground vehicles, a speed bump that provided longer response time history measurements was developed. Figure 2 shows a schematic of the measurement approach that was used in this extended diagnostic speed bump. In this configuration, the rubberized speed bump provided the excitation force to the wheels of the vehicle and the plates positioned behind the speed bump measured the response of the vehicle for approximately 1 second after the vehicle traversed the speed bump. From this perspective, the extended diagnostic speed bump was akin to the use of modal impact testing for exciting broadband frequency ranges in mechanical systems for use in vibration analysis of such systems.

Figure 3 is a photograph of the test setup along with a HMMWV about to traverse the extended diagnostic speed bump. Four sensors were attached to two steel plates, which were 85 inches long and $\frac{1}{2}$ inch thick. Steel was selected to avoid excessive deformation due to the dynamic weight of the vehicle – excessive deformation of the plate would result in filtering of the response measurement. In the future, aluminum plates will be constructed to determine if lighter plates could be used. The plates were placed on a thin rubber sheet on the roadway immediately behind the rubberized speed bump underneath the tracking lanes of the left and right wheels of the vehicle. The rubber sheet was used to correct for small differences in elevation of the roadway surface, much like rubber couplings that are used in rotating machines to account for misalignment of drivelines. Sensors 1 and 2 were placed 60 inches behind the speed bump whereas sensors 3 and 4 were placed 30 inches behind the speed bump. Four sensors were used so that the effects of sensor position could be studied. Triaxial accelerometers (PCB 356B18) were used so that the effects of measurement direction (vertical, tracking, and lateral) on diagnostic capability could be studied. Figure 3 shows the attachment of the sensors to a National Instruments NI cDAQ-9178 compact eight slot data acquisition chassis with NI 9234 data acquisition cards.

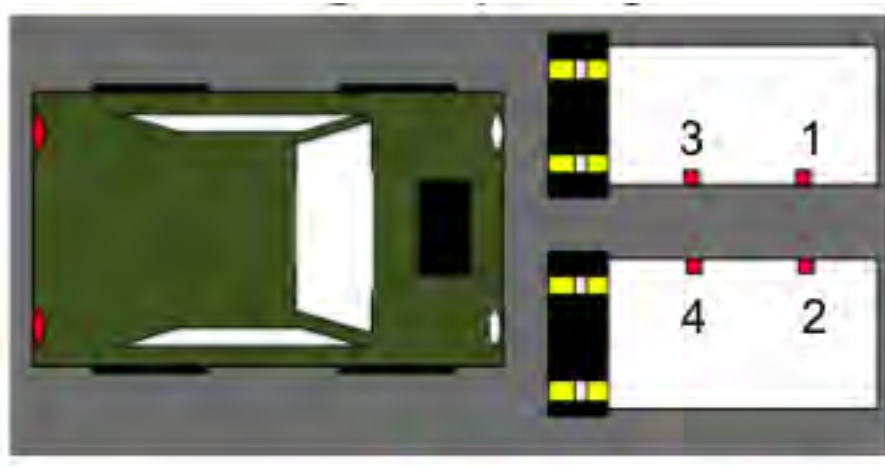


Figure 2. Extended cleat diagnostic speed bump configuration that was selected to provide longer response time histories with enhanced frequency resolution.



Figure 3. Photograph of extended diagnostic speed bump measurement configuration with rubberized cleat, measurement plates, sensors, and data acquisition system.

The tests that were run and analyzed for this quarterly report are listed below:

- Baseline condition of vehicle (30 runs)
- Driver front tire pressure reduction from 20 psi to 10 psi (30 runs)
- Baseline condition of vehicle (11 runs)
- Passenger front tire pressure reduction from 20 psi to 10 psi (30 runs)
- Baseline condition of vehicle (11 runs)
- Driver rear tire pressure reduction from 24 psi to 10 psi (30 runs)
- Baseline condition of vehicle (11 runs)
- Passenger rear tire pressure reduction from 24 psi to 10 psi (30 runs)
- Baseline condition of vehicle (11 runs)

3. Results

3.1 Baseline data analysis

The acceleration spectra at sensor 3 in the vertical direction for the first through the fifth baseline series of data for the front wheel excitation were plotted in Figure 4. A Hanning window was used to process the portion of the response time history that was acquired immediately after the front wheels crossed over the cleat. The narrowband operational response with center frequency 7.5 Hz was apparently the response of the extended cleat (plate) due to its interaction with the vehicle as it was directly excited when the vehicle traversed the cleat. In contrast, the narrowband spectral responses with center frequencies at 15, 36, 72, and 100 Hz appeared to be harmonics of the lower frequency operational response. It is not yet known if these harmonics are due to the cleat's response on the elastic foundation, the vehicle dynamics, or a combination of these two sources of nonlinear response. It was clear from the analysis presented in subsequent figures that these higher frequency operational responses could be attributed to the tracking and lateral degrees of freedom, whereas the lower frequency response with center frequency near 7.5 Hz could be attributed primarily to the vertical degree of freedom.

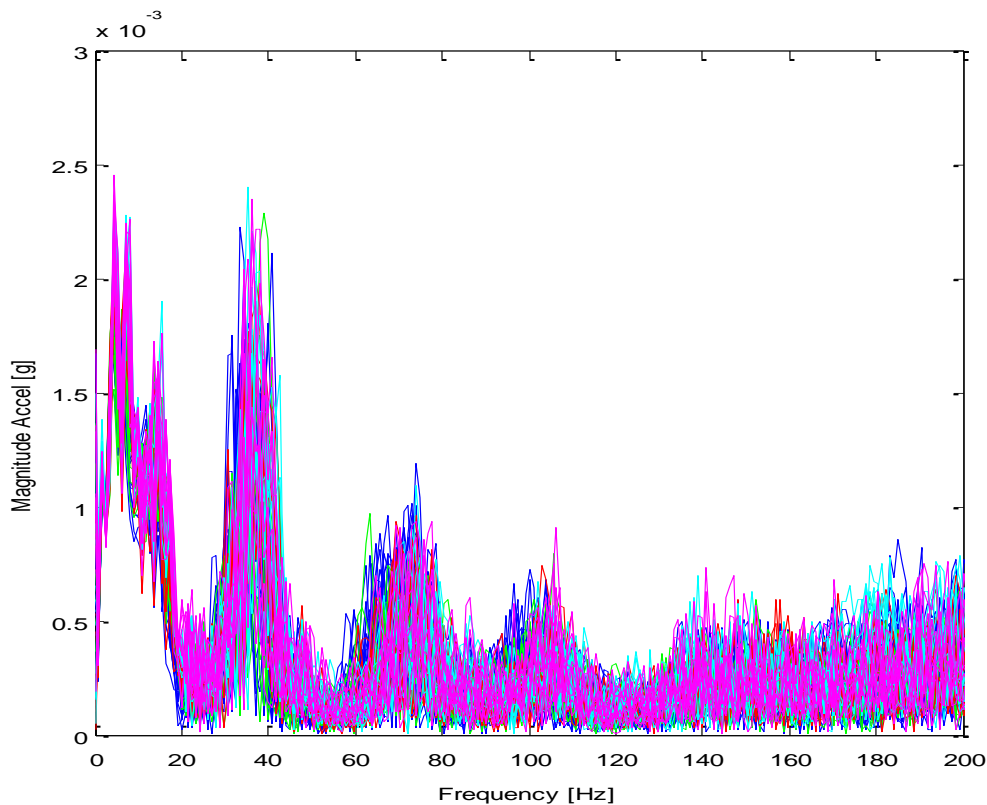


Figure 4. Baseline frequency spectra from sensor 3 (driver's side), vertical direction acceleration for a front axle wheel crossing measured using long cleat for (—) first 30, (—) second 11, (—) third 11, (—) fourth 11, and (—) fifth 11 data series.

The average spectra for the baseline series of data were plotted in Figure 5. This plot exhibited the same characteristics as the individual spectra in Figure 4. It was also evident in Figure 5 that the first two baseline data series were similar to one another and the last three series of baseline datasets were similar to one another, but these two groups of spectra were different across the entire frequency range. The similarity of the last three baseline datasets suggested that there was not a strong memory effect in the vertical response of the extended cleat due to the simulated tire faults that were introduced by reducing tire pressures one at a time. But there was a definite difference between the first two baseline datasets and the last three datasets that will be further examined in future analyses.

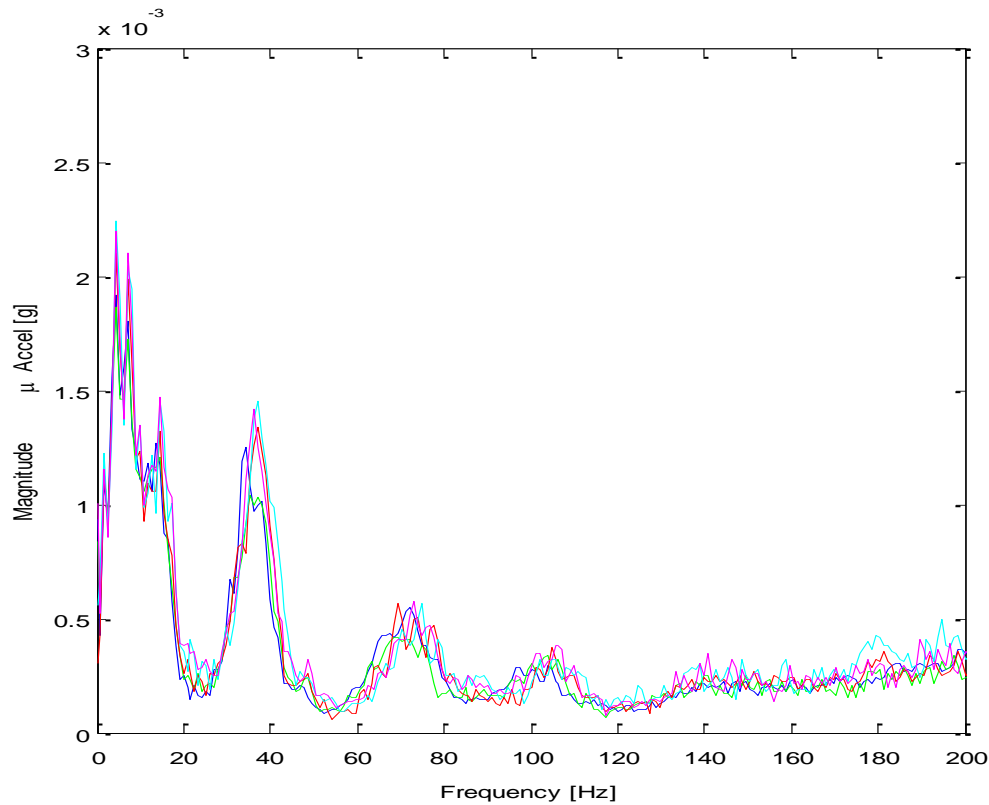


Figure 5. Mean baseline frequency spectra from sensor 3 (driver's side), vertical direction acceleration for a front axle wheel crossing measured using long cleat for (—) first 30, (—) second 11, (—) third 11, (—) fourth 11, and (—) fifth 11 data series.

To better understand the variation in the individual measurements that were conducted in the baseline state of the vehicle, the standard deviation as a function of frequency across the five sets of baseline data plotted in Figures 4 and 5 were calculated and plotted in Figure 6. Note that the standard deviation was largest near 37.5 Hz, and smallest near 20, 59, 90, and 120 Hz. Although this information was useful for defining the inherent variability in the measurements acquired using the long cleat, these standard deviation spectra were normalized as shown in Figure 7 to draw additional insight from the data. This result was interesting because it indicated that the least normalized variation in the

baseline data was between 2 and 20 Hz. Throughout the remainder of the frequency range, the normalized variation was nearly constant at 50% of the mean value of the spectrum of interest. It was important to focus the diagnostic analysis in the frequency range where the normalized standard deviation was a minimum because smaller changes in the spectra due to simulated faults in the vehicle should theoretically be observed in this frequency range. Figure 8 shows a comparison between the normalized standard deviations for sensors 1 through 4 in the vertical direction acceleration (sensors 1 and 2 were furthest from the cleat, and sensors 3 and 4 were closest to the cleat). It was evident in this figure that sensors 3 and 4 exhibited the lowest normalized standard deviation suggesting that these two sensors would increase the detectability of faults. The subsequent analysis focused on the data acquired from sensors 3 and 4 due to the lower variation in this sensor data.

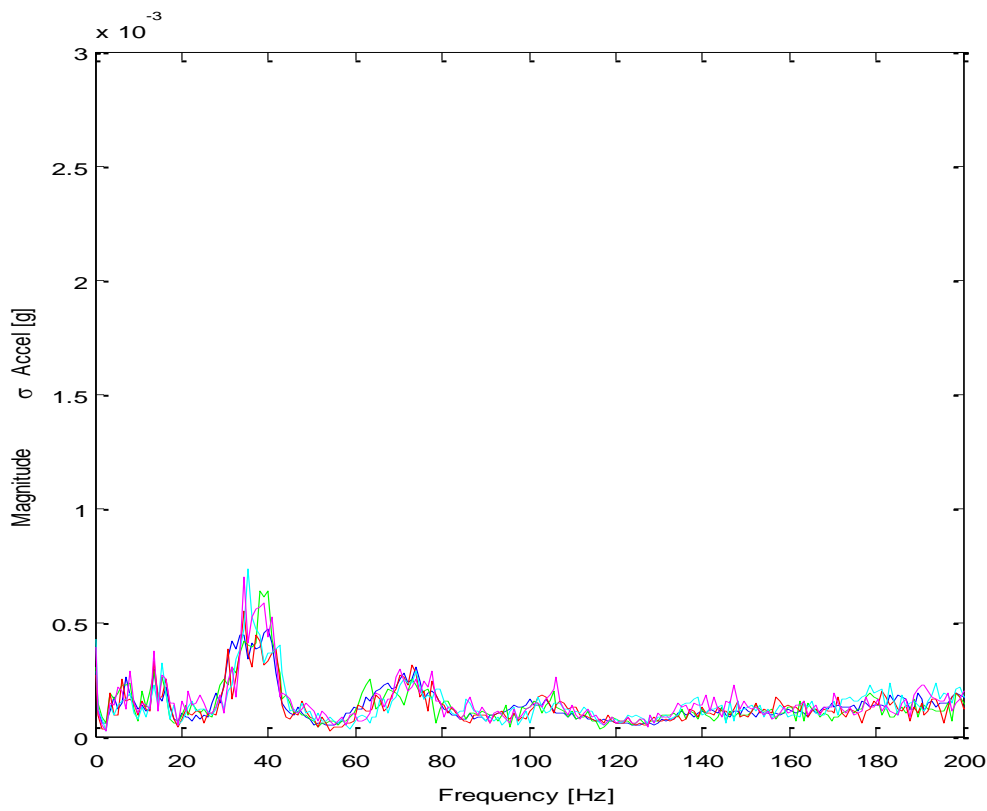


Figure 6. Baseline standard deviations of frequency spectra from sensor 3 (driver's side), vertical direction acceleration for a front axle wheel crossing measured using long cleat for (—) first 30, (—) second 11, (—) third 11, (—) fourth 11, and (—) fifth 11 data series.

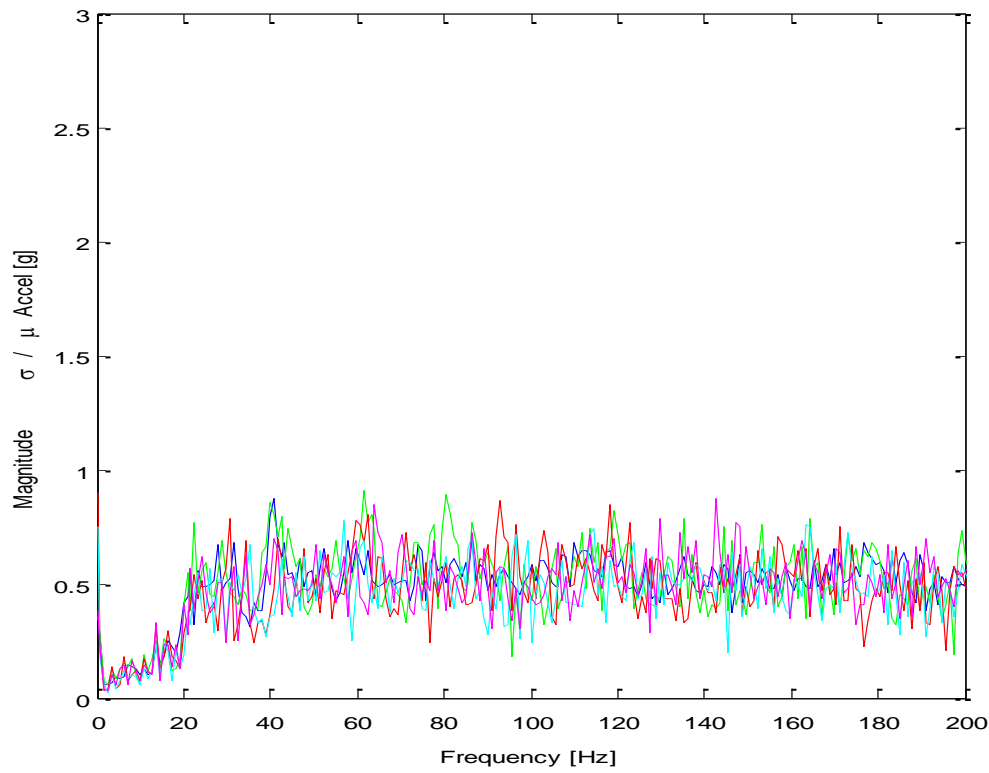


Figure 7. Normalized baseline standard deviations of frequency spectra from sensor 3 (driver's side), vertical direction acceleration for a front axle wheel crossing measured using long cleat (—) first 30, (—) second 11, (—) third 11, (—) fourth 11, and (—) fifth 11 data series.

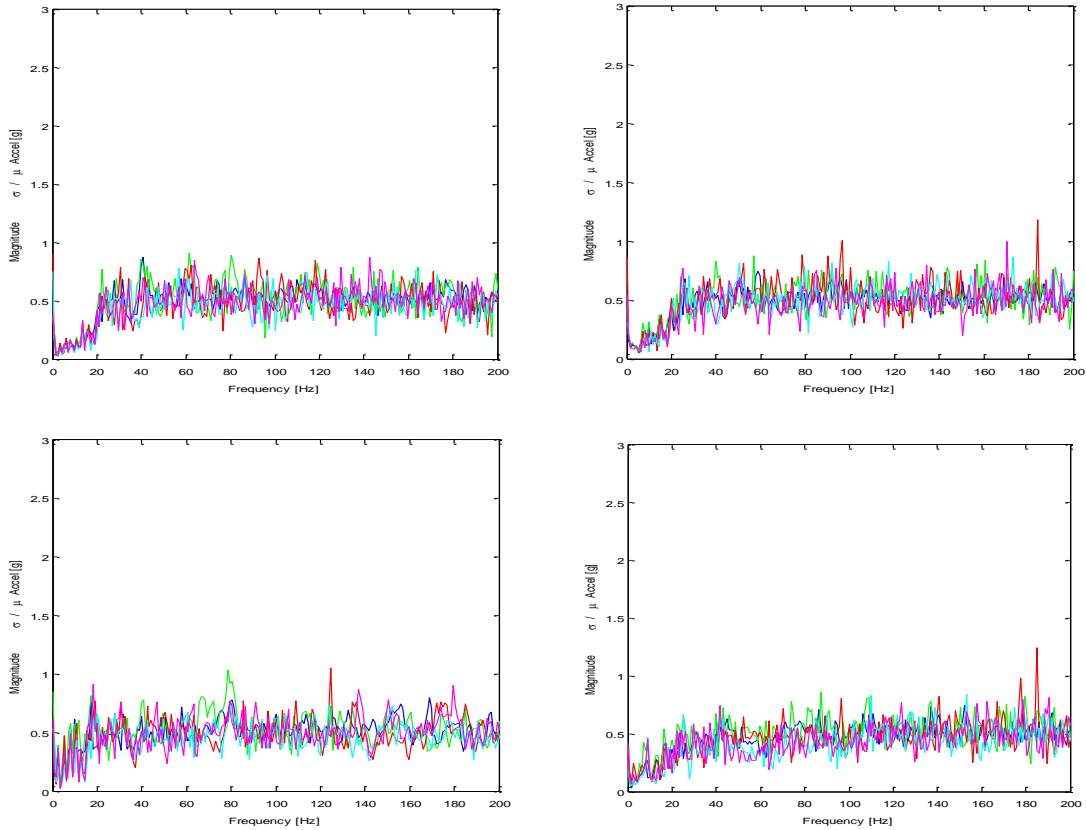


Figure 8. Normalized baseline standard deviations of frequency spectra from (a) sensor 3 (driver), (b) sensor 4 (passenger), (c) sensor 1 (driver), and (d) sensor 2 (passenger) vertical direction accelerations for front axle wheel crossings measured using long cleat (—) first 30, (—) second 11, (—) third 11, (—) fourth 11, and (—) fifth 11 data series.

The other two measurement degrees of freedom measured on the extended cleat in the tracking (Y) and lateral (X) degrees of freedom were also analyzed to assess any qualitative differences with the vertical direction (Z) degree of freedom. Figure 9 is a comparison between the (a) vertical and (b) lateral degrees of freedom for sensor 3, and Figure 10 is a comparison between the (a) vertical and (b) tracking degrees of freedom for sensor 3. Note that the lateral direction measurement in Figure 9(b) exhibited a narrowband peak near 70 Hz in contrast to the vertical direction measurement, which exhibited a peak in its response near 7.5 Hz. This result indicated that the lateral direction measurement was either a harmonic byproduct of the low frequency response in the vertical direction, forced response directly due to the cleat, or a combination of these two response contributions. Also, note that both the lateral direction and vertical direction exhibited peaks near 70 Hz suggesting that these two narrowband responses were correlated to one another, but the lateral direction was clearly dominating in this frequency range. The same statements hold for the comparison of the vertical and tracking direction accelerations in Figure 10 for the narrowband response that peaks near 37 Hz in both of the mean spectral amplitudes. It can also be seen in Figure 9(b) and

Figure 10(b) that both the lateral and tracking direction acceleration spectra exhibited peaks around 2 Hz. It is unknown at this time if this response was due to the extended cleat (elastically supported plates on the backside of the cleat) or the vehicle dynamics. Based on these results, Figure 11 was produced to highlight the dominant degrees of freedom in the sensor 3, vertical direction acceleration narrowband frequency ranges that were peaking to some degree in all of the measurements.

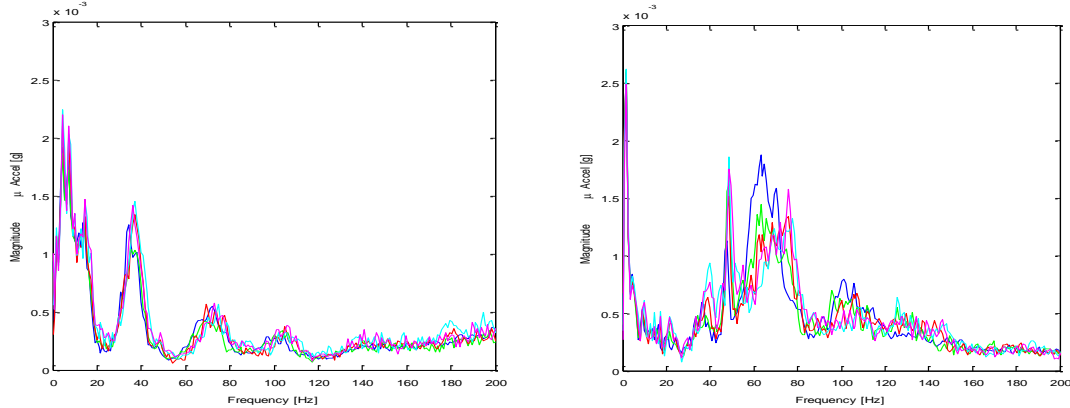


Figure 9. Mean baseline frequency spectra from sensor 3 (driver's side), (a) vertical and (b) lateral direction accelerations for a front axle wheel crossing measured using long cleat for (—) first 30, (—) second 11, (—) third 11, (—) fourth 11, and (—) fifth 11 data series.

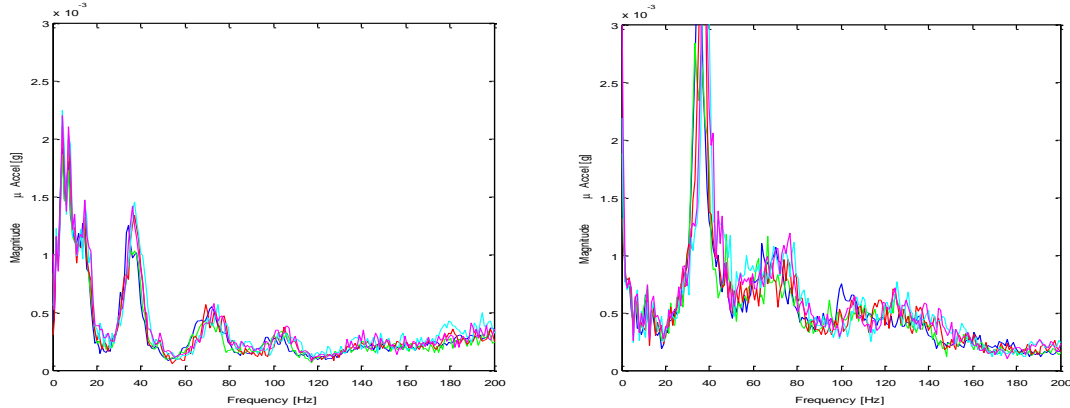


Figure 10. Mean baseline frequency spectra from sensor 3 (driver's side), (a) vertical and (b) tracking direction accelerations for a front axle wheel crossing measured using long cleat for (—) first 30, (—) second 11, (—) third 11, (—) fourth 11, and (—) fifth 11 data series.

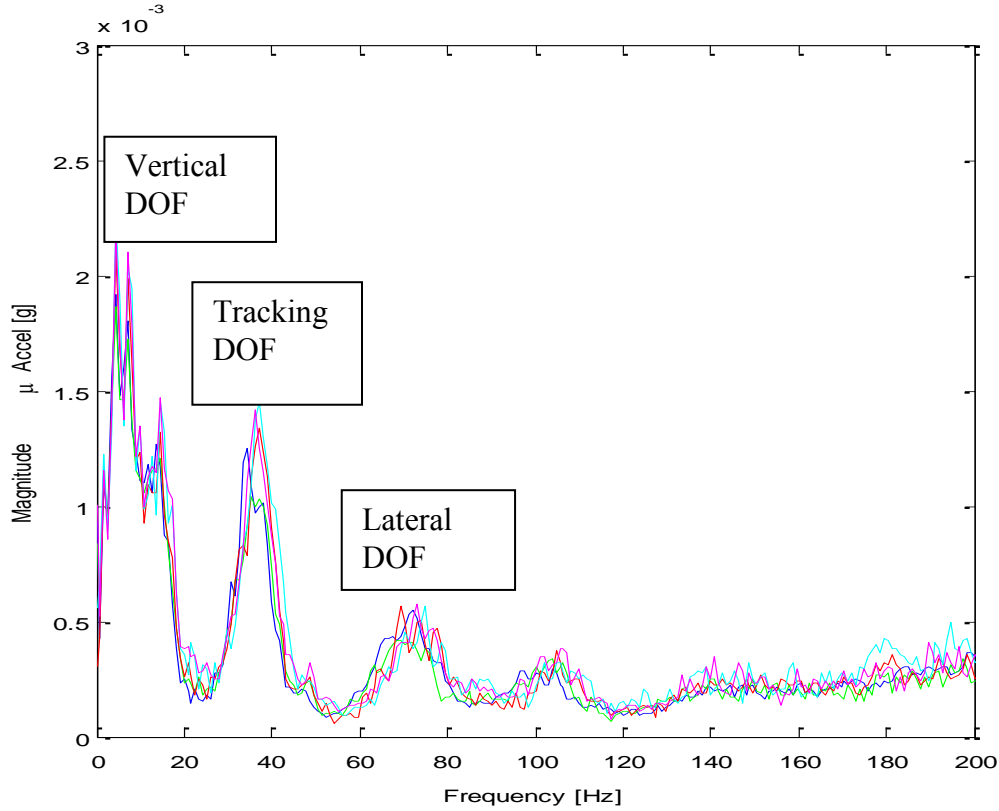


Figure 11. Mean baseline frequency spectra from sensor 3 (driver's side) vertical direction acceleration for a front axle wheel crossing measured using long cleat for (—) first 30, (—) second 11, (—) third 11, (—) fourth 11, and (—) fifth 11 data series showing dominant degrees of freedom as a function of frequency.

The normalized standard deviations for the tracking and lateral acceleration degrees of freedom at sensor 3 were plotted in Figure 12. Note that the deviation was not as low as for the vertical direction in the 1-20 Hz range; however, the deviation was still lowest in this frequency range despite the fact that the tracking and lateral acceleration spectra exhibited peaks in different narrowband frequency ranges. This result suggested that the small normalized deviation in all of these measurements was indicative of the primary forced response in the vertical direction below 20 Hz, whereas the higher frequency narrowband band responses in the tracking and lateral directions (see Figure 11) were harmonically coupled to the low frequency response.

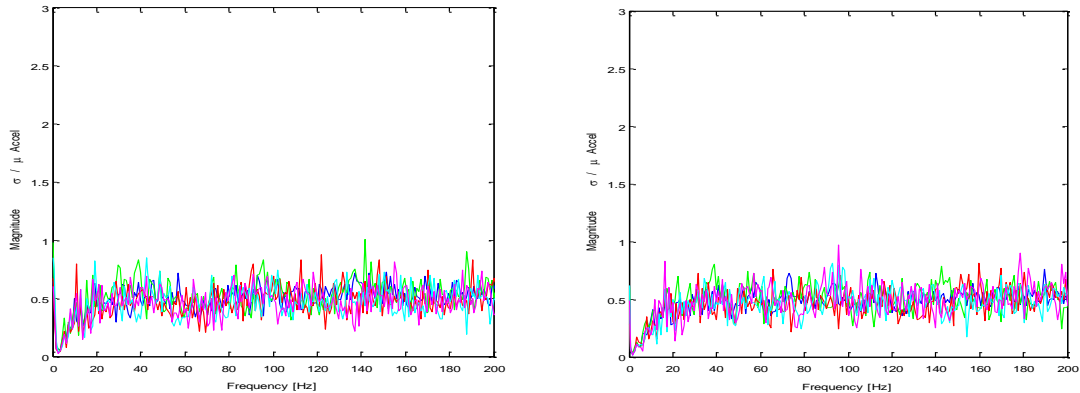


Figure 12. Normalized baseline standard deviations of frequency spectra from sensor 3 (driver's side) for the (a) lateral and (b) tracking direction accelerations for front axle wheel crossings measured using long cleat (—) first 30, (—) second 11, (—) third 11, (—) fourth 11, and (—) fifth 11 data series.

The (a) spectra and (b) normalized standard deviations for a rear wheel crossing were plotted in Figure 13 for comparison with the results obtained for the front wheel crossing. Note that the response characteristics were similar in the spectra in terms of the frequency ranges that exhibited peaks in the response amplitude; however, the normalized deviation in Figure 13(b) was larger below 20 Hz than it was for the front wheel crossing. This result suggested that rear wheel faults would be less detectable than front wheel faults.

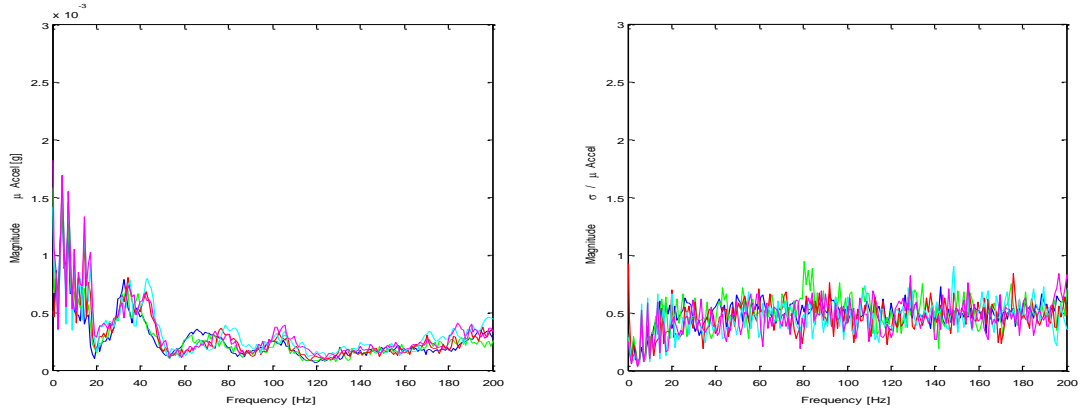


Figure 13. Mean spectra and normalized baseline standard deviations from sensor 3 (driver's side) for the vertical direction acceleration for rear axle wheel crossing measured using long cleat (—) first 30, (—) second 11, (—) third 11, (—) fourth 11, and (—) fifth 11 data series.

3.2 Variations with vehicle speed

Figure 14 shows the variations in the acquired vertical acceleration data from sensors 3 and 4 on the diagnostic speed bump plates as a function of vehicle speed. The speed was estimated by normalizing the wheelbase with the time period during which the vehicle wheels were in contact with the plates. The data plotted on the y axis was a fault index that was calculated by summing the magnitudes of the respective frequency spectra from 0-200 Hz (see Figure 11 for example of spectra). The color code for the plotted symbols was the same as in the previous plots – the plots in Figure 14 corresponded to the baseline (undamaged) vehicle condition at various stages in the series of tests that were listed previously. The centerline of points was a second order polynomial curve fit of the data as a function of speed. The two outer lines of points were the 99% confidence bounds of this curve fit (i.e., centerline ± 3 standard deviations).

It was evident by examining these figures that the spectral energy in the frequency range 0-200 Hz increased as a function of vehicle speed. This result was anticipated because higher vehicle speeds resulted in larger changes in momentum when the vehicle wheels traversed the speed bump leading to larger responses measured by the extended diagnostic speed bump plates. It was also evident that the passenger and driver side measurements by the diagnostic speed bump exhibited similar variations as a function of vehicle speed; however, the passenger side response (Figure 14(b)) was roughly an order of magnitude larger than the driver side response (Figure 14(a)). It was also interesting that the baseline data that was acquired later in the series of datasets listed previously exhibited higher vehicle speeds and, therefore, larger magnitude responses than the data acquired earlier in the series of datasets. The passenger side response also exhibited a larger change with speed than the driver side response.

To quantify the quality of curve fit that these second order polynomials provided, the error in the fit for each of the datasets was calculated and a histogram was generated using these errors. Figure 15 is a plot of the histograms for the driver side (Figure 15(a)) and passenger side (Figure 15(b)) responses. Both sets of error exhibited nearly Gaussian characteristics with zero means suggesting that the curve fits captured the underlying trends in the variability as a function of speed. The passenger side error exhibited two times the spread as the driver side error, but as a proportion of the measured response magnitude, the passenger side error was smaller in magnitude than the driver side error.

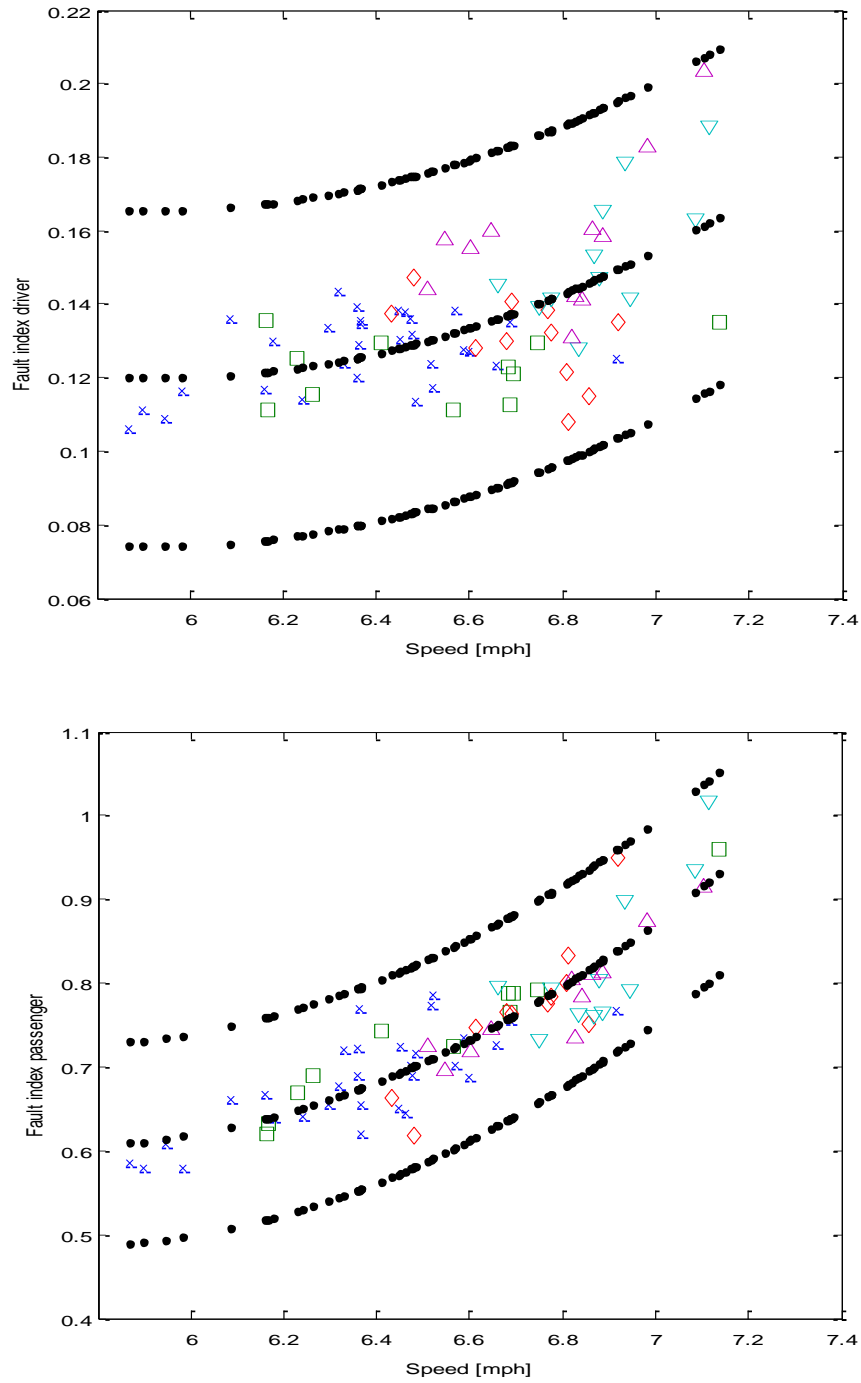


Figure 14. Variation in fault index over frequency range from 0-200 Hz from (a) sensor 3 (driver's side) and (b) sensor 4 (passenger's side) for the vertical direction acceleration for front axle wheel crossing measured using long cleat (—) first 30, (—) second 11, (—) third 11, (—) fourth 11, (—) fifth 11 data series, and (—) second order polynomial curve fit with 99% confidence bands.

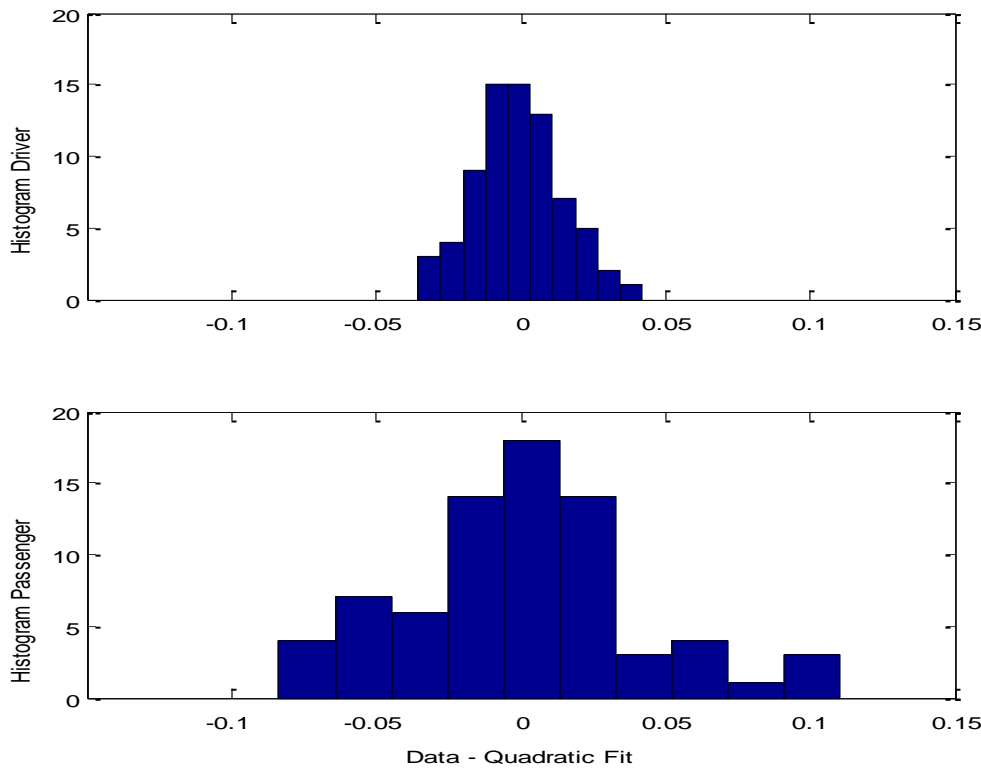


Figure 15. Histogram of errors in second order polynomial curve fit of fault index with speed over frequency range from 0-200 Hz from (a) sensor 3 (driver's side) and (b) sensor 4 (passenger's side) for the vertical direction acceleration for front axle wheel crossing measured using long cleat indicating nearly Gaussian error distribution.

3.3 Tire fault data analysis

The next step was to investigate the diagnostic capability due to tire faults in the form of reductions in tire air pressure. The prescribed healthy front and rear tire pressures were 20 and 22 psi, respectively. To simulate a tire fault in one tire at a time, the air pressure in the tire of interest was reduced to 10 psi. Thirty datasets were then acquired for the faulty tire condition. A comparison of the mean baseline datasets and the datasets for the driver front faulty tire were plotted in Figure 16 for the vertical response measured by sensor 3 on the extended diagnostic speed bump. It was evident that the largest percent change in the responses due to the tire fault occurred in the frequency ranges 30-40 Hz, 60-80 Hz, and 95-110 Hz. Given the conclusions made in the baseline data analysis conducted in the previous sections, it has been postulated that these frequency ranges exhibited the largest magnitude changes due to the tire fault because the responses in these frequency ranges were dominated by the lateral and tracking wheel degrees of freedom whereas the frequency range from 0-20 Hz was dominated by the vehicle chassis vertical degree of freedom (recall Figure 11).

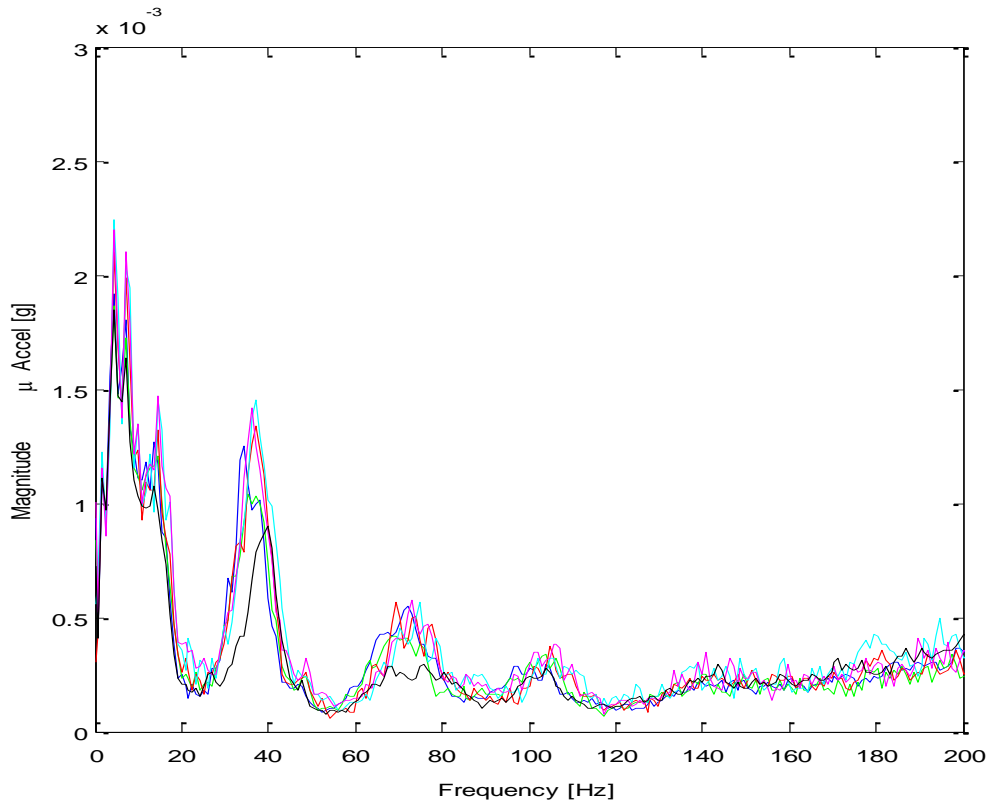


Figure 16. Mean baseline frequency spectra from sensor 3 (driver's side) vertical direction acceleration for a front axle wheel crossing measured using long cleat for baseline data series including (—) first 30, (—) second 11, (—) third 11, (—) fourth 11, and (—) fifth 11 data series, and (—) 10 psi under pressure in driver front tire indicating frequency ranges in which change due to fault could be observed.

A fault index was then extracted from the measured data for each dataset by calculating the sum of the spectral magnitudes for sensors 3 and 4 in the vertical direction across all three of these frequency ranges after the front wheels traversed the speed bump. The resulting fault indices were plotted in Figure 17 for the driver (Figure 17(a)) and passenger side (Figure 17(b)) measurements. Note that the driver side fault index plot detects all of the 10 psi drive front tire pressure datasets (in red) because each of these datasets falls outside of the 99% confidence bands for the quadratic curve fit that was made using the baseline data (in blue). It was interesting that the quadratic curve fits for the driver side and passenger side datasets were qualitatively different in these frequency ranges in contrast to the similarities observed in these curve fits in Figure 14 for the entire frequency range from 0-200 Hz. The reason for these differences is not yet well understood but, given the dominant measurement degrees of freedom in the restricted frequency ranges used to produce Figure 17, it is believed that the quadratic curve fits differed for the driver and passenger sides perhaps due to variation in the plate boundary conditions. In some areas underneath the plates that form the extended diagnostic speed bump, small gaps were observed that might have contributed to the differences between the driver and passenger side responses.

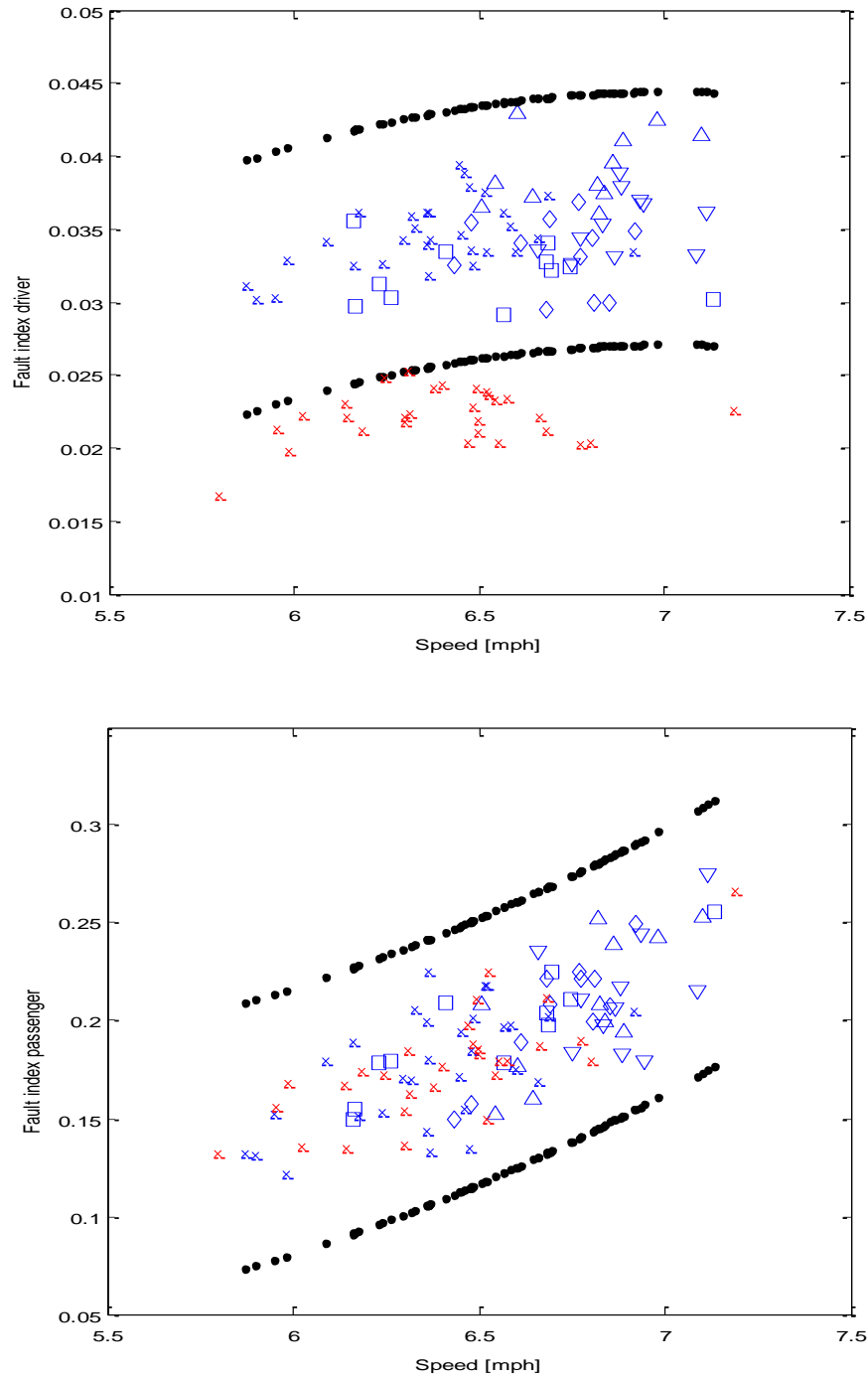


Figure 17. Fault index over frequency ranges 30-40 Hz, 60-80 Hz, and 95-110 Hz from (a) sensor 3 (driver's side) and (b) sensor 4 (passenger's side) for the vertical direction acceleration for front axle wheel crossing measured using long cleat with (—) all baseline datasets, (—) second order polynomial curve fit with 99% confidence bands, and (—) driver front 10 psi tire pressure.

A comparison of the mean baseline datasets and the datasets for the driver front faulty tire were also plotted in Figure 18 for the tracking response measured by sensor 3 on the extended diagnostic speed bump. It was evident that the largest percent change in the responses due to the tire fault occurred in the frequency range from 5-60 Hz. The tire fault clearly affects the tracking response throughout a broad frequency range. This result suggests that the tracking direction of response is more broadly sensitive to the presence of a tire fault. For a passenger front tire fault, the plot in Figure 19 does not indicate differences across such a broad frequency range.

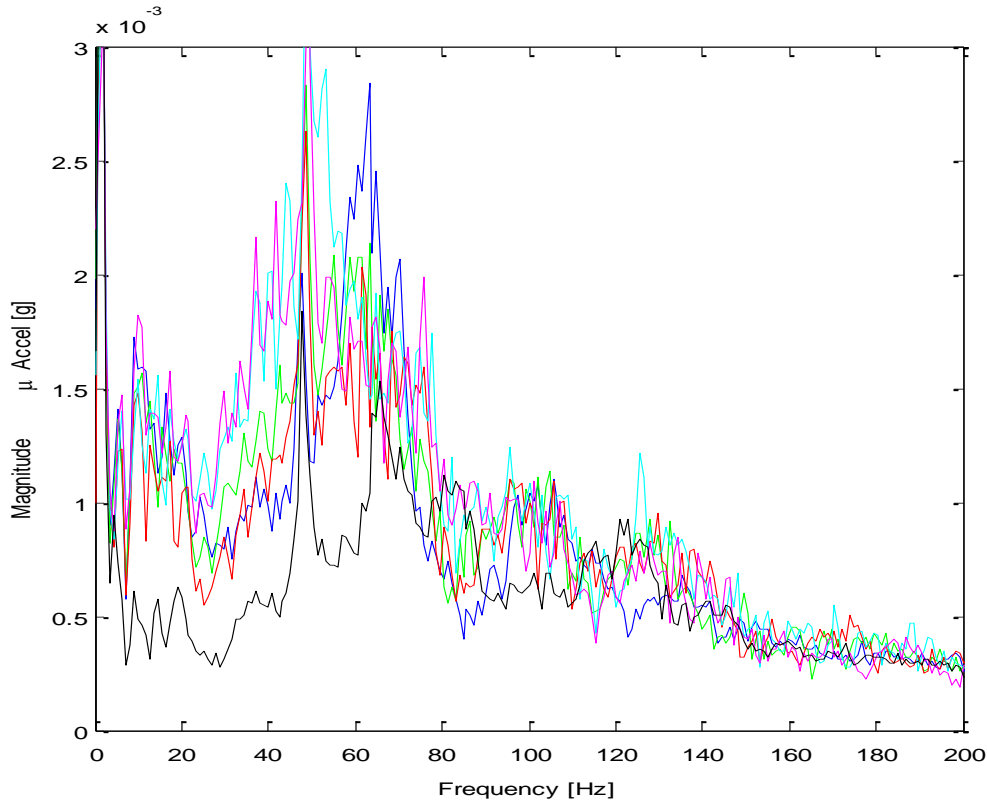


Figure 18. Mean baseline frequency spectra from sensor 3 (driver's side) tracking direction acceleration for a front axle wheel crossing measured using long cleat for baseline data series including (—) first 30, (—) second 11, (—) third 11, (—) fourth 11, and (—) fifth 11 data series, and (—) 10 psi under pressure in driver front tire indicating frequency ranges in which change due to fault could be observed.

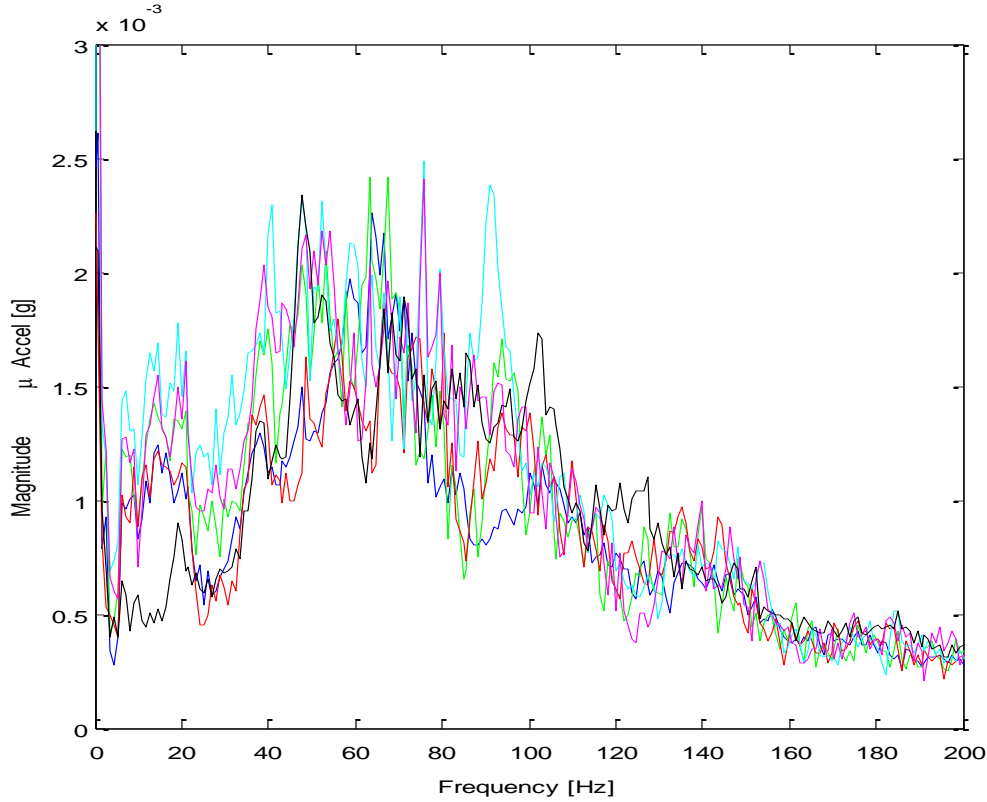


Figure 19. Mean baseline frequency spectra from sensor 4 (passenger's side) tracking direction acceleration for a front axle wheel crossing measured using long cleat for baseline data series including (—) first 30, (—) second 11, (—) third 11, (—) fourth 11, and (—) fifth 11 data series, and (—) 10 psi under pressure in passenger front tire indicating frequency ranges in which change due to fault could be observed.

To better understand the various sensitivities of the extended diagnostic cleat to faults in all four corners of the vehicle, the mean baseline frequency spectra from sensors 3 and 4 were plotted for these four plots. Figure 20 shows the mean spectra for the four fault conditions as indicated in the figure caption. The similarities between the fault characteristics in Figures 20(a) and 20(c) are evident as are the similarities between the fault characteristics in Figures 20(b) and (d). Despite the difference in the frequency ranges that exhibit the largest changes due to faults in the driver side and passenger side of the vehicle, the frequency ranges selected for further analysis of these faults were 30-40 Hz, 60-80 Hz, and 95-110 Hz as were used in Figure 17.

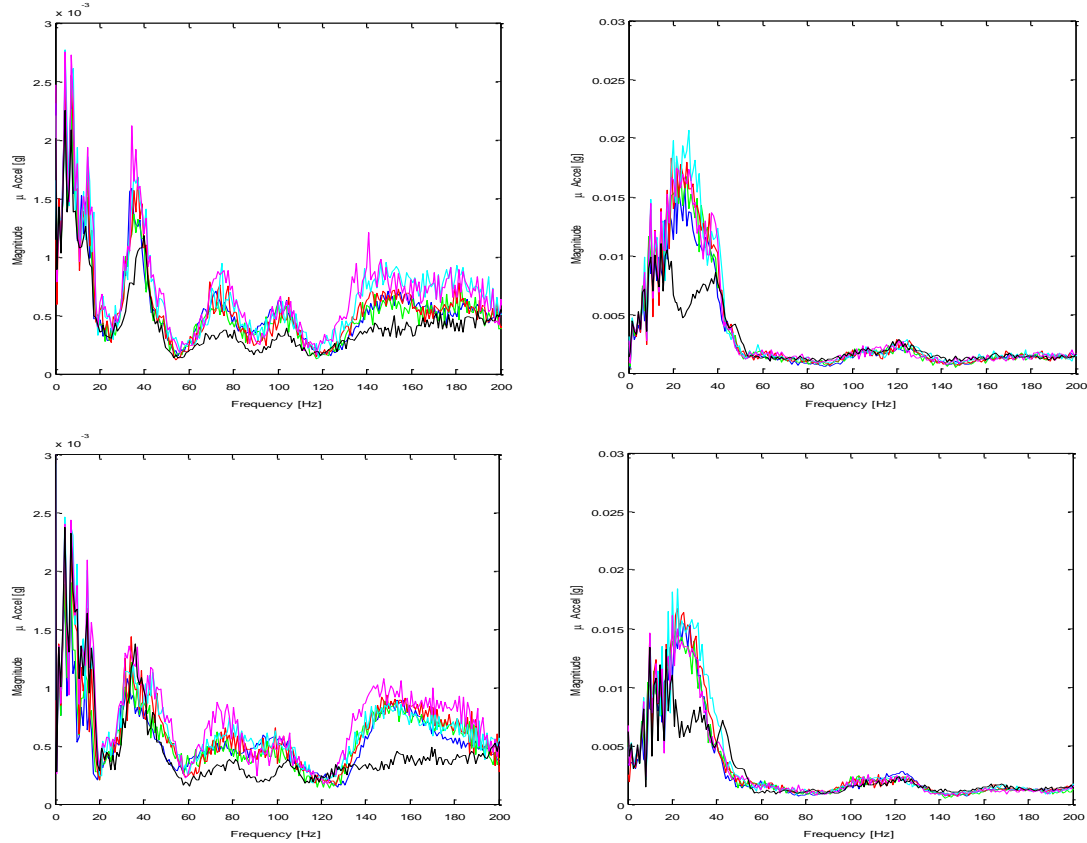


Figure 20. Mean baseline frequency spectra from (a,c) sensor 3 and (b,d) sensor 4 in the vertical direction for a front axle wheel crossing measured using long cleat for baseline data series including (—) first 30, (—) second 11, (—) third 11, (—) fourth 11, and (—) fifth 11 data series, and (—) 10 psi under pressure in (a) driver front, (b) passenger front, (c) driver rear, and (d) passenger rear tire indicating frequency ranges in which change due to faults could be observed.

3.4 Receiver Operator Characteristics for fault detection

The results in the previous section in Figure 17 showed how the damage indices for the faulty front driver tire and faulty front passenger tire fell outside of the normal distribution of damage indices in the baseline case. To quantify the number of false positive and false negative indications of damage that are obtained using this approach, Receiver Operator Characteristic (ROC) curves were generated. These curves were generated by selecting a threshold beyond which faults would be flagged (some fraction of the standard deviation of the healthy distribution of the baseline data), counting the number of false indications of damage, and iterating until the ROC curve was generated. False positive and negative rates were counted using data from front and rear datasets for all four tire fault conditions as well as the baseline datasets. The total number of datasets for calculating the false positive rates was 127 whereas the total number of datasets for calculating the false negative rates was 30. Figure 21 shows the resulting ROC curve for

the driver front tire fault (∇), passenger front tire fault (Δ), driver rear tire fault (\blacktriangleleft), and passenger rear tire fault (\triangleright). For a driver side tire fault, a 70% false negative rate is achieved for a 1% false positive rate. When the false negative rate goes to zero (i.e., when all of the driver front tire fault cases are flagged as faulty), a 3.7% false positive rate is achieved. It is interesting to note that the passenger side tire fault exhibits no false negatives regardless of the threshold that was selected. The reason that this was the case is because the passenger side data exhibits less deviation from the mean as discussed previously. This type of ROC analysis can be used as a design aid in selecting the threshold that must be used to achieve the desired level of false positives/negatives.

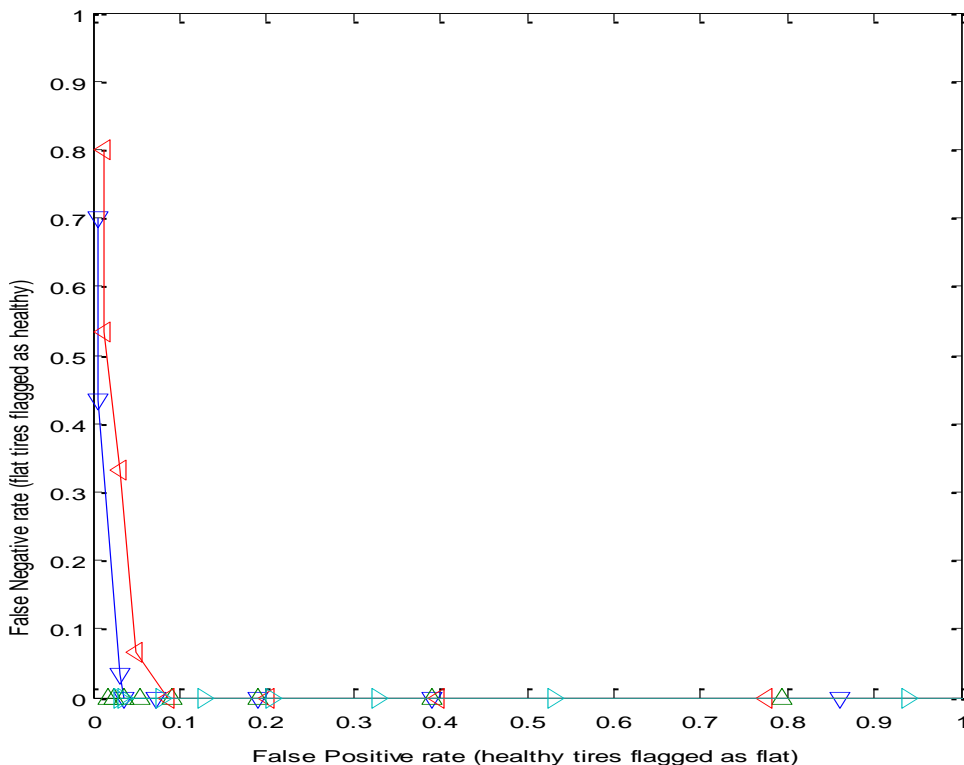


Figure 21. Receiver Operating Characteristic curves for sensors 3 and 4 vertical direction accelerations for front and rear axle wheel crossings measured using long cleat for 10 psi under pressure in driver and passenger front and rear tires, respectively. False positive and negative rates were counted using data from front and rear datasets for these two fault conditions as well as the baseline datasets.

Figure 22 is a close up of the ROC results from Figure 21 in the lower-left hand corner of that figure. As stated above, note that when detecting passenger side tire faults, no false negatives were obtained regardless of the threshold that was selected. The minimum number of false positives that were obtained for the front and rear passenger side faults were 1.5% and 3%, respectively.

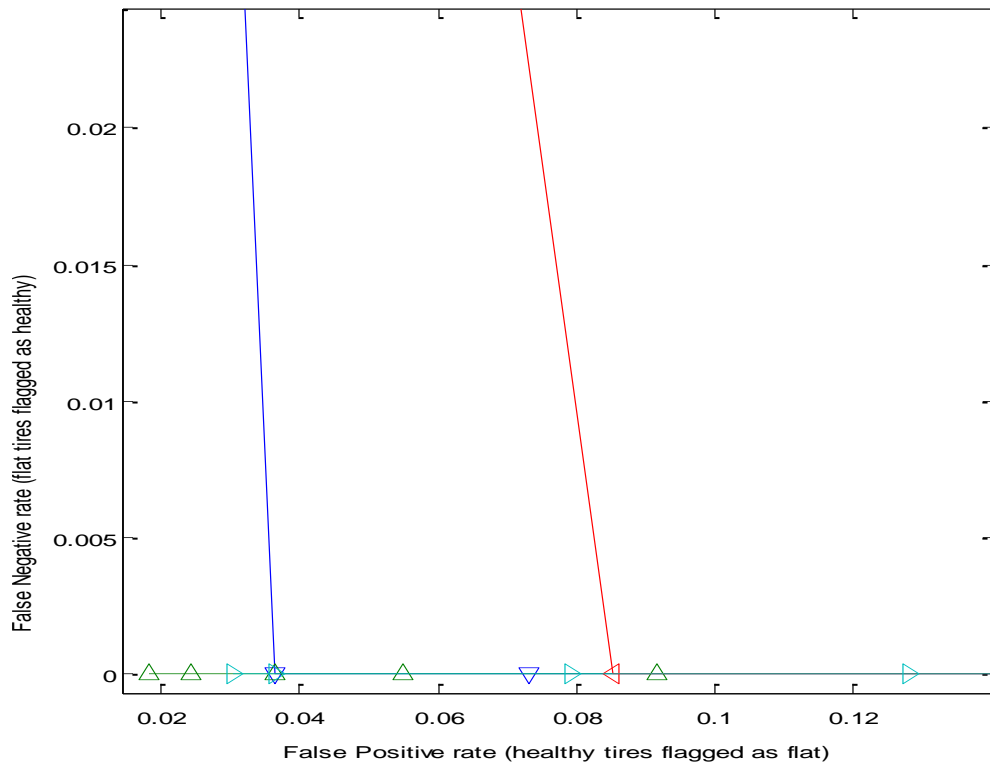


Figure 22. Receiver Operating Characteristic curves (close up of Figure 21 in lower-left-hand corner).

Other ROC curves were also generated for the tracking and lateral directions of response. Figures 23 and 24 show these ROC curves for the two cases involving faults in the driver front and passenger front tires. The diagnostic performance using the tracking and lateral direction measurements was not as good as the performance achieved using the vertical direction measurement (Figure 21). However, for other types of faults it is possible that all three of these directional responses will be useful for detecting faults.

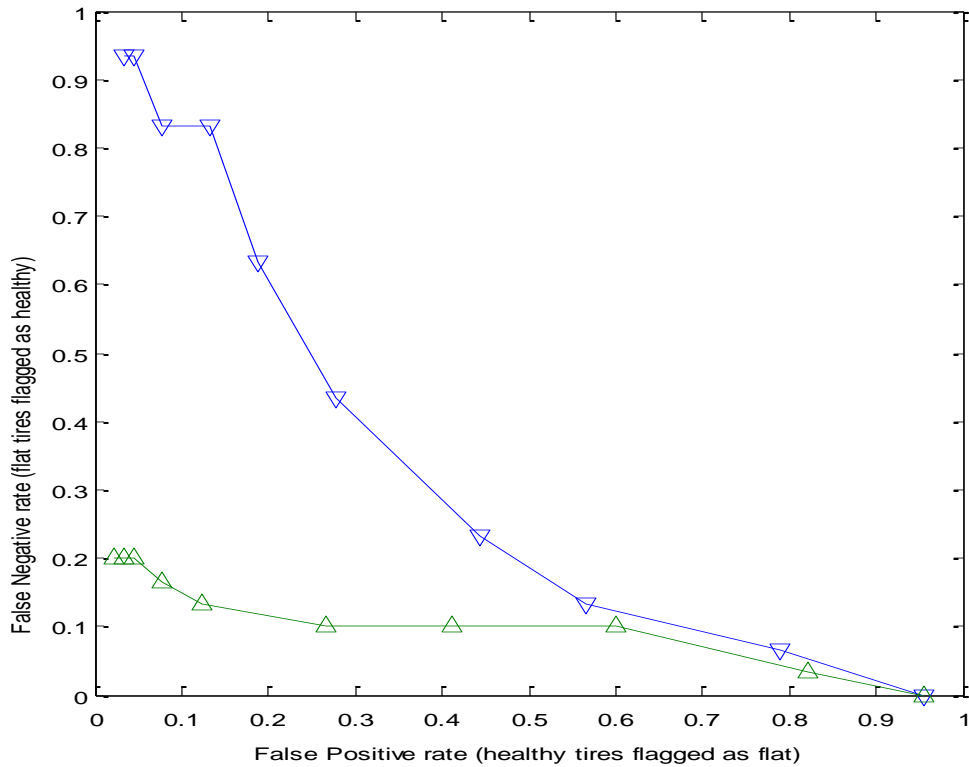


Figure 23. Receiver Operating Characteristic curves for sensors 3 (∇) and 4 (Δ) tracking direction accelerations for front and rear axle wheel crossings measured using long cleat for 10 psi under pressure in driver and passenger front tires, respectively. False positive and negative rates were counted using data from front and rear datasets for these two fault conditions as well as the baseline datasets.

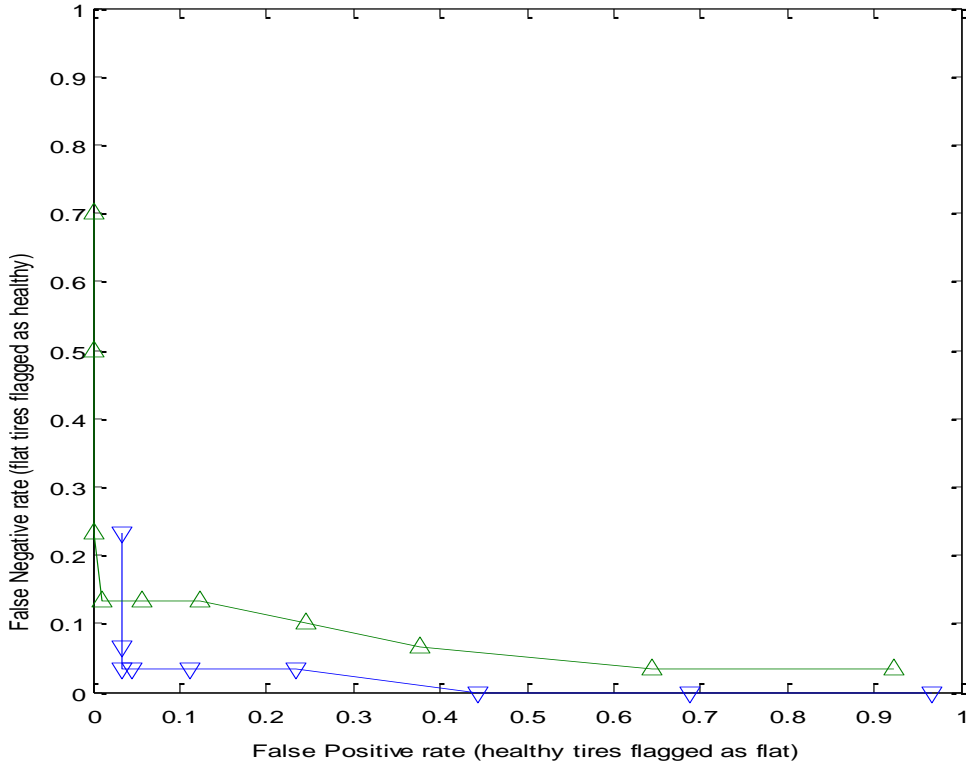


Figure 24. Receiver Operating Characteristic curves for sensors 3 (∇) and 4 (Δ) lateral direction accelerations for front and rear axle wheel crossings measured using long cleat for 10 psi under pressure in driver and passenger front tires, respectively. False positive and negative rates were counted using data from front and rear datasets for these two fault conditions as well as the baseline datasets.

3.5 Extended diagnostic speed bump modal data analysis

The data in the previous sections indicated that the plates on the driver side and passenger side exhibited large differences in their measured response amplitudes. Such differences will complicate the calibration procedure for the instrumented diagnostic cleat. To develop a better understanding of whether or not these differences are due to the vehicle or the extended diagnostic cleat hardware, a modal impact test was conducted on the plates. Figure 25(a) shows the configuration of the plates that were tested where the sensors mounted to the plates are indicated in red (at point 13 on each of the plates). The numbers started with point 1 in the upper right hand corner, went to point 18 in the lower right hand corner, started again at point 19 in the upper center, went to point 36 in the lower center, started at point 37 in the upper left hand corner, and went to point 54 in the lower left hand corner. Figure 25(b) shows the schematic of the driver side plate where each point indicates a modal impact location (modal hammer was used to impact the plate in the vertical downward direction).

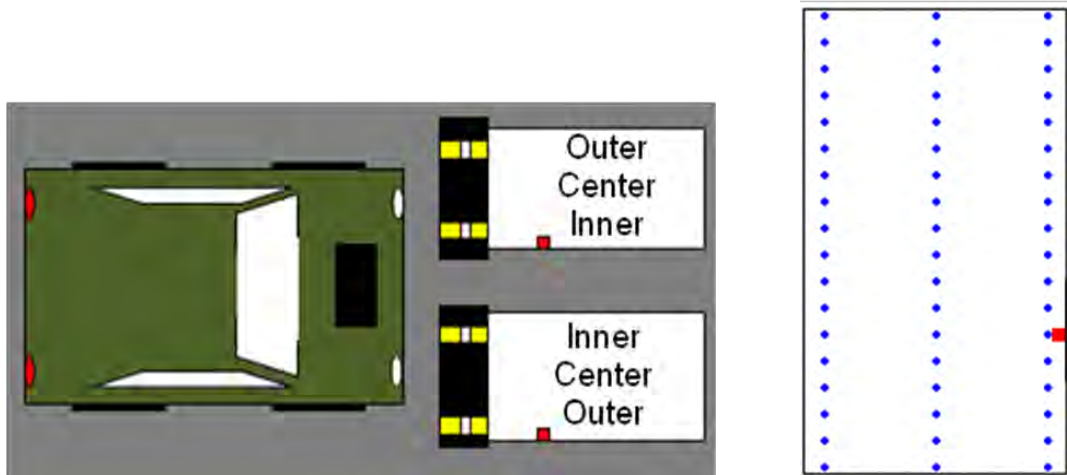


Figure 25: (a) Driver side and passenger side extended cleat plates showing locations of accelerometers used in modal impact test, and (b) schematic of modal test grid on driver side plate.

Figure 26 is a plot of the modal impact driving point frequency response function magnitudes (blue) between the forces applied at points 13 on the (a) driver and (b) passenger side plates and the associated vertical acceleration responses on those plates. The driver side frequency response function magnitude is actually plotted transparently on top of the passenger side frequency response function to make it easier to compare the two plots. The associated coherence functions are plotted in green on the same axes. The coherence functions are plotted on a log scale so it is somewhat difficult to see the drops in coherence but these drops are modest beyond 5 Hz. It is evident from the frequency response functions that the passenger side frequency response function magnitude is much larger (at least a factor of 10) than the driver side frequency response function. This result helps to explain the differences that were observed in the previous sections in the damage indices for the driver side (Figure 14(a)) and passenger side (Figure 14(b)) measurements that were obtained as the vehicle traversed the diagnostic cleat.

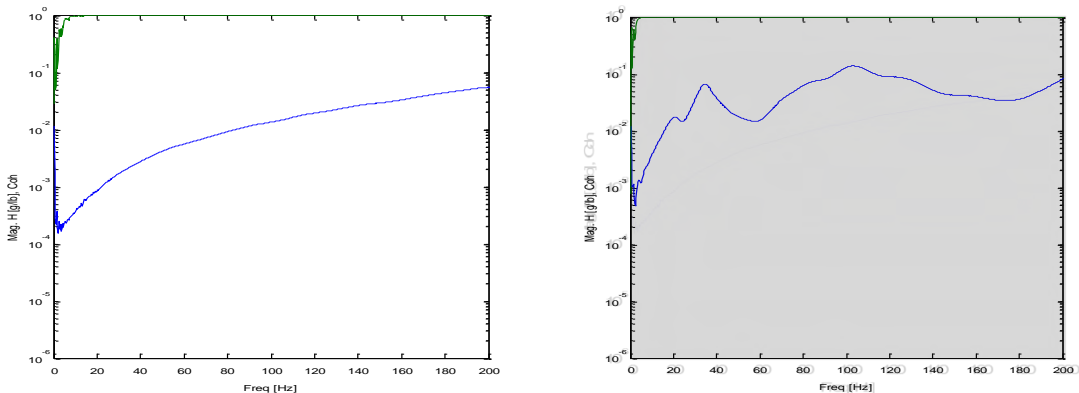


Figure 26: (a) Driver side driving point frequency response function magnitude (blue) and coherence function (green), and (b) passenger side frequency response magnitude and coherence functions (with driver side measurements shown beneath).

To further illuminate the differences in magnitude of the driver side and passenger side measurements, all 54 of the frequency response function magnitudes for the driver side and passenger side plates were plotted in Figure 27(a) and (b), respectively. Several observations can be made when comparing these two sets of frequency response function magnitudes. First, it is clear that the passenger side frequency response function magnitudes are much higher than the driver side frequency response functions. This finding is consistent with the discussions surrounding Figure 26(b). Second, it is also evident that the driver side frequency response functions exhibit fewer peaks (more heavily damped) – Figure 27(b) shows that the passenger side frequency response has a number of lightly damped modes throughout the frequency range from 0-200 Hz. Third, it is also seen that the passenger side inner and outer rows of points exhibit more symmetry than the corresponding rows in the driver side data.

To attempt to reveal the source of these differences in the measured frequency response functions, the operating deflection shapes at various frequencies in the two sets of frequency response measurements were extracted and plotted in Figures 28-31. At a given frequency, such as 35 Hz, the magnitude and phase of the complex frequency response functions for all 54 modal impacts (using the vertical direction measurement as a reference) were extracted. These magnitudes and phases were then converted into a sinusoidal amplitude, Magnitude $\times \sin(\text{Phase})$, and plotted at the corresponding geometric point as shown in Figures 28-31. Note that the geometries were created from left to right to match the modal grids pictured in Figure 25(b) from top to bottom. Therefore, the sensor locations are at length location 13 for both the driver and passenger sides. The operating deflection shapes at 18.5 Hz and 21 Hz for the two sides plotted in Figure 28 indicate that the motion of the sensor at length location 13 is large relative to the others points for the passenger side deflection shape (Figure 28(b)) but is small relative to the other points for the driver side deflection shape (Figure 28(a)). This observation may be related to the lower amplitude measurements that are made using the driver side plate. The same can be said of the operating deflection shapes for the 35 Hz motions in Figure 29. This characteristic is not as evident in Figure 30, but is again evident in Figure 31 for the 102 Hz and 105 Hz motions, respectively, for the driver side and passenger side plates.

Assuming the two plates are nearly identical, it can be concluded that the boundary condition created by the rubber foundation beneath the driver side plate is quite different than the corresponding boundary condition beneath the passenger side plate. And these boundary conditions lead to a difference in the operating deflection shapes for the two plates. These differences in the deflection shapes of the two plates lead to large amplitudes of response in the passenger side plate. The difference in damping is also noteworthy and must also be due to the difference in how the passenger side plate is resting on the rubber foundation.

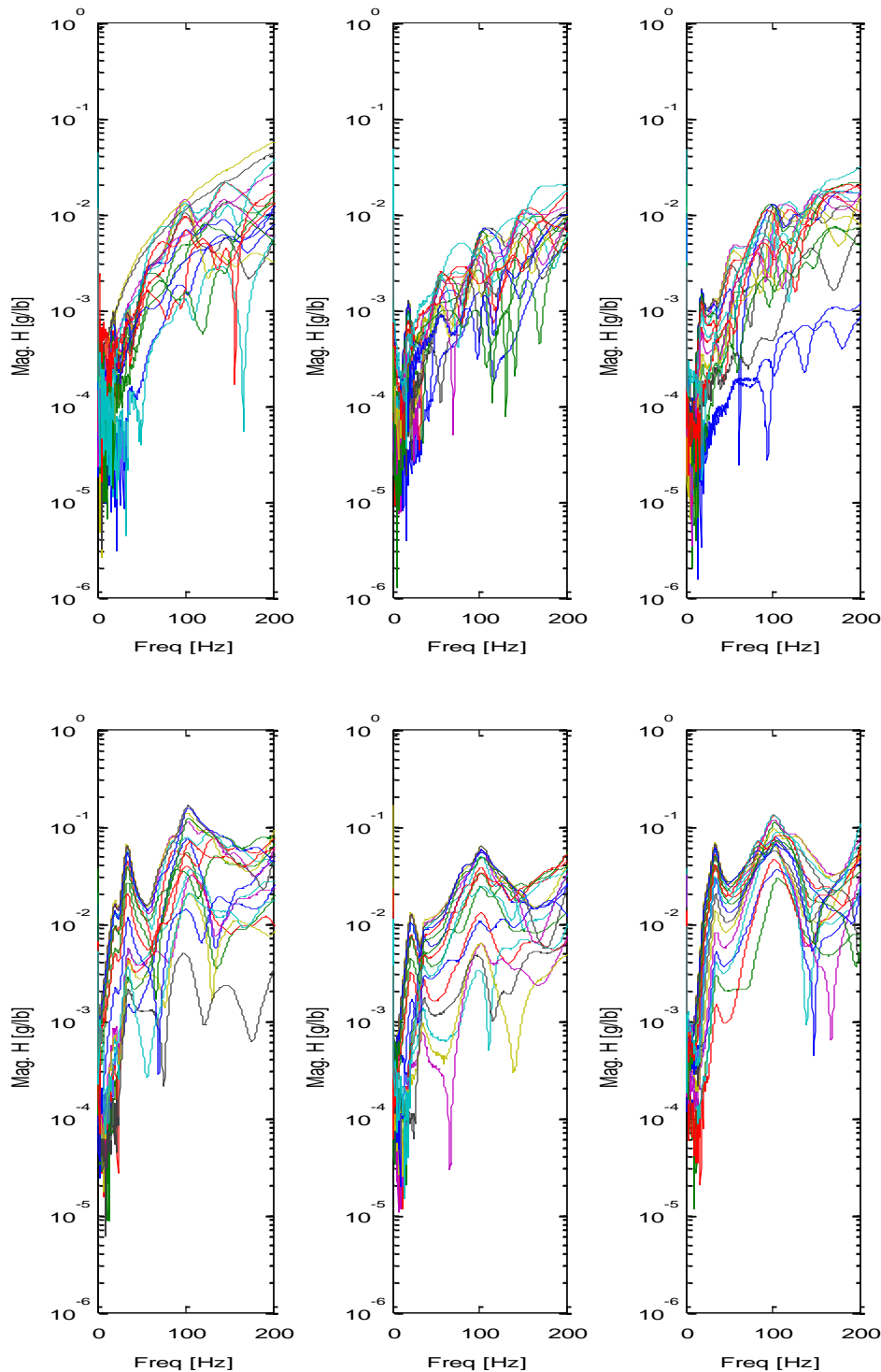


Figure 27: (a) Driver side frequency response functions for inner, center, and outer rows, and (b) passenger side frequency response functions for outer, center, and inner rows showing larger amplitude responses of passenger side plate.

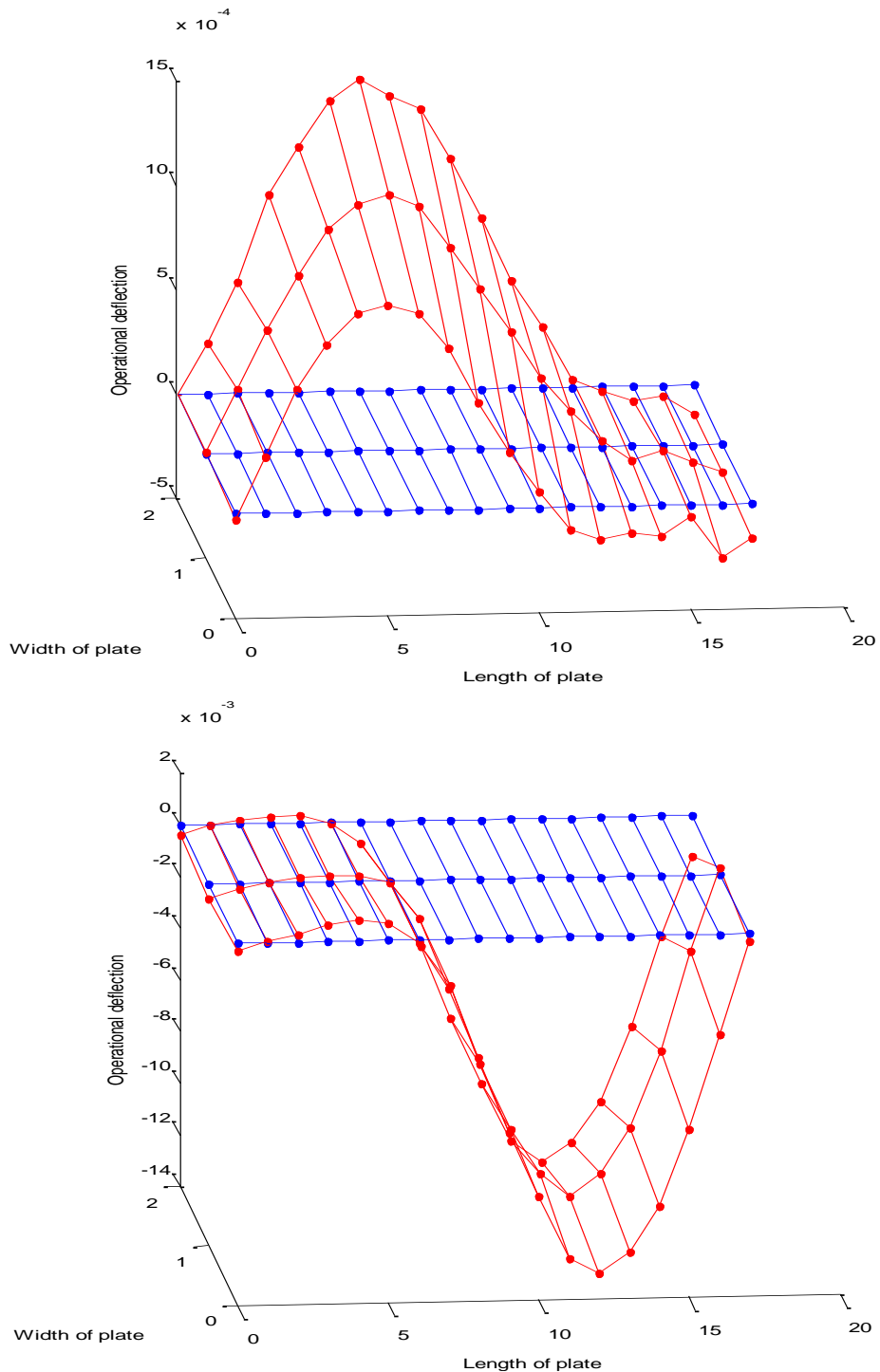


Figure 28: (a) Driver side modal deflection shape at 18.5 Hz, and (b) passenger side modal deflection shape at 21 Hz.

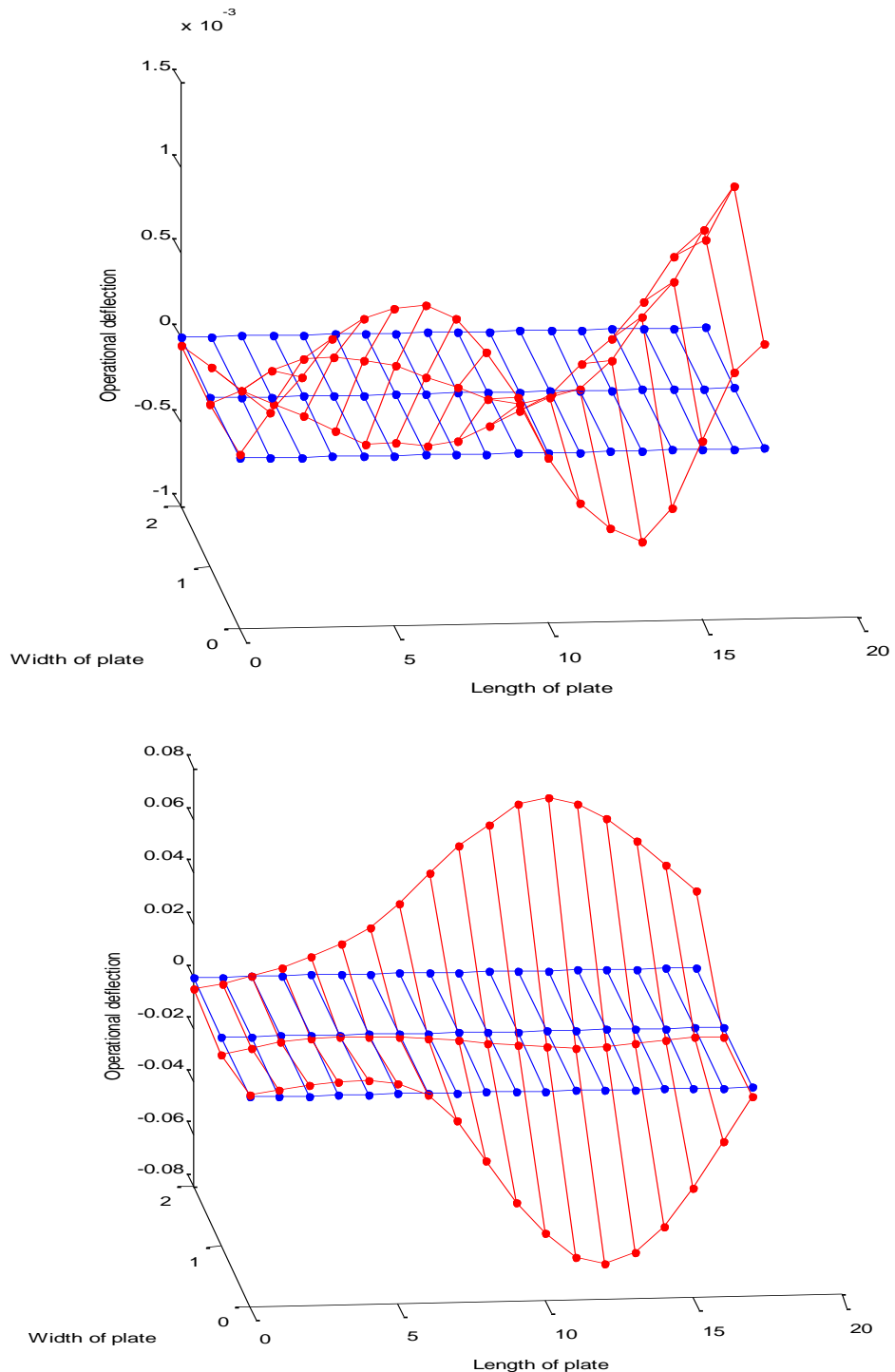


Figure 29: (a) Driver side modal deflection shape at 35 Hz, and (b) passenger side modal deflection shape at 35 Hz.

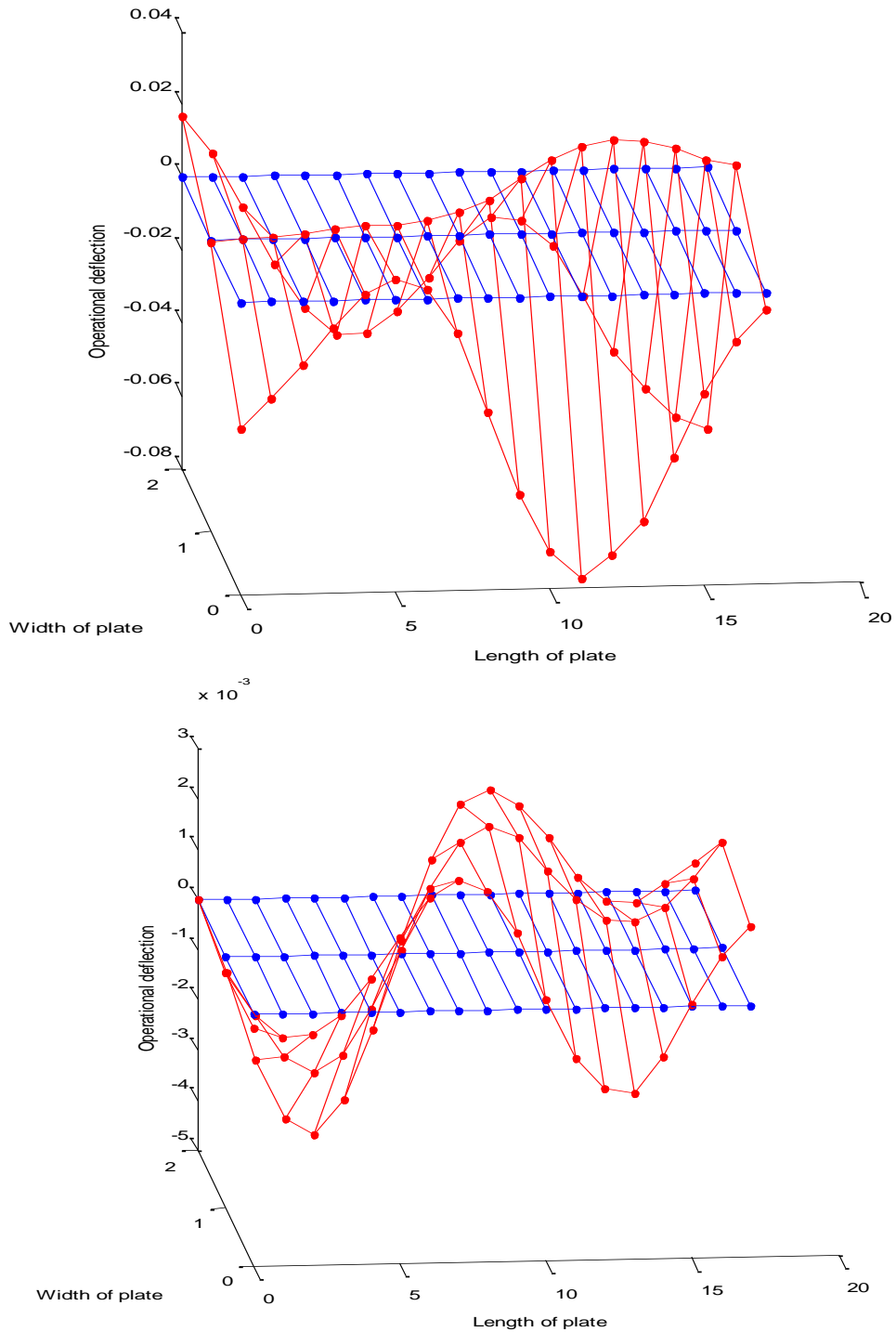


Figure 30: (a) Driver side modal deflection shape at 57 Hz, and (b) passenger side modal deflection shape at 86 Hz.

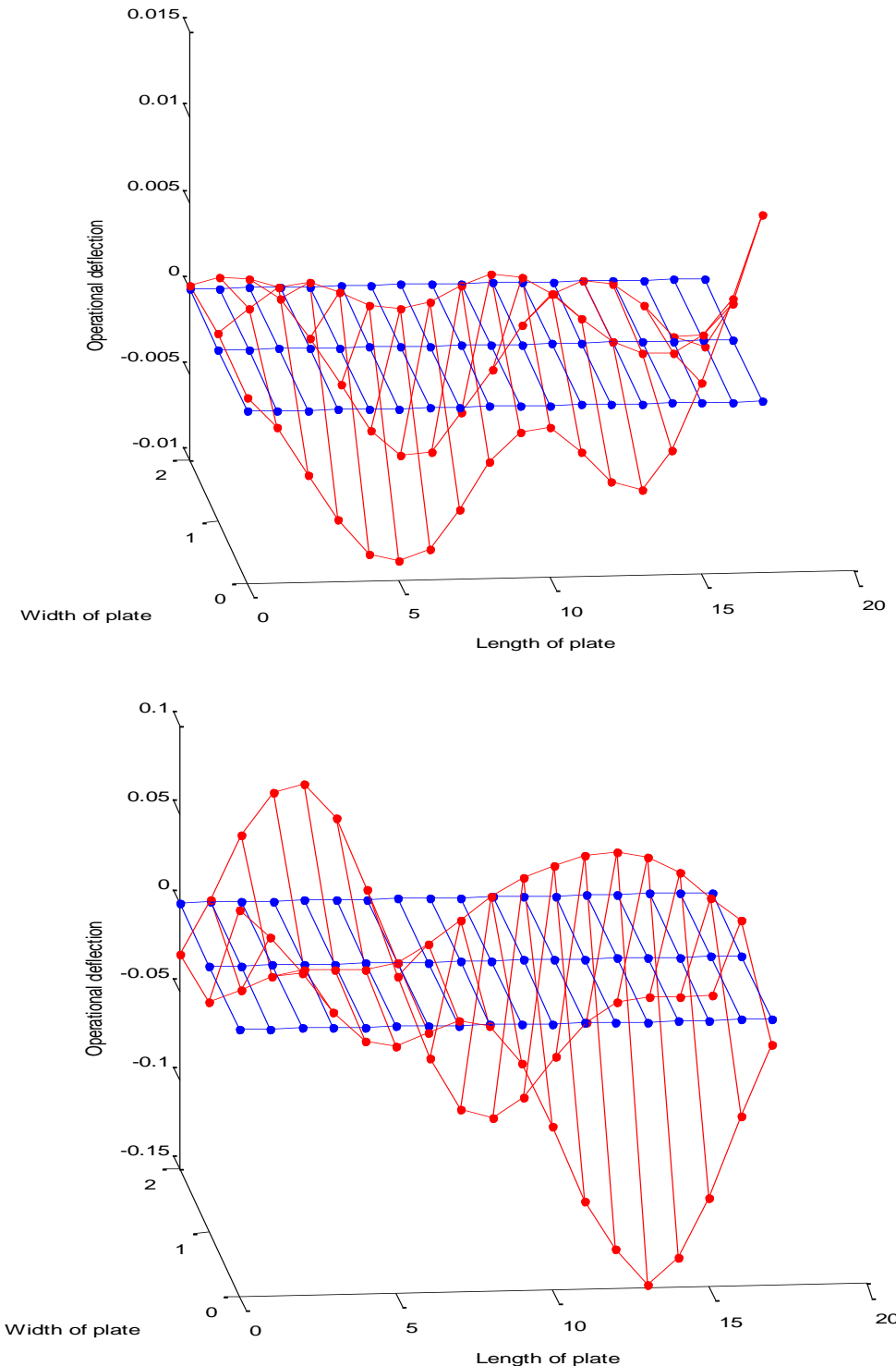


Figure 31: (a) Driver side modal deflection shape at 102 Hz, and (b) passenger side modal deflection shape at 105 Hz.

3.6 Kinematic analysis of tracking wheels

The data in Figure 27 indicated that the plates on the driver side and passenger side of the extended diagnostic speed bump exhibited different frequency response amplitudes as a function of the vertical force location. Therefore, if the vehicle tracks as shown in Figure 32 with an angle of approach as small as ± 5 degrees, the tires can track as far as 7.1 inches away from the center line of the plates that comprise the extended diagnostic speed bump. In addition, the location at which the tires cross over the speed bump will change where the 0 degree line is positioned on the measurement plates.

In this section, the angle of approach of the vehicle for the datasets studied in the previous sections is analyzed and this variation in angle of approach is also interpreted in light of the changes in plate frequency response functions that are plotted in Figure 27. Likewise, the effects of crossing location on the speed bump are considered using this same type of frequency response function analysis approach. Based on this analysis, a dynamic model is pursued in the next section in an effort to develop a methodology for normalizing data to reduce the effects of these two sources of variability on the diagnostic results. That is, if it can be (a) determined that the wheels are approaching the speed bump with a certain angle of approach and (b) determined that the wheels are crossing at a given position along the length of the speed bump, then (c) the data can be normalized using frequency response function data from the plates (that indicate the amplitude of response will change as a function of the angle of approach as well as the point at which the vehicle crossed over the speed bump as it enters the measurement plate).

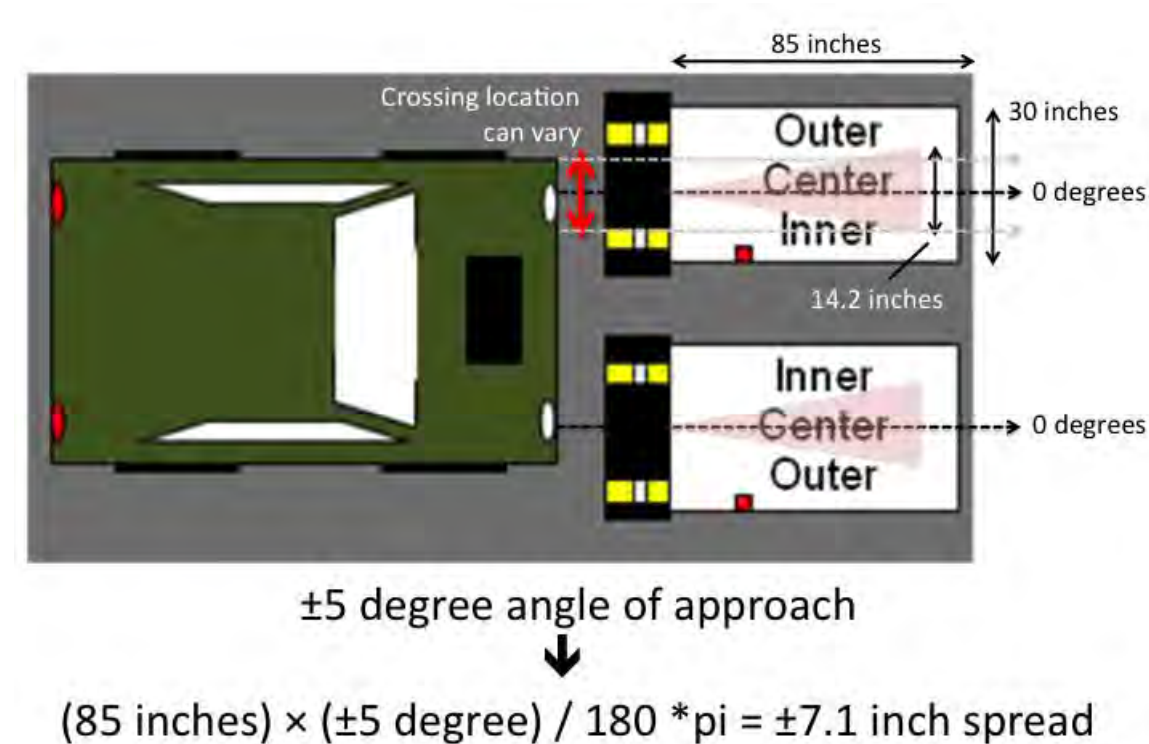


Figure 32: Spread in wheel track for small angles of approach resulting in variation in response of plates due to changes in frequency response as shown in Figure 27.

The driver side plate is considered in Figure 33. This schematic of the modal grid on the driver side plate indicates that the wheel is initially tracking on the points down the middle of the plate (e.g., points 36, 35, and 34). If the vehicle is tracking with a small but non-zero positive or negative angle of approach, then the wheel will travel within the shaded area in Figure 33. If the vehicle is tracking right (positive angle of approach), then the forces applied by the tire to the plate will cause the measured frequency response to be more strongly correlated with measurements that are obtained with the force acts closer to points 1-18. On the other hand, if the vehicle is tracking to the left (with a negative angle of approach), then the measured response will be more similar to the response that is obtained when forces are applied closer to points 37-54. In addition, as the vehicle traverses the plate, the frequency response characteristics that govern the measurement stem from forces by the tire that change their points of action from points 36 to 35 to 34 and so on. If it desirable to normalize the measured data, then these two sources of variation due to the tracking wheel and angle of approach must be taken into account. The following paragraphs analyze these sources of variation and then the next section develops a model that can be used to compensate for these variations.

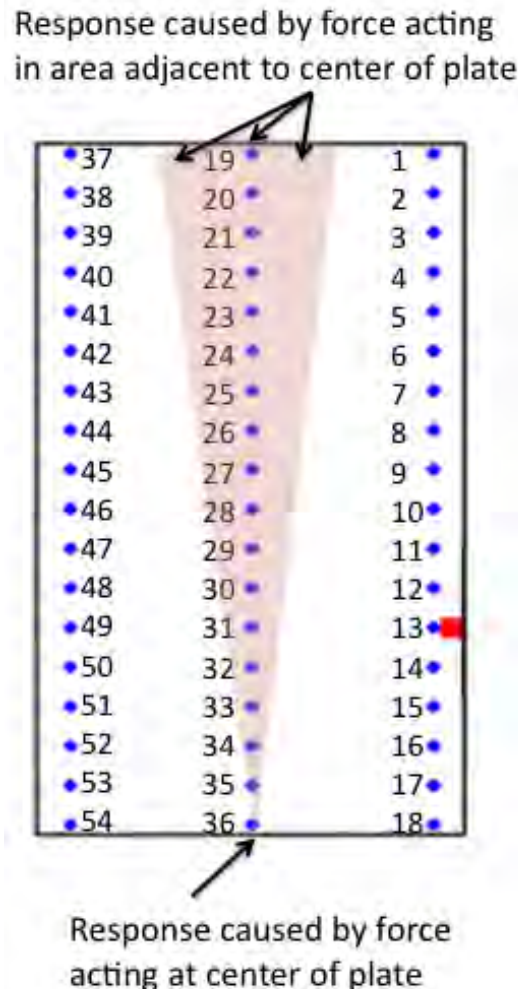


Figure 33: Spread in wheel track for small angles of approach causes contribution from wheel forces in wider area as wheel exits plate.

Because of the asymmetrical nature of the data on the driver side plate (see Figure 27(a)), the passenger side plate data was analyzed instead. When analyzing the data, it was assumed that, due to symmetry, the frequency response data relating forces applied to the plate at various points and the responses measured by the sensor on the right hand side (outer side on passenger plate indicated in Figure 32) were equivalent to the frequency responses when the sensor on the left hand side of the plate was used (inner side on passenger plate indicated in Figure 32). The modal data was analyzed up to 60 Hz because the results in Figure 20 indicated that the majority of the diagnostic data content was in the frequency range below 60 Hz.

To gain an understanding of the variation in forced response of the passenger plate, the frequency response functions for forces applied at points 36, 35, 34, 33, 32, 31; points 30, 29, 28, 27, 26, 25; and points 24, 23, 22, 21, 20, 19 were plotted in Figure 34 (a-c). Note that in Figure 34(a) the frequency response on the edge of the plate at point 36 is small and then increases steadily as the force is moved from points 35 through 31. Then as the force moves from point 30 to point 25, the frequency response decreases. Then the frequency response again increases gradually as the force moves from points 24 to 19. If the measured spectra in Figure 20(b,d) are analyzed in light of these findings, it is evident that from 20-40 Hz where all of the changes due to the tire fault were observed, there are substantial changes in the frequency response function magnitude as the tire force moves from the front edge of the plate to the back edge of the plate in the diagnostic speed bump in this frequency range. Likewise, Figure 35 shows a comparison between these frequency response functions along the centerline (.....) of points and the frequency response functions along the inner line (____) of points on the passenger side plate. Note that frequency response functions along the centerline of points have lower magnitudes in general than those along the inner line of points. These differences will cause significant changes in amplitude of the measured signal in the frequency range from 20-40 Hz depending on the angle of approach as explained in Figure 33, especially as the wheel tracks towards the back edge of the plate (Figure 35(c)).

The changes in fault index as a function of angle of approach were also examined by subtracting the influence of the vehicle speed from the fault indices for the passenger side measurements corresponding to undamaged passenger front conditions, and plotting the fault index residual versus the angle of approach. Figure 36 shows this result, which indicates that there might be some modest correlation in the change in fault index with angle of approach. But the correlation is not at all strong.

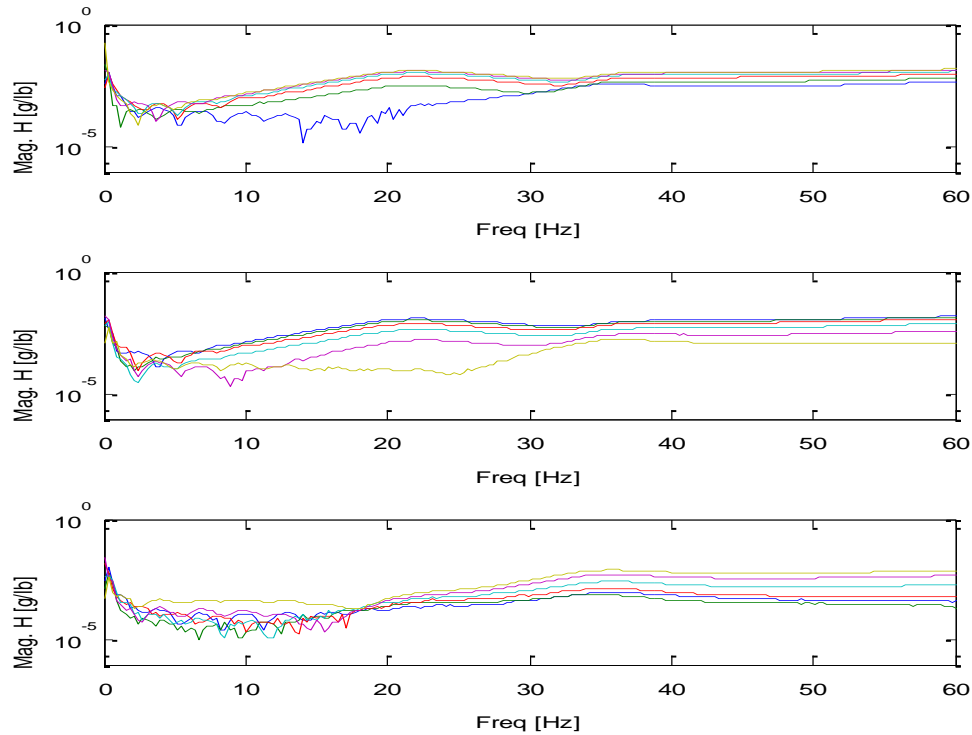


Figure 34: Frequency response function magnitudes for forces applied along centerline of passenger plate for (a) points 36-31, (b) points 30-25, and (c) points 24-19.

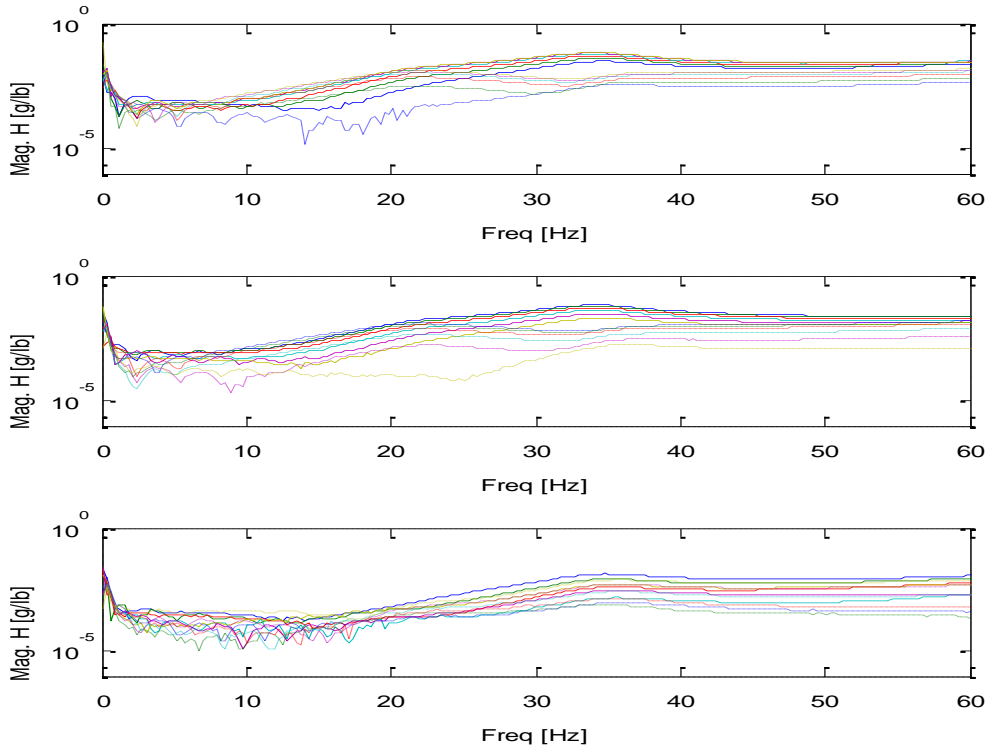


Figure 35: Frequency response function magnitudes for forces applied along (.....) centerline and inner line (____) of passenger plate for (a) points 36-31, (b) points 30-25, and (c) points 24-19.

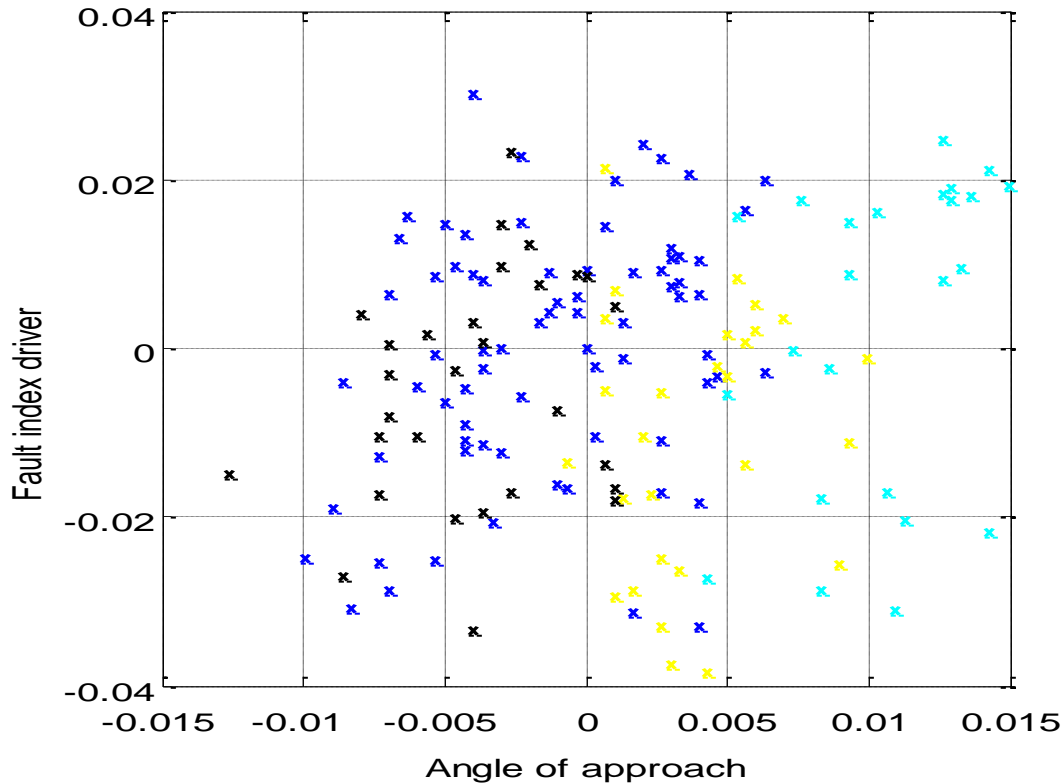


Figure 36: Fault index after subtracting changes due to variation in vehicle speed as a function of angle of approach for passenger side measurements for baseline (x), driver front tire fault (y), driver rear tire fault (z), and passenger rear tire fault (x) datasets.

Figures 32 and 33 indicated that the angle of approach taken by the vehicle as it crosses the extended diagnostic speed bump can lead to variations in the frequency response functions as shown in Figures 34 and 35. However, the result in Figure 36 indicates that there is not a strong correlation between the changes in the fault index and the angle of approach. Figure 37 is a plot of these same residual fault indices as a function of angle of approach along with a best quadratic curve fit. This plot clearly indicates that the correlation is weak between changes in angle of approach and the resulting changes in the fault index. It is, therefore, believed that there are other sources of variability that lead to the variations in the fault index from test to test that cannot be explained by the variations in speed as discussed in Section 3.3.

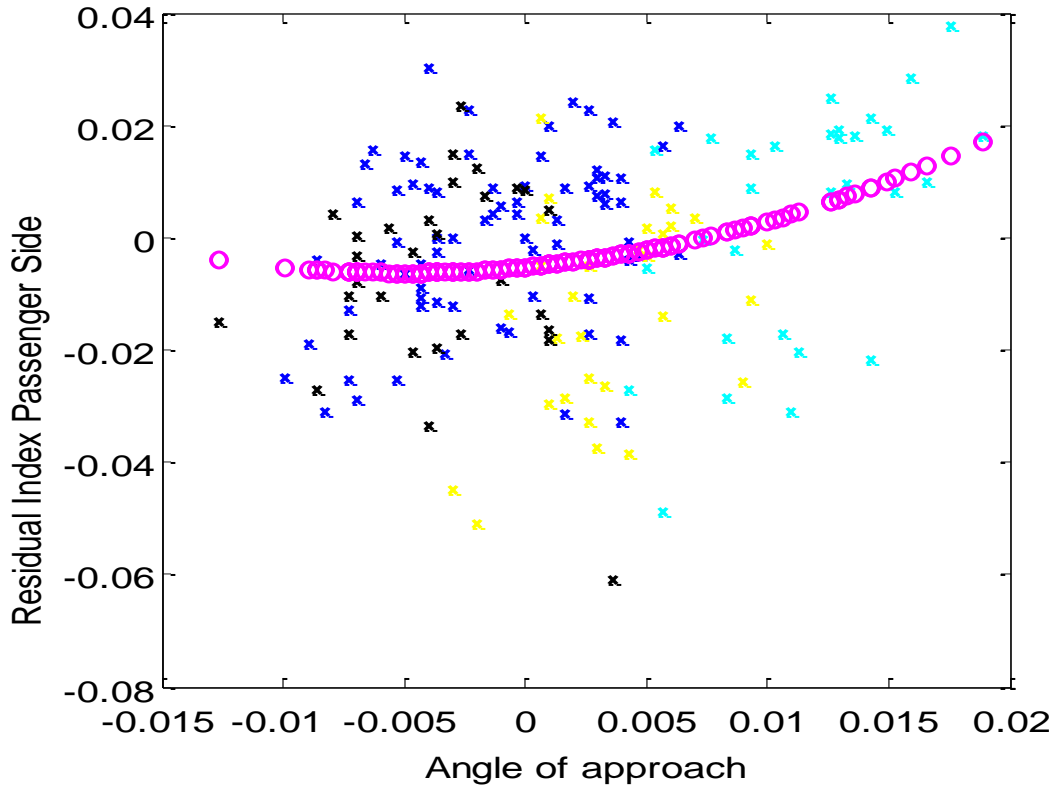
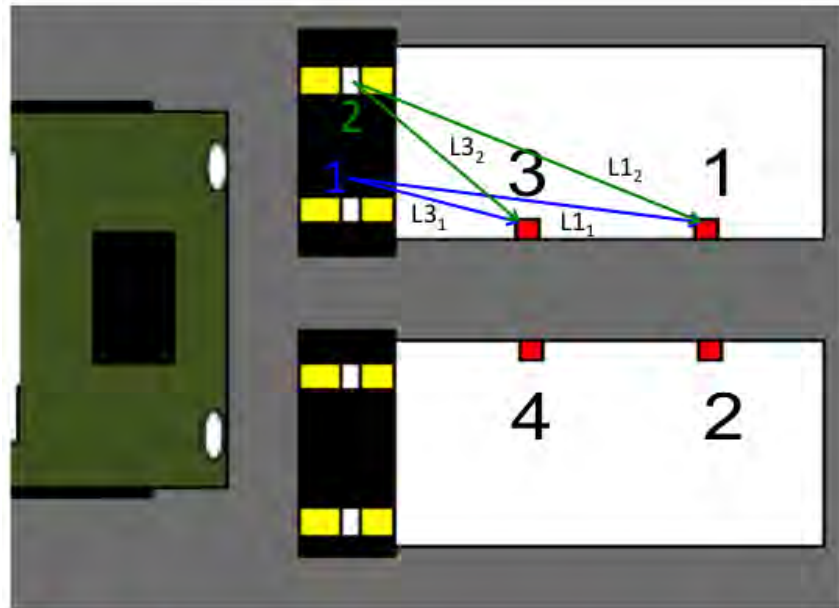


Figure 37: Fault index after subtracting changes due to variation in vehicle speed as a function of angle of approach for passenger side measurements along with quadratic curve fit.

Figure 38 illustrates another source of variability in the way in which the wheel of the vehicle traverses the diagnostic speed bump. In this figure, it is assumed that the drive front wheel can cross at point 1 on the speed bump or at point 2. Depending on where the wheel crosses the speed bump, the distance from that point to sensors 3 and 1 on the driver side plate changes. This difference leads to different delays in the responses measured by accelerometers 3 and 1. It is postulated that this difference in the measurement delay can potentially be used to further normalize the test data. Figure 39 shows the calculation of the distances, L_{3k} and L_{1k} , from a point k on the speed bump to accelerometers 3 and 1, respectively. Note that L_{1k} is always longer than L_{3k} but that the ratio L_{1k} / L_{3k} of these two distances becomes smaller as C_k increases, i.e., as the wheel crossing moves towards the upper edge of the plate. In the subsequent plots and analysis, the passenger side plate is considered due to the greater repeatability in the data that was found in previous analyses.



■ Accelerometers

Figure 38: Illustration of changes in path from tire crossing locations 1 and 2 to sensor degrees of freedom at accelerometers 1 and 3.

$$L3_k = \sqrt{A^2 + C_k^2}$$

$$L1_k = \sqrt{B^2 + C_k^2}$$

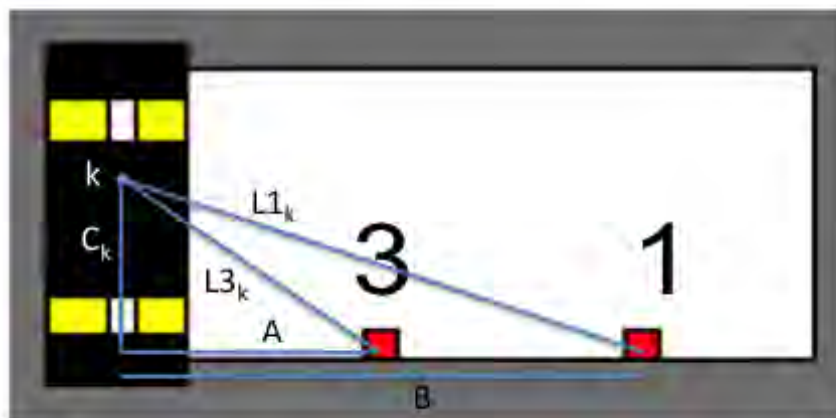


Figure 39: Calculation of distance from point k to accelerometers 3 and 1.

The potential correlation between the residual fault index and the phase differences in the measurements that were acquired by sensors at different distances from the forcing function on the plate were analyzed next. Figure 40(a) shows the spectral magnitudes for seven baseline datasets from channel 12 (sensor 4) on the passenger side plate of the extended diagnostic speed bump. It is evident that the data from the black, cyan (light blue), and yellow datasets are generally larger. Figure 40(b) shows the differences in phase in the measurements acquired at sensor 4 (channel 12) and sensor 2 (channel 6). Note that the phase differences that are largest, which indicate longer time delay between the measurements, correspond to the spectral magnitudes that are largest. The largest phase differences are associated with the wheel crossings that are nearest to the sensors as illustrated in Figure 39. This result suggests that the closer the wheel crossing is to the sensors (as indicated in Figure 39), the larger the residual amplitudes. It is also evident from these spectral magnitudes that the standard deviation in the measured response is largest for these wheel crossing locations closest to the sensors. Figure 41 shows additional results for twenty baseline datasets indicating similar findings to those in Figure 40.

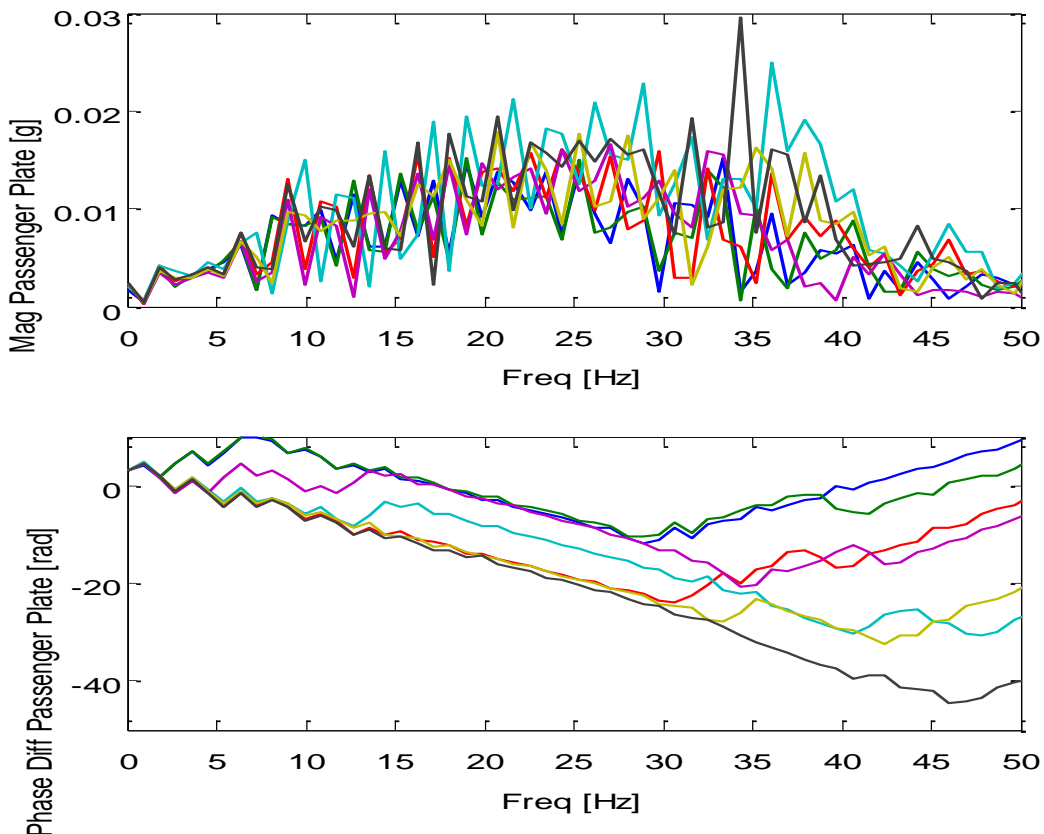


Figure 40: (a) Magnitude of response of channel 12 for sensor 4 on passenger side plate for seven baseline tests, and (b) corresponding difference in unwrapped phase between channels 12 and 6 (see Figure 39 for driver side plate sensor locations).

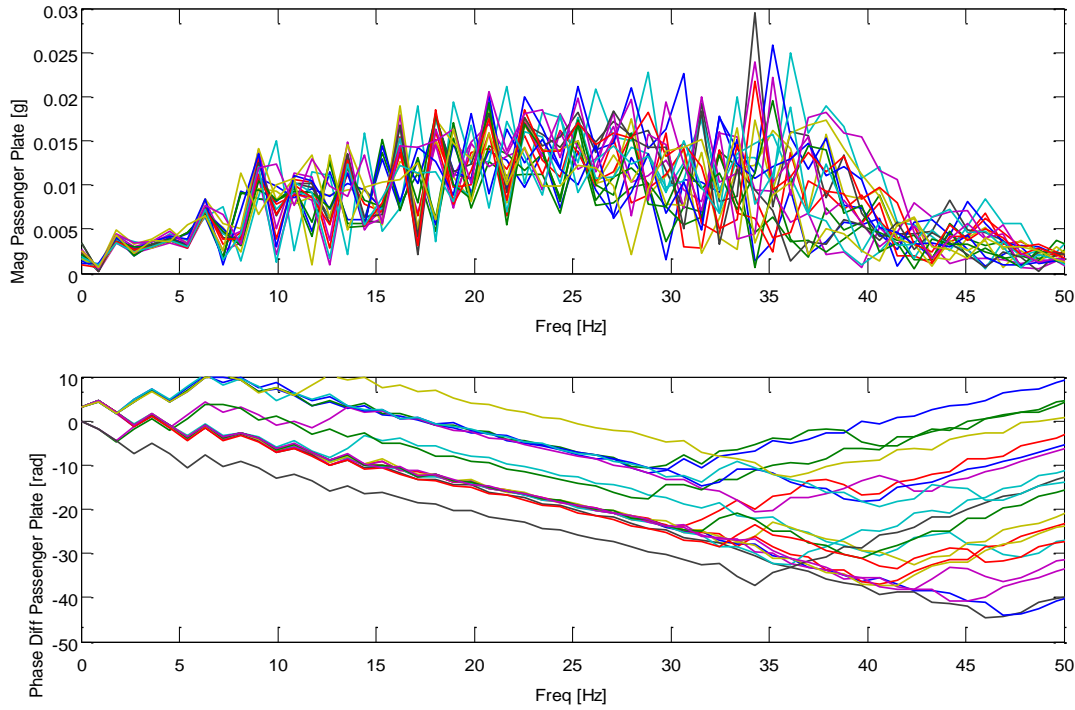


Figure 41: (a) Magnitude of response of channel 12 for sensor 4 on passenger side plate for twenty baseline tests, and (b) corresponding difference in unwrapped phase between channels 12 and 6 (see Figure 39 for driver side plate sensor locations).

The residual fault indices were then plotted in Figure 42 versus the average unwrapped phase difference from 0-45 Hz between channels 12 and 6 for the passenger side plate in the extended speed bump in the diagnostic frequency range. The absolute values of the fault indices were plotted because it was found that the fault indices were nearly symmetric about a fault index of zero. The quadratic (pink) and linear (red) curve fits were then applied to the residual fault indices for all of the baseline datasets for the passenger front wheel crossing. There are two important conclusions that can be drawn from this result. First, there is a strong correlation between the average phase difference in these two acceleration measurements and the residual fault index – larger (more negative) phase differences translate into larger residual fault indices. Second, larger phase differences also result in more deviation in the residual fault indices that are measured from test to test. Therefore, the summary conclusion is that the phase difference in the measurements should be minimized to reduce the variability in the diagnostic speed bump measurement. To reduce the phase difference, the wheel should track further away from the sensors (e.g., close to point 2 than point 1 in Figure 38).

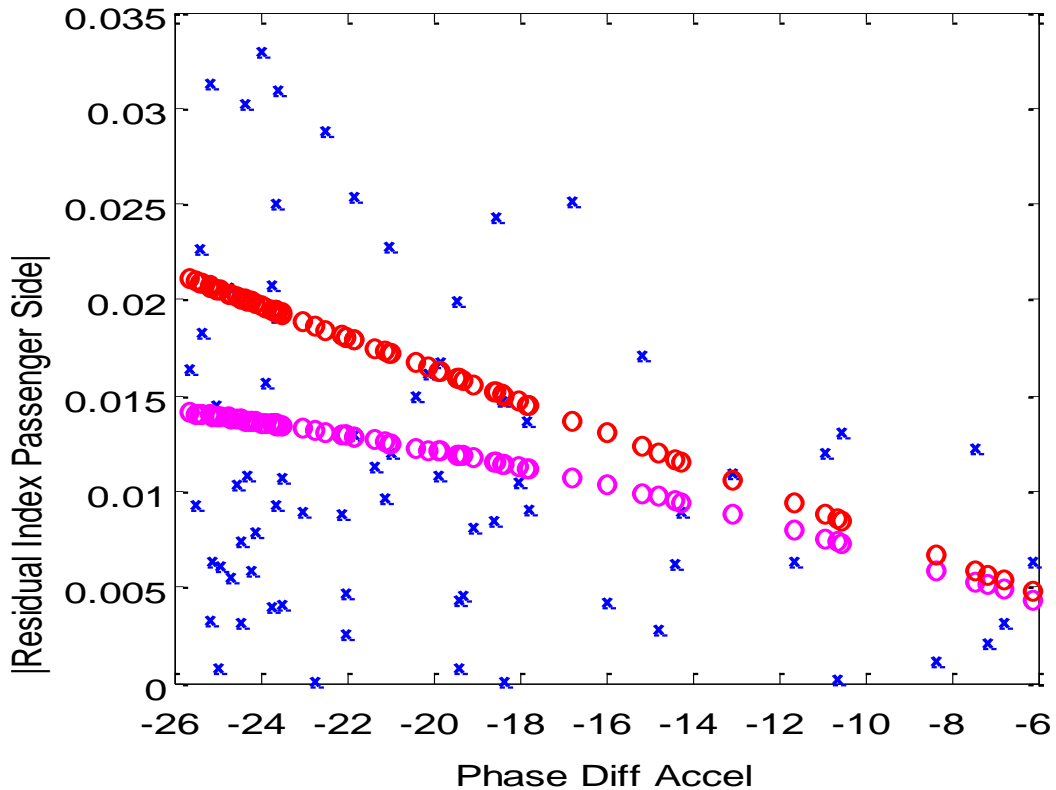


Figure 42: Absolute value of fault index after subtracting changes due to variation in vehicle speed as a function of mean difference in unwrapped phase from 0-45 Hz in channels 6 and 12 for passenger side data along with quadratic and linear curve fits.

3.7 Dynamic analysis of diagnostic speed bump

Figure 43 shows a simulated forcing function that was used to study the forced response of the plate due to the tracking motion of the tire. This force centered around 20 Hz was assumed to translate over the plate along the centerline as pictured in Figure 33; in other words, the tire was assumed to start at point 36 and end at point 19. In order to apply this force to the plate using the measured frequency response functions, the force was decomposed using a series of translating boxcar windows as illustrated in Figure 44. This series of plots represents the first five decompositions of the force into forces components that act one after the other at points 36, 35, 34, 33, and 32 in Figure 33.

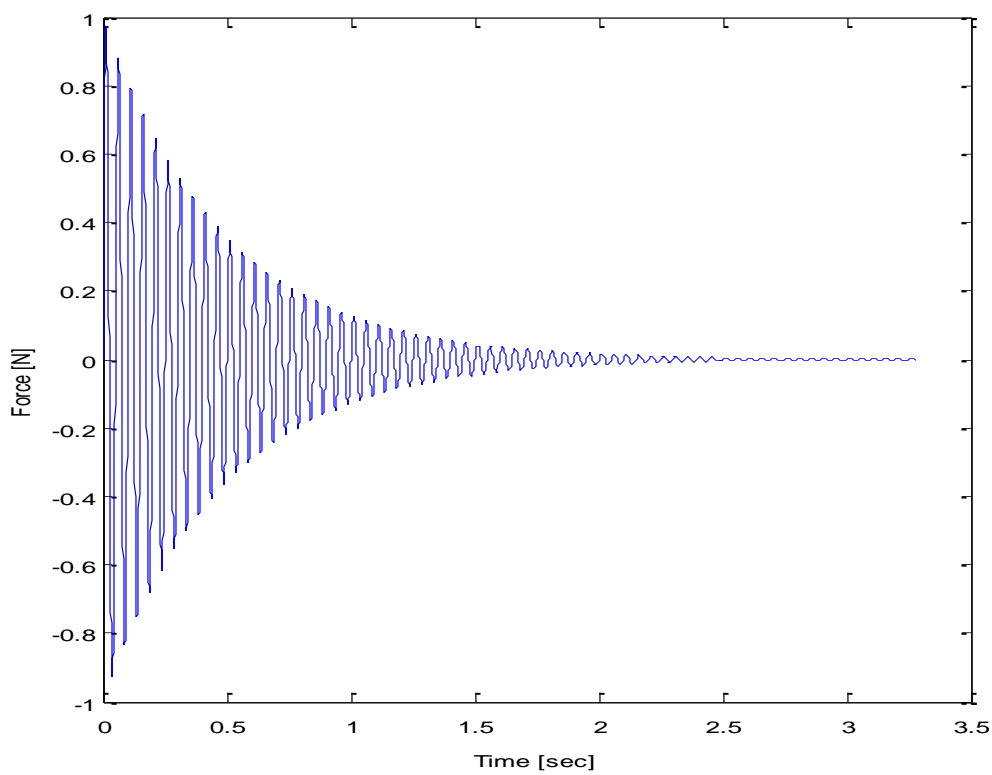


Figure 43: Simulated forcing function due to tracking of tire along plate.

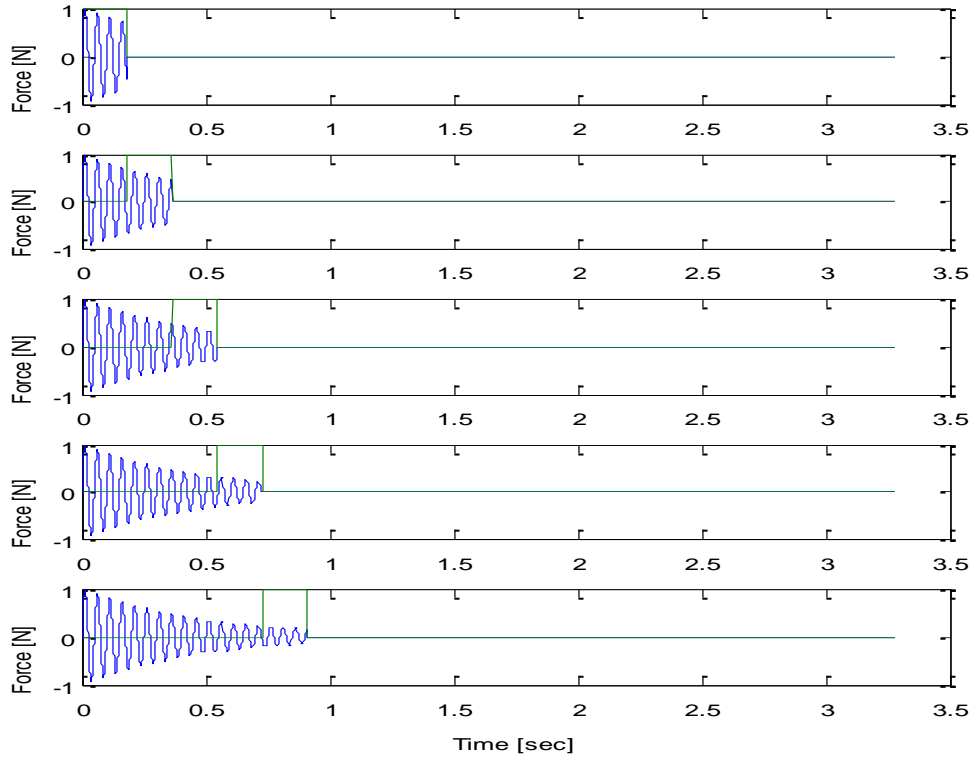


Figure 44: Summation of force components created using a translating boxcar window that moves at a speed equal to the vehicle speed along the plate.

In order to develop a dynamic model of the plate's forced response due to this translating force by the tire, the mathematical representation of the forcing function that was used to generate Figure 43 is given by,

$$f(t) = e^{-\frac{t}{\tau}} \sin(\omega t) \quad (1)$$

where the time constant and frequency were selected arbitrarily. It is desired to measure the variations in this forcing function due to faults using the diagnostic speed bump as a measurement system. This force was then decomposed as shown in Figure 44. Mathematically, this decomposition of the force can be expressed as follows:

$$f(t) = \sum_{b=1}^{18} w(t-t_b) f_b(t) = \sum_{b=1}^{18} f_b(t) \text{ where } t_b = (b-1) \frac{L}{18V} \quad (2)$$

where V is the vehicle speed, L is the plate length, and the sliding boxcar window is given by,

□

$$w(t) = u_s(t) - u_s\left(t - \frac{L}{18V}\right) \quad (3)$$

where $u_s(t)$ is the step function. The time delay, $L/18V$, represents the time it takes for the tire to travel from one point to another along the centerline in the schematic shown in Figure 33. \square

Each of the decomposed force components, $f_b(t)$, in Eq. (2) was then transformed into the frequency domain, and these forces were multiplied by the respective frequency response functions shown in 34(a-c) to produce the responses to each of these decomposed forces. These responses were then summed to produce the total measured response at the sensor:

$$\begin{aligned} A(\omega) &= \sum_{b=1}^{18} H_{a,b}(\omega) F_b(\omega) \\ &= \sum_{b=1}^{18} H_{a,b}(\omega) [W_b(\omega) * F(\omega)] \\ &= \sum_{b=1}^{18} H_{a,b}(\omega) W_b(\omega) * F(\omega) \\ &= \left[\sum_{b=1}^{18} H_{a,b}(\omega) W_b(\omega) \right] * F(\omega) \end{aligned} \quad (4)$$

where $W_b(\omega) = \frac{e^{-j\omega(b-1)\frac{L}{18V}} - e^{-j\omega b \frac{L}{18V}}}{j\omega}$

where $H_{a,b}(\omega)$ denotes the frequency response function between the points along the centerline of the plate in Figure 33 starting at point 36 and ending at point 19 and the response measured by the accelerometer, a , on the plate. $F_b(\omega)$ denotes the Fourier transform of each of the 18 decomposed force components in Eq. (2). The Fourier transform of the translating boxcar function is given in the third line of Eq. (4). The “**” symbol denotes the convolution of the frequency transform of the translating window function with the frequency transform of the forcing function imposed by the tire on the plate. \square

In Eq. (4), $H_{a,b}(\omega)$, $A(\omega)$, and $W_b(\omega)$ are known quantities based on the speed of the vehicle, the dimensions of the extended diagnostic speed bump, and the modal impact testing that was performed on the plates of the speed bump. Eq. (4) can also be expressed in the time domain as follows using multiplication as opposed to convolution:

$$a(t) = \left| \sum_{b=1}^{18} h_{w(a,b)}(t) \right| \times f(t) \quad (5)$$

\square

where the definition of the windowed impulse response function, $h_{w(a,b)}(t)$ is evident from the fourth row of Eq. (4). By inverting the expression in brackets, the forcing function from the tire can theoretically be recovered directly from Eq. (5).

It is evident in Eq. (4) that if the tire is tracking along a different line on the plate of the extended diagnostic speed bump, there will be a change in the measured acceleration even if the condition of the vehicle is the same. The goal of developing the model in Eq. (4) was to determine a method for normalizing the measured data to reduce this variability in the acceleration measurement. Based on the re-expression in Eq. (5), it appears that it may be possible to normalize the measured acceleration data in this manner.

3.8 Modeling of extended diagnostic speed bump

The findings that were presented in the previous sections were for the most part empirical in nature; therefore, a simulation model was developed to verify these findings. For example, one of the intents of this model was to verify that there are variations of the type observed experimentally in the frequency response of the plate within the extended diagnostic speed bump. Another intent of the model was to show that there is variation due to the crossing point of the tire on the cleat and that this variation is largest when the plate is positioned symmetrically with respect to the cleat. An illustration of the simulation model that was developed is shown in Figure 45.

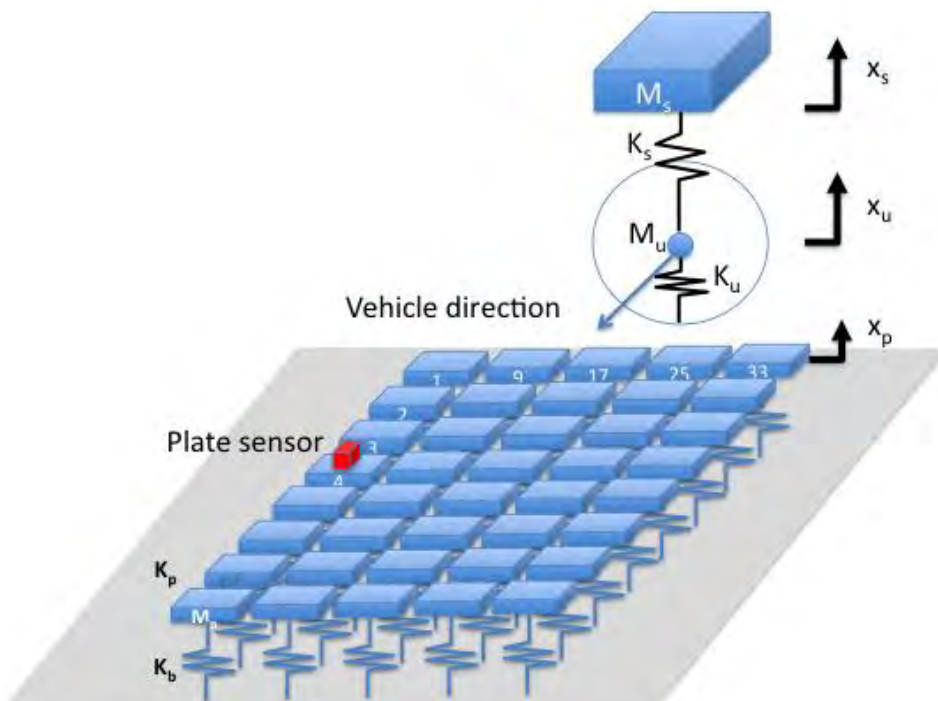


Figure 45: Dynamic model of extended diagnostic cleat plate placed on the driver or passenger side of the vehicle.

The plate is modeled as a network of coupled translational degrees of freedom resting on an elastic foundation. The passenger or driver side of the vehicle is modeled as a quarter car with sprung and unsprung masses, which are supported by tire and suspension springs. The vehicle moves across the plate after it has encountered the cleat in the simulation. The cleat introduces initial conditions of the sprung and unsprung masses and then, as the quarter car translates across the plate, initial conditions are passed from one time sequence in the simulation to the next sequence. It is assumed that the sensor is placed on the plate on degree of freedom 4.

The first set of analysis results that were obtained using this model consisted of the frequency response functions relating the forces applied at various points along the plate to the acceleration measured by the sensor. The centerline of points along the plate model were considered first (points 17 through 24). The frequency response functions corresponding to forces applied in three consecutive set of points along this centerline are plotted in Figure 46 (a) points 17-19, (b) 20-21, and (c) 22-24. Although the magnitudes are not identical to the measured magnitudes in Figure 34, the trends in the experimental and simulation frequency response functions along the centerline of the plate are similar. That is, forcing functions on the edges of the plate produce larger measured response accelerations than forces at the center of the plate. Also, the experimental and simulation frequency response function magnitudes both exhibit a peak just above 0 Hz. This peak corresponds to the rigid body modal deflection shape of the plate resting on the elastic foundation. The simulated rigid body mode of the plate is much more lightly damped than was found in the experimental data. This difference will result in a lightly damped oscillation of the measured acceleration on the plate.

The second set of analysis results compared the frequency response functions for forces applied along the centerline of points to the functions for forces applied along the inner line of points. Figure 47 shows the comparison of these two sets of frequency response functions. Note that these results are qualitatively similar to the results in Figure 35 for the experimentally measured frequency response functions. The inner line of points exhibit smaller magnitude frequency response functions across most of the frequency range in both the simulated and experimental frequency response functions.

The third set of analysis results for the simulation model consisted of the modal deflection shapes of the plate model. Figures 48 through 51 show the modal deflection shapes for the first four modes of vibration of the plate. These figures show some agreement with the experimentally measured modes shapes in Figures 28 through 31. But it is clear that the boundary condition of the plate in the experimental setup is not a uniform elastic foundation as simulated in Figure 45. Despite these discrepancies between the experimental and theoretical modal deflection shapes, the simulation model will be utilized to study the forced response due to the moving quarter car excitation in subsequent sections.

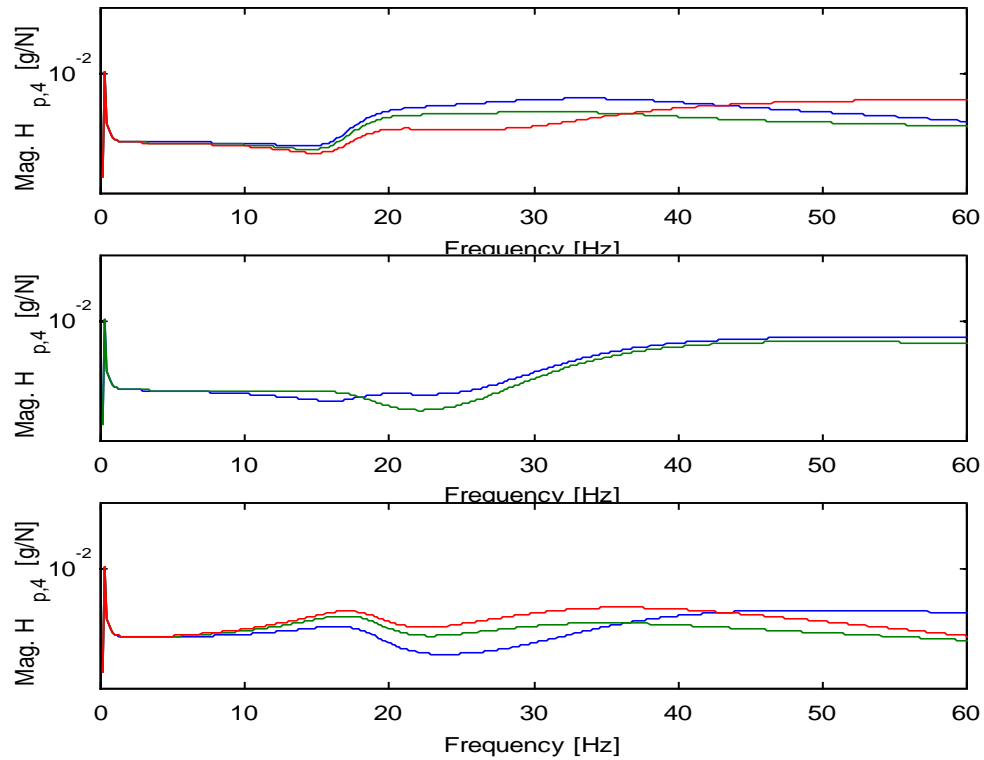


Figure 46: Frequency response function magnitudes for forces applied along centerline of plate in Figure 45 for (a) points 17-19, (b) 20-21, and (b) points 22-24.

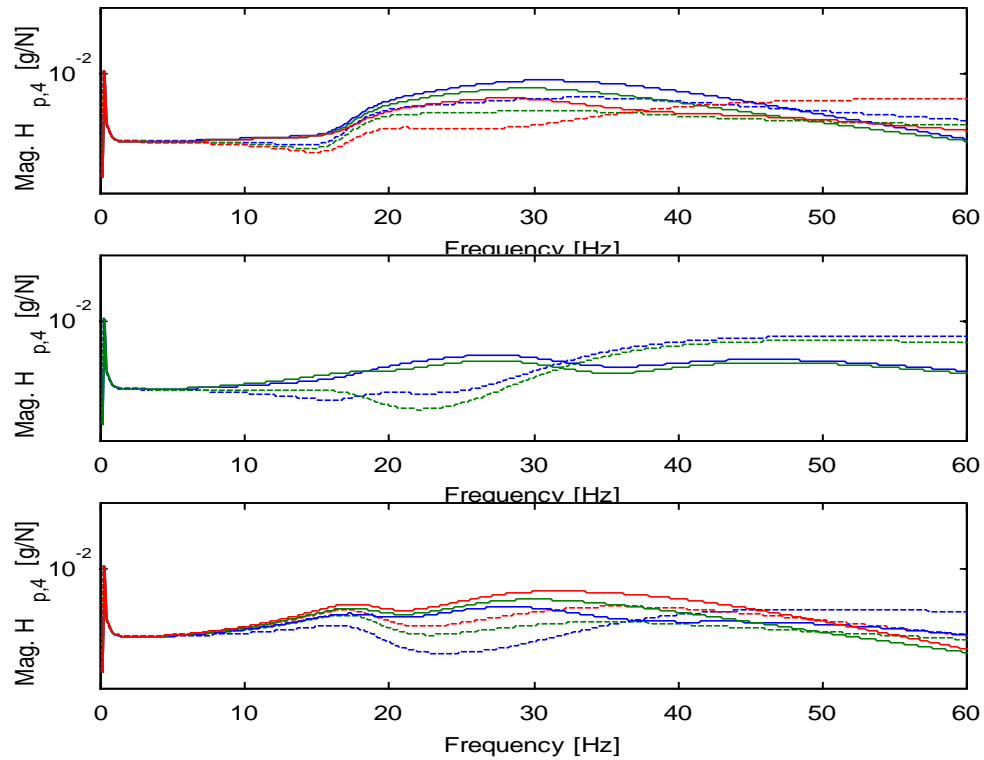


Figure 47: Frequency response function magnitudes for forces applied along (.....) centerline and inner line (____) of passenger plate for (a) points 17-19 (33-35), (b) points 20-21 (36-37), and (c) points 22-24 (38-40).

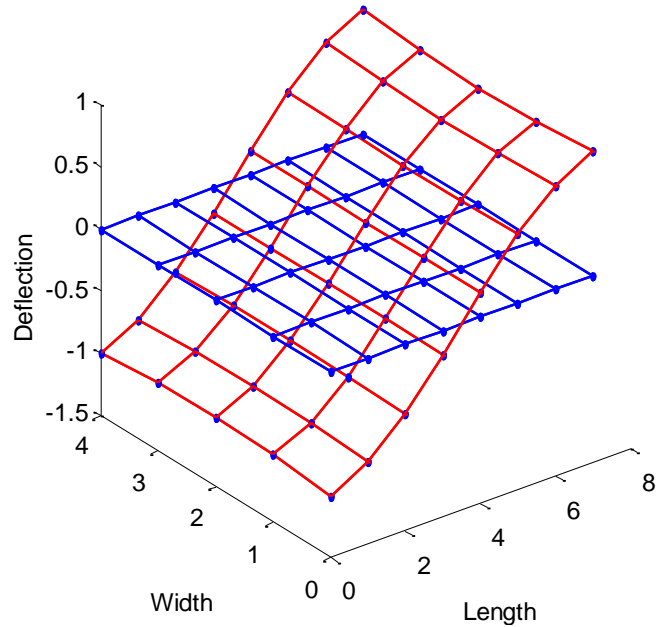


Figure 48: Plate modal deflection shape at 18.1 Hz.

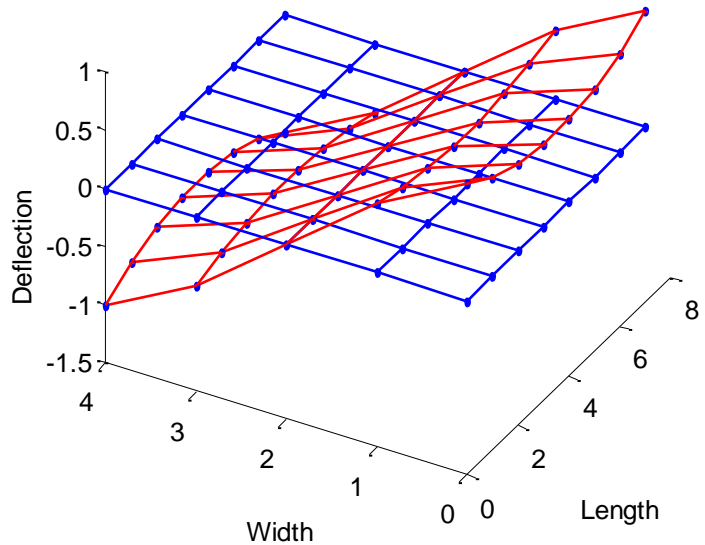


Figure 49: Plate modal deflection shape at 29.4 Hz.

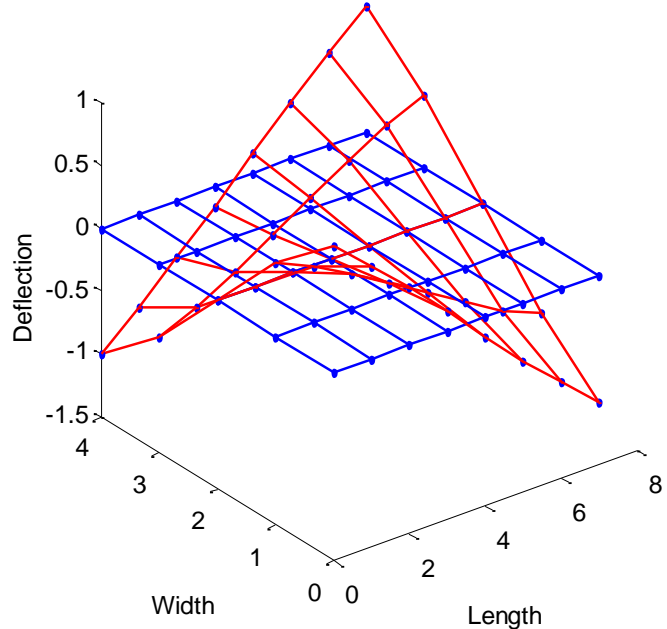


Figure 50: Plate modal deflection shape at 32.2 Hz.

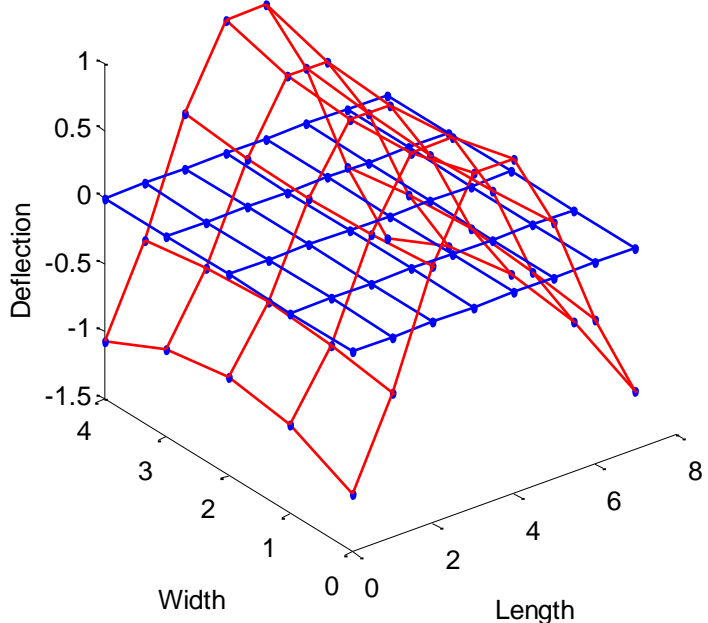


Figure 51: Plate modal deflection shape at 35.4 Hz.

3.9 Simulation of extended diagnostic speed bump

The model that was developed in Section 3.8 was used in this section to simulate the response of the extended diagnostic speed bump for various types of faults in the quarter-car model. The goal of these simulations was to better understand the variability in measurements due to variability in vehicle operating conditions such as the crossing point on cleat, speed, and payload of the vehicle. The initial simulations assumed that there were no dynamic interactions between the plate in the model and the quarter car that traverses the plate. It was also assumed that moving weight of the wheel had no effect on the dynamic response of the plate in the initial simulations; however, this assumption will be lifted in later simulations to examine the effects of changes in vehicle payload.

The simulation was run assuming a vehicle speed of 5 mph with the plate initial conditions equal to zero (zero displacement and velocity across the 40 degrees of freedom of the plate). The parameters in the quarter car model and plate model are given in the appendix in the Matlab source code. In this first set of simulations, the force imposed by the tire on the plate was assumed to transition instantaneously from one degree of freedom to the next on the plate model in Figure 45. In other words, a sliding boxcar window was applied to the forcing function in the tire to move that forcing function along the plate surface as the quarter car traverses the simulated diagnostic cleat.

Figure 52 shows the baseline response of the measured displacement at degree of freedom 4 in the plate model (blue curve), the force in the quarter car tire as it traversed the plate (green curve), and the acceleration (obtained through numerical integration) of degree of freedom 4 of the plate model (red dashed curve). This simulation result led to several interesting insights.

- First, the force (in green) exhibited two natural frequencies of vibration initially after it crossed the cleat and began to traverse the plate. The highest natural frequency was initially present but decayed quickly whereas the lowest natural frequency of the quarter car model persisted until the end of the plate. This result was consistent with the findings from the extended diagnostic cleat experimental data.
- Second, although the displacement (in blue) did not follow this force time history, the acceleration (in red) at degree of freedom 4 did follow the force time history reasonable well. The additional frequency components in the plate acceleration response were at higher frequencies of vibration. This result indicated that the acceleration of the plate was a good measure of the force in the tire of the vehicle.
- Third, the frequency spectrum of the acceleration response in Figure 53 also resembled the force spectrum fairly well. Specifically, the two resonant frequencies in the quarter car model were evident in the acceleration spectrum. However, the acceleration spectrum also exhibited frequency content above the second resonant frequency due in part to signal processing leakage (since the time history does not die out by the end of the time window in Figure 52) and the technique that was used to move the forcing function from one degree of freedom to the next on the plate model.

To attempt to reduce these effects on the acceleration spectrum due to the movement of the forcing function from one degree of freedom to the next, a Hanning window was used to smooth out this transition of the force between the degrees of freedom. Figure 54 shows the corresponding time histories that were obtained in these simulations and Figure 55 shows the spectral amplitude plots. Note that there are still frequency components at frequencies other than the resonant frequencies of the quarter car.

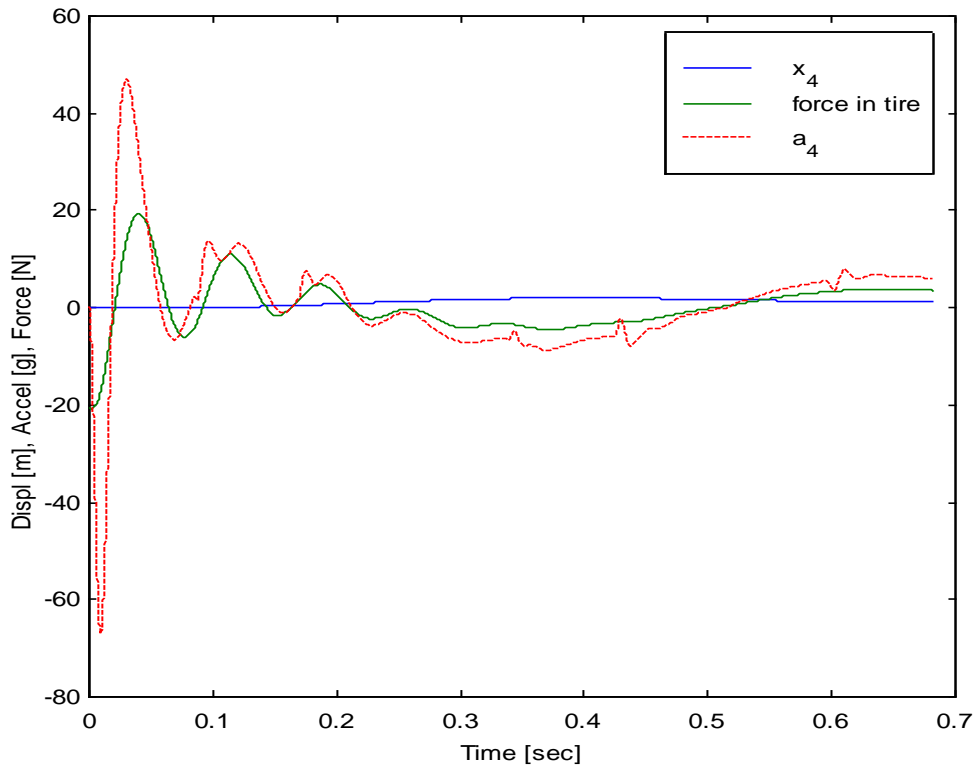


Figure 52: Response time histories of the plate displacement (—), tire force (—), and acceleration (---) using boxcar window to transition force between degrees of freedom.

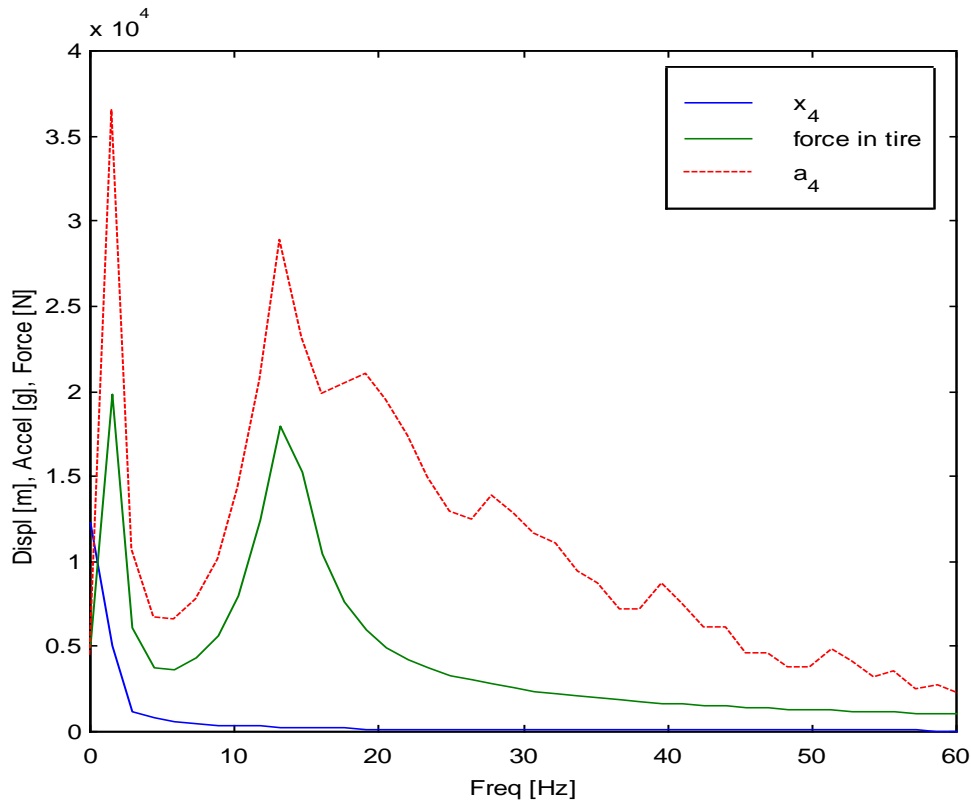


Figure 53: Response spectra of the plate displacement (), tire force (), and acceleration (- -) using boxcar window to transition force between degrees of freedom.

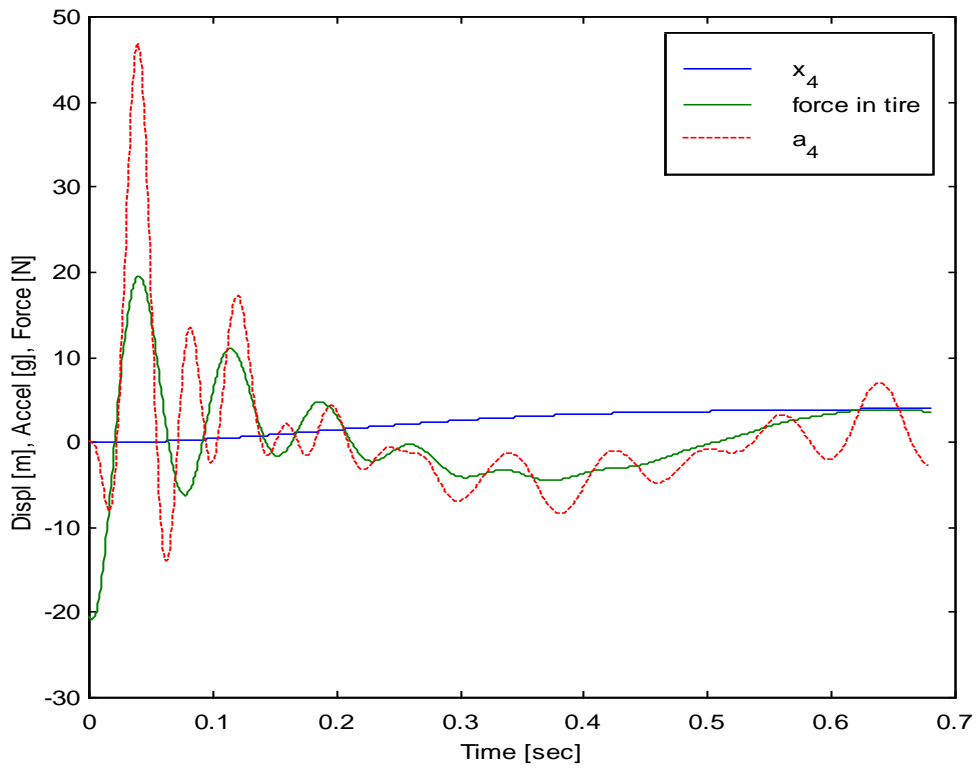


Figure 54: Response time histories of the plate displacement (____), tire force (____), and acceleration (- - -) using Hanning window to transition force between degrees of freedom.

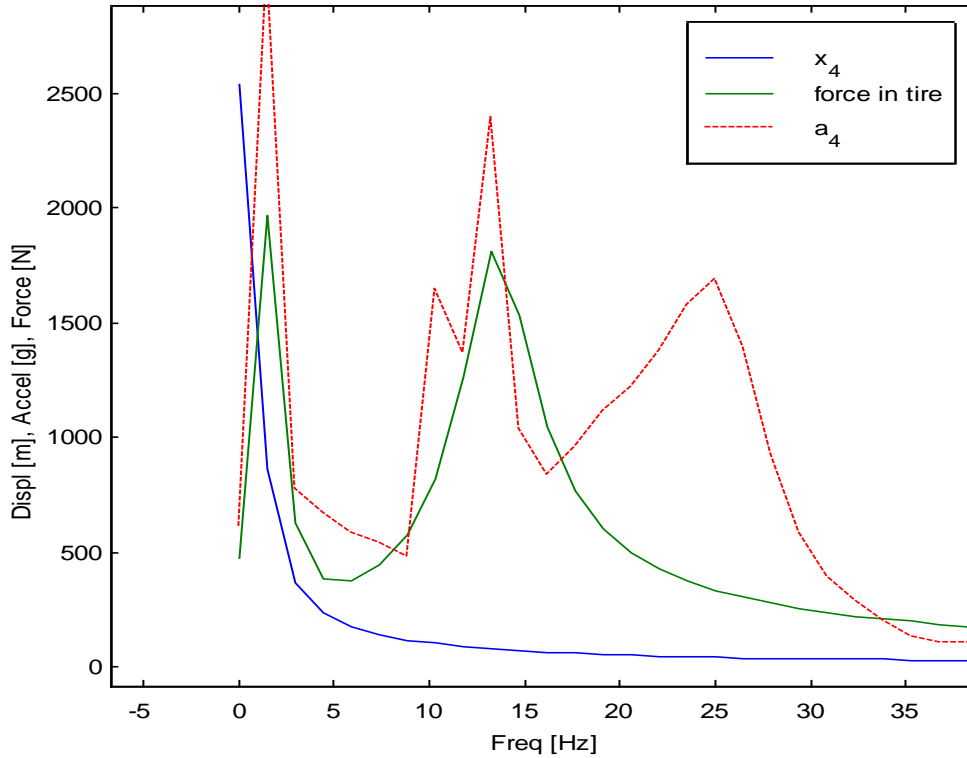


Figure 55: Response spectra of the plate displacement (____), tire force (____), and acceleration (- - -) using Hanning window to transition force between degrees of freedom.

To better understand the frequency content of the acceleration spectrum that was obtained for the extended diagnostic cleat plate model, the force time history in the tire was plotted together with the sliding force time history using a boxcar window (Figure 56(a)) and a Hanning window (Figure 57(a)). Note that the contiguous force time histories that were windowed with the sliding boxcar function in Figure 56(a) were identical to the actual force imposed by the tire on the plate; however, these contiguous time histories had sharp discontinuities each time the tire moved from one degree of freedom to the next degree of freedom on the plate. In contrast, the contiguous set of windowed force time histories using the Hanning window in Figure 57(a) did not exhibit discontinuities; however, the windowed series of force time histories did not exactly match the actual force time history imposed by the vehicle on the plate using the Hanning window.

The force spectra corresponding to the time domain functions are shown in Figures 56(b) and 57(b). Note that the spectra generated using the series of sliding box car windows produced a peak initially at the second mode of the quarter car model and then the energy in the spectra shifted towards the first mode of the model as time increased. Also note that the spectra that were initially produced by the first windowed force produced ripples that caused similar ripples in the measured response on the plate (see Figure 53). The

link between the force spectra using the Hanning window in Figure 57(b) and the measured response of the plate in Figure 55 was not as evident based on this analysis.

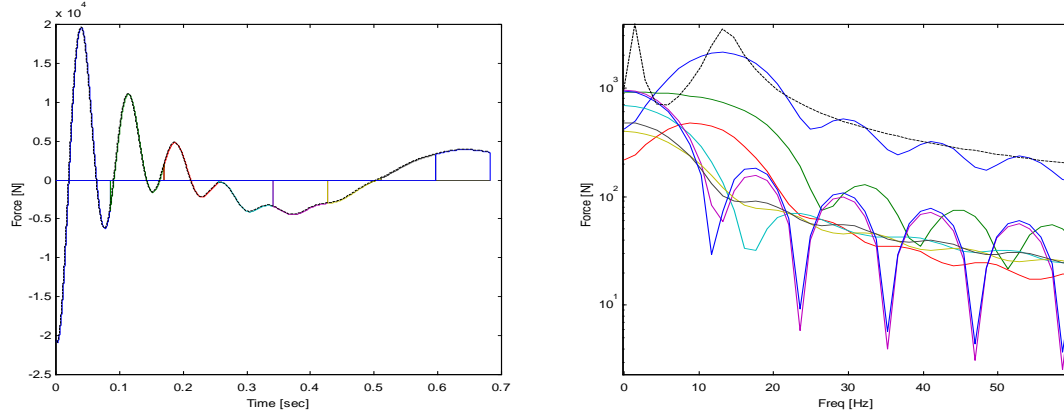


Figure 56: (a) Force time history from quarter car model (---) and windowed force time history using series of eight boxcar windows that slide along the time history, and (b) corresponding frequency spectra for original force (---) and windowed forces.

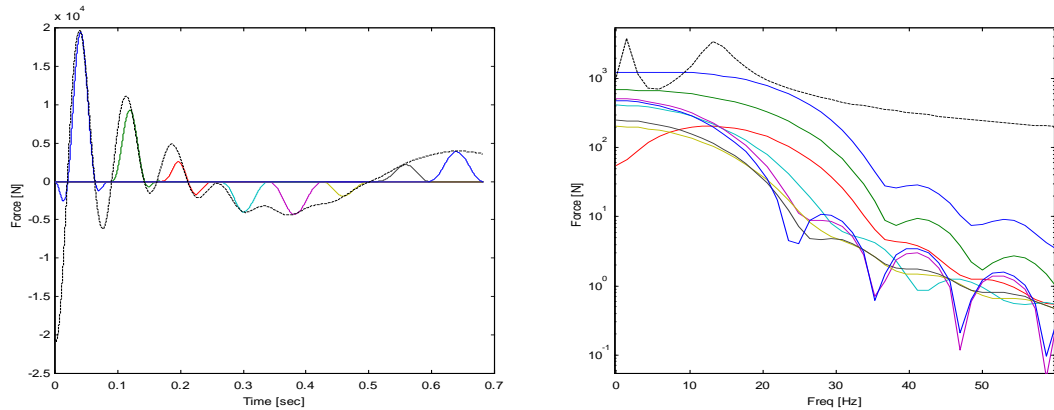


Figure 57: (a) Force time history from quarter car model (---) and windowed force time history using series of eight Hanning windows that slide along the time history, and (b) corresponding frequency spectra for original force (---) and windowed forces.

The analysis above did not reveal any significant insights into how the effects of the sliding window selection could be minimized in the simulation results. Therefore, a series of simulations was conducted using both the boxcar and Hanning window types. The simulations were conducted over a range of quarter car vehicle speeds from 4 to 7 mph. The results of the simulations are plotted in Figures 58(a,b) for the boxcar window and Figures 58(c,d) for the Hanning window. The force spectrum in the wheel of the quarter car is plotted in both Figures 58(a) and (c) for reference. This force spectrum indicated that more energy was delivered to the higher frequency range of the quarter car as the vehicle traveled more quickly over the simulated speed bump as expected. The second mode of vibration of the quarter car, consequently, responded with greater amplitude for greater vehicle speed. Interestingly, the sprung mass resonance (first mode of vibration) did not exhibit an appreciable change in amplitude when the speed of the vehicle increased.

Note that below 20 Hz, the boxcar window led to a plate response in Figure 58(b) that was very similar to the actual quarter car force in Figure 58(a). However, the Hanning window response led to a plate response in Figure 58(d) that was not at all similar to the force in the quarter car in Figure 58(c). This result suggested that the boxcar wind should be used to perform the simulations because it led to a plate response that was most similar to the force in the quarter car wheel.

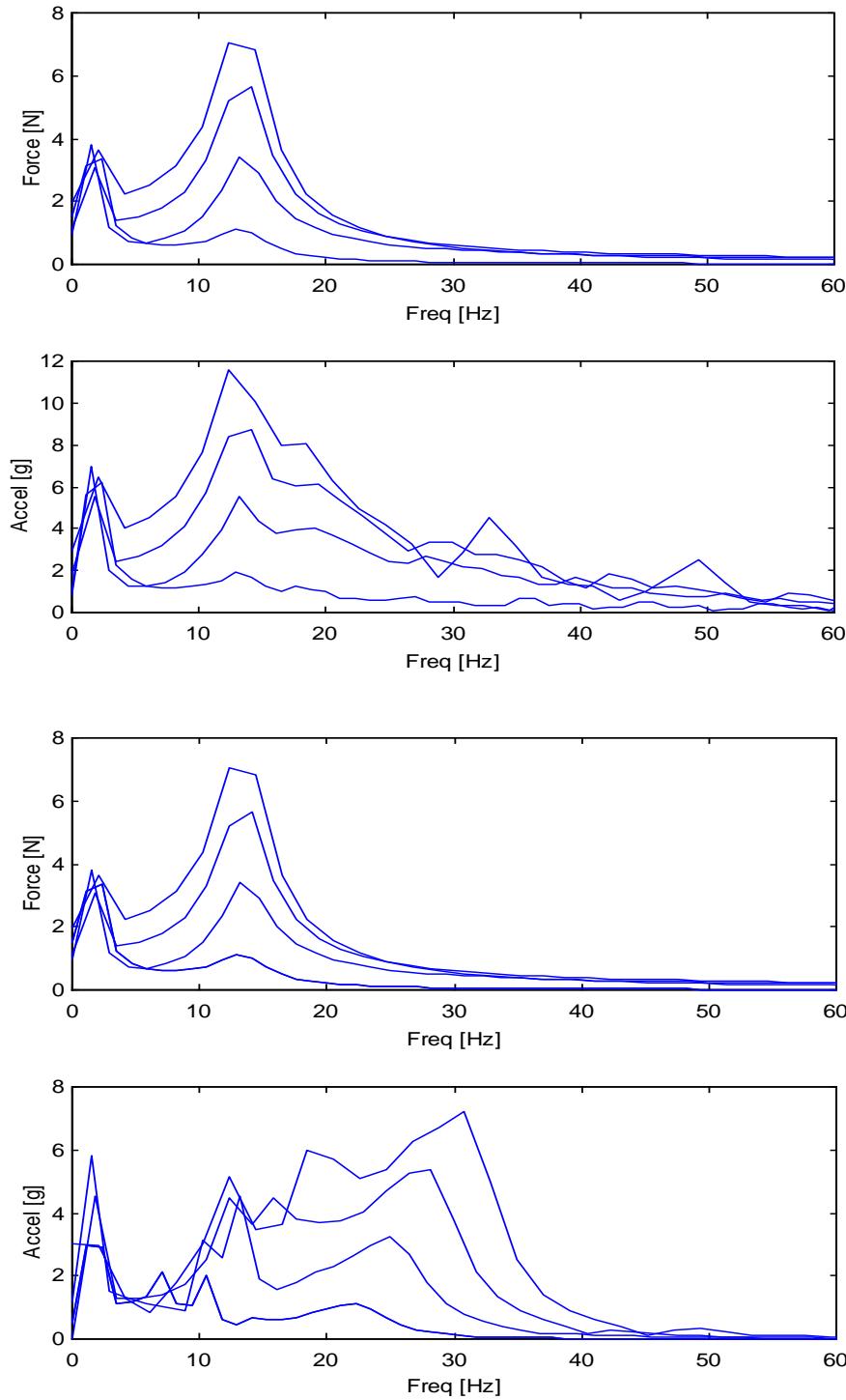


Figure 58: (a) Force spectrum from quarter car model for speeds ranging from 4 to 7 mph, (b) corresponding frequency spectra for plate accelerations using sliding boxcar window to apply the forcing function from the quarter car model to the plate, (c) (repeat) force spectrum from quarter car model for speeds ranging from 4 to 7 mph, and (d) corresponding frequency spectra for plate accelerations using sliding Hanning window to apply the forcing function from the quarter car model to the plate.

3.10 Simulation of faults in quarter car using extended cleat model

The model that was developed in Sections 3.8 and 3.9 was used in this section to simulate the effects of faults in the quarter car model on the resultant force in the wheel and measured acceleration on the plate.

First, the suspension stiffness was reduced to 95%, 90%, 80%, and 50% of the original stiffness and the wheel force and plate acceleration at degree of freedom 4 were plotted in Figures 39(a) and (b). The plots indicated that the second resonant frequency decreased as the stiffness decreased while the amplitude at the first resonance decreased and the amplitude of the second resonance increased. This result was expected because a decrease in stiffness of the suspension would result in less transfer of force to the plate near the first resonance but a greater transfer near the second resonance due to the lowering of that resonant frequency. For the closely spaced modes of vibration in the actual wheeled vehicle that has been tested, the net effect of this reduction in suspension stiffness was observed to be a reduction in the measured response amplitudes, which is consistent with this simulation result.

Second, the tire stiffness was reduced to 95%, 90%, 80%, and 50% of the original stiffness and the wheel force and plate acceleration at degree of freedom 4 were again plotted in Figures 39(c) and (d). The plots again indicated a reduction in the natural frequency of the second mode of vibration and a smaller but noticeable increase in that mode's of vibration resonant response amplitude. At other frequencies, the reduction in tire stiffness led to a reduction in the force amplitude that was transmitted and to which the plate responded as expected. This result was also consistent qualitatively with the experimental observations for reductions in tire air pressure.

The third and fourth fault simulations were conducted by reducing the damping in the suspension and then the damping in the tire. The results obtained for a reduction in the suspension damping were plotted in Figures 40(a) and (b), whereas the results for a reduction in the tire damping were plotted in Figures 40(c) and (d). For both of these cases where damping parameters in the quarter car were reduced, the amplitude of response increased because less damping resulted in greater forced response of the vehicle and, therefore, greater force transmitted to the plate. Assuming the experiments that were performed in the previous sections resulted in an increase in the amount of damping in the tire due to a decrease in the tire pressure, these simulation results in Figures 40(a-d) were also consistent with the experimental observations. This result was also interesting because it suggested that the force in the wheel and the subsequent response of the extended diagnostic cleat plate were most sensitive to changes in the stiffness of the tire and suspension. However, it should be noted that changes in damping were difficult to simulate because it was probably the case that the actual changes in damping in the experiments were nonlinear in nature but the simulations failed to capture these nonlinearities.

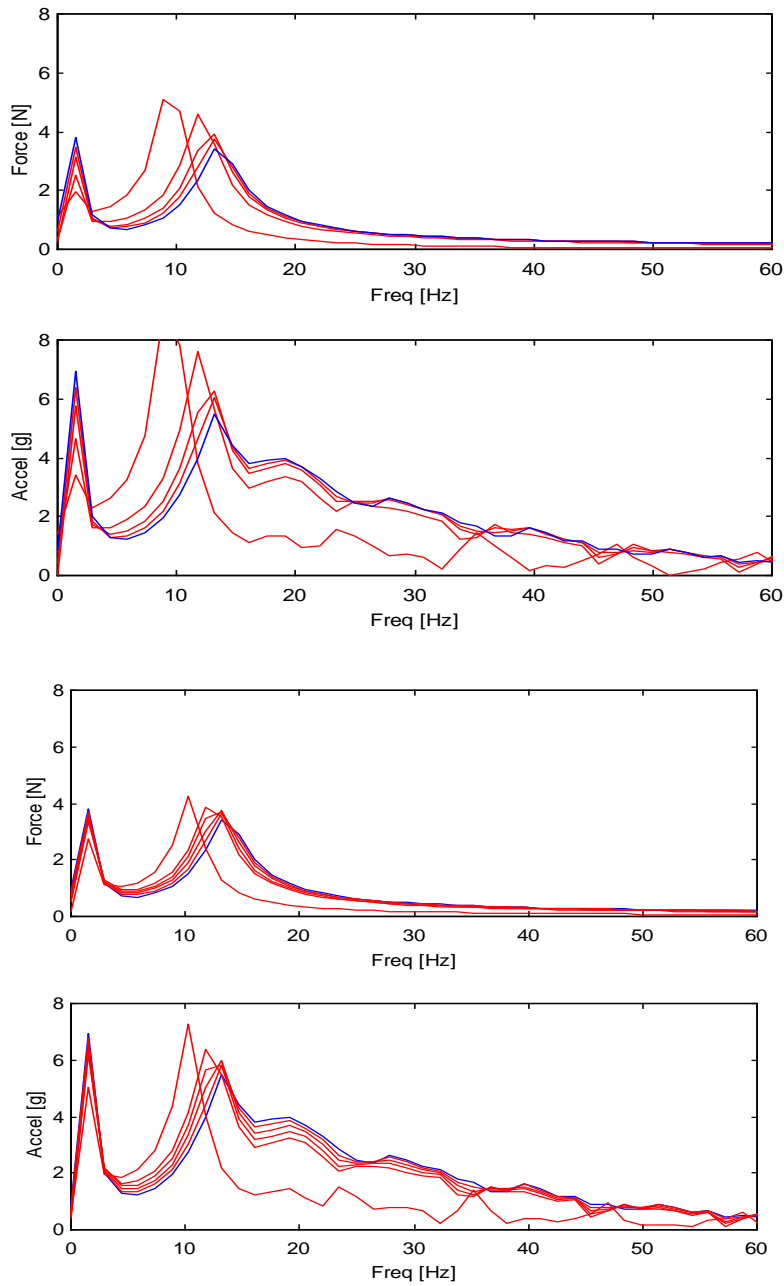


Figure 59: (a) Force spectrum from quarter car model with (—) 100% and (—) 95%, 85%, 80%, and 50% suspension stiffness, (b) corresponding frequency spectra to (a) for plate acceleration at degree of freedom four, (c) force spectrum from quarter car model with (—) 100% and (—) 95%, 85%, 80%, and 50% tire stiffness, and (d) corresponding frequency spectra to (c) for plate acceleration at degree of freedom four.

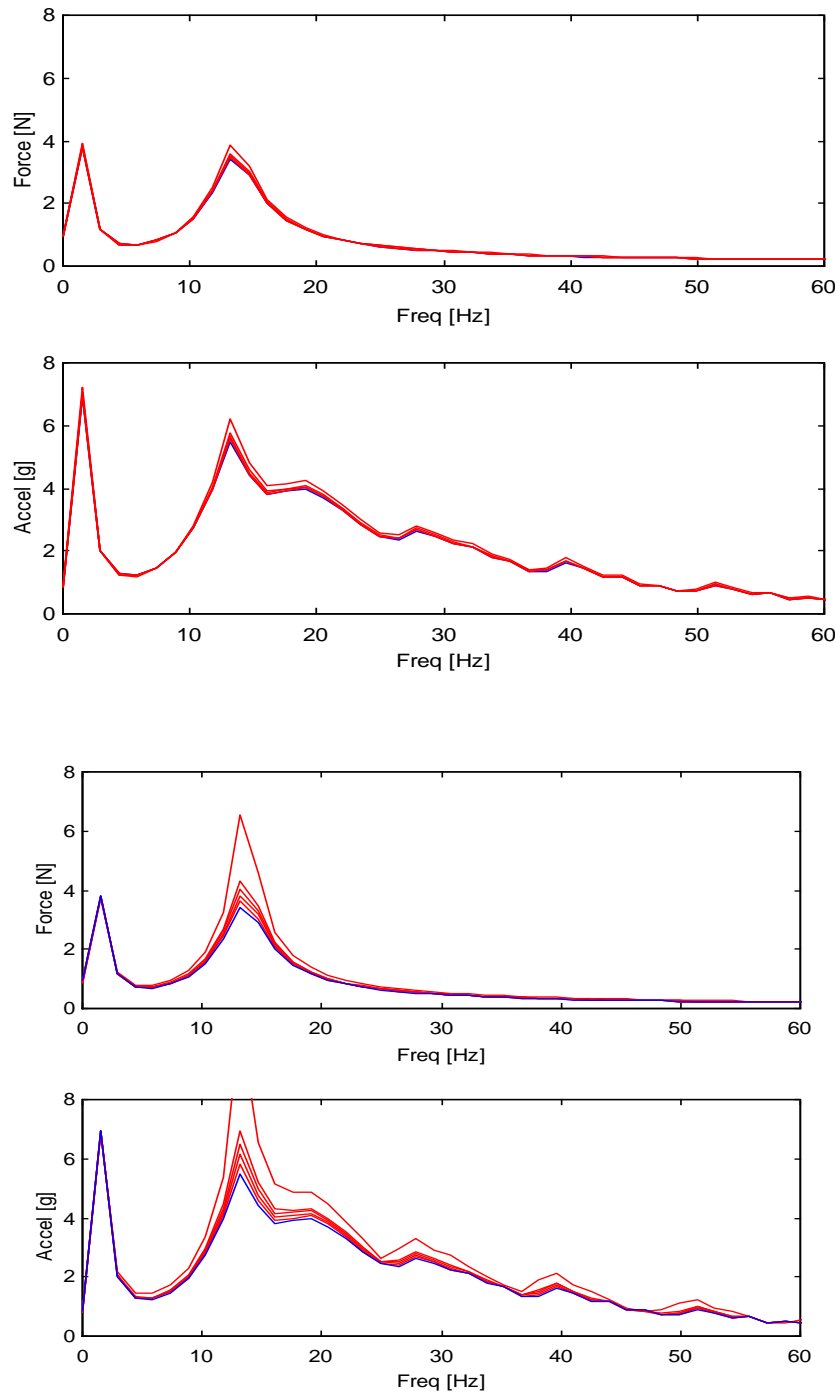


Figure 60: (a) Force spectrum from quarter car model with (—) 100% and (—) 95%, 85%, 80%, 75%, and 50% suspension damping, (b) corresponding frequency spectra to (a) for plate acceleration at degree of freedom four, (c) force spectrum from quarter car model with (—) 100% and (—) 95%, 85%, 80%, 75%, and 50% tire damping, and (d) corresponding frequency spectra to (c) for plate acceleration at degree of freedom four.

3.11 Simulation of changes in wheel crossing location using extended cleat model

The model that was developed in Sections 3.8 and 3.9 was used in this section to simulate the effects of changes in the wheel crossing location on the response of the plate in the extended diagnostic cleat. Recall that the crossing location is believed to have caused some of the variability that was observed in the experimental data. Based on Figure 42, it was determined that if the wheel tracks on the opposite side as the sensor was located on the plate of the extended diagnostic plate, there would be less variability introduced into the measurement. The goal of this section was to validate this hypothesis using the simulation model.

The plate response in the simulation model was calculated for a sensor positioned at degree of freedom four and the time response was transformed into the frequency domain. The simulation was carried out for a wheel position along the centerline of the plate model, along the left or right lines adjacent to the centerline of the plate, and along the left and right edges of the plate (see Figure 45). The lines left of center corresponded to locations on the plate on the side closest to the sensor degree of freedom. The lines right of center corresponded to location on the opposite side of the plate as the sensor degree of freedom. According to the hypothesis made using the experimental data, variation in the measured response of the plate for the wheel cracking locations right of center on the plate would be less than those left of center on the plate.

Figure 61(a) shows the acceleration spectra for these various simulations of the quarter car model in the baseline (healthy) condition. Figure 61(b) shows a close up view of the second peak in the acceleration spectra. The following conclusions be drawn based on these simulation results:

- There was very little change in the acceleration spectra near the first mode of vibration of the quarter car model as a function of the wheel crossing location on the diagnostic cleat. This trend was also observed in the experimental data from Figure 16 as illustrated in Figure 62, where more variation was observed above 5 Hz than below 5 Hz. This result together with the result in Figure 45 suggested that the quarter car model correctly captured the source of variability due to the wheel crossing location.
- As indicated in Figure 45, the quarter car model simulation also verified that a target crossing point of the wheel that was along the centerline of the plates in the extended diagnostic cleat led to inherently large variations in the measured response on the plate when the crossing point of the wheel deviated either to the left or right of center. This result suggested that the plates in the extended diagnostic cleat should indeed be placed in a manner that the centerline of the plate is offset from the centerline of the rubber cleat over which the wheel rolls.
- As indicated in Figure 61(b), the variations in the observed plate acceleration magnitudes were larger when the wheel rolls down the plate to the left of center (dashed arrows) than to the right of center (solid arrows). In other words, $L1 > R1$ and $L2 > R2$ in Figure 61(b). This result together with the result in Figure 45 suggested

that the quarter car model correctly captured the trends in variability as a function of the wheel crossing location on the extended diagnostic cleat.

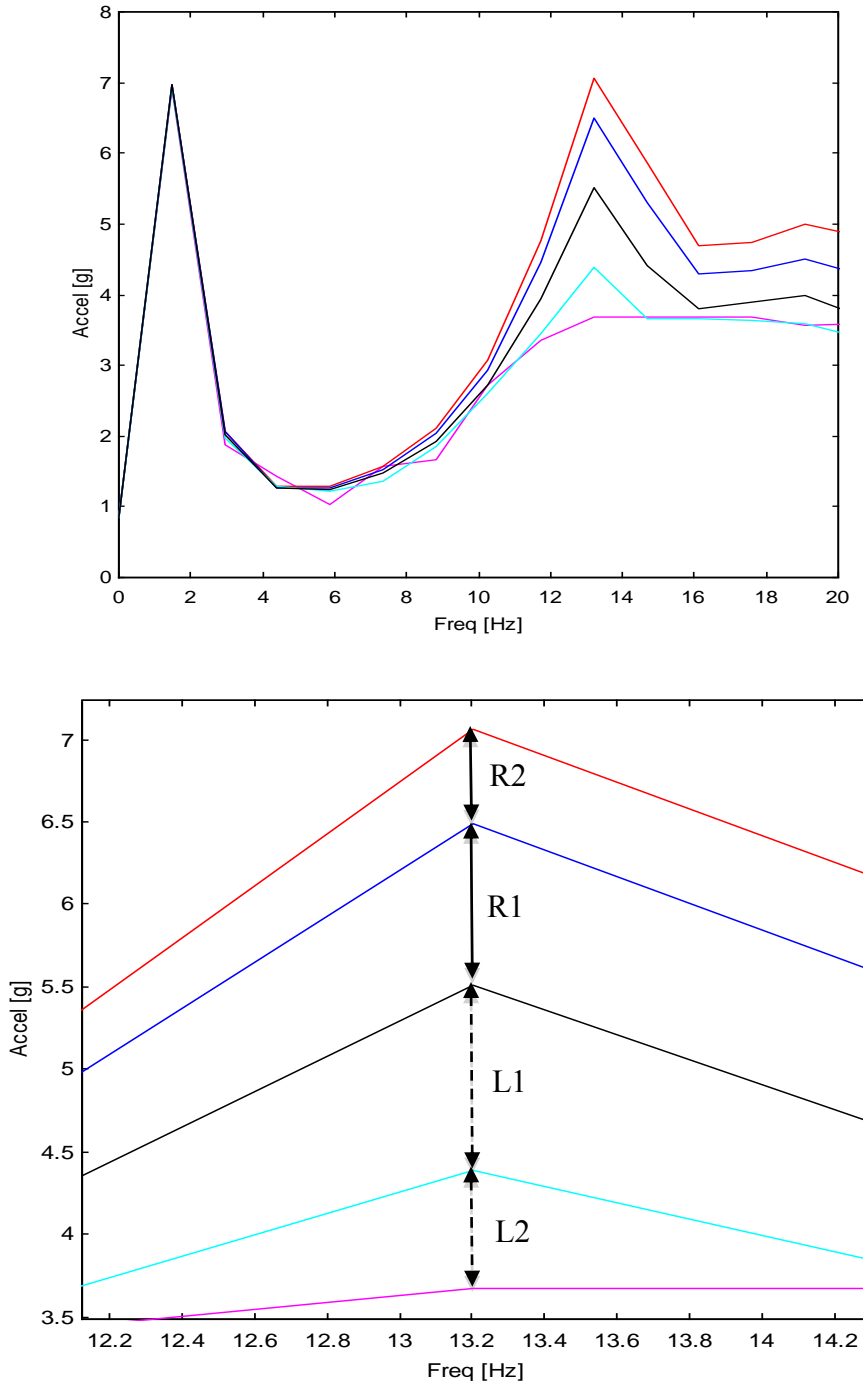


Figure 61: Frequency spectra for plate acceleration at degree of freedom four for wheel crossing location down center of plate (—), on right and left sides of center (—, —), and on right and left edges of plate (—, —) where crossing locations left of center are closer to the sensor on the plate: (a) 0 to 20 Hz, and (b) close up of second peak showing differences in amplitude for different wheel crossing locations.

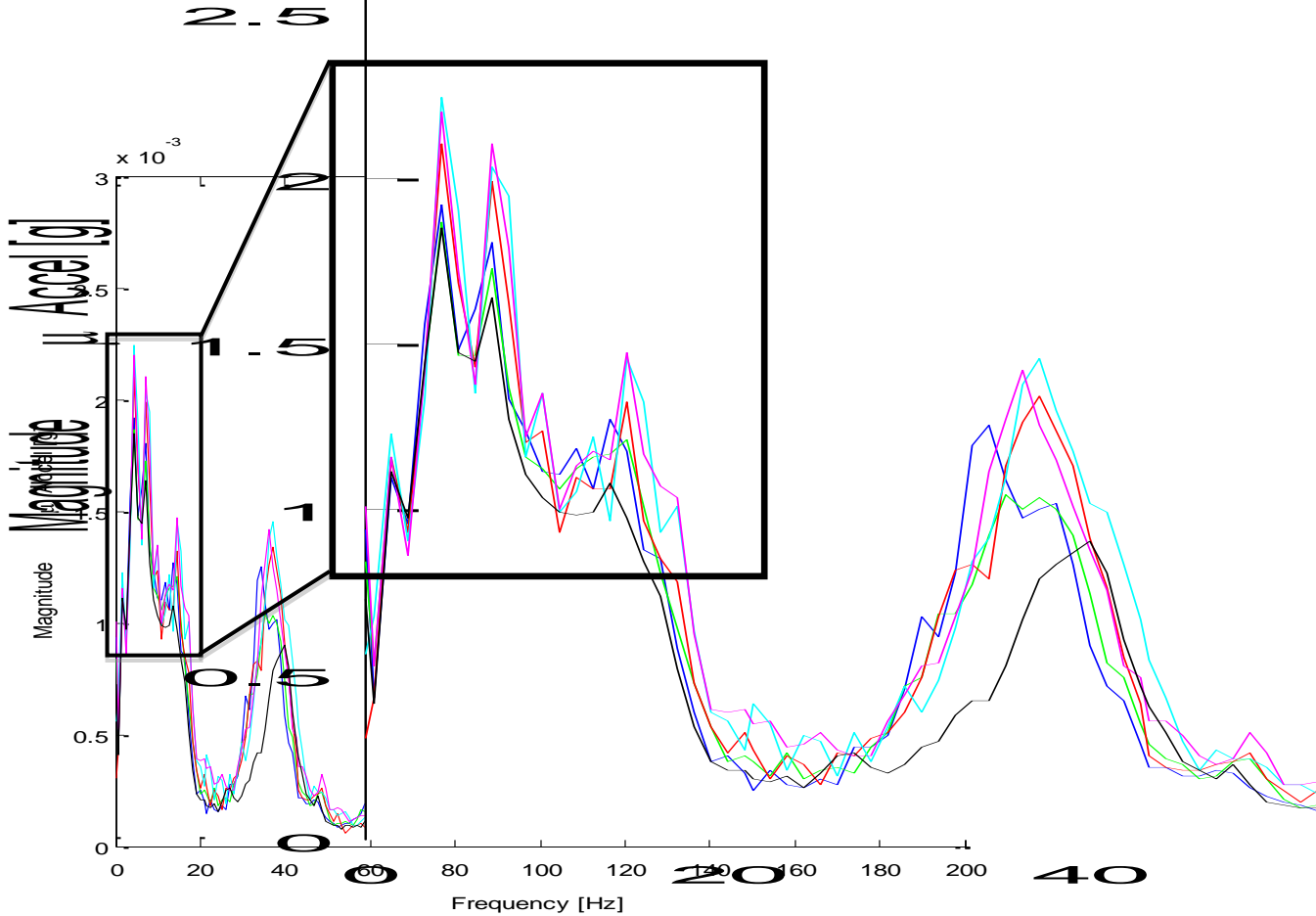


Figure 62: Frequency spectra measured experimentally (recall legend from Figure 16) with close up view of low frequency range indicating that there is less variation in the response below 5 Hz than in the response above 5 Hz as reflected in the simulation data in Figure 61(a).

To quantify how these changes in the response of the extended diagnostic speed bump plate affect the ability to diagnose faults, simulations were then conducted for four fault conditions including 20% reductions in the suspension and tire stiffness as well as 50% reductions in the suspension and tire damping parameters. The spectral responses were found for each of these fault conditions and the baseline responses corresponding to the given wheel tracking location were subtracted from the faulty response. The energy in these difference spectra was then calculated (area under the curve) and plotted in Figure 63. Several interesting findings were extracted from this plot:

- For all faults, the largest magnitude change in the spectral energy was observed when the wheel traversed the extended diagnostic speed bump on the side opposite where the sensor was located (right of the centerline of the plate). This result suggested that the sensitivity to faults could be increased by positioning the plate in the diagnostic cleat such that the centerline of the plate was offset from the wheel tracking position putting the wheel furthest from the side of the plate on which the sensor was located.

- The largest fault was observed for a reduction in damping of the tire followed by a reduction in stiffness of the suspension, stiffness of the tire, and finally damping in the suspension. This result suggested that it is likely the tire pressure faults may be introducing more of a change in damping as opposed to a change in stiffness resulting in tire faults being detected using the extended diagnostic speed bump.

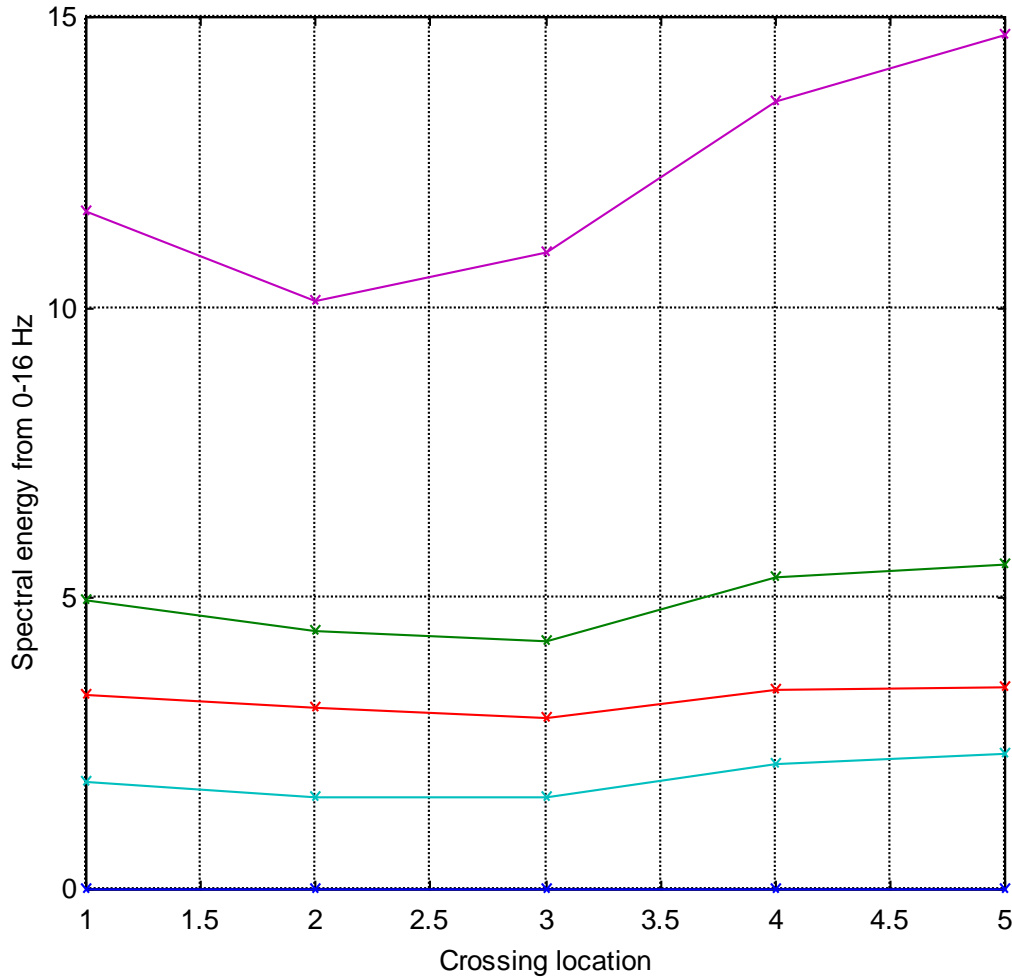


Figure 63: Difference in spectral energy for sensor degree of freedom four for quarter car from 0-16 Hz with respect to the baseline energy for different crossing locations (center, left of center, left edge, right of center, and right edge) for four types of faults including (—) 20% loss of stiffness in suspension, (—) 20% loss of stiffness in tire, (—) 50% loss of damping in suspension, and (—) 20% loss of damping in tire.

3.12 Analysis of vehicle response measured using extended diagnostic cleat

The experimental results that were presented in the previous sections focused on the analysis of measurements that were acquired from the plates of the extended diagnostic cleat. In these previous results, the vehicle was tested with and without faults in the tires and the dampers in order to determine the effectiveness of the diagnostic cleat measurement for detecting these faults. In this section, the issue of the vehicle response was considered to determine how the vehicle was responding with and without faults.

Accelerometers were installed on the lower suspension control arms of each corner, and the front and rear wheels of the vehicle were driven over the cleat 20 times at a speed of 5 mph. The measurement was triggered when one of the accelerometers on the driver front control arm reached a minimum acceleration value indicated a wheel crossing. Figure 64 shows the averaged time histories for the four control arm acceleration measurements in the vertical direction. The front wheel crossing was evident in the acceleration data for the driver and passenger front control arm measurements, whereas the rear wheel crossing was most evident in the data for the driver and passenger rear control arm measurements. There was some coupling between front and rear but very little. The lower frequency components in the response measurements were most evident towards the end of the respective time histories because these motions possessed the lowest amounts of damping. It was also evident that the front control arm response measurements contained a dominant mode of vibration that was higher in frequency than the dominant mode of vibration in the rear control arm measurements. This result suggested that a different mode of vibration of the vehicle was being excited by the front wheel crossing than the rear wheel crossing.

Next, the damper on the passenger front corner was disabled and the acceleration measurements on that corner of the vehicle in the vertical direction were compared to the baseline measurements without any fault present. Figure 65 shows a comparison of the responses that were measured on the passenger front control arm with and without disabling the damper in that corner. This figure indicated that the disabled damper led to less damping in the response of the vehicle. Note that around 1 second immediately after the rear wheels traversed the cleat, there was a low amplitude transient in the response that also exhibit a change in the response amplitude due the disabled damper, albeit not as large of a change as in the initial portion of the response measurement. This result was expected because the relative motion across the damper would be smaller in this portion of the response when the passenger front corner was being excited indirectly after the wheel wheels traversed the cleat.

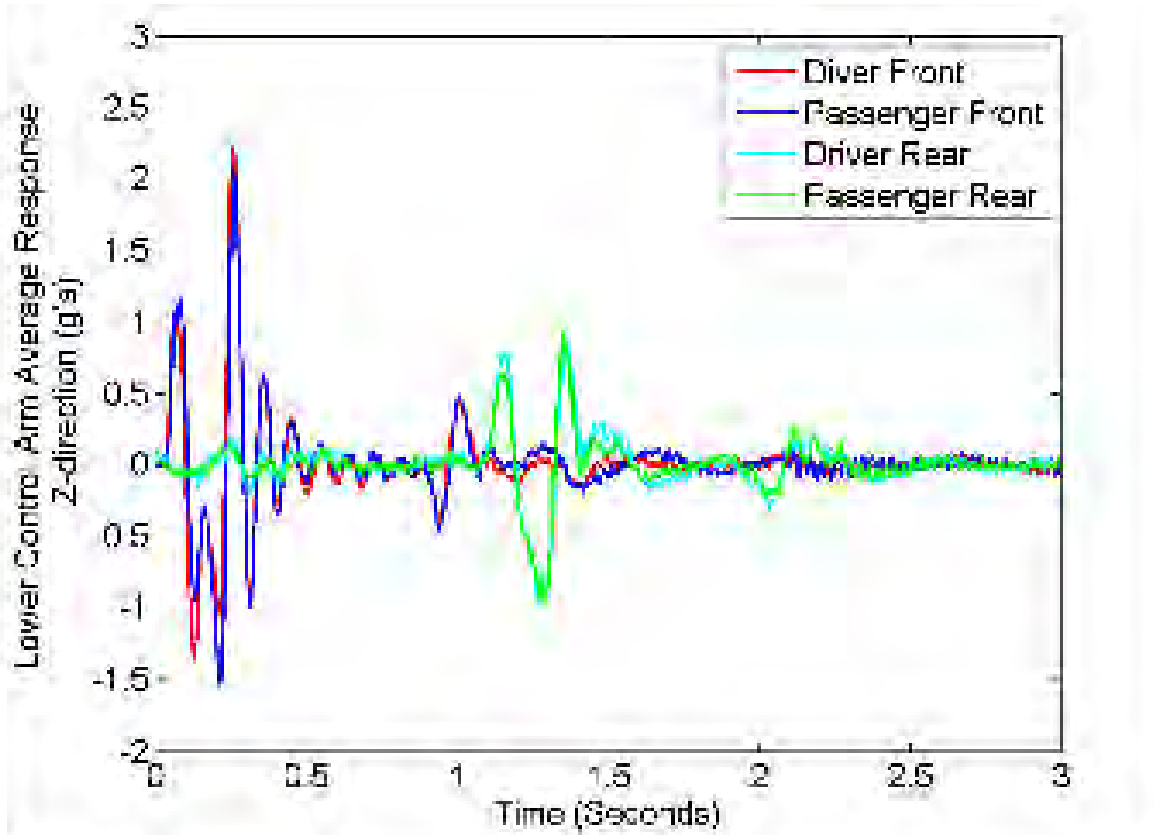


Figure 64: Averaged vertical response on lower control arms of vehicle for 20 vehicle runs at 5 mph (Courtesy T. DiPetta, Purdue University).

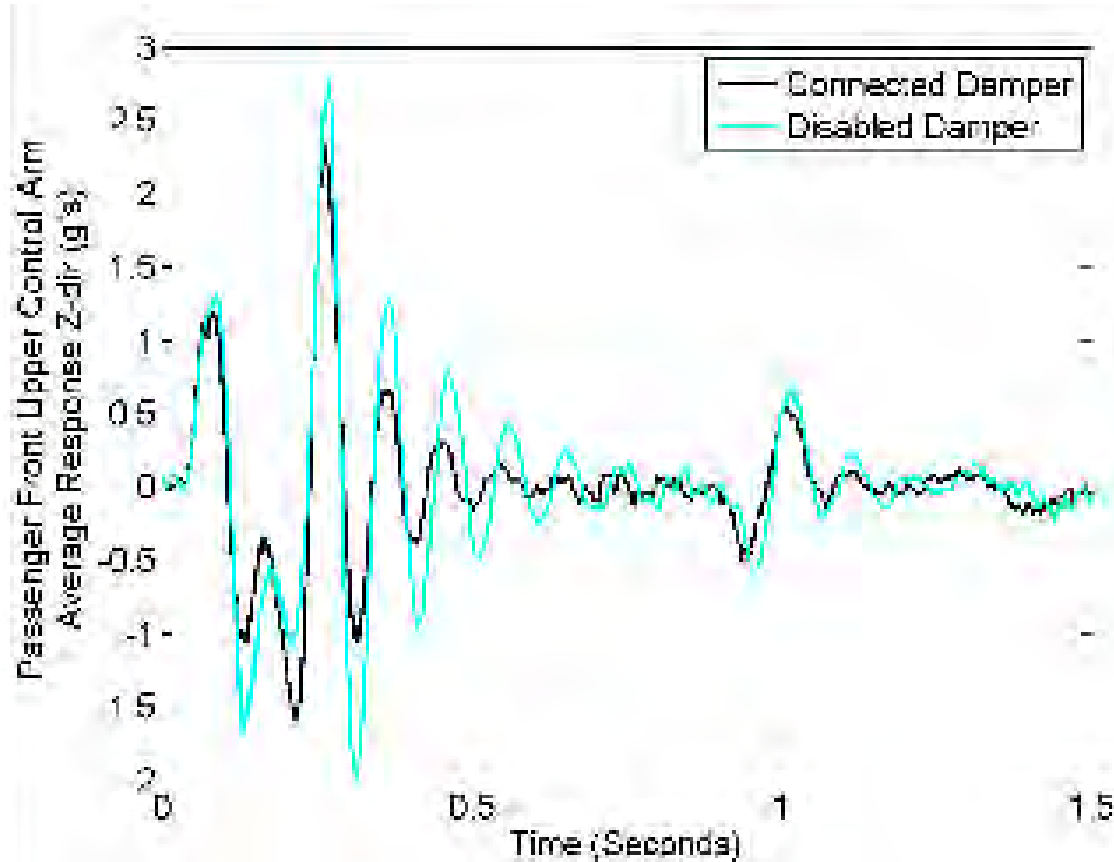


Figure 65: Averaged vertical response on the passenger front lower control arms of vehicle for 20 vehicle runs at 5 mph with connected and disabled damper on passenger front corner (Courtesy T. DiPetta, Purdue University).

The power spectral density functions corresponding to test runs of the vehicle with (10 runs) and without (10 runs) the damper disabled were plotted in Figure 66 for the vertical acceleration measurements. These results were consistent with the observed changes in the averaged time histories in Figure 65. Specifically, the spectra in Figure 66 exhibited a shift upward in amplitude for all of the disabled damper datasets compared to the connected damper datasets. The result was also consistent with the result from the simulation model in Figure 60; however, the experimental spectra exhibited changes in the low frequency peak and the high frequency peak, whereas the simulation result only exhibited changes in the higher frequency peak. When the lateral and tracking direction responses were instead analyzed, the power spectral densities in Figure 67 were obtained. Unlike the vertical direction acceleration measurements, the tracking and lateral direction measurements were not as affected by the disabled damper.

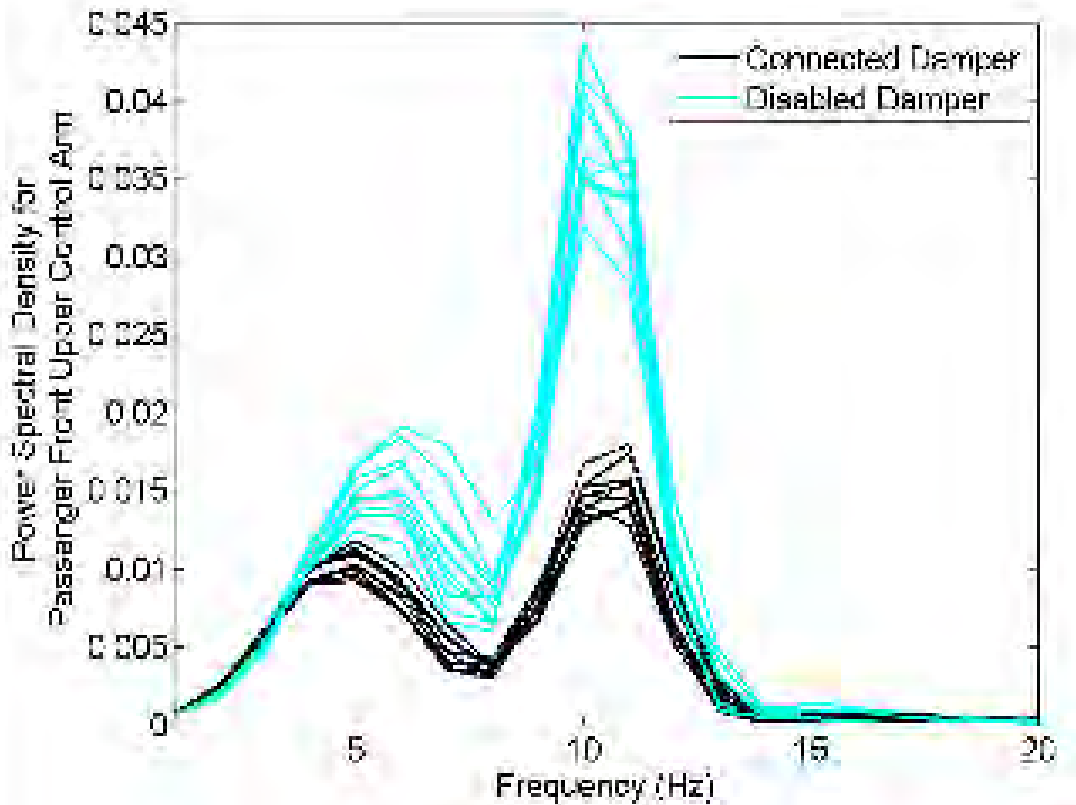


Figure 66: Power Spectral Density calculated using Welch's method for vertical response on passenger front lower control arm of vehicle with connected and disabled damper on that corner of the vehicle (Courtesy T. DiPetta, Purdue University).

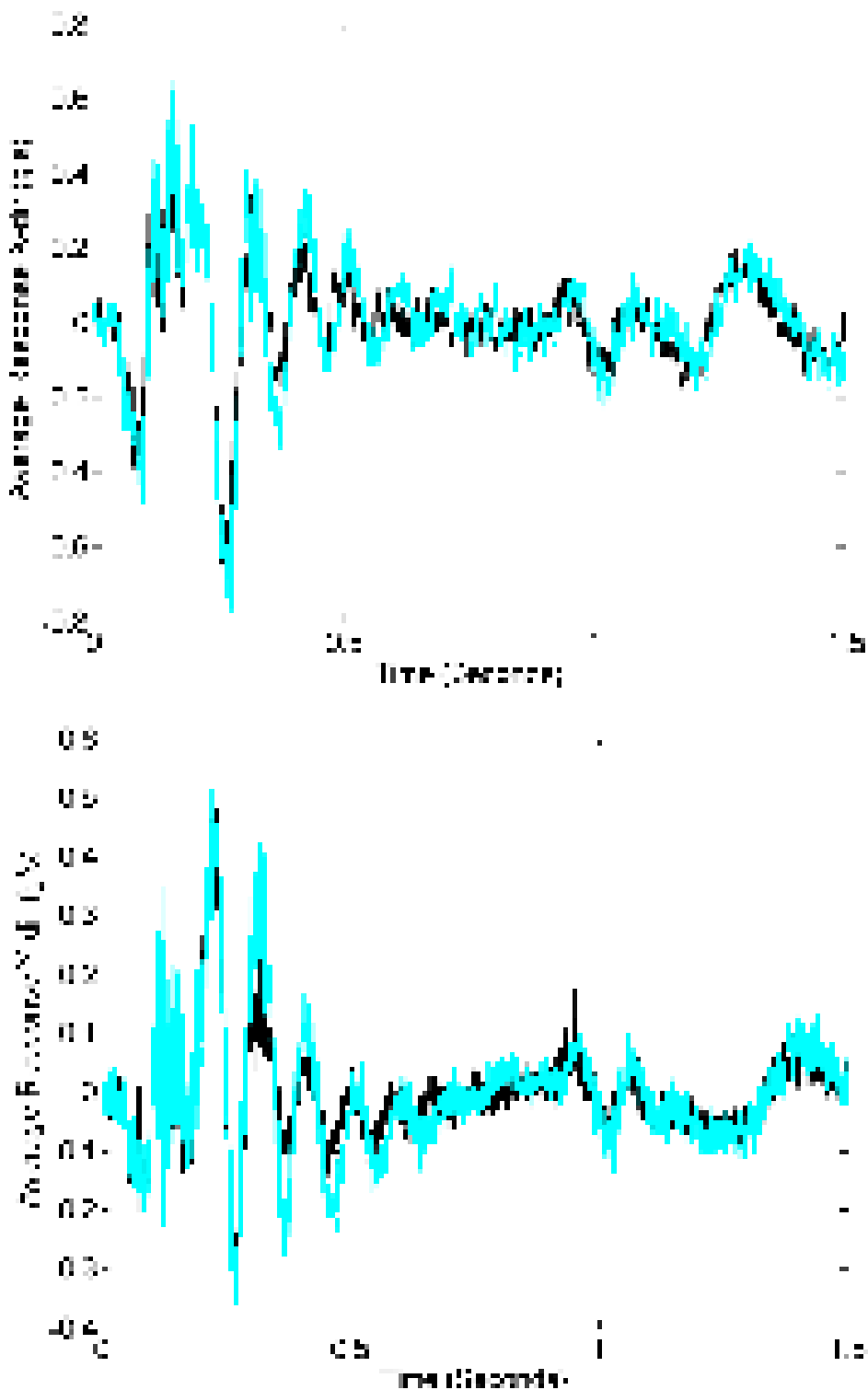


Figure 67: Averaged tracking (top) and lateral (bottom) responses on passenger front lower control arm of vehicle for 20 vehicle runs at 5 mph with connected and disabled damper on that corner of the vehicle (Courtesy T. DiPetta, Purdue University).

For comparison with the on-vehicle sensor measurements for the connected and disabled damper, the data from the extended diagnostic cleat plates were also analyzed for the driver side (accelerometer 1) and passenger side (accelerometer 4) sensors. Figure 68 contains the plots of the power spectral density functions for the driver side (top) and passenger side (bottom) accelerometer measurements in the lateral direction for disabled dampers in the four different corners of the vehicle along with the baseline (no fault) condition. There were several interesting results noted in these plots:

- First, for disabled dampers in the front of the vehicle, the largest changes in the response measurements that were made using the diagnostic cleat over the whole frequency range were observed in the lateral direction rather than the vertical direction. This result was initially thought to have contradicted the results in Figure 66 that were obtained using the on-vehicle sensors; however, it was determined that a disabled damper in one corner would result in larger vertical response in that corner, more roll motion of the front of the vehicle, and, hence, more lateral response on the opposite corner.
- Second, for disabled dampers in the rear of the vehicle, the largest changes were observed on the same side of the vehicle as the side on which the damper was disabled.

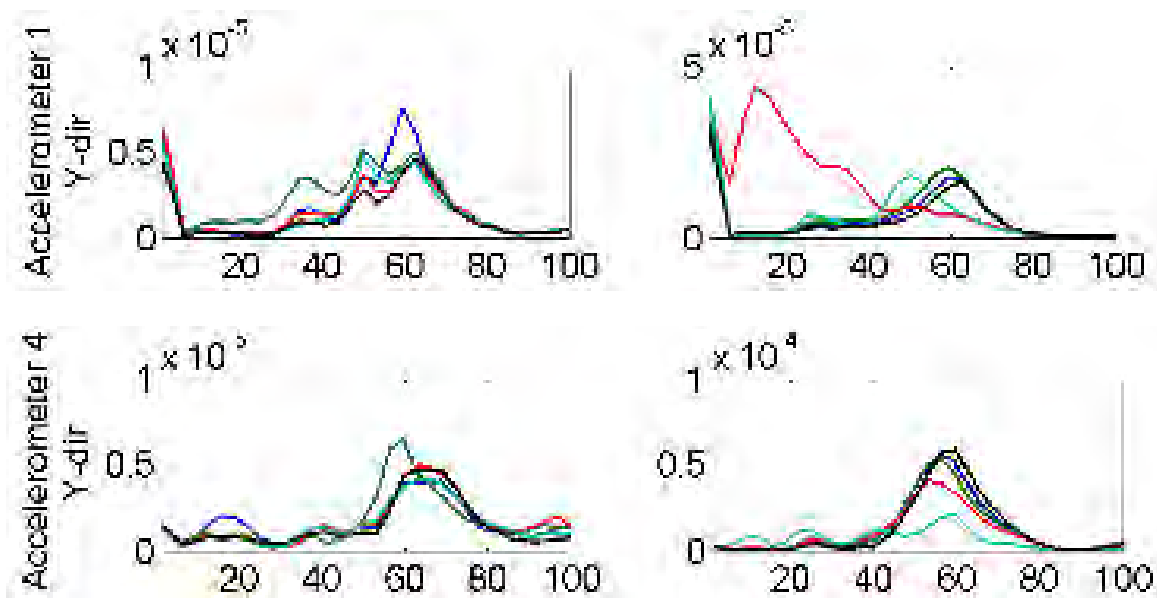


Figure 68: Power Spectral Density functions for lateral responses on extended diagnostic cleat for driver side (top) and passenger side (bottom) plates for 20 vehicle runs at 5 mph with connected and disabled damper on various corners of the vehicle
 (—, no fault, — driver front, — passenger front, — driver rear, and — passenger rear)
 (Courtesy T. DiPetta, Purdue University).

3.13 Final demonstration of diagnostic speed bump

On June 21 2011, a demonstration was performed at U.S. Army TARDEC in Warren, MI. A briefing was also provided and is attached to this final report along with a journal paper that was cleared for public release through OPSEC and has been submitted for review. Both the briefing and the demonstration were well received. Tire faults were detected and located during the demonstration despite poor weather on the day of the demonstration in the form of precipitation. A graphical user interface was used to present the results of these demonstrations. Recommendations were made by several individuals who attended the demonstration about how the technology could be further developed. Figure 69(a) and (b) show photographs of the H1 that was used in the demonstration as well as individuals who observed the results of the diagnostic tests.



Figure 69: (a) Photo of H1 driving over the diagnostic speed bump setup at U.S. Army TARDEC and (b) photo of participants who observed demonstration.

Appendix

```
% Analysis of extended diagnostic speed bump data
% 8/21/2010
% DEA

% Import data
%
% Baseline 1
% Baseline 2 after driver front tire fault
% Baseline 3 after passenger front tire fault
% Baseline 4 after driver rear tire fault
% Baseline 5 after driver passenger tire fault
%
% Sensors 1 and 3 on driver side; 3 closest to cleat
% Sensors 2 and 4 on passenger side; 4 closest to cleat
%

% Generate time vector
t=(0:0.000332:9034*0.000332)';

% Load baseline data
importfile('Baseline1st_1/Acceleration.txt');
base11=data;
speedb11=speed(data,t);
aoadb11=angleofa(data,t);
importfile('Baseline1st_2/Acceleration.txt');
base12=data;
speedb12=speed(data,t);
aoadb12=angleofa(data,t);
importfile('Baseline1st_3/Acceleration.txt');
base13=data;
speedb13=speed(data,t);
aoadb13=angleofa(data,t);
importfile('Baseline1st_4/Acceleration.txt');
base14=data;
speedb14=speed(data,t);
aoadb14=angleofa(data,t);
importfile('Baseline1st_5/Acceleration.txt');
base15=data;
speedb15=speed(data,t);
aoadb15=angleofa(data,t);
importfile('Baseline1st_6/Acceleration.txt');
base16=data;
speedb16=speed(data,t);
aoadb16=angleofa(data,t);
importfile('Baseline1st_7/Acceleration.txt');
base17=data;
speedb17=speed(data,t);
aoadb17=angleofa(data,t);
importfile('Baseline1st_8/Acceleration.txt');
base18=data;
speedb18=speed(data,t);
aoadb18=angleofa(data,t);
importfile('Baseline1st_9/Acceleration.txt');
base19=data;
```

```
speedb19=speed(data,t);
aoadb19=angleofa(data,t);
importfile('Baseline1st_10/Acceleration.txt');
base110=data;
speedb110=speed(data,t);
aoadb110=angleofa(data,t);
importfile('Baseline1st_11/Acceleration.txt');
base111=data;
speedb111=speed(data,t);
aoadb111=angleofa(data,t);
importfile('Baseline1st_12/Acceleration.txt');
base112=data;
speedb112=speed(data,t);
aoadb112=angleofa(data,t);
importfile('Baseline1st_13/Acceleration.txt');
base113=data;
speedb113=speed(data,t);
aoadb113=angleofa(data,t);
importfile('Baseline1st_14/Acceleration.txt');
base114=data;
speedb114=speed(data,t);
aoadb114=angleofa(data,t);
importfile('Baseline1st_15/Acceleration.txt');
base115=data;
speedb115=speed(data,t);
aoadb115=angleofa(data,t);
importfile('Baseline1st_16/Acceleration.txt');
base116=data;
speedb116=speed(data,t);
aoadb116=angleofa(data,t);
importfile('Baseline1st_17/Acceleration.txt');
base117=data;
speedb117=speed(data,t);
aoadb117=angleofa(data,t);
importfile('Baseline1st_18/Acceleration.txt');
base118=data;
speedb118=speed(data,t);
aoadb118=angleofa(data,t);
importfile('Baseline1st_19/Acceleration.txt');
base119=data;
speedb119=speed(data,t);
aoadb119=angleofa(data,t);
importfile('Baseline1st_20/Acceleration.txt');
base120=data;
speedb120=speed(data,t);
aoadb120=angleofa(data,t);
importfile('Baseline1st_21/Acceleration.txt');
base121=data;
speedb121=speed(data,t);
aoadb121=angleofa(data,t);
importfile('Baseline1st_22/Acceleration.txt');
base122=data;
speedb122=speed(data,t);
aoadb122=angleofa(data,t);
importfile('Baseline1st_23/Acceleration.txt');
base123=data;
speedb123=speed(data,t);
```

```
aoadb123=angleofa(data,t);
importfile('Baseline1st_24/Acceleration.txt');
base124=data;
speedb124=speed(data,t);
aoadb124=angleofa(data,t);
importfile('Baseline1st_25/Acceleration.txt');
base125=data;
speedb125=speed(data,t);
aoadb125=angleofa(data,t);
importfile('Baseline1st_26/Acceleration.txt');
base126=data;
speedb126=speed(data,t);
aoadb126=angleofa(data,t);
importfile('Baseline1st_27/Acceleration.txt');
base127=data;
speedb127=speed(data,t);
aoadb127=angleofa(data,t);
importfile('Baseline1st_28/Acceleration.txt');
base128=data;
speedb128=speed(data,t);
aoadb128=angleofa(data,t);
importfile('Baseline1st_29/Acceleration.txt');
base129=data;
speedb129=speed(data,t);
aoadb129=angleofa(data,t);
importfile('Baseline1st_30/Acceleration.txt');
base130=data;
speedb130=speed(data,t);
aoadb130=angleofa(data,t);

importfile('Baseline2nd_1/Acceleration.txt');
base21=data;
speedb21=speed(data,t);
aoadb21=angleofa(data,t);
importfile('Baseline2nd_2/Acceleration.txt');
base22=data;
speedb22=speed(data,t);
aoadb22=angleofa(data,t);
importfile('Baseline2nd_3/Acceleration.txt');
base23=data;
speedb23=speed(data,t);
aoadb23=angleofa(data,t);
importfile('Baseline2nd_4/Acceleration.txt');
base24=data;
speedb24=speed(data,t);
aoadb24=angleofa(data,t);
importfile('Baseline2nd_5/Acceleration.txt');
base25=data;
speedb25=speed(data,t);
aoadb25=angleofa(data,t);
importfile('Baseline2nd_6/Acceleration.txt');
base26=data;
speedb26=speed(data,t);
aoadb26=angleofa(data,t);
importfile('Baseline2nd_7/Acceleration.txt');
base27=data;
speedb27=speed(data,t);
```

```
aoadb27=angleofa(data,t);
importfile('Baseline2nd_8/Acceleration.txt');
base28=data;
speedb28=speed(data,t);
aoadb28=angleofa(data,t);
importfile('Baseline2nd_9/Acceleration.txt');
base29=data;
speedb29=speed(data,t);
aoadb29=angleofa(data,t);
importfile('Baseline2nd_10/Acceleration.txt');
base210=data;
speedb210=speed(data,t);
aoadb210=angleofa(data,t);
importfile('Baseline2nd_11/Acceleration.txt');
base211=data;
speedb211=speed(data,t);
aoadb211=angleofa(data,t);

importfile('Baseline3rd_1/Acceleration.txt');
base31=data;
speedb31=speed(data,t);
aoadb31=angleofa(data,t);
importfile('Baseline3rd_2/Acceleration.txt');
base32=data;
speedb32=speed(data,t);
aoadb32=angleofa(data,t);
importfile('Baseline3rd_3/Acceleration.txt');
base33=data;
speedb33=speed(data,t);
aoadb33=angleofa(data,t);
importfile('Baseline3rd_4/Acceleration.txt');
base34=data;
speedb34=speed(data,t);
aoadb34=angleofa(data,t);
importfile('Baseline3rd_5/Acceleration.txt');
base35=data;
speedb35=speed(data,t);
aoadb35=angleofa(data,t);
importfile('Baseline3rd_6/Acceleration.txt');
base36=data;
speedb36=speed(data,t);
aoadb36=angleofa(data,t);
importfile('Baseline3rd_7/Acceleration.txt');
base37=data;
speedb37=speed(data,t);
aoadb37=angleofa(data,t);
importfile('Baseline3rd_8/Acceleration.txt');
base38=data;
speedb38=speed(data,t);
aoadb38=angleofa(data,t);
importfile('Baseline3rd_9/Acceleration.txt');
base39=data;
speedb39=speed(data,t);
aoadb39=angleofa(data,t);
importfile('Baseline3rd_10/Acceleration.txt');
base310=data;
speedb310=speed(data,t);
```

```
aoadb310=angleofa(data,t);
importfile('Baseline3rd_11/Acceleration.txt');
base311=data;
speedb311=speed(data,t);
aoadb311=angleofa(data,t);

importfile('Baseline4th_1/Acceleration.txt');
base41=data;
speedb41=speed(data,t);
aoadb41=angleofa(data,t);
importfile('Baseline4th_2/Acceleration.txt');
base42=data;
speedb42=speed(data,t);
aoadb42=angleofa(data,t);
importfile('Baseline4th_3/Acceleration.txt');
base43=data;
speedb43=speed(data,t);
aoadb43=angleofa(data,t);
importfile('Baseline4th_4/Acceleration.txt');
base44=data;
speedb44=speed(data,t);
aoadb44=angleofa(data,t);
importfile('Baseline4th_5/Acceleration.txt');
base45=data;
speedb45=speed(data,t);
aoadb45=angleofa(data,t);
importfile('Baseline4th_6/Acceleration.txt');
base46=data;
speedb46=speed(data,t);
aoadb46=angleofa(data,t);
importfile('Baseline4th_7/Acceleration.txt');
base47=data;
speedb47=speed(data,t);
aoadb47=angleofa(data,t);
importfile('Baseline4th_8/Acceleration.txt');
base48=data;
speedb48=speed(data,t);
aoadb48=angleofa(data,t);
importfile('Baseline4th_9/Acceleration.txt');
base49=data;
speedb49=speed(data,t);
aoadb49=angleofa(data,t);
importfile('Baseline4th_10/Acceleration.txt');
base410=data;
speedb410=speed(data,t);
aoadb410=angleofa(data,t);
importfile('Baseline4th_11/Acceleration.txt');
base411=data;
speedb411=speed(data,t);
aoadb411=angleofa(data,t);

importfile('Baseline5th_1/Acceleration.txt');
base51=data;
speedb51=speed(data,t);
aoadb51=angleofa(data,t);
importfile('Baseline5th_2/Acceleration.txt');
```

```
base52=data;
speedb52=speed(data,t);
aoadb52=angleofa(data,t);
importfile('Baseline5th_3/Acceleration.txt');
base53=data;
speedb53=speed(data,t);
aoadb53=angleofa(data,t);
importfile('Baseline5th_4/Acceleration.txt');
base54=data;
speedb54=speed(data,t);
aoadb54=angleofa(data,t);
importfile('Baseline5th_5/Acceleration.txt');
base55=data;
speedb55=speed(data,t);
aoadb55=angleofa(data,t);
importfile('Baseline5th_6/Acceleration.txt');
base56=data;
speedb56=speed(data,t);
aoadb56=angleofa(data,t);
importfile('Baseline5th_7/Acceleration.txt');
base57=data;
speedb57=speed(data,t);
aoadb57=angleofa(data,t);
importfile('Baseline5th_8/Acceleration.txt');
base58=data;
speedb58=speed(data,t);
aoadb58=angleofa(data,t);
importfile('Baseline5th_9/Acceleration.txt');
base59=data;
speedb59=speed(data,t);
aoadb59=angleofa(data,t);
importfile('Baseline5th_10/Acceleration.txt');
base510=data;
speedb510=speed(data,t);
aoadb510=angleofa(data,t);
importfile('Baseline5th_11/Acceleration.txt');
base511=data;
speedb511=speed(data,t);
aoadb511=angleofa(data,t);

% Analyze spectra

% Set range of time points to analyze for
% Front axle
fsti=401;
feni=3740;

% Rear axle
bsti=3741;
beni=3741+(feni-fsti);

% Define frequency vector for length of time points considered
f=(0:1/t(feni-fsti+1):(feni-fsti)/t(feni-fsti+1))';

% Set sensor channels to analyze
Nchd=9;
```

```

Nchp=12;

% Set frequency range to analyze
%frng=[round(1+5/f(2)):round(1+15/f(2))
%round(1+60/f(2)):round(1+80/f(2)) round(1+95/f(2)):round(1+110/f(2))];
%frng=[round(1+2/f(2)):round(1+200/f(2))];
%frng=[round(1+30/f(2)):round(1+40/f(2))
%round(1+60/f(2)):round(1+80/f(2)) round(1+95/f(2)):round(1+110/f(2))];
%frng=[round(1+10/f(2)):round(1+60/f(2))];
%frng=[round(1+25/f(2)):round(1+35/f(2))];

% Set type of window to use in analysis
%wind=hanning(feni-fsti+1);
wind=ones(feni-fsti+1,1);

% Calculate spectra for driver side baseline
base11sf=fft(base11(fsti:feni,Nchd).*wind)/(feni-fsti+1)*2;
base11sr=fft(base11(bsti:beni,Nchd).*wind)/(beni-bsti+1)*2;
base12sf=fft(base12(fsti:feni,Nchd).*wind)/(feni-fsti+1)*2;
base12sr=fft(base12(bsti:beni,Nchd).*wind)/(beni-bsti+1)*2;
base13sf=fft(base13(fsti:feni,Nchd).*wind)/(feni-fsti+1)*2;
base13sr=fft(base13(bsti:beni,Nchd).*wind)/(beni-bsti+1)*2;
base14sf=fft(base14(fsti:feni,Nchd).*wind)/(feni-fsti+1)*2;
base14sr=fft(base14(bsti:beni,Nchd).*wind)/(beni-bsti+1)*2;
base15sf=fft(base15(fsti:feni,Nchd).*wind)/(feni-fsti+1)*2;
base15sr=fft(base15(bsti:beni,Nchd).*wind)/(beni-bsti+1)*2;
base16sf=fft(base16(fsti:feni,Nchd).*wind)/(feni-fsti+1)*2;
base16sr=fft(base16(bsti:beni,Nchd).*wind)/(beni-bsti+1)*2;
base17sf=fft(base17(fsti:feni,Nchd).*wind)/(feni-fsti+1)*2;
base17sr=fft(base17(bsti:beni,Nchd).*wind)/(beni-bsti+1)*2;
base18sf=fft(base18(fsti:feni,Nchd).*wind)/(feni-fsti+1)*2;
base18sr=fft(base18(bsti:beni,Nchd).*wind)/(beni-bsti+1)*2;
base19sf=fft(base19(fsti:feni,Nchd).*wind)/(feni-fsti+1)*2;
base19sr=fft(base19(bsti:beni,Nchd).*wind)/(beni-bsti+1)*2;
base110sf=fft(base110(fsti:feni,Nchd).*wind)/(feni-fsti+1)*2;
base110sr=fft(base110(bsti:beni,Nchd).*wind)/(beni-bsti+1)*2;
base111sf=fft(base111(fsti:feni,Nchd).*wind)/(feni-fsti+1)*2;
base111sr=fft(base111(bsti:beni,Nchd).*wind)/(beni-bsti+1)*2;
base112sf=fft(base112(fsti:feni,Nchd).*wind)/(feni-fsti+1)*2;
base112sr=fft(base112(bsti:beni,Nchd).*wind)/(beni-bsti+1)*2;
base113sf=fft(base113(fsti:feni,Nchd).*wind)/(feni-fsti+1)*2;
base113sr=fft(base113(bsti:beni,Nchd).*wind)/(beni-bsti+1)*2;
base114sf=fft(base114(fsti:feni,Nchd).*wind)/(feni-fsti+1)*2;
base114sr=fft(base114(bsti:beni,Nchd).*wind)/(beni-bsti+1)*2;
base115sf=fft(base115(fsti:feni,Nchd).*wind)/(feni-fsti+1)*2;
base115sr=fft(base115(bsti:beni,Nchd).*wind)/(beni-bsti+1)*2;
base116sf=fft(base116(fsti:feni,Nchd).*wind)/(feni-fsti+1)*2;
base116sr=fft(base116(bsti:beni,Nchd).*wind)/(beni-bsti+1)*2;
base117sf=fft(base117(fsti:feni,Nchd).*wind)/(feni-fsti+1)*2;
base117sr=fft(base117(bsti:beni,Nchd).*wind)/(beni-bsti+1)*2;
base118sf=fft(base118(fsti:feni,Nchd).*wind)/(feni-fsti+1)*2;
base118sr=fft(base118(bsti:beni,Nchd).*wind)/(beni-bsti+1)*2;
base119sf=fft(base119(fsti:feni,Nchd).*wind)/(feni-fsti+1)*2;
base119sr=fft(base119(bsti:beni,Nchd).*wind)/(beni-bsti+1)*2;
base120sf=fft(base120(fsti:feni,Nchd).*wind)/(feni-fsti+1)*2;
base120sr=fft(base120(bsti:beni,Nchd).*wind)/(beni-bsti+1)*2;

```

```

base121sf=fft(base121(fsti:feni,Nchd).*wind)/(feni-fsti+1)*2;
base121sr=fft(base121(bsti:beni,Nchd).*wind)/(beni-bsti+1)*2;
base122sf=fft(base122(fsti:feni,Nchd).*wind)/(feni-fsti+1)*2;
base122sr=fft(base122(bsti:beni,Nchd).*wind)/(beni-bsti+1)*2;
base123sf=fft(base123(fsti:feni,Nchd).*wind)/(feni-fsti+1)*2;
base123sr=fft(base123(bsti:beni,Nchd).*wind)/(beni-bsti+1)*2;
base124sf=fft(base124(fsti:feni,Nchd).*wind)/(feni-fsti+1)*2;
base124sr=fft(base124(bsti:beni,Nchd).*wind)/(beni-bsti+1)*2;
base125sf=fft(base125(fsti:feni,Nchd).*wind)/(feni-fsti+1)*2;
base125sr=fft(base125(bsti:beni,Nchd).*wind)/(beni-bsti+1)*2;
base126sf=fft(base126(fsti:feni,Nchd).*wind)/(feni-fsti+1)*2;
base126sr=fft(base126(bsti:beni,Nchd).*wind)/(beni-bsti+1)*2;
base127sf=fft(base127(fsti:feni,Nchd).*wind)/(feni-fsti+1)*2;
base127sr=fft(base127(bsti:beni,Nchd).*wind)/(beni-bsti+1)*2;
base128sf=fft(base128(fsti:feni,Nchd).*wind)/(feni-fsti+1)*2;
base128sr=fft(base128(bsti:beni,Nchd).*wind)/(beni-bsti+1)*2;
base129sf=fft(base129(fsti:feni,Nchd).*wind)/(feni-fsti+1)*2;
base129sr=fft(base129(bsti:beni,Nchd).*wind)/(beni-bsti+1)*2;
base130sf=fft(base130(fsti:feni,Nchd).*wind)/(feni-fsti+1)*2;
base130sr=fft(base130(bsti:beni,Nchd).*wind)/(beni-bsti+1)*2;

base21sf=fft(base21(fsti:feni,Nchd).*wind)/(feni-fsti+1)*2;
base21sr=fft(base21(bsti:beni,Nchd).*wind)/(beni-bsti+1)*2;
base22sf=fft(base22(fsti:feni,Nchd).*wind)/(feni-fsti+1)*2;
base22sr=fft(base22(bsti:beni,Nchd).*wind)/(beni-bsti+1)*2;
base23sf=fft(base23(fsti:feni,Nchd).*wind)/(feni-fsti+1)*2;
base23sr=fft(base23(bsti:beni,Nchd).*wind)/(beni-bsti+1)*2;
base24sf=fft(base24(fsti:feni,Nchd).*wind)/(feni-fsti+1)*2;
base24sr=fft(base24(bsti:beni,Nchd).*wind)/(beni-bsti+1)*2;
base25sf=fft(base25(fsti:feni,Nchd).*wind)/(feni-fsti+1)*2;
base25sr=fft(base25(bsti:beni,Nchd).*wind)/(beni-bsti+1)*2;
base26sf=fft(base26(fsti:feni,Nchd).*wind)/(feni-fsti+1)*2;
base26sr=fft(base26(bsti:beni,Nchd).*wind)/(beni-bsti+1)*2;
base27sf=fft(base27(fsti:feni,Nchd).*wind)/(feni-fsti+1)*2;
base27sr=fft(base27(bsti:beni,Nchd).*wind)/(beni-bsti+1)*2;
base28sf=fft(base28(fsti:feni,Nchd).*wind)/(feni-fsti+1)*2;
base28sr=fft(base28(bsti:beni,Nchd).*wind)/(beni-bsti+1)*2;
base29sf=fft(base29(fsti:feni,Nchd).*wind)/(feni-fsti+1)*2;
base29sr=fft(base29(bsti:beni,Nchd).*wind)/(beni-bsti+1)*2;
base210sf=fft(base210(fsti:feni,Nchd).*wind)/(feni-fsti+1)*2;
base210sr=fft(base210(bsti:beni,Nchd).*wind)/(beni-bsti+1)*2;
base211sf=fft(base211(fsti:feni,Nchd).*wind)/(feni-fsti+1)*2;
base211sr=fft(base211(bsti:beni,Nchd).*wind)/(beni-bsti+1)*2;

base31sf=fft(base31(fsti:feni,Nchd).*wind)/(feni-fsti+1)*2;
base31sr=fft(base31(bsti:beni,Nchd).*wind)/(beni-bsti+1)*2;
base32sf=fft(base32(fsti:feni,Nchd).*wind)/(feni-fsti+1)*2;
base32sr=fft(base32(bsti:beni,Nchd).*wind)/(beni-bsti+1)*2;
base33sf=fft(base33(fsti:feni,Nchd).*wind)/(feni-fsti+1)*2;
base33sr=fft(base33(bsti:beni,Nchd).*wind)/(beni-bsti+1)*2;
base34sf=fft(base34(fsti:feni,Nchd).*wind)/(feni-fsti+1)*2;
base34sr=fft(base34(bsti:beni,Nchd).*wind)/(beni-bsti+1)*2;
base35sf=fft(base35(fsti:feni,Nchd).*wind)/(feni-fsti+1)*2;
base35sr=fft(base35(bsti:beni,Nchd).*wind)/(beni-bsti+1)*2;
base36sf=fft(base36(fsti:feni,Nchd).*wind)/(feni-fsti+1)*2;
base36sr=fft(base36(bsti:beni,Nchd).*wind)/(beni-bsti+1)*2;

```

```

base37sf=fft (base37 (fsti:feni,Nchd) .*wind) / (feni-fsti+1)*2;
base37sr=fft (base37 (bsti:beni,Nchd) .*wind) / (beni-bsti+1)*2;
base38sf=fft (base38 (fsti:feni,Nchd) .*wind) / (feni-fsti+1)*2;
base38sr=fft (base38 (bsti:beni,Nchd) .*wind) / (beni-bsti+1)*2;
base39sf=fft (base39 (fsti:feni,Nchd) .*wind) / (feni-fsti+1)*2;
base39sr=fft (base39 (bsti:beni,Nchd) .*wind) / (beni-bsti+1)*2;
base310sf=fft (base310 (fsti:feni,Nchd) .*wind) / (feni-fsti+1)*2;
base310sr=fft (base310 (bsti:beni,Nchd) .*wind) / (beni-bsti+1)*2;
base311sf=fft (base311 (fsti:feni,Nchd) .*wind) / (feni-fsti+1)*2;
base311sr=fft (base311 (bsti:beni,Nchd) .*wind) / (beni-bsti+1)*2;

base41sf=fft (base41 (fsti:feni,Nchd) .*wind) / (feni-fsti+1)*2;
base41sr=fft (base41 (bsti:beni,Nchd) .*wind) / (beni-bsti+1)*2;
base42sf=fft (base42 (fsti:feni,Nchd) .*wind) / (feni-fsti+1)*2;
base42sr=fft (base42 (bsti:beni,Nchd) .*wind) / (beni-bsti+1)*2;
base43sf=fft (base43 (fsti:feni,Nchd) .*wind) / (feni-fsti+1)*2;
base43sr=fft (base43 (bsti:beni,Nchd) .*wind) / (beni-bsti+1)*2;
base44sf=fft (base44 (fsti:feni,Nchd) .*wind) / (feni-fsti+1)*2;
base44sr=fft (base44 (bsti:beni,Nchd) .*wind) / (beni-bsti+1)*2;
base45sf=fft (base45 (fsti:feni,Nchd) .*wind) / (feni-fsti+1)*2;
base45sr=fft (base45 (bsti:beni,Nchd) .*wind) / (beni-bsti+1)*2;
base46sf=fft (base46 (fsti:feni,Nchd) .*wind) / (feni-fsti+1)*2;
base46sr=fft (base46 (bsti:beni,Nchd) .*wind) / (beni-bsti+1)*2;
base47sf=fft (base47 (fsti:feni,Nchd) .*wind) / (feni-fsti+1)*2;
base47sr=fft (base47 (bsti:beni,Nchd) .*wind) / (beni-bsti+1)*2;
base48sf=fft (base48 (fsti:feni,Nchd) .*wind) / (feni-fsti+1)*2;
base48sr=fft (base48 (bsti:beni,Nchd) .*wind) / (beni-bsti+1)*2;
base49sf=fft (base49 (fsti:feni,Nchd) .*wind) / (feni-fsti+1)*2;
base49sr=fft (base49 (bsti:beni,Nchd) .*wind) / (beni-bsti+1)*2;
base410sf=fft (base410 (fsti:feni,Nchd) .*wind) / (feni-fsti+1)*2;
base410sr=fft (base410 (bsti:beni,Nchd) .*wind) / (beni-bsti+1)*2;
base411sf=fft (base411 (fsti:feni,Nchd) .*wind) / (feni-fsti+1)*2;
base411sr=fft (base411 (bsti:beni,Nchd) .*wind) / (beni-bsti+1)*2;

base51sf=fft (base51 (fsti:feni,Nchd) .*wind) / (feni-fsti+1)*2;
base51sr=fft (base51 (bsti:beni,Nchd) .*wind) / (beni-bsti+1)*2;
base52sf=fft (base52 (fsti:feni,Nchd) .*wind) / (feni-fsti+1)*2;
base52sr=fft (base52 (bsti:beni,Nchd) .*wind) / (beni-bsti+1)*2;
base53sf=fft (base53 (fsti:feni,Nchd) .*wind) / (feni-fsti+1)*2;
base53sr=fft (base53 (bsti:beni,Nchd) .*wind) / (beni-bsti+1)*2;
base54sf=fft (base54 (fsti:feni,Nchd) .*wind) / (feni-fsti+1)*2;
base54sr=fft (base54 (bsti:beni,Nchd) .*wind) / (beni-bsti+1)*2;
base55sf=fft (base55 (fsti:feni,Nchd) .*wind) / (feni-fsti+1)*2;
base55sr=fft (base55 (bsti:beni,Nchd) .*wind) / (beni-bsti+1)*2;
base56sf=fft (base56 (fsti:feni,Nchd) .*wind) / (feni-fsti+1)*2;
base56sr=fft (base56 (bsti:beni,Nchd) .*wind) / (beni-bsti+1)*2;
base57sf=fft (base57 (fsti:feni,Nchd) .*wind) / (feni-fsti+1)*2;
base57sr=fft (base57 (bsti:beni,Nchd) .*wind) / (beni-bsti+1)*2;
base58sf=fft (base58 (fsti:feni,Nchd) .*wind) / (feni-fsti+1)*2;
base58sr=fft (base58 (bsti:beni,Nchd) .*wind) / (beni-bsti+1)*2;
base59sf=fft (base59 (fsti:feni,Nchd) .*wind) / (feni-fsti+1)*2;
base59sr=fft (base59 (bsti:beni,Nchd) .*wind) / (beni-bsti+1)*2;
base510sf=fft (base510 (fsti:feni,Nchd) .*wind) / (feni-fsti+1)*2;
base510sr=fft (base510 (bsti:beni,Nchd) .*wind) / (beni-bsti+1)*2;
base511sf=fft (base511 (fsti:feni,Nchd) .*wind) / (feni-fsti+1)*2;
base511sr=fft (base511 (bsti:beni,Nchd) .*wind) / (beni-bsti+1)*2;

```

```
% Calculate spectra for passenger side
base11sfp=fft(base11(fsti:feni,Nchp).*wind)/(feni-fsti+1)*2;
base11srp=fft(base11(bsti:beni,Nchp).*wind)/(beni-bsti+1)*2;
base12sfp=fft(base12(fsti:feni,Nchp).*wind)/(feni-fsti+1)*2;
base12srp=fft(base12(bsti:beni,Nchp).*wind)/(beni-bsti+1)*2;
base13sfp=fft(base13(fsti:feni,Nchp).*wind)/(feni-fsti+1)*2;
base13srp=fft(base13(bsti:beni,Nchp).*wind)/(beni-bsti+1)*2;
base14sfp=fft(base14(fsti:feni,Nchp).*wind)/(feni-fsti+1)*2;
base14srp=fft(base14(bsti:beni,Nchp).*wind)/(beni-bsti+1)*2;
base15sfp=fft(base15(fsti:feni,Nchp).*wind)/(feni-fsti+1)*2;
base15srp=fft(base15(bsti:beni,Nchp).*wind)/(beni-bsti+1)*2;
base16sfp=fft(base16(fsti:feni,Nchp).*wind)/(feni-fsti+1)*2;
base16srp=fft(base16(bsti:beni,Nchp).*wind)/(beni-bsti+1)*2;
base17sfp=fft(base17(fsti:feni,Nchp).*wind)/(feni-fsti+1)*2;
base17srp=fft(base17(bsti:beni,Nchp).*wind)/(beni-bsti+1)*2;
base18sfp=fft(base18(fsti:feni,Nchp).*wind)/(feni-fsti+1)*2;
base18srp=fft(base18(bsti:beni,Nchp).*wind)/(beni-bsti+1)*2;
base19sfp=fft(base19(fsti:feni,Nchp).*wind)/(feni-fsti+1)*2;
base19srp=fft(base19(bsti:beni,Nchp).*wind)/(beni-bsti+1)*2;
base110sfp=fft(base110(fsti:feni,Nchp).*wind)/(feni-fsti+1)*2;
base110srp=fft(base110(bsti:beni,Nchp).*wind)/(beni-bsti+1)*2;
base111sfp=fft(base111(fsti:feni,Nchp).*wind)/(feni-fsti+1)*2;
base111srp=fft(base111(bsti:beni,Nchp).*wind)/(beni-bsti+1)*2;
base112sfp=fft(base112(fsti:feni,Nchp).*wind)/(feni-fsti+1)*2;
base112srp=fft(base112(bsti:beni,Nchp).*wind)/(beni-bsti+1)*2;
base113sfp=fft(base113(fsti:feni,Nchp).*wind)/(feni-fsti+1)*2;
base113srp=fft(base113(bsti:beni,Nchp).*wind)/(beni-bsti+1)*2;
base114sfp=fft(base114(fsti:feni,Nchp).*wind)/(feni-fsti+1)*2;
base114srp=fft(base114(bsti:beni,Nchp).*wind)/(beni-bsti+1)*2;
base115sfp=fft(base115(fsti:feni,Nchp).*wind)/(feni-fsti+1)*2;
base115srp=fft(base115(bsti:beni,Nchp).*wind)/(beni-bsti+1)*2;
base116sfp=fft(base116(fsti:feni,Nchp).*wind)/(feni-fsti+1)*2;
base116srp=fft(base116(bsti:beni,Nchp).*wind)/(beni-bsti+1)*2;
base117sfp=fft(base117(fsti:feni,Nchp).*wind)/(feni-fsti+1)*2;
base117srp=fft(base117(bsti:beni,Nchp).*wind)/(beni-bsti+1)*2;
base118sfp=fft(base118(fsti:feni,Nchp).*wind)/(feni-fsti+1)*2;
base118srp=fft(base118(bsti:beni,Nchp).*wind)/(beni-bsti+1)*2;
base119sfp=fft(base119(fsti:feni,Nchp).*wind)/(feni-fsti+1)*2;
base119srp=fft(base119(bsti:beni,Nchp).*wind)/(beni-bsti+1)*2;
base120sfp=fft(base120(fsti:feni,Nchp).*wind)/(feni-fsti+1)*2;
base120srp=fft(base120(bsti:beni,Nchp).*wind)/(beni-bsti+1)*2;
base121sfp=fft(base121(fsti:feni,Nchp).*wind)/(feni-fsti+1)*2;
base121srp=fft(base121(bsti:beni,Nchp).*wind)/(beni-bsti+1)*2;
base122sfp=fft(base122(fsti:feni,Nchp).*wind)/(feni-fsti+1)*2;
base122srp=fft(base122(bsti:beni,Nchp).*wind)/(beni-bsti+1)*2;
base123sfp=fft(base123(fsti:feni,Nchp).*wind)/(feni-fsti+1)*2;
base123srp=fft(base123(bsti:beni,Nchp).*wind)/(beni-bsti+1)*2;
base124sfp=fft(base124(fsti:feni,Nchp).*wind)/(feni-fsti+1)*2;
base124srp=fft(base124(bsti:beni,Nchp).*wind)/(beni-bsti+1)*2;
base125sfp=fft(base125(fsti:feni,Nchp).*wind)/(feni-fsti+1)*2;
base125srp=fft(base125(bsti:beni,Nchp).*wind)/(beni-bsti+1)*2;
base126sfp=fft(base126(fsti:feni,Nchp).*wind)/(feni-fsti+1)*2;
base126srp=fft(base126(bsti:beni,Nchp).*wind)/(beni-bsti+1)*2;
base127sfp=fft(base127(fsti:feni,Nchp).*wind)/(feni-fsti+1)*2;
base127srp=fft(base127(bsti:beni,Nchp).*wind)/(beni-bsti+1)*2;
base128sfp=fft(base128(fsti:feni,Nchp).*wind)/(feni-fsti+1)*2;
```

```

base128srp=fft(base128(bsti:beni,Nchp).*wind)/(beni-bsti+1)*2;
base129sfp=fft(base129(fsti:feni,Nchp).*wind)/(feni-fsti+1)*2;
base129srp=fft(base129(bsti:beni,Nchp).*wind)/(beni-bsti+1)*2;
base130sfp=fft(base130(fsti:feni,Nchp).*wind)/(feni-fsti+1)*2;
base130srp=fft(base130(bsti:beni,Nchp).*wind)/(beni-bsti+1)*2;

base21sfp=fft(base21(fsti:feni,Nchp).*wind)/(feni-fsti+1)*2;
base21srp=fft(base21(bsti:beni,Nchp).*wind)/(beni-bsti+1)*2;
base22sfp=fft(base22(fsti:feni,Nchp).*wind)/(feni-fsti+1)*2;
base22srp=fft(base22(bsti:beni,Nchp).*wind)/(beni-bsti+1)*2;
base23sfp=fft(base23(fsti:feni,Nchp).*wind)/(feni-fsti+1)*2;
base23srp=fft(base23(bsti:beni,Nchp).*wind)/(beni-bsti+1)*2;
base24sfp=fft(base24(fsti:feni,Nchp).*wind)/(feni-fsti+1)*2;
base24srp=fft(base24(bsti:beni,Nchp).*wind)/(beni-bsti+1)*2;
base25sfp=fft(base25(fsti:feni,Nchp).*wind)/(feni-fsti+1)*2;
base25srp=fft(base25(bsti:beni,Nchp).*wind)/(beni-bsti+1)*2;
base26sfp=fft(base26(fsti:feni,Nchp).*wind)/(feni-fsti+1)*2;
base26srp=fft(base26(bsti:beni,Nchp).*wind)/(beni-bsti+1)*2;
base27sfp=fft(base27(fsti:feni,Nchp).*wind)/(feni-fsti+1)*2;
base27srp=fft(base27(bsti:beni,Nchp).*wind)/(beni-bsti+1)*2;
base28sfp=fft(base28(fsti:feni,Nchp).*wind)/(feni-fsti+1)*2;
base28srp=fft(base28(bsti:beni,Nchp).*wind)/(beni-bsti+1)*2;
base29sfp=fft(base29(fsti:feni,Nchp).*wind)/(feni-fsti+1)*2;
base29srp=fft(base29(bsti:beni,Nchp).*wind)/(beni-bsti+1)*2;
base210sfp=fft(base210(fsti:feni,Nchp).*wind)/(feni-fsti+1)*2;
base210srp=fft(base210(bsti:beni,Nchp).*wind)/(beni-bsti+1)*2;
base211sfp=fft(base211(fsti:feni,Nchp).*wind)/(feni-fsti+1)*2;
base211srp=fft(base211(bsti:beni,Nchp).*wind)/(beni-bsti+1)*2;

base31sfp=fft(base31(fsti:feni,Nchp).*wind)/(feni-fsti+1)*2;
base31srp=fft(base31(bsti:beni,Nchp).*wind)/(beni-bsti+1)*2;
base32sfp=fft(base32(fsti:feni,Nchp).*wind)/(feni-fsti+1)*2;
base32srp=fft(base32(bsti:beni,Nchp).*wind)/(beni-bsti+1)*2;
base33sfp=fft(base33(fsti:feni,Nchp).*wind)/(feni-fsti+1)*2;
base33srp=fft(base33(bsti:beni,Nchp).*wind)/(beni-bsti+1)*2;
base34sfp=fft(base34(fsti:feni,Nchp).*wind)/(feni-fsti+1)*2;
base34srp=fft(base34(bsti:beni,Nchp).*wind)/(beni-bsti+1)*2;
base35sfp=fft(base35(fsti:feni,Nchp).*wind)/(feni-fsti+1)*2;
base35srp=fft(base35(bsti:beni,Nchp).*wind)/(beni-bsti+1)*2;
base36sfp=fft(base36(fsti:feni,Nchp).*wind)/(feni-fsti+1)*2;
base36srp=fft(base36(bsti:beni,Nchp).*wind)/(beni-bsti+1)*2;
base37sfp=fft(base37(fsti:feni,Nchp).*wind)/(feni-fsti+1)*2;
base37srp=fft(base37(bsti:beni,Nchp).*wind)/(beni-bsti+1)*2;
base38sfp=fft(base38(fsti:feni,Nchp).*wind)/(feni-fsti+1)*2;
base38srp=fft(base38(bsti:beni,Nchp).*wind)/(beni-bsti+1)*2;
base39sfp=fft(base39(fsti:feni,Nchp).*wind)/(feni-fsti+1)*2;
base39srp=fft(base39(bsti:beni,Nchp).*wind)/(beni-bsti+1)*2;
base310sfp=fft(base310(fsti:feni,Nchp).*wind)/(feni-fsti+1)*2;
base310srp=fft(base310(bsti:beni,Nchp).*wind)/(beni-bsti+1)*2;
base311sfp=fft(base311(fsti:feni,Nchp).*wind)/(feni-fsti+1)*2;
base311srp=fft(base311(bsti:beni,Nchp).*wind)/(beni-bsti+1)*2;

base41sfp=fft(base41(fsti:feni,Nchp).*wind)/(feni-fsti+1)*2;
base41srp=fft(base41(bsti:beni,Nchp).*wind)/(beni-bsti+1)*2;
base42sfp=fft(base42(fsti:feni,Nchp).*wind)/(feni-fsti+1)*2;
base42srp=fft(base42(bsti:beni,Nchp).*wind)/(beni-bsti+1)*2;

```

```

base43sfp=fft(base43(fsti:feni,Nchp).*wind)/(feni-fsti+1)*2;
base43srp=fft(base43(bsti:beni,Nchp).*wind)/(beni-bsti+1)*2;
base44sfp=fft(base44(fsti:feni,Nchp).*wind)/(feni-fsti+1)*2;
base44srp=fft(base44(bsti:beni,Nchp).*wind)/(beni-bsti+1)*2;
base45sfp=fft(base45(fsti:feni,Nchp).*wind)/(feni-fsti+1)*2;
base45srp=fft(base45(bsti:beni,Nchp).*wind)/(beni-bsti+1)*2;
base46sfp=fft(base46(fsti:feni,Nchp).*wind)/(feni-fsti+1)*2;
base46srp=fft(base46(bsti:beni,Nchp).*wind)/(beni-bsti+1)*2;
base47sfp=fft(base47(fsti:feni,Nchp).*wind)/(feni-fsti+1)*2;
base47srp=fft(base47(bsti:beni,Nchp).*wind)/(beni-bsti+1)*2;
base48sfp=fft(base48(fsti:feni,Nchp).*wind)/(feni-fsti+1)*2;
base48srp=fft(base48(bsti:beni,Nchp).*wind)/(beni-bsti+1)*2;
base49sfp=fft(base49(fsti:feni,Nchp).*wind)/(feni-fsti+1)*2;
base49srp=fft(base49(bsti:beni,Nchp).*wind)/(beni-bsti+1)*2;
base410sfp=fft(base410(fsti:feni,Nchp).*wind)/(feni-fsti+1)*2;
base410srp=fft(base410(bsti:beni,Nchp).*wind)/(beni-bsti+1)*2;
base411sfp=fft(base411(fsti:feni,Nchp).*wind)/(feni-fsti+1)*2;
base411srp=fft(base411(bsti:beni,Nchp).*wind)/(beni-bsti+1)*2;

base51sfp=fft(base51(fsti:feni,Nchp).*wind)/(feni-fsti+1)*2;
base51srp=fft(base51(bsti:beni,Nchp).*wind)/(beni-bsti+1)*2;
base52sfp=fft(base52(fsti:feni,Nchp).*wind)/(feni-fsti+1)*2;
base52srp=fft(base52(bsti:beni,Nchp).*wind)/(beni-bsti+1)*2;
base53sfp=fft(base53(fsti:feni,Nchp).*wind)/(feni-fsti+1)*2;
base53srp=fft(base53(bsti:beni,Nchp).*wind)/(beni-bsti+1)*2;
base54sfp=fft(base54(fsti:feni,Nchp).*wind)/(feni-fsti+1)*2;
base54srp=fft(base54(bsti:beni,Nchp).*wind)/(beni-bsti+1)*2;
base55sfp=fft(base55(fsti:feni,Nchp).*wind)/(feni-fsti+1)*2;
base55srp=fft(base55(bsti:beni,Nchp).*wind)/(beni-bsti+1)*2;
base56sfp=fft(base56(fsti:feni,Nchp).*wind)/(feni-fsti+1)*2;
base56srp=fft(base56(bsti:beni,Nchp).*wind)/(beni-bsti+1)*2;
base57sfp=fft(base57(fsti:feni,Nchp).*wind)/(feni-fsti+1)*2;
base57srp=fft(base57(bsti:beni,Nchp).*wind)/(beni-bsti+1)*2;
base58sfp=fft(base58(fsti:feni,Nchp).*wind)/(feni-fsti+1)*2;
base58srp=fft(base58(bsti:beni,Nchp).*wind)/(beni-bsti+1)*2;
base59sfp=fft(base59(fsti:feni,Nchp).*wind)/(feni-fsti+1)*2;
base59srp=fft(base59(bsti:beni,Nchp).*wind)/(beni-bsti+1)*2;
base510sfp=fft(base510(fsti:feni,Nchp).*wind)/(feni-fsti+1)*2;
base510srp=fft(base510(bsti:beni,Nchp).*wind)/(beni-bsti+1)*2;
base511sfp=fft(base511(fsti:feni,Nchp).*wind)/(feni-fsti+1)*2;
base511srp=fft(base511(bsti:beni,Nchp).*wind)/(beni-bsti+1)*2;

% Load data from tire pressure fault	driver front
importfile('DriverFrontTP10psi_1/Acceleration.txt');
tiredf11=data;
speedtdf11=speed(data,t);
aoadtdf11=angleofa(data,t);
importfile('DriverFrontTP10psi_2/Acceleration.txt');
tiredf12=data;
speedtdf12=speed(data,t);
aoadtdf12=angleofa(data,t);
importfile('DriverFrontTP10psi_3/Acceleration.txt');
tiredf13=data;
speedtdf13=speed(data,t);
aoadtdf13=angleofa(data,t);
importfile('DriverFrontTP10psi_4/Acceleration.txt');

```

```
tiredf14=data;
speedtdf14=speed(data,t);
aoadtdf14=angleofa(data,t);
importfile('DriverFrontTP10psi_5/Acceleration.txt');
tiredf15=data;
speedtdf15=speed(data,t);
aoadtdf15=angleofa(data,t);
importfile('DriverFrontTP10psi_6/Acceleration.txt');
tiredf16=data;
speedtdf16=speed(data,t);
aoadtdf16=angleofa(data,t);
importfile('DriverFrontTP10psi_7/Acceleration.txt');
tiredf17=data;
speedtdf17=speed(data,t);
aoadtdf17=angleofa(data,t);
importfile('DriverFrontTP10psi_8/Acceleration.txt');
tiredf18=data;
speedtdf18=speed(data,t);
aoadtdf18=angleofa(data,t);
importfile('DriverFrontTP10psi_9/Acceleration.txt');
tiredf19=data;
speedtdf19=speed(data,t);
aoadtdf19=angleofa(data,t);
importfile('DriverFrontTP10psi_10/Acceleration.txt');
tiredf110=data;
speedtdf110=speed(data,t);
aoadtdf110=angleofa(data,t);
importfile('DriverFrontTP10psi_11/Acceleration.txt');
tiredf111=data;
speedtdf111=speed(data,t);
aoadtdf111=angleofa(data,t);
importfile('DriverFrontTP10psi_12/Acceleration.txt');
tiredf112=data;
speedtdf112=speed(data,t);
aoadtdf112=angleofa(data,t);
importfile('DriverFrontTP10psi_13/Acceleration.txt');
tiredf113=data;
speedtdf113=speed(data,t);
aoadtdf113=angleofa(data,t);
importfile('DriverFrontTP10psi_14/Acceleration.txt');
tiredf114=data;
speedtdf114=speed(data,t);
aoadtdf114=angleofa(data,t);
importfile('DriverFrontTP10psi_15/Acceleration.txt');
tiredf115=data;
speedtdf115=speed(data,t);
aoadtdf115=angleofa(data,t);
importfile('DriverFrontTP10psi_16/Acceleration.txt');
tiredf116=data;
speedtdf116=speed(data,t);
aoadtdf116=angleofa(data,t);
importfile('DriverFrontTP10psi_17/Acceleration.txt');
tiredf117=data;
speedtdf117=speed(data,t);
aoadtdf117=angleofa(data,t);
importfile('DriverFrontTP10psi_18/Acceleration.txt');
tiredf118=data;
```

```

speedtdf118=speed(data,t);
aoadtdf118=angleofa(data,t);
importfile('DriverFrontTP10psi_19/Acceleration.txt');
tiredf119=data;
speedtdf119=speed(data,t);
aoadtdf119=angleofa(data,t);
importfile('DriverFrontTP10psi_20/Acceleration.txt');
tiredf120=data;
speedtdf120=speed(data,t);
aoadtdf120=angleofa(data,t);
importfile('DriverFrontTP10psi_21/Acceleration.txt');
tiredf121=data;
speedtdf121=speed(data,t);
aoadtdf121=angleofa(data,t);
importfile('DriverFrontTP10psi_22/Acceleration.txt');
tiredf122=data;
speedtdf122=speed(data,t);
aoadtdf122=angleofa(data,t);
importfile('DriverFrontTP10psi_23/Acceleration.txt');
tiredf123=data;
speedtdf123=speed(data,t);
aoadtdf123=angleofa(data,t);
importfile('DriverFrontTP10psi_24/Acceleration.txt');
tiredf124=data;
speedtdf124=speed(data,t);
aoadtdf124=angleofa(data,t);
importfile('DriverFrontTP10psi_25/Acceleration.txt');
tiredf125=data;
speedtdf125=speed(data,t);
aoadtdf125=angleofa(data,t);
importfile('DriverFrontTP10psi_26/Acceleration.txt');
tiredf126=data;
speedtdf126=speed(data,t);
aoadtdf126=angleofa(data,t);
importfile('DriverFrontTP10psi_27/Acceleration.txt');
tiredf127=data;
speedtdf127=speed(data,t);
aoadtdf127=angleofa(data,t);
importfile('DriverFrontTP10psi_28/Acceleration.txt');
tiredf128=data;
speedtdf128=speed(data,t);
aoadtdf128=angleofa(data,t);
importfile('DriverFrontTP10psi_29/Acceleration.txt');
tiredf129=data;
speedtdf129=speed(data,t);
aoadtdf129=angleofa(data,t);
importfile('DriverFrontTP10psi_30/Acceleration.txt');
tiredf130=data;
speedtdf130=speed(data,t);
aoadtdf130=angleofa(data,t);

% Calculate spectra for driver side tire fault
tiredf11sf=fft(tiredf11(fsti:feni,Nchd).*wind)/(feni-fsti+1)*2;
tiredf11sr=fft(tiredf11(bsti:beni,Nchd).*wind)/(beni-bsti+1)*2;
tiredf12sf=fft(tiredf12(fsti:feni,Nchd).*wind)/(feni-fsti+1)*2;
tiredf12sr=fft(tiredf12(bsti:beni,Nchd).*wind)/(beni-bsti+1)*2;
tiredf13sf=fft(tiredf13(fsti:feni,Nchd).*wind)/(feni-fsti+1)*2;

```



```
tiredf130sfp=fft(tiredf130(fsti:feni,Nchp).*wind)/(feni-fsti+1)*2;
tiredf130srp=fft(tiredf130(bsti:beni,Nchp).*wind)/(beni-bsti+1)*2;

% Load passenger front tire data
importfile('PassengerFrontTP10psi_1/Acceleration.txt');
tirepf11=data;
speedtpf11=speed(data,t);
aoadtpf11=angleofa(data,t);
importfile('PassengerFrontTP10psi_2/Acceleration.txt');
tirepf12=data;
speedtpf12=speed(data,t);
aoadtpf12=angleofa(data,t);
importfile('PassengerFrontTP10psi_3/Acceleration.txt');
tirepf13=data;
speedtpf13=speed(data,t);
aoadtpf13=angleofa(data,t);
importfile('PassengerFrontTP10psi_4/Acceleration.txt');
tirepf14=data;
speedtpf14=speed(data,t);
aoadtpf14=angleofa(data,t);
importfile('PassengerFrontTP10psi_5/Acceleration.txt');
tirepf15=data;
speedtpf15=speed(data,t);
aoadtpf15=angleofa(data,t);
importfile('PassengerFrontTP10psi_6/Acceleration.txt');
tirepf16=data;
speedtpf16=speed(data,t);
aoadtpf16=angleofa(data,t);
importfile('PassengerFrontTP10psi_7/Acceleration.txt');
tirepf17=data;
speedtpf17=speed(data,t);
aoadtpf17=angleofa(data,t);
importfile('PassengerFrontTP10psi_8/Acceleration.txt');
tirepf18=data;
speedtpf18=speed(data,t);
aoadtpf18=angleofa(data,t);
importfile('PassengerFrontTP10psi_9/Acceleration.txt');
tirepf19=data;
speedtpf19=speed(data,t);
aoadtpf19=angleofa(data,t);
importfile('PassengerFrontTP10psi_10/Acceleration.txt');
tirepf110=data;
speedtpf110=speed(data,t);
aoadtpf110=angleofa(data,t);
importfile('PassengerFrontTP10psi_11/Acceleration.txt');
tirepf111=data;
speedtpf111=speed(data,t);
aoadtpf111=angleofa(data,t);
importfile('PassengerFrontTP10psi_12/Acceleration.txt');
tirepf112=data;
speedtpf112=speed(data,t);
aoadtpf112=angleofa(data,t);
importfile('PassengerFrontTP10psi_13/Acceleration.txt');
tirepf113=data;
speedtpf113=speed(data,t);
aoadtpf113=angleofa(data,t);
importfile('PassengerFrontTP10psi_14/Acceleration.txt');
```

```
tirepf114=data;
speedtpf114=speed(data,t);
aoadtpf114=angleofa(data,t);
importfile('PassengerFrontTP10psi_15/Acceleration.txt');
tirepf115=data;
speedtpf115=speed(data,t);
aoadtpf115=angleofa(data,t);
importfile('PassengerFrontTP10psi_16/Acceleration.txt');
tirepf116=data;
speedtpf116=speed(data,t);
aoadtpf116=angleofa(data,t);
importfile('PassengerFrontTP10psi_17/Acceleration.txt');
tirepf117=data;
speedtpf117=speed(data,t);
aoadtpf117=angleofa(data,t);
importfile('PassengerFrontTP10psi_18/Acceleration.txt');
tirepf118=data;
speedtpf118=speed(data,t);
aoadtpf118=angleofa(data,t);
importfile('PassengerFrontTP10psi_19/Acceleration.txt');
tirepf119=data;
speedtpf119=speed(data,t);
aoadtpf119=angleofa(data,t);
importfile('PassengerFrontTP10psi_20/Acceleration.txt');
tirepf120=data;
speedtpf120=speed(data,t);
aoadtpf120=angleofa(data,t);
importfile('PassengerFrontTP10psi_21/Acceleration.txt');
tirepf121=data;
speedtpf121=speed(data,t);
aoadtpf121=angleofa(data,t);
importfile('PassengerFrontTP10psi_22/Acceleration.txt');
tirepf122=data;
speedtpf122=speed(data,t);
aoadtpf122=angleofa(data,t);
importfile('PassengerFrontTP10psi_23/Acceleration.txt');
tirepf123=data;
speedtpf123=speed(data,t);
aoadtpf123=angleofa(data,t);
importfile('PassengerFrontTP10psi_24/Acceleration.txt');
tirepf124=data;
speedtpf124=speed(data,t);
aoadtpf124=angleofa(data,t);
importfile('PassengerFrontTP10psi_25/Acceleration.txt');
tirepf125=data;
speedtpf125=speed(data,t);
aoadtpf125=angleofa(data,t);
importfile('PassengerFrontTP10psi_26/Acceleration.txt');
tirepf126=data;
speedtpf126=speed(data,t);
aoadtpf126=angleofa(data,t);
importfile('PassengerFrontTP10psi_27/Acceleration.txt');
tirepf127=data;
speedtpf127=speed(data,t);
aoadtpf127=angleofa(data,t);
importfile('PassengerFrontTP10psi_28/Acceleration.txt');
tirepf128=data;
```

```

speedtpf128=speed(data,t);
aoadtpf128=angleofa(data,t);
importfile('PassengerFrontTP10psi_29/Acceleration.txt');
tirepf129=data;
speedtpf129=speed(data,t);
aoadtpf129=angleofa(data,t);
importfile('PassengerFrontTP10psi_30/Acceleration.txt');
tirepf130=data;
speedtpf130=speed(data,t);
aoadtpf130=angleofa(data,t);

tirepf11sf=fft(tirepf11(fsti:feni,Nchd).*wind)/(feni-fsti+1)*2;
tirepf11sr=fft(tirepf11(bsti:beni,Nchd).*wind)/(beni-bsti+1)*2;
tirepf12sf=fft(tirepf12(fsti:feni,Nchd).*wind)/(feni-fsti+1)*2;
tirepf12sr=fft(tirepf12(bsti:beni,Nchd).*wind)/(beni-bsti+1)*2;
tirepf13sf=fft(tirepf13(fsti:feni,Nchd).*wind)/(feni-fsti+1)*2;
tirepf13sr=fft(tirepf13(bsti:beni,Nchd).*wind)/(beni-bsti+1)*2;
tirepf14sf=fft(tirepf14(fsti:feni,Nchd).*wind)/(feni-fsti+1)*2;
tirepf14sr=fft(tirepf14(bsti:beni,Nchd).*wind)/(beni-bsti+1)*2;
tirepf15sf=fft(tirepf15(fsti:feni,Nchd).*wind)/(feni-fsti+1)*2;
tirepf15sr=fft(tirepf15(bsti:beni,Nchd).*wind)/(beni-bsti+1)*2;
tirepf16sf=fft(tirepf16(fsti:feni,Nchd).*wind)/(feni-fsti+1)*2;
tirepf16sr=fft(tirepf16(bsti:beni,Nchd).*wind)/(beni-bsti+1)*2;
tirepf17sf=fft(tirepf17(fsti:feni,Nchd).*wind)/(feni-fsti+1)*2;
tirepf17sr=fft(tirepf17(bsti:beni,Nchd).*wind)/(beni-bsti+1)*2;
tirepf18sf=fft(tirepf18(fsti:feni,Nchd).*wind)/(feni-fsti+1)*2;
tirepf18sr=fft(tirepf18(bsti:beni,Nchd).*wind)/(beni-bsti+1)*2;
tirepf19sf=fft(tirepf19(fsti:feni,Nchd).*wind)/(feni-fsti+1)*2;
tirepf19sr=fft(tirepf19(bsti:beni,Nchd).*wind)/(beni-bsti+1)*2;
tirepf110sf=fft(tirepf110(fsti:feni,Nchd).*wind)/(feni-fsti+1)*2;
tirepf110sr=fft(tirepf110(bsti:beni,Nchd).*wind)/(beni-bsti+1)*2;
tirepf111sf=fft(tirepf111(fsti:feni,Nchd).*wind)/(feni-fsti+1)*2;
tirepf111sr=fft(tirepf111(bsti:beni,Nchd).*wind)/(beni-bsti+1)*2;
tirepf112sf=fft(tirepf112(fsti:feni,Nchd).*wind)/(feni-fsti+1)*2;
tirepf112sr=fft(tirepf112(bsti:beni,Nchd).*wind)/(beni-bsti+1)*2;
tirepf113sf=fft(tirepf113(fsti:feni,Nchd).*wind)/(feni-fsti+1)*2;
tirepf113sr=fft(tirepf113(bsti:beni,Nchd).*wind)/(beni-bsti+1)*2;
tirepf114sf=fft(tirepf114(fsti:feni,Nchd).*wind)/(feni-fsti+1)*2;
tirepf114sr=fft(tirepf114(bsti:beni,Nchd).*wind)/(beni-bsti+1)*2;
tirepf115sf=fft(tirepf115(fsti:feni,Nchd).*wind)/(feni-fsti+1)*2;
tirepf115sr=fft(tirepf115(bsti:beni,Nchd).*wind)/(beni-bsti+1)*2;
tirepf116sf=fft(tirepf116(fsti:feni,Nchd).*wind)/(feni-fsti+1)*2;
tirepf116sr=fft(tirepf116(bsti:beni,Nchd).*wind)/(beni-bsti+1)*2;
tirepf117sf=fft(tirepf117(fsti:feni,Nchd).*wind)/(feni-fsti+1)*2;
tirepf117sr=fft(tirepf117(bsti:beni,Nchd).*wind)/(beni-bsti+1)*2;
tirepf118sf=fft(tirepf118(fsti:feni,Nchd).*wind)/(feni-fsti+1)*2;
tirepf118sr=fft(tirepf118(bsti:beni,Nchd).*wind)/(beni-bsti+1)*2;
tirepf119sf=fft(tirepf119(fsti:feni,Nchd).*wind)/(feni-fsti+1)*2;
tirepf119sr=fft(tirepf119(bsti:beni,Nchd).*wind)/(beni-bsti+1)*2;
tirepf120sf=fft(tirepf120(fsti:feni,Nchd).*wind)/(feni-fsti+1)*2;
tirepf120sr=fft(tirepf120(bsti:beni,Nchd).*wind)/(beni-bsti+1)*2;
tirepf121sf=fft(tirepf121(fsti:feni,Nchd).*wind)/(feni-fsti+1)*2;
tirepf121sr=fft(tirepf121(bsti:beni,Nchd).*wind)/(beni-bsti+1)*2;
tirepf122sf=fft(tirepf122(fsti:feni,Nchd).*wind)/(feni-fsti+1)*2;
tirepf122sr=fft(tirepf122(bsti:beni,Nchd).*wind)/(beni-bsti+1)*2;
tirepf123sf=fft(tirepf123(fsti:feni,Nchd).*wind)/(feni-fsti+1)*2;
tirepf123sr=fft(tirepf123(bsti:beni,Nchd).*wind)/(beni-bsti+1)*2;

```



```

tirepf122sfp=fft(tirepf122(fsti:feni,Nchp).*wind)/(feni-fsti+1)*2;
tirepf122srp=fft(tirepf122(bsti:beni,Nchp).*wind)/(beni-bsti+1)*2;
tirepf123sfp=fft(tirepf123(fsti:feni,Nchp).*wind)/(feni-fsti+1)*2;
tirepf123srp=fft(tirepf123(bsti:beni,Nchp).*wind)/(beni-bsti+1)*2;
tirepf124sfp=fft(tirepf124(fsti:feni,Nchp).*wind)/(feni-fsti+1)*2;
tirepf124srp=fft(tirepf124(bsti:beni,Nchp).*wind)/(beni-bsti+1)*2;
tirepf125sfp=fft(tirepf125(fsti:feni,Nchp).*wind)/(feni-fsti+1)*2;
tirepf125srp=fft(tirepf125(bsti:beni,Nchp).*wind)/(beni-bsti+1)*2;
tirepf126sfp=fft(tirepf126(fsti:feni,Nchp).*wind)/(feni-fsti+1)*2;
tirepf126srp=fft(tirepf126(bsti:beni,Nchp).*wind)/(beni-bsti+1)*2;
tirepf127sfp=fft(tirepf127(fsti:feni,Nchp).*wind)/(feni-fsti+1)*2;
tirepf127srp=fft(tirepf127(bsti:beni,Nchp).*wind)/(beni-bsti+1)*2;
tirepf128sfp=fft(tirepf128(fsti:feni,Nchp).*wind)/(feni-fsti+1)*2;
tirepf128srp=fft(tirepf128(bsti:beni,Nchp).*wind)/(beni-bsti+1)*2;
tirepf129sfp=fft(tirepf129(fsti:feni,Nchp).*wind)/(feni-fsti+1)*2;
tirepf129srp=fft(tirepf129(bsti:beni,Nchp).*wind)/(beni-bsti+1)*2;
tirepf130sfp=fft(tirepf130(fsti:feni,Nchp).*wind)/(feni-fsti+1)*2;
tirepf130srp=fft(tirepf130(bsti:beni,Nchp).*wind)/(beni-bsti+1)*2;

% Load data from tire pressure fault/driver rear
importfile('DriverRearTP10psi_1/Acceleration.txt');
tiredr11=data;
speedtdr11=speed(data,t);
aoadtdr11=angleofa(data,t);
importfile('DriverRearTP10psi_2/Acceleration.txt');
tiredr12=data;
speedtdr12=speed(data,t);
aoadtdr12=angleofa(data,t);
importfile('DriverRearTP10psi_3/Acceleration.txt');
tiredr13=data;
speedtdr13=speed(data,t);
aoadtdr13=angleofa(data,t);
importfile('DriverRearTP10psi_4/Acceleration.txt');
tiredr14=data;
speedtdr14=speed(data,t);
aoadtdr14=angleofa(data,t);
importfile('DriverRearTP10psi_5/Acceleration.txt');
tiredr15=data;
speedtdr15=speed(data,t);
aoadtdr15=angleofa(data,t);
importfile('DriverRearTP10psi_6/Acceleration.txt');
tiredr16=data;
speedtdr16=speed(data,t);
aoadtdr16=angleofa(data,t);
importfile('DriverRearTP10psi_7/Acceleration.txt');
tiredr17=data;
speedtdr17=speed(data,t);
aoadtdr17=angleofa(data,t);
importfile('DriverRearTP10psi_8/Acceleration.txt');
tiredr18=data;
speedtdr18=speed(data,t);
aoadtdr18=angleofa(data,t);
importfile('DriverRearTP10psi_9/Acceleration.txt');
tiredr19=data;
speedtdr19=speed(data,t);
aoadtdr19=angleofa(data,t);
importfile('DriverRearTP10psi_10/Acceleration.txt');

```

```
tiredr110=data;
speedtdr110=speed(data,t);
aoadtdr110=angleofa(data,t);
importfile('DriverRearTP10psi_11/Acceleration.txt');
tiredr111=data;
speedtdr111=speed(data,t);
aoadtdr111=angleofa(data,t);
importfile('DriverRearTP10psi_12/Acceleration.txt');
tiredr112=data;
speedtdr112=speed(data,t);
aoadtdr112=angleofa(data,t);
importfile('DriverRearTP10psi_13/Acceleration.txt');
tiredr113=data;
speedtdr113=speed(data,t);
aoadtdr113=angleofa(data,t);
importfile('DriverRearTP10psi_14/Acceleration.txt');
tiredr114=data;
speedtdr114=speed(data,t);
aoadtdr114=angleofa(data,t);
importfile('DriverRearTP10psi_15/Acceleration.txt');
tiredr115=data;
speedtdr115=speed(data,t);
aoadtdr115=angleofa(data,t);
importfile('DriverRearTP10psi_16/Acceleration.txt');
tiredr116=data;
speedtdr116=speed(data,t);
aoadtdr116=angleofa(data,t);
importfile('DriverRearTP10psi_17/Acceleration.txt');
tiredr117=data;
speedtdr117=speed(data,t);
aoadtdr117=angleofa(data,t);
importfile('DriverRearTP10psi_18/Acceleration.txt');
tiredr118=data;
speedtdr118=speed(data,t);
aoadtdr118=angleofa(data,t);
importfile('DriverRearTP10psi_19/Acceleration.txt');
tiredr119=data;
speedtdr119=speed(data,t);
aoadtdr119=angleofa(data,t);
importfile('DriverRearTP10psi_20/Acceleration.txt');
tiredr120=data;
speedtdr120=speed(data,t);
aoadtdr120=angleofa(data,t);
importfile('DriverRearTP10psi_21/Acceleration.txt');
tiredr121=data;
speedtdr121=speed(data,t);
aoadtdr121=angleofa(data,t);
importfile('DriverRearTP10psi_22/Acceleration.txt');
tiredr122=data;
speedtdr122=speed(data,t);
aoadtdr122=angleofa(data,t);
importfile('DriverRearTP10psi_23/Acceleration.txt');
tiredr123=data;
speedtdr123=speed(data,t);
aoadtdr123=angleofa(data,t);
importfile('DriverRearTP10psi_24/Acceleration.txt');
tiredr124=data;
```

```

speedtdr124=speed(data,t);
aoadtdr124=angleofa(data,t);
importfile('DriverRearTP10psi_25/Acceleration.txt');
tiredr125=data;
speedtdr125=speed(data,t);
aoadtdr125=angleofa(data,t);
importfile('DriverRearTP10psi_26/Acceleration.txt');
tiredr126=data;
speedtdr126=speed(data,t);
aoadtdr126=angleofa(data,t);
importfile('DriverRearTP10psi_27/Acceleration.txt');
tiredr127=data;
speedtdr127=speed(data,t);
aoadtdr127=angleofa(data,t);
importfile('DriverRearTP10psi_28/Acceleration.txt');
tiredr128=data;
speedtdr128=speed(data,t);
aoadtdr128=angleofa(data,t);
importfile('DriverRearTP10psi_29/Acceleration.txt');
tiredr129=data;
speedtdr129=speed(data,t);
aoadtdr129=angleofa(data,t);
importfile('DriverRearTP10psi_30/Acceleration.txt');
tiredr130=data;
speedtdr130=speed(data,t);
aoadtdr130=angleofa(data,t);

% Calculate spectra for driver side tire fault
tiredr11sf=fft(tiredr11(fsti:feni,Nchd).*wind)/(feni-fsti+1)*2;
tiredr11sr=fft(tiredr11(bsti:beni,Nchd).*wind)/(beni-bsti+1)*2;
tiredr12sf=fft(tiredr12(fsti:feni,Nchd).*wind)/(feni-fsti+1)*2;
tiredr12sr=fft(tiredr12(bsti:beni,Nchd).*wind)/(beni-bsti+1)*2;
tiredr13sf=fft(tiredr13(fsti:feni,Nchd).*wind)/(feni-fsti+1)*2;
tiredr13sr=fft(tiredr13(bsti:beni,Nchd).*wind)/(beni-bsti+1)*2;
tiredr14sf=fft(tiredr14(fsti:feni,Nchd).*wind)/(feni-fsti+1)*2;
tiredr14sr=fft(tiredr14(bsti:beni,Nchd).*wind)/(beni-bsti+1)*2;
tiredr15sf=fft(tiredr15(fsti:feni,Nchd).*wind)/(feni-fsti+1)*2;
tiredr15sr=fft(tiredr15(bsti:beni,Nchd).*wind)/(beni-bsti+1)*2;
tiredr16sf=fft(tiredr16(fsti:feni,Nchd).*wind)/(feni-fsti+1)*2;
tiredr16sr=fft(tiredr16(bsti:beni,Nchd).*wind)/(beni-bsti+1)*2;
tiredr17sf=fft(tiredr17(fsti:feni,Nchd).*wind)/(feni-fsti+1)*2;
tiredr17sr=fft(tiredr17(bsti:beni,Nchd).*wind)/(beni-bsti+1)*2;
tiredr18sf=fft(tiredr18(fsti:feni,Nchd).*wind)/(feni-fsti+1)*2;
tiredr18sr=fft(tiredr18(bsti:beni,Nchd).*wind)/(beni-bsti+1)*2;
tiredr19sf=fft(tiredr19(fsti:feni,Nchd).*wind)/(feni-fsti+1)*2;
tiredr19sr=fft(tiredr19(bsti:beni,Nchd).*wind)/(beni-bsti+1)*2;
tiredr110sf=fft(tiredr110(fsti:feni,Nchd).*wind)/(feni-fsti+1)*2;
tiredr110sr=fft(tiredr110(bsti:beni,Nchd).*wind)/(beni-bsti+1)*2;
tiredr111sf=fft(tiredr111(fsti:feni,Nchd).*wind)/(feni-fsti+1)*2;
tiredr111sr=fft(tiredr111(bsti:beni,Nchd).*wind)/(beni-bsti+1)*2;
tiredr112sf=fft(tiredr112(fsti:feni,Nchd).*wind)/(feni-fsti+1)*2;
tiredr112sr=fft(tiredr112(bsti:beni,Nchd).*wind)/(beni-bsti+1)*2;
tiredr113sf=fft(tiredr113(fsti:feni,Nchd).*wind)/(feni-fsti+1)*2;
tiredr113sr=fft(tiredr113(bsti:beni,Nchd).*wind)/(beni-bsti+1)*2;
tiredr114sf=fft(tiredr114(fsti:feni,Nchd).*wind)/(feni-fsti+1)*2;
tiredr114sr=fft(tiredr114(bsti:beni,Nchd).*wind)/(beni-bsti+1)*2;
tiredr115sf=fft(tiredr115(fsti:feni,Nchd).*wind)/(feni-fsti+1)*2;

```

```

tiredr115sr=fft(tiredr115(bsti:beni,Nchd).*wind)/(beni-bsti+1)*2;
tiredr116sf=fft(tiredr116(fsti:feni,Nchd).*wind)/(feni-fsti+1)*2;
tiredr116sr=fft(tiredr116(bsti:beni,Nchd).*wind)/(beni-bsti+1)*2;
tiredr117sf=fft(tiredr117(fsti:feni,Nchd).*wind)/(feni-fsti+1)*2;
tiredr117sr=fft(tiredr117(bsti:beni,Nchd).*wind)/(beni-bsti+1)*2;
tiredr118sf=fft(tiredr118(fsti:feni,Nchd).*wind)/(feni-fsti+1)*2;
tiredr118sr=fft(tiredr118(bsti:beni,Nchd).*wind)/(beni-bsti+1)*2;
tiredr119sf=fft(tiredr119(fsti:feni,Nchd).*wind)/(feni-fsti+1)*2;
tiredr119sr=fft(tiredr119(bsti:beni,Nchd).*wind)/(beni-bsti+1)*2;
tiredr120sf=fft(tiredr120(fsti:feni,Nchd).*wind)/(feni-fsti+1)*2;
tiredr120sr=fft(tiredr120(bsti:beni,Nchd).*wind)/(beni-bsti+1)*2;
tiredr121sf=fft(tiredr121(fsti:feni,Nchd).*wind)/(feni-fsti+1)*2;
tiredr121sr=fft(tiredr121(bsti:beni,Nchd).*wind)/(beni-bsti+1)*2;
tiredr122sf=fft(tiredr122(fsti:feni,Nchd).*wind)/(feni-fsti+1)*2;
tiredr122sr=fft(tiredr122(bsti:beni,Nchd).*wind)/(beni-bsti+1)*2;
tiredr123sf=fft(tiredr123(fsti:feni,Nchd).*wind)/(feni-fsti+1)*2;
tiredr123sr=fft(tiredr123(bsti:beni,Nchd).*wind)/(beni-bsti+1)*2;
tiredr124sf=fft(tiredr124(fsti:feni,Nchd).*wind)/(feni-fsti+1)*2;
tiredr124sr=fft(tiredr124(bsti:beni,Nchd).*wind)/(beni-bsti+1)*2;
tiredr125sf=fft(tiredr125(fsti:feni,Nchd).*wind)/(feni-fsti+1)*2;
tiredr125sr=fft(tiredr125(bsti:beni,Nchd).*wind)/(beni-bsti+1)*2;
tiredr126sf=fft(tiredr126(fsti:feni,Nchd).*wind)/(feni-fsti+1)*2;
tiredr126sr=fft(tiredr126(bsti:beni,Nchd).*wind)/(beni-bsti+1)*2;
tiredr127sf=fft(tiredr127(fsti:feni,Nchd).*wind)/(feni-fsti+1)*2;
tiredr127sr=fft(tiredr127(bsti:beni,Nchd).*wind)/(beni-bsti+1)*2;
tiredr128sf=fft(tiredr128(fsti:feni,Nchd).*wind)/(feni-fsti+1)*2;
tiredr128sr=fft(tiredr128(bsti:beni,Nchd).*wind)/(beni-bsti+1)*2;
tiredr129sf=fft(tiredr129(fsti:feni,Nchd).*wind)/(feni-fsti+1)*2;
tiredr129sr=fft(tiredr129(bsti:beni,Nchd).*wind)/(beni-bsti+1)*2;
tiredr130sf=fft(tiredr130(fsti:feni,Nchd).*wind)/(feni-fsti+1)*2;
tiredr130sr=fft(tiredr130(bsti:beni,Nchd).*wind)/(beni-bsti+1)*2;

tiredr11sf=fft(tiredr11(fsti:feni,Nchp).*wind)/(feni-fsti+1)*2;
tiredr11srp=fft(tiredr11(bsti:beni,Nchp).*wind)/(beni-bsti+1)*2;
tiredr12sf=fft(tiredr12(fsti:feni,Nchp).*wind)/(feni-fsti+1)*2;
tiredr12srp=fft(tiredr12(bsti:beni,Nchp).*wind)/(beni-bsti+1)*2;
tiredr13sf=fft(tiredr13(fsti:feni,Nchp).*wind)/(feni-fsti+1)*2;
tiredr13srp=fft(tiredr13(bsti:beni,Nchp).*wind)/(beni-bsti+1)*2;
tiredr14sf=fft(tiredr14(fsti:feni,Nchp).*wind)/(feni-fsti+1)*2;
tiredr14srp=fft(tiredr14(bsti:beni,Nchp).*wind)/(beni-bsti+1)*2;
tiredr15sf=fft(tiredr15(fsti:feni,Nchp).*wind)/(feni-fsti+1)*2;
tiredr15srp=fft(tiredr15(bsti:beni,Nchp).*wind)/(beni-bsti+1)*2;
tiredr16sf=fft(tiredr16(fsti:feni,Nchp).*wind)/(feni-fsti+1)*2;
tiredr16srp=fft(tiredr16(bsti:beni,Nchp).*wind)/(beni-bsti+1)*2;
tiredr17sf=fft(tiredr17(fsti:feni,Nchp).*wind)/(feni-fsti+1)*2;
tiredr17srp=fft(tiredr17(bsti:beni,Nchp).*wind)/(beni-bsti+1)*2;
tiredr18sf=fft(tiredr18(fsti:feni,Nchp).*wind)/(feni-fsti+1)*2;
tiredr18srp=fft(tiredr18(bsti:beni,Nchp).*wind)/(beni-bsti+1)*2;
tiredr19sf=fft(tiredr19(fsti:feni,Nchp).*wind)/(feni-fsti+1)*2;
tiredr19srp=fft(tiredr19(bsti:beni,Nchp).*wind)/(beni-bsti+1)*2;
tiredr110sf=fft(tiredr110(fsti:feni,Nchp).*wind)/(feni-fsti+1)*2;
tiredr110srp=fft(tiredr110(bsti:beni,Nchp).*wind)/(beni-bsti+1)*2;
tiredr111sf=fft(tiredr111(fsti:feni,Nchp).*wind)/(feni-fsti+1)*2;
tiredr111srp=fft(tiredr111(bsti:beni,Nchp).*wind)/(beni-bsti+1)*2;
tiredr112sf=fft(tiredr112(fsti:feni,Nchp).*wind)/(feni-fsti+1)*2;
tiredr112srp=fft(tiredr112(bsti:beni,Nchp).*wind)/(beni-bsti+1)*2;
tiredr113sf=fft(tiredr113(fsti:feni,Nchp).*wind)/(feni-fsti+1)*2;

```

```
tiredr113srp=fft(tiredr113(bsti:beni,Nchp).*wind)/(beni-bsti+1)*2;
tiredr114sfp=fft(tiredr114(fsti:feni,Nchp).*wind)/(feni-fsti+1)*2;
tiredr114srp=fft(tiredr114(bsti:beni,Nchp).*wind)/(beni-bsti+1)*2;
tiredr115sfp=fft(tiredr115(fsti:feni,Nchp).*wind)/(feni-fsti+1)*2;
tiredr115srp=fft(tiredr115(bsti:beni,Nchp).*wind)/(beni-bsti+1)*2;
tiredr116sfp=fft(tiredr116(fsti:feni,Nchp).*wind)/(feni-fsti+1)*2;
tiredr116srp=fft(tiredr116(bsti:beni,Nchp).*wind)/(beni-bsti+1)*2;
tiredr117sfp=fft(tiredr117(fsti:feni,Nchp).*wind)/(feni-fsti+1)*2;
tiredr117srp=fft(tiredr117(bsti:beni,Nchp).*wind)/(beni-bsti+1)*2;
tiredr118sfp=fft(tiredr118(fsti:feni,Nchp).*wind)/(feni-fsti+1)*2;
tiredr118srp=fft(tiredr118(bsti:beni,Nchp).*wind)/(beni-bsti+1)*2;
tiredr119sfp=fft(tiredr119(fsti:feni,Nchp).*wind)/(feni-fsti+1)*2;
tiredr119srp=fft(tiredr119(bsti:beni,Nchp).*wind)/(beni-bsti+1)*2;
tiredr120sfp=fft(tiredr120(fsti:feni,Nchp).*wind)/(feni-fsti+1)*2;
tiredr120srp=fft(tiredr120(bsti:beni,Nchp).*wind)/(beni-bsti+1)*2;
tiredr121sfp=fft(tiredr121(fsti:feni,Nchp).*wind)/(feni-fsti+1)*2;
tiredr121srp=fft(tiredr121(bsti:beni,Nchp).*wind)/(beni-bsti+1)*2;
tiredr122sfp=fft(tiredr122(fsti:feni,Nchp).*wind)/(feni-fsti+1)*2;
tiredr122srp=fft(tiredr122(bsti:beni,Nchp).*wind)/(beni-bsti+1)*2;
tiredr123sfp=fft(tiredr123(fsti:feni,Nchp).*wind)/(feni-fsti+1)*2;
tiredr123srp=fft(tiredr123(bsti:beni,Nchp).*wind)/(beni-bsti+1)*2;
tiredr124sfp=fft(tiredr124(fsti:feni,Nchp).*wind)/(feni-fsti+1)*2;
tiredr124srp=fft(tiredr124(bsti:beni,Nchp).*wind)/(beni-bsti+1)*2;
tiredr125sfp=fft(tiredr125(fsti:feni,Nchp).*wind)/(feni-fsti+1)*2;
tiredr125srp=fft(tiredr125(bsti:beni,Nchp).*wind)/(beni-bsti+1)*2;
tiredr126sfp=fft(tiredr126(fsti:feni,Nchp).*wind)/(feni-fsti+1)*2;
tiredr126srp=fft(tiredr126(bsti:beni,Nchp).*wind)/(beni-bsti+1)*2;
tiredr127sfp=fft(tiredr127(fsti:feni,Nchp).*wind)/(feni-fsti+1)*2;
tiredr127srp=fft(tiredr127(bsti:beni,Nchp).*wind)/(beni-bsti+1)*2;
tiredr128sfp=fft(tiredr128(fsti:feni,Nchp).*wind)/(feni-fsti+1)*2;
tiredr128srp=fft(tiredr128(bsti:beni,Nchp).*wind)/(beni-bsti+1)*2;
tiredr129sfp=fft(tiredr129(fsti:feni,Nchp).*wind)/(feni-fsti+1)*2;
tiredr129srp=fft(tiredr129(bsti:beni,Nchp).*wind)/(beni-bsti+1)*2;
tiredr130sfp=fft(tiredr130(fsti:feni,Nchp).*wind)/(feni-fsti+1)*2;
tiredr130srp=fft(tiredr130(bsti:beni,Nchp).*wind)/(beni-bsti+1)*2;

% Load passenger rear tire data
importfile('PassengerRearTP10psi_1/Acceleration.txt');
tirepr11=data;
speedptr11=speed(data,t);
aoadptr11=angleofa(data,t);
importfile('PassengerRearTP10psi_2/Acceleration.txt');
tirepr12=data;
speedptr12=speed(data,t);
aoadptr12=angleofa(data,t);
importfile('PassengerRearTP10psi_3/Acceleration.txt');
tirepr13=data;
speedptr13=speed(data,t);
aoadptr13=angleofa(data,t);
importfile('PassengerRearTP10psi_4/Acceleration.txt');
tirepr14=data;
speedptr14=speed(data,t);
aoadptr14=angleofa(data,t);
importfile('PassengerRearTP10psi_5/Acceleration.txt');
tirepr15=data;
speedptr15=speed(data,t);
aoadptr15=angleofa(data,t);
```

```
importfile('PassengerRearTP10psi_6/Acceleration.txt');
tirepr16=data;
speedptr16=speed(data,t);
aoadptr16=angleofa(data,t);
importfile('PassengerRearTP10psi_7/Acceleration.txt');
tirepr17=data;
speedptr17=speed(data,t);
aoadptr17=angleofa(data,t);
importfile('PassengerRearTP10psi_8/Acceleration.txt');
tirepr18=data;
speedptr18=speed(data,t);
aoadptr18=angleofa(data,t);
importfile('PassengerRearTP10psi_9/Acceleration.txt');
tirepr19=data;
speedptr19=speed(data,t);
aoadptr19=angleofa(data,t);
importfile('PassengerRearTP10psi_10/Acceleration.txt');
tirepr110=data;
speedptr110=speed(data,t);
aoadptr110=angleofa(data,t);
importfile('PassengerRearTP10psi_11/Acceleration.txt');
tirepr111=data;
speedptr111=speed(data,t);
aoadptr111=angleofa(data,t);
importfile('PassengerRearTP10psi_12/Acceleration.txt');
tirepr112=data;
speedptr112=speed(data,t);
aoadptr112=angleofa(data,t);
importfile('PassengerRearTP10psi_13/Acceleration.txt');
tirepr113=data;
speedptr113=speed(data,t);
aoadptr113=angleofa(data,t);
importfile('PassengerRearTP10psi_14/Acceleration.txt');
tirepr114=data;
speedptr114=speed(data,t);
aoadptr114=angleofa(data,t);
importfile('PassengerRearTP10psi_15/Acceleration.txt');
tirepr115=data;
speedptr115=speed(data,t);
aoadptr115=angleofa(data,t);
importfile('PassengerRearTP10psi_16/Acceleration.txt');
tirepr116=data;
speedptr116=speed(data,t);
aoadptr116=angleofa(data,t);
importfile('PassengerRearTP10psi_17/Acceleration.txt');
tirepr117=data;
speedptr117=speed(data,t);
aoadptr117=angleofa(data,t);
importfile('PassengerRearTP10psi_18/Acceleration.txt');
tirepr118=data;
speedptr118=speed(data,t);
aoadptr118=angleofa(data,t);
importfile('PassengerRearTP10psi_19/Acceleration.txt');
tirepr119=data;
speedptr119=speed(data,t);
aoadptr119=angleofa(data,t);
importfile('PassengerRearTP10psi_20/Acceleration.txt');
```

```
tirepr120=data;
speedtpr120=speed(data,t);
aoadtp120=angleofa(data,t);
importfile('PassengerRearTP10psi_21/Acceleration.txt');
tirepr121=data;
speedtpr121=speed(data,t);
aoadtp121=angleofa(data,t);
importfile('PassengerRearTP10psi_22/Acceleration.txt');
tirepr122=data;
speedtpr122=speed(data,t);
aoadtp122=angleofa(data,t);
importfile('PassengerRearTP10psi_23/Acceleration.txt');
tirepr123=data;
speedtpr123=speed(data,t);
aoadtp123=angleofa(data,t);
importfile('PassengerRearTP10psi_24/Acceleration.txt');
tirepr124=data;
speedtpr124=speed(data,t);
aoadtp124=angleofa(data,t);
importfile('PassengerRearTP10psi_25/Acceleration.txt');
tirepr125=data;
speedtpr125=speed(data,t);
aoadtp125=angleofa(data,t);
importfile('PassengerRearTP10psi_26/Acceleration.txt');
tirepr126=data;
speedtpr126=speed(data,t);
aoadtp126=angleofa(data,t);
importfile('PassengerRearTP10psi_27/Acceleration.txt');
tirepr127=data;
speedtpr127=speed(data,t);
aoadtp127=angleofa(data,t);
importfile('PassengerRearTP10psi_28/Acceleration.txt');
tirepr128=data;
speedtpr128=speed(data,t);
aoadtp128=angleofa(data,t);
importfile('PassengerRearTP10psi_29/Acceleration.txt');
tirepr129=data;
speedtpr129=speed(data,t);
aoadtp129=angleofa(data,t);
importfile('PassengerRearTP10psi_30/Acceleration.txt');
tirepr130=data;
speedtpr130=speed(data,t);
aoadtp130=angleofa(data,t);

tirepr11sf=fft(tirepr11(fsti:feni,Nchd).*wind)/(feni-fsti+1)*2;
tirepr11sr=fft(tirepr11(bsti:beni,Nchd).*wind)/(beni-bsti+1)*2;
tirepr12sf=fft(tirepr12(fsti:feni,Nchd).*wind)/(feni-fsti+1)*2;
tirepr12sr=fft(tirepr12(bsti:beni,Nchd).*wind)/(beni-bsti+1)*2;
tirepr13sf=fft(tirepr13(fsti:feni,Nchd).*wind)/(feni-fsti+1)*2;
tirepr13sr=fft(tirepr13(bsti:beni,Nchd).*wind)/(beni-bsti+1)*2;
tirepr14sf=fft(tirepr14(fsti:feni,Nchd).*wind)/(feni-fsti+1)*2;
tirepr14sr=fft(tirepr14(bsti:beni,Nchd).*wind)/(beni-bsti+1)*2;
tirepr15sf=fft(tirepr15(fsti:feni,Nchd).*wind)/(feni-fsti+1)*2;
tirepr15sr=fft(tirepr15(bsti:beni,Nchd).*wind)/(beni-bsti+1)*2;
tirepr16sf=fft(tirepr16(fsti:feni,Nchd).*wind)/(feni-fsti+1)*2;
tirepr16sr=fft(tirepr16(bsti:beni,Nchd).*wind)/(beni-bsti+1)*2;
tirepr17sf=fft(tirepr17(fsti:feni,Nchd).*wind)/(feni-fsti+1)*2;
```



```

tirepr15srp=fft(tirepr15(bsti:beni,Nchp).*wind)/(beni-bsti+1)*2;
tirepr16sfp=fft(tirepr16(fsti:feni,Nchp).*wind)/(feni-fsti+1)*2;
tirepr16srp=fft(tirepr16(bsti:beni,Nchp).*wind)/(beni-bsti+1)*2;
tirepr17sfp=fft(tirepr17(fsti:feni,Nchp).*wind)/(feni-fsti+1)*2;
tirepr17srp=fft(tirepr17(bsti:beni,Nchp).*wind)/(beni-bsti+1)*2;
tirepr18sfp=fft(tirepr18(fsti:feni,Nchp).*wind)/(feni-fsti+1)*2;
tirepr18srp=fft(tirepr18(bsti:beni,Nchp).*wind)/(beni-bsti+1)*2;
tirepr19sfp=fft(tirepr19(fsti:feni,Nchp).*wind)/(feni-fsti+1)*2;
tirepr19srp=fft(tirepr19(bsti:beni,Nchp).*wind)/(beni-bsti+1)*2;
tirepr110sfp=fft(tirepr110(fsti:feni,Nchp).*wind)/(feni-fsti+1)*2;
tirepr110srp=fft(tirepr110(bsti:beni,Nchp).*wind)/(beni-bsti+1)*2;
tirepr111sfp=fft(tirepr111(fsti:feni,Nchp).*wind)/(feni-fsti+1)*2;
tirepr111srp=fft(tirepr111(bsti:beni,Nchp).*wind)/(beni-bsti+1)*2;
tirepr112sfp=fft(tirepr112(fsti:feni,Nchp).*wind)/(feni-fsti+1)*2;
tirepr112srp=fft(tirepr112(bsti:beni,Nchp).*wind)/(beni-bsti+1)*2;
tirepr113sfp=fft(tirepr113(fsti:feni,Nchp).*wind)/(feni-fsti+1)*2;
tirepr113srp=fft(tirepr113(bsti:beni,Nchp).*wind)/(beni-bsti+1)*2;
tirepr114sfp=fft(tirepr114(fsti:feni,Nchp).*wind)/(feni-fsti+1)*2;
tirepr114srp=fft(tirepr114(bsti:beni,Nchp).*wind)/(beni-bsti+1)*2;
tirepr115sfp=fft(tirepr115(fsti:feni,Nchp).*wind)/(feni-fsti+1)*2;
tirepr115srp=fft(tirepr115(bsti:beni,Nchp).*wind)/(beni-bsti+1)*2;
tirepr116sfp=fft(tirepr116(fsti:feni,Nchp).*wind)/(feni-fsti+1)*2;
tirepr116srp=fft(tirepr116(bsti:beni,Nchp).*wind)/(beni-bsti+1)*2;
tirepr117sfp=fft(tirepr117(fsti:feni,Nchp).*wind)/(feni-fsti+1)*2;
tirepr117srp=fft(tirepr117(bsti:beni,Nchp).*wind)/(beni-bsti+1)*2;
tirepr118sfp=fft(tirepr118(fsti:feni,Nchp).*wind)/(feni-fsti+1)*2;
tirepr118srp=fft(tirepr118(bsti:beni,Nchp).*wind)/(beni-bsti+1)*2;
tirepr119sfp=fft(tirepr119(fsti:feni,Nchp).*wind)/(feni-fsti+1)*2;
tirepr119srp=fft(tirepr119(bsti:beni,Nchp).*wind)/(beni-bsti+1)*2;
tirepr120sfp=fft(tirepr120(fsti:feni,Nchp).*wind)/(feni-fsti+1)*2;
tirepr120srp=fft(tirepr120(bsti:beni,Nchp).*wind)/(beni-bsti+1)*2;
tirepr121sfp=fft(tirepr121(fsti:feni,Nchp).*wind)/(feni-fsti+1)*2;
tirepr121srp=fft(tirepr121(bsti:beni,Nchp).*wind)/(beni-bsti+1)*2;
tirepr122sfp=fft(tirepr122(fsti:feni,Nchp).*wind)/(feni-fsti+1)*2;
tirepr122srp=fft(tirepr122(bsti:beni,Nchp).*wind)/(beni-bsti+1)*2;
tirepr123sfp=fft(tirepr123(fsti:feni,Nchp).*wind)/(feni-fsti+1)*2;
tirepr123srp=fft(tirepr123(bsti:beni,Nchp).*wind)/(beni-bsti+1)*2;
tirepr124sfp=fft(tirepr124(fsti:feni,Nchp).*wind)/(feni-fsti+1)*2;
tirepr124srp=fft(tirepr124(bsti:beni,Nchp).*wind)/(beni-bsti+1)*2;
tirepr125sfp=fft(tirepr125(fsti:feni,Nchp).*wind)/(feni-fsti+1)*2;
tirepr125srp=fft(tirepr125(bsti:beni,Nchp).*wind)/(beni-bsti+1)*2;
tirepr126sfp=fft(tirepr126(fsti:feni,Nchp).*wind)/(feni-fsti+1)*2;
tirepr126srp=fft(tirepr126(bsti:beni,Nchp).*wind)/(beni-bsti+1)*2;
tirepr127sfp=fft(tirepr127(fsti:feni,Nchp).*wind)/(feni-fsti+1)*2;
tirepr127srp=fft(tirepr127(bsti:beni,Nchp).*wind)/(beni-bsti+1)*2;
tirepr128sfp=fft(tirepr128(fsti:feni,Nchp).*wind)/(feni-fsti+1)*2;
tirepr128srp=fft(tirepr128(bsti:beni,Nchp).*wind)/(beni-bsti+1)*2;
tirepr129sfp=fft(tirepr129(fsti:feni,Nchp).*wind)/(feni-fsti+1)*2;
tirepr129srp=fft(tirepr129(bsti:beni,Nchp).*wind)/(beni-bsti+1)*2;
tirepr130sfp=fft(tirepr130(fsti:feni,Nchp).*wind)/(feni-fsti+1)*2;
tirepr130srp=fft(tirepr130(bsti:beni,Nchp).*wind)/(beni-bsti+1)*2;

% Loop through diagnostic parameters (thresholds, etc.)
% to generate receiver operating characteristic

for kk=1:10,

```

```

temp=linspace(0.1,4,10); % Iterate on threshold for fault detection
0.1sigma to 4sigma
thresh=temp(kk)

% Best ranges for front tire pressure faults
frng=[round(1+20/f(2)):round(1+30/f(2))
round(1+60/f(2)):round(1+80/f(2)) round(1+95/f(2)):round(1+110/f(2))
round(1+140/f(2)):round(1+180/f(2))]; % Best for z direction
acceleration
frng=[round(1+20/f(2)):round(1+30/f(2))
round(1+60/f(2)):round(1+80/f(2)) round(1+95/f(2)):round(1+110/f(2))];
% Best for z direction acceleration
%frng=[round(1+10/f(2)):round(1+15/f(2))]; % Best for Y direction
acceleration
%frng=[round(1+10/f(2)):round(1+15/f(2))]; % Best for x direction
acceleration

% Regression analysis of baseline data

X=[speedb11 speedb12 speedb13 speedb14 speedb15 speedb16 speedb17
speedb18 speedb19 ...
    speedb110 speedb111 speedb112 speedb113 speedb114 speedb115
speedb116 speedb117 speedb118 ...
    speedb119 speedb120 speedb121 speedb122 speedb123 speedb124
speedb125 speedb126 speedb127 ...
    speedb128 speedb129 speedb130 speedb21 speedb22 speedb23 speedb24
speedb25 speedb26 ...
    speedb27 speedb28 speedb29 speedb210 speedb211 speedb31 speedb32
speedb33 speedb34 speedb35 speedb36 ...
    speedb37 speedb38 speedb39 speedb310 speedb311 speedb41 speedb42
speedb43 speedb44 speedb45 speedb46 ...
    speedb47 speedb48 speedb49 speedb410 speedb411 speedb51 speedb52
speedb53 speedb54 speedb55 speedb56 ...
    speedb57 speedb58 speedb59 speedb510 speedb511];
Y=[aoadb11 aoadb12 aoadb13 aoadb14 aoadb15 aoadb16 aoadb17 aoadb18
aoadb19 ...
    aoadb110 aoadb111 aoadb112 aoadb113 aoadb114 aoadb115 aoadb116
aoadb117 aoadb118 ...
    aoadb119 aoadb120 aoadb121 aoadb122 aoadb123 aoadb124 aoadb125
aoadb126 aoadb127 ...
    aoadb128 aoadb129 aoadb130 aoadb21 aoadb22 aoadb23 aoadb24 aoadb25
aoadb26 ...
    aoadb27 aoadb28 aoadb29 aoadb210 aoadb211 aoadb31 aoadb32 aoadb33
aoadb34 aoadb35 aoadb36 ...
    aoadb37 aoadb38 aoadb39 aoadb310 aoadb311 aoadb41 aoadb42 aoadb43
aoadb44 aoadb45 aoadb46 ...
    aoadb47 aoadb48 aoadb49 aoadb410 aoadb411 aoadb51 aoadb52 aoadb53
aoadb54 aoadb55 aoadb56 ...
    aoadb57 aoadb58 aoadb59 aoadb510 aoadb511];

% Calculate indices for use in regression analysis

% Driver front
fibd=[sum(abs(base11sf(frng))) sum(abs(base12sf(frng)))
sum(abs(base13sf(frng))) ...

```

```

        sum(abs(base14sf(frng))) sum(abs(base15sf(frng)))
sum(abs(base16sf(frng))) ...
    sum(abs(base17sf(frng))) sum(abs(base18sf(frng)))
sum(abs(base19sf(frng))) ...
    sum(abs(base110sf(frng))) sum(abs(base111sf(frng)))
sum(abs(base112sf(frng))) ...
    sum(abs(base113sf(frng))) sum(abs(base114sf(frng)))
sum(abs(base115sf(frng))) ...
    sum(abs(base116sf(frng))) sum(abs(base117sf(frng)))
sum(abs(base118sf(frng))) ...
    sum(abs(base119sf(frng))) sum(abs(base120sf(frng)))
sum(abs(base121sf(frng))) ...
    sum(abs(base122sf(frng))) sum(abs(base123sf(frng)))
sum(abs(base124sf(frng))) ...
    sum(abs(base125sf(frng))) sum(abs(base126sf(frng)))
sum(abs(base127sf(frng))) ...
    sum(abs(base128sf(frng))) sum(abs(base129sf(frng)))
sum(abs(base130sf(frng)))];
fib2d=[sum(abs(base21sf(frng))) sum(abs(base22sf(frng)))
sum(abs(base23sf(frng))) ...
    sum(abs(base24sf(frng))) sum(abs(base25sf(frng)))
sum(abs(base26sf(frng))) ...
    sum(abs(base27sf(frng))) sum(abs(base28sf(frng)))
sum(abs(base29sf(frng))) ...
    sum(abs(base210sf(frng))) sum(abs(base211sf(frng)))]];
fib3d=[sum(abs(base31sf(frng))) sum(abs(base32sf(frng)))
sum(abs(base33sf(frng))) ...
    sum(abs(base34sf(frng))) sum(abs(base35sf(frng)))
sum(abs(base36sf(frng))) ...
    sum(abs(base37sf(frng))) sum(abs(base38sf(frng)))
sum(abs(base39sf(frng))) ...
    sum(abs(base310sf(frng))) sum(abs(base311sf(frng)))]];
fib4d=[sum(abs(base41sf(frng))) sum(abs(base42sf(frng)))
sum(abs(base43sf(frng))) ...
    sum(abs(base44sf(frng))) sum(abs(base45sf(frng)))
sum(abs(base46sf(frng))) ...
    sum(abs(base47sf(frng))) sum(abs(base48sf(frng)))
sum(abs(base49sf(frng))) ...
    sum(abs(base410sf(frng))) sum(abs(base411sf(frng)))]];
fib5d=[sum(abs(base51sf(frng))) sum(abs(base52sf(frng)))
sum(abs(base53sf(frng))) ...
    sum(abs(base54sf(frng))) sum(abs(base55sf(frng)))
sum(abs(base56sf(frng))) ...
    sum(abs(base57sf(frng))) sum(abs(base58sf(frng)))
sum(abs(base59sf(frng))) ...
    sum(abs(base510sf(frng))) sum(abs(base511sf(frng)))]];

Zd=[fibd fib2d fib3d fib4d fib5d];

% Curve fit baseline driver front
pd=polyfit(X,Zd,2);
md=mean(Zd-(pd(1)*X.^2+pd(2)*X+pd(3)));
stdd=std(Zd-(pd(1)*X.^2+pd(2)*X+pd(3)));

% Driver rear
fibdr=[sum(abs(base11sr(frng))) sum(abs(base12sr(frng)))

```

```

sum(abs(base13sr(frng))) ...
    sum(abs(base14sr(frng))) sum(abs(base15sr(frng)))
sum(abs(base16sr(frng))) ...
    sum(abs(base17sr(frng))) sum(abs(base18sr(frng)))
sum(abs(base19sr(frng))) ...
    sum(abs(base10sr(frng))) sum(abs(base11sr(frng)))
sum(abs(base12sr(frng))) ...
    sum(abs(base13sr(frng))) sum(abs(base14sr(frng)))
sum(abs(base15sr(frng))) ...
    sum(abs(base16sr(frng))) sum(abs(base17sr(frng)))
sum(abs(base18sr(frng))) ...
    sum(abs(base19sr(frng))) sum(abs(base20sr(frng)))
sum(abs(base21sr(frng))) ...
    sum(abs(base22sr(frng))) sum(abs(base23sr(frng)))
sum(abs(base24sr(frng))) ...
    sum(abs(base25sr(frng))) sum(abs(base26sr(frng)))
sum(abs(base27sr(frng))) ...
    sum(abs(base28sr(frng))) sum(abs(base29sr(frng)))
sum(abs(base29sr(frng))) ...
    sum(abs(base210sr(frng))) sum(abs(base211sr(frng)));
fib2dr=[sum(abs(base21sr(frng))) sum(abs(base22sr(frng)))
sum(abs(base23sr(frng))) ...
    sum(abs(base24sr(frng))) sum(abs(base25sr(frng)))
sum(abs(base26sr(frng))) ...
    sum(abs(base27sr(frng))) sum(abs(base28sr(frng)))
sum(abs(base29sr(frng))) ...
    sum(abs(base210sr(frng))) sum(abs(base211sr(frng)));
fib3dr=[sum(abs(base31sr(frng))) sum(abs(base32sr(frng)))
sum(abs(base33sr(frng))) ...
    sum(abs(base34sr(frng))) sum(abs(base35sr(frng)))
sum(abs(base36sr(frng))) ...
    sum(abs(base37sr(frng))) sum(abs(base38sr(frng)))
sum(abs(base39sr(frng))) ...
    sum(abs(base310sr(frng))) sum(abs(base311sr(frng)));
fib4dr=[sum(abs(base41sr(frng))) sum(abs(base42sr(frng)))
sum(abs(base43sr(frng))) ...
    sum(abs(base44sr(frng))) sum(abs(base45sr(frng)))
sum(abs(base46sr(frng))) ...
    sum(abs(base47sr(frng))) sum(abs(base48sr(frng)))
sum(abs(base49sr(frng))) ...
    sum(abs(base410sr(frng))) sum(abs(base411sr(frng)));
fib5dr=[sum(abs(base51sr(frng))) sum(abs(base52sr(frng)))
sum(abs(base53sr(frng))) ...
    sum(abs(base54sr(frng))) sum(abs(base55sr(frng)))
sum(abs(base56sr(frng))) ...
    sum(abs(base57sr(frng))) sum(abs(base58sr(frng)))
sum(abs(base59sr(frng))) ...
    sum(abs(base510sr(frng))) sum(abs(base511sr(frng)));
Zdr=[fibdr fib2dr fib3dr fib4dr fib5dr];

% Curve fit baseline driver rear
pdr=polyfit(X,Zdr,2);
mdr=mean(Zdr-(pdr(1)*X.^2+pdr(2)*X+pdr(3)));
stddr=std(Zdr-(pdr(1)*X.^2+pdr(2)*X+pdr(3)));

% Passenger front

```

```

fibp=[sum(abs(base11sfp(frng))) sum(abs(base12sfp(frng)))
sum(abs(base13sfp(frng))) ...
    sum(abs(base14sfp(frng))) sum(abs(base15sfp(frng)))
sum(abs(base16sfp(frng))) ...
    sum(abs(base17sfp(frng))) sum(abs(base18sfp(frng)))
sum(abs(base19sfp(frng))) ...
    sum(abs(base110sfp(frng))) sum(abs(base111sfp(frng)))
sum(abs(base112sfp(frng))) ...
    sum(abs(base113sfp(frng))) sum(abs(base114sfp(frng)))
sum(abs(base115sfp(frng))) ...
    sum(abs(base116sfp(frng))) sum(abs(base117sfp(frng)))
sum(abs(base118sfp(frng))) ...
    sum(abs(base119sfp(frng))) sum(abs(base120sfp(frng)))
sum(abs(base121sfp(frng))) ...
    sum(abs(base122sfp(frng))) sum(abs(base123sfp(frng)))
sum(abs(base124sfp(frng))) ...
    sum(abs(base125sfp(frng))) sum(abs(base126sfp(frng)))
sum(abs(base127sfp(frng))) ...
    sum(abs(base128sfp(frng))) sum(abs(base129sfp(frng)))
sum(abs(base130sfp(frng))];;
fib2p=[sum(abs(base21sfp(frng))) sum(abs(base22sfp(frng)))
sum(abs(base23sfp(frng))) ...
    sum(abs(base24sfp(frng))) sum(abs(base25sfp(frng)))
sum(abs(base26sfp(frng))) ...
    sum(abs(base27sfp(frng))) sum(abs(base28sfp(frng)))
sum(abs(base29sfp(frng))) ...
    sum(abs(base210sfp(frng))) sum(abs(base211sfp(frng)))];;
fib3p=[sum(abs(base31sfp(frng))) sum(abs(base32sfp(frng)))
sum(abs(base33sfp(frng))) ...
    sum(abs(base34sfp(frng))) sum(abs(base35sfp(frng)))
sum(abs(base36sfp(frng))) ...
    sum(abs(base37sfp(frng))) sum(abs(base38sfp(frng)))
sum(abs(base39sfp(frng))) ...
    sum(abs(base310sfp(frng))) sum(abs(base311sfp(frng)))];;
fib4p=[sum(abs(base41sfp(frng))) sum(abs(base42sfp(frng)))
sum(abs(base43sfp(frng))) ...
    sum(abs(base44sfp(frng))) sum(abs(base45sfp(frng)))
sum(abs(base46sfp(frng))) ...
    sum(abs(base47sfp(frng))) sum(abs(base48sfp(frng)))
sum(abs(base49sfp(frng))) ...
    sum(abs(base410sfp(frng))) sum(abs(base411sfp(frng)))];;
fib5p=[sum(abs(base51sfp(frng))) sum(abs(base52sfp(frng)))
sum(abs(base53sfp(frng))) ...
    sum(abs(base54sfp(frng))) sum(abs(base55sfp(frng)))
sum(abs(base56sfp(frng))) ...
    sum(abs(base57sfp(frng))) sum(abs(base58sfp(frng)))
sum(abs(base59sfp(frng))) ...
    sum(abs(base510sfp(frng))) sum(abs(base511sfp(frng)))];;
Zp=[fibp fib2p fib3p fib4p fib5p];

% Curve fit baseline passenger front
pp=polyfit(X,Zp,2);
mp=mean(Zp-(pp(1)*X.^2+pp(2)*X+pp(3)));
stdp=std(Zp-(pp(1)*X.^2+pp(2)*X+pp(3)));

```

```
% Passenger rear
fibpr=[sum(abs(base11srp(frng))) sum(abs(base12srp(frng)))
sum(abs(base13srp(frng))) ...
    sum(abs(base14srp(frng))) sum(abs(base15srp(frng)))
sum(abs(base16srp(frng))) ...
    sum(abs(base17srp(frng))) sum(abs(base18srp(frng)))
sum(abs(base19srp(frng))) ...
    sum(abs(base110srp(frng))) sum(abs(base111srp(frng)))
sum(abs(base112srp(frng))) ...
    sum(abs(base113srp(frng))) sum(abs(base114srp(frng)))
sum(abs(base115srp(frng))) ...
    sum(abs(base116srp(frng))) sum(abs(base117srp(frng)))
sum(abs(base118srp(frng))) ...
    sum(abs(base119srp(frng))) sum(abs(base120srp(frng)))
sum(abs(base121srp(frng))) ...
    sum(abs(base122srp(frng))) sum(abs(base123srp(frng)))
sum(abs(base124srp(frng))) ...
    sum(abs(base125srp(frng))) sum(abs(base126srp(frng)))
sum(abs(base127srp(frng))) ...
    sum(abs(base128srp(frng))) sum(abs(base129srp(frng)))
sum(abs(base130srp(frng))]];
fib2pr=[sum(abs(base21srp(frng))) sum(abs(base22srp(frng)))
sum(abs(base23srp(frng))) ...
    sum(abs(base24srp(frng))) sum(abs(base25srp(frng)))
sum(abs(base26srp(frng))) ...
    sum(abs(base27srp(frng))) sum(abs(base28srp(frng)))
sum(abs(base29srp(frng))) ...
    sum(abs(base210srp(frng))) sum(abs(base211srp(frng)))];
fib3pr=[sum(abs(base31srp(frng))) sum(abs(base32srp(frng)))
sum(abs(base33srp(frng))) ...
    sum(abs(base34srp(frng))) sum(abs(base35srp(frng)))
sum(abs(base36srp(frng))) ...
    sum(abs(base37srp(frng))) sum(abs(base38srp(frng)))
sum(abs(base39srp(frng))) ...
    sum(abs(base310srp(frng))) sum(abs(base311srp(frng)))];
fib4pr=[sum(abs(base41srp(frng))) sum(abs(base42srp(frng)))
sum(abs(base43srp(frng))) ...
    sum(abs(base44srp(frng))) sum(abs(base45srp(frng)))
sum(abs(base46srp(frng))) ...
    sum(abs(base47srp(frng))) sum(abs(base48srp(frng)))
sum(abs(base49srp(frng))) ...
    sum(abs(base410srp(frng))) sum(abs(base411srp(frng)))];
fib5pr=[sum(abs(base51srp(frng))) sum(abs(base52srp(frng)))
sum(abs(base53srp(frng))) ...
    sum(abs(base54srp(frng))) sum(abs(base55srp(frng)))
sum(abs(base56srp(frng))) ...
    sum(abs(base57srp(frng))) sum(abs(base58srp(frng)))
sum(abs(base59srp(frng))) ...
    sum(abs(base510srp(frng))) sum(abs(base511srp(frng))];

Zpr=[fibpr fib2pr fib3pr fib4pr fib5pr];

% Curve fit baseline passenger rear
ppr=polyfit(X,Zpr,2);
mpr=mean(Zpr-(ppr(1)*X.^2+ppr(2)*X+ppr(3)));
stdpr=std(Zpr-(ppr(1)*X.^2+ppr(2)*X+ppr(3))];
```

```
% Count number of false positives/negatives for baseline

% Driver front
flagd=0;
for ii=1:74,
    if Zd(ii) > pd(1)*X(ii)^2+pd(2)*X(ii)+pd(3)+thresh*std,
        flagd=flagd+1;
    elseif Zd(ii) < pd(1)*X(ii)^2+pd(2)*X(ii)+pd(3)-thresh*std,
        flagd=flagd+1;
    end
end
NoFPd=flagd;

% Passenger front
flagp=0;
for ii=1:74,
    if Zp(ii) > pp(1)*X(ii)^2+pp(2)*X(ii)+pp(3)+thresh*stdp,
        flagp=flagp+1;
    elseif Zp(ii) < pp(1)*X(ii)^2+pp(2)*X(ii)+pp(3)-thresh*stdp,
        flagp=flagp+1;
    end
end
NoFPp=flagp;

% Driver rear
flagd=0;
for ii=1:74,
    if Zdr(ii) > pdr(1)*X(ii)^2+pdr(2)*X(ii)+pdr(3)+thresh*stddr,
        flagd=flagd+1;
    elseif Zdr(ii) < pdr(1)*X(ii)^2+pdr(2)*X(ii)+pdr(3)-thresh*stddr,
        flagd=flagd+1;
    end
end
NoFPdr=flagd;

% Passenger rear
flagp=0;
for ii=1:74,
    if Zpr(ii) > ppr(1)*X(ii)^2+ppr(2)*X(ii)+ppr(3)+thresh*stdpr,
        flagp=flagp+1;
    elseif Zpr(ii) < ppr(1)*X(ii)^2+ppr(2)*X(ii)+ppr(3)-thresh*stdpr,
        flagp=flagp+1;
    end
end
NoFPpr=flagp;

% Define damage indices for driver front tire fault
Ztdf=[sum(abs(tiredf1sf(frng))) sum(abs(tiredf12sf(frng)))
sum(abs(tiredf13sf(frng))) ...
sum(abs(tiredf14sf(frng))) sum(abs(tiredf15sf(frng)))
sum(abs(tiredf16sf(frng))) sum(abs(tiredf17sf(frng))) ...
sum(abs(tiredf18sf(frng))) sum(abs(tiredf19sf(frng)))
sum(abs(tiredf110sf(frng))) sum(abs(tiredf111sf(frng))) ...
sum(abs(tiredf112sf(frng))) sum(abs(tiredf113sf(frng)))
sum(abs(tiredf114sf(frng))) sum(abs(tiredf115sf(frng))) ...
```

```

    sum(abs(tiredf116sf(frng))) sum(abs(tiredf117sf(frng)))
sum(abs(tiredf118sf(frng))) sum(abs(tiredf119sf(frng))) ...
    sum(abs(tiredf120sf(frng))) sum(abs(tiredf121sf(frng)))
sum(abs(tiredf122sf(frng))) sum(abs(tiredf123sf(frng))) ...
    sum(abs(tiredf124sf(frng))) sum(abs(tiredf125sf(frng)))
sum(abs(tiredf126sf(frng))) sum(abs(tiredf127sf(frng))) ...
    sum(abs(tiredf128sf(frng))) sum(abs(tiredf129sf(frng)))
sum(abs(tiredf130sf(frng))];

Ztdfp=[sum(abs(tiredf11sfp(frng))) sum(abs(tiredf12sfp(frng)))
sum(abs(tiredf13sfp(frng))) ...
    sum(abs(tiredf14sfp(frng))) sum(abs(tiredf15sfp(frng)))
sum(abs(tiredf16sfp(frng))) sum(abs(tiredf17sfp(frng))) ...
    sum(abs(tiredf18sfp(frng))) sum(abs(tiredf19sfp(frng)))
sum(abs(tiredf110sfp(frng))) sum(abs(tiredf111sfp(frng))) ...
    sum(abs(tiredf112sfp(frng))) sum(abs(tiredf113sfp(frng)))
sum(abs(tiredf114sfp(frng))) sum(abs(tiredf115sfp(frng))) ...
    sum(abs(tiredf116sfp(frng))) sum(abs(tiredf117sfp(frng)))
sum(abs(tiredf118sfp(frng))) sum(abs(tiredf119sfp(frng))) ...
    sum(abs(tiredf120sfp(frng))) sum(abs(tiredf121sfp(frng)))
sum(abs(tiredf122sfp(frng))) sum(abs(tiredf123sfp(frng))) ...
    sum(abs(tiredf124sfp(frng))) sum(abs(tiredf125sfp(frng)))
sum(abs(tiredf126sfp(frng))) sum(abs(tiredf127sfp(frng))) ...
    sum(abs(tiredf128sfp(frng))) sum(abs(tiredf129sfp(frng)))
sum(abs(tiredf130sfp(frng))];

Ztdfr=[sum(abs(tiredf11sr(frng))) sum(abs(tiredf12sr(frng)))
sum(abs(tiredf13sr(frng))) ...
    sum(abs(tiredf14sr(frng))) sum(abs(tiredf15sr(frng)))
sum(abs(tiredf16sr(frng))) sum(abs(tiredf17sr(frng))) ...
    sum(abs(tiredf18sr(frng))) sum(abs(tiredf19sr(frng)))
sum(abs(tiredf110sr(frng))) sum(abs(tiredf111sr(frng))) ...
    sum(abs(tiredf112sr(frng))) sum(abs(tiredf113sr(frng)))
sum(abs(tiredf114sr(frng))) sum(abs(tiredf115sr(frng))) ...
    sum(abs(tiredf116sr(frng))) sum(abs(tiredf117sr(frng)))
sum(abs(tiredf118sr(frng))) sum(abs(tiredf119sr(frng))) ...
    sum(abs(tiredf120sr(frng))) sum(abs(tiredf121sr(frng)))
sum(abs(tiredf122sr(frng))) sum(abs(tiredf123sr(frng))) ...
    sum(abs(tiredf124sr(frng))) sum(abs(tiredf125sr(frng)))
sum(abs(tiredf126sr(frng))) sum(abs(tiredf127sr(frng))) ...
    sum(abs(tiredf128sr(frng))) sum(abs(tiredf129sr(frng)))
sum(abs(tiredf130sr(frng))];

Ztdfpr=[sum(abs(tiredf11srp(frng))) sum(abs(tiredf12srp(frng)))
sum(abs(tiredf13srp(frng))) ...
    sum(abs(tiredf14srp(frng))) sum(abs(tiredf15srp(frng)))
sum(abs(tiredf16srp(frng))) sum(abs(tiredf17srp(frng))) ...
    sum(abs(tiredf18srp(frng))) sum(abs(tiredf19srp(frng)))
sum(abs(tiredf110srp(frng))) sum(abs(tiredf111srp(frng))) ...
    sum(abs(tiredf112srp(frng))) sum(abs(tiredf113srp(frng)))
sum(abs(tiredf114srp(frng))) sum(abs(tiredf115srp(frng))) ...
    sum(abs(tiredf116srp(frng))) sum(abs(tiredf117srp(frng)))
sum(abs(tiredf118srp(frng))) sum(abs(tiredf119srp(frng))) ...
    sum(abs(tiredf120srp(frng))) sum(abs(tiredf121srp(frng)))
sum(abs(tiredf122srp(frng))) sum(abs(tiredf123srp(frng))) ...
    sum(abs(tiredf124srp(frng))) sum(abs(tiredf125srp(frng)))

```

```

sum(abs(tiredf126srp(frng))) sum(abs(tiredf127srp(frng))) ...
    sum(abs(tiredf128srp(frng))) sum(abs(tiredf129srp(frng))) ...
sum(abs(tiredf130srp(frng))];

Xt=[speedtdf11 speedtdf12 speedtdf13 speedtdf14 speedtdf15 speedtdf16
speedtdf17 speedtdf18 speedtdf19 ...
    speedtdf10 speedtdf11 speedtdf12 speedtdf13 speedtdf14
speedtdf15 speedtdf16 speedtdf17 speedtdf18 ...
    speedtdf19 speedtdf10 speedtdf11 speedtdf12 speedtdf13
speedtdf14 speedtdf15 speedtdf16 speedtdf17 ...
    speedtdf18 speedtdf19 speedtdf130];

% Calculate false negatives
flagtd=0;
for ii=1:30,
    if Ztdf(ii) > pd(1)*Xt(ii)^2+pd(2)*Xt(ii)+pd(3)+thresh*stdd,
        flagtd=flagtd+1;
    elseif Ztdf(ii) < pd(1)*Xt(ii)^2+pd(2)*Xt(ii)+pd(3)-thresh*stdd,
        flagtd=flagtd+1;
    end
end
NoFNtd=30-flagtd;

% Calculate false positives
flagtd=0;
for ii=1:30,
    if Ztdfp(ii) > pp(1)*Xt(ii)^2+pp(2)*Xt(ii)+pp(3)+thresh*stdp,
        flagtd=flagtd+1;
    elseif Ztdfp(ii) < pp(1)*Xt(ii)^2+pp(2)*Xt(ii)+pp(3)-thresh*stdp,
        flagtd=flagtd+1;
    end
end
NoFPtd1=flagtd;

% Calculate false positives
flagtd=0;
for ii=1:30,
    if Ztdfr(ii) > pdr(1)*Xt(ii)^2+pdr(2)*Xt(ii)+pdr(3)+thresh*stddr,
        flagtd=flagtd+1;
    elseif Ztdfr(ii) < pdr(1)*Xt(ii)^2+pdr(2)*Xt(ii)+pdr(3)-thresh*stddr,
        flagtd=flagtd+1;
    end
end
NoFPtd2=flagtd;

% Calculate false positives
flagtd=0;
for ii=1:30,
    if Ztdfpr(ii) > ppr(1)*Xt(ii)^2+ppr(2)*Xt(ii)+ppr(3)+thresh*stdpr,
        flagtd=flagtd+1;
    elseif Ztdfpr(ii) < ppr(1)*Xt(ii)^2+ppr(2)*Xt(ii)+ppr(3)-thresh*stdpr,
        flagtd=flagtd+1;
    end
end

```

```
NoFPtd3=flagtd;

% Define damage indices for passenger front tire fault
Ztpf=[sum(abs(tirepf11sf(frng))) sum(abs(tirepf12sf(frng)))
sum(abs(tirepf13sf(frng))) ...
sum(abs(tirepf14sf(frng))) sum(abs(tirepf15sf(frng)))
sum(abs(tirepf16sf(frng))) sum(abs(tirepf17sf(frng))) ...
sum(abs(tirepf18sf(frng))) sum(abs(tirepf19sf(frng)))
sum(abs(tirepf110sf(frng))) sum(abs(tirepf111sf(frng))) ...
sum(abs(tirepf112sf(frng))) sum(abs(tirepf113sf(frng)))
sum(abs(tirepf114sf(frng))) sum(abs(tirepf115sf(frng))) ...
sum(abs(tirepf116sf(frng))) sum(abs(tirepf117sf(frng)))
sum(abs(tirepf118sf(frng))) sum(abs(tirepf119sf(frng))) ...
sum(abs(tirepf120sf(frng))) sum(abs(tirepf121sf(frng)))
sum(abs(tirepf122sf(frng))) sum(abs(tirepf123sf(frng))) ...
sum(abs(tirepf124sf(frng))) sum(abs(tirepf125sf(frng)))
sum(abs(tirepf126sf(frng))) sum(abs(tirepf127sf(frng))) ...
sum(abs(tirepf128sf(frng))) sum(abs(tirepf129sf(frng)))
sum(abs(tirepf130sf(frng))];

Ztpfp=[sum(abs(tirepf11sfp(frng))) sum(abs(tirepf12sfp(frng)))
sum(abs(tirepf13sfp(frng))) ...
sum(abs(tirepf14sfp(frng))) sum(abs(tirepf15sfp(frng)))
sum(abs(tirepf16sfp(frng))) sum(abs(tirepf17sfp(frng))) ...
sum(abs(tirepf18sfp(frng))) sum(abs(tirepf19sfp(frng)))
sum(abs(tirepf110sfp(frng))) sum(abs(tirepf111sfp(frng))) ...
sum(abs(tirepf112sfp(frng))) sum(abs(tirepf113sfp(frng)))
sum(abs(tirepf114sfp(frng))) sum(abs(tirepf115sfp(frng))) ...
sum(abs(tirepf116sfp(frng))) sum(abs(tirepf117sfp(frng)))
sum(abs(tirepf118sfp(frng))) sum(abs(tirepf119sfp(frng))) ...
sum(abs(tirepf120sfp(frng))) sum(abs(tirepf121sfp(frng)))
sum(abs(tirepf122sfp(frng))) sum(abs(tirepf123sfp(frng))) ...
sum(abs(tirepf124sfp(frng))) sum(abs(tirepf125sfp(frng)))
sum(abs(tirepf126sfp(frng))) sum(abs(tirepf127sfp(frng))) ...
sum(abs(tirepf128sfp(frng))) sum(abs(tirepf129sfp(frng)))
sum(abs(tirepf130sfp(frng))];

Ztpfr=[sum(abs(tirepf11sr(frng))) sum(abs(tirepf12sr(frng)))
sum(abs(tirepf13sr(frng))) ...
sum(abs(tirepf14sr(frng))) sum(abs(tirepf15sr(frng)))
sum(abs(tirepf16sr(frng))) sum(abs(tirepf17sr(frng))) ...
sum(abs(tirepf18sr(frng))) sum(abs(tirepf19sr(frng)))
sum(abs(tirepf110sr(frng))) sum(abs(tirepf111sr(frng))) ...
sum(abs(tirepf112sr(frng))) sum(abs(tirepf113sr(frng)))
sum(abs(tirepf114sr(frng))) sum(abs(tirepf115sr(frng))) ...
sum(abs(tirepf116sr(frng))) sum(abs(tirepf117sr(frng)))
sum(abs(tirepf118sr(frng))) sum(abs(tirepf119sr(frng))) ...
sum(abs(tirepf120sr(frng))) sum(abs(tirepf121sr(frng)))
sum(abs(tirepf122sr(frng))) sum(abs(tirepf123sr(frng))) ...
sum(abs(tirepf124sr(frng))) sum(abs(tirepf125sr(frng)))
sum(abs(tirepf126sr(frng))) sum(abs(tirepf127sr(frng))) ...
sum(abs(tirepf128sr(frng))) sum(abs(tirepf129sr(frng)))
sum(abs(tirepf130sr(frng))];

Ztpfpr=[sum(abs(tirepf11srp(frng))) sum(abs(tirepf12srp(frng)))
sum(abs(tirepf13srp(frng))) ...
```

```

    sum(abs(tirepf14srp(frng))) sum(abs(tirepf15srp(frng)))
sum(abs(tirepf16srp(frng))) sum(abs(tirepf17srp(frng))) ...
    sum(abs(tirepf18srp(frng))) sum(abs(tirepf19srp(frng)))
sum(abs(tirepf110srp(frng))) sum(abs(tirepf111srp(frng))) ...
    sum(abs(tirepf112srp(frng))) sum(abs(tirepf113srp(frng)))
sum(abs(tirepf114srp(frng))) sum(abs(tirepf115srp(frng))) ...
    sum(abs(tirepf116srp(frng))) sum(abs(tirepf117srp(frng)))
sum(abs(tirepf118srp(frng))) sum(abs(tirepf119srp(frng))) ...
    sum(abs(tirepf120srp(frng))) sum(abs(tirepf121srp(frng)))
sum(abs(tirepf122srp(frng))) sum(abs(tirepf123srp(frng))) ...
    sum(abs(tirepf124srp(frng))) sum(abs(tirepf125srp(frng)))
sum(abs(tirepf126srp(frng))) sum(abs(tirepf127srp(frng))) ...
    sum(abs(tirepf128srp(frng))) sum(abs(tirepf129srp(frng)))
sum(abs(tirepf130srp(frng))];

Xtp=[speedtpf11 speedtpf12 speedtpf13 speedtpf14 speedtpf15 speedtpf16
speedtpf17 speedtpf18 speedtpf19 ...
    speedtpf110 speedtpf111 speedtpf112 speedtpf113 speedtpf114
speedtpf115 speedtpf116 speedtpf117 speedtpf118 ...
    speedtpf119 speedtpf120 speedtpf121 speedtpf122 speedtpf123
speedtpf124 speedtpf125 speedtpf126 speedtpf127 ...
    speedtpf128 speedtpf129 speedtpf130];

% Calculate false positives
flagtd=0;
for ii=1:30,
    if Ztpf(ii) > pd(1)*Xtp(ii)^2+pd(2)*Xtp(ii)+pd(3)+thresh*stdd,
        flagtd=flagtd+1;
    elseif Ztpf(ii) < pd(1)*Xtp(ii)^2+pd(2)*Xtp(ii)+pd(3)-thresh*stdd,
        flagtd=flagtd+1;
    end
end
NoFPtp1=flagtd;

% Calculate false negatives
flagtd=0;
for ii=1:30,
    if Ztpfp(ii) > pp(1)*Xtp(ii)^2+pp(2)*Xtp(ii)+pp(3)+thresh*stdp,
        flagtd=flagtd+1;
    elseif Ztpfp(ii) < pp(1)*Xtp(ii)^2+pp(2)*Xtp(ii)+pp(3)-thresh*stdp,
        flagtd=flagtd+1;
    end
end
NoFNtp=30-flagtd;

% Calculate false positives
flagtd=0;
for ii=1:30,
    if Ztpfr(ii) > pdr(1)*Xtp(ii)^2+pdr(2)*Xtp(ii)+pdr(3)+thresh*stddr,
        flagtd=flagtd+1;
    elseif Ztpfr(ii) < pdr(1)*Xtp(ii)^2+pdr(2)*Xtp(ii)+pdr(3)-
thresh*stddr,
        flagtd=flagtd+1;
    end
end
NoFPtp2=flagtd;

```

```
% Calculate false positives
flagtd=0;
for ii=1:30,
    if Ztpfpr(ii) >
        ppr(1)*Xtp(ii)^2+ppr(2)*Xtp(ii)+ppr(3)+thresh*stdpr,
            flagtd=flagtd+1;
    elseif Ztpfpr(ii) < ppr(1)*Xtp(ii)^2+ppr(2)*Xtp(ii)+ppr(3)-
        thresh*stdpr,
            flagtd=flagtd+1;
    end
end
NoFPtp3=flagtd;

% Define damage indices for driver rear tire fault
Ztdr=[sum(abs(tiredr11sf(frng))) sum(abs(tiredr12sf(frng)))
sum(abs(tiredr13sf(frng))) ...
    sum(abs(tiredr14sf(frng))) sum(abs(tiredr15sf(frng)))
sum(abs(tiredr16sf(frng))) sum(abs(tiredr17sf(frng))) ...
    sum(abs(tiredr18sf(frng))) sum(abs(tiredr19sf(frng)))
sum(abs(tiredr110sf(frng))) sum(abs(tiredr111sf(frng))) ...
    sum(abs(tiredr112sf(frng))) sum(abs(tiredr113sf(frng)))
sum(abs(tiredr114sf(frng))) sum(abs(tiredr115sf(frng))) ...
    sum(abs(tiredr116sf(frng))) sum(abs(tiredr117sf(frng)))
sum(abs(tiredr118sf(frng))) sum(abs(tiredr119sf(frng))) ...
    sum(abs(tiredr120sf(frng))) sum(abs(tiredr121sf(frng)))
sum(abs(tiredr122sf(frng))) sum(abs(tiredr123sf(frng))) ...
    sum(abs(tiredr124sf(frng))) sum(abs(tiredr125sf(frng)))
sum(abs(tiredr126sf(frng))) sum(abs(tiredr127sf(frng))) ...
    sum(abs(tiredr128sf(frng))) sum(abs(tiredr129sf(frng)))
sum(abs(tiredr130sf(frng))];

Ztdrp=[sum(abs(tiredr11sfp(frng))) sum(abs(tiredr12sfp(frng)))
sum(abs(tiredr13sfp(frng))) ...
    sum(abs(tiredr14sfp(frng))) sum(abs(tiredr15sfp(frng)))
sum(abs(tiredr16sfp(frng))) sum(abs(tiredr17sfp(frng))) ...
    sum(abs(tiredr18sfp(frng))) sum(abs(tiredr19sfp(frng)))
sum(abs(tiredr110sfp(frng))) sum(abs(tiredr111sfp(frng))) ...
    sum(abs(tiredr112sfp(frng))) sum(abs(tiredr113sfp(frng)))
sum(abs(tiredr114sfp(frng))) sum(abs(tiredr115sfp(frng))) ...
    sum(abs(tiredr116sfp(frng))) sum(abs(tiredr117sfp(frng)))
sum(abs(tiredr118sfp(frng))) sum(abs(tiredr119sfp(frng))) ...
    sum(abs(tiredr120sfp(frng))) sum(abs(tiredr121sfp(frng)))
sum(abs(tiredr122sfp(frng))) sum(abs(tiredr123sfp(frng))) ...
    sum(abs(tiredr124sfp(frng))) sum(abs(tiredr125sfp(frng)))
sum(abs(tiredr126sfp(frng))) sum(abs(tiredr127sfp(frng))) ...
    sum(abs(tiredr128sfp(frng))) sum(abs(tiredr129sfp(frng)))
sum(abs(tiredr130sfp(frng))];

Ztdrr=[sum(abs(tiredr11sr(frng))) sum(abs(tiredr12sr(frng)))
sum(abs(tiredr13sr(frng))) ...
    sum(abs(tiredr14sr(frng))) sum(abs(tiredr15sr(frng)))
sum(abs(tiredr16sr(frng))) sum(abs(tiredr17sr(frng))) ...
    sum(abs(tiredr18sr(frng))) sum(abs(tiredr19sr(frng)))
sum(abs(tiredr110sr(frng))) sum(abs(tiredr111sr(frng))) ...
    sum(abs(tiredr112sr(frng))) sum(abs(tiredr113sr(frng)))
```

```

sum(abs(tiredr114sr(frng))) sum(abs(tiredr115sr(frng))) ...
    sum(abs(tiredr116sr(frng))) sum(abs(tiredr117sr(frng)))
sum(abs(tiredr118sr(frng))) sum(abs(tiredr119sr(frng))) ...
    sum(abs(tiredr120sr(frng))) sum(abs(tiredr121sr(frng)))
sum(abs(tiredr122sr(frng))) sum(abs(tiredr123sr(frng))) ...
    sum(abs(tiredr124sr(frng))) sum(abs(tiredr125sr(frng)))
sum(abs(tiredr126sr(frng))) sum(abs(tiredr127sr(frng))) ...
    sum(abs(tiredr128sr(frng))) sum(abs(tiredr129sr(frng)))
sum(abs(tiredr130sr(frng))];

Ztdrpr=[sum(abs(tiredr11srp(frng))) sum(abs(tiredr12srp(frng)))
sum(abs(tiredr13srp(frng))) ...
    sum(abs(tiredr14srp(frng))) sum(abs(tiredr15srp(frng)))
sum(abs(tiredr16srp(frng))) sum(abs(tiredr17srp(frng))) ...
    sum(abs(tiredr18srp(frng))) sum(abs(tiredr19srp(frng)))
sum(abs(tiredr110srp(frng))) sum(abs(tiredr111srp(frng))) ...
    sum(abs(tiredr112srp(frng))) sum(abs(tiredr113srp(frng)))
sum(abs(tiredr114srp(frng))) sum(abs(tiredr115srp(frng))) ...
    sum(abs(tiredr116srp(frng))) sum(abs(tiredr117srp(frng)))
sum(abs(tiredr118srp(frng))) sum(abs(tiredr119srp(frng))) ...
    sum(abs(tiredr120srp(frng))) sum(abs(tiredr121srp(frng)))
sum(abs(tiredr122srp(frng))) sum(abs(tiredr123srp(frng))) ...
    sum(abs(tiredr124srp(frng))) sum(abs(tiredr125srp(frng)))
sum(abs(tiredr126srp(frng))) sum(abs(tiredr127srp(frng))) ...
    sum(abs(tiredr128srp(frng))) sum(abs(tiredr129srp(frng)))
sum(abs(tiredr130srp(frng))];

Xt=[speedtdr11 speedtdr12 speedtdr13 speedtdr14 speedtdr15 speedtdr16
speedtdr17 speedtdr18 speedtdr19 ...
    speedtdr10 speedtdr11 speedtdr12 speedtdr113 speedtdr114
speedtdr115 speedtdr116 speedtdr117 speedtdr118 ...
    speedtdr119 speedtdr120 speedtdr121 speedtdr122 speedtdr123
speedtdr124 speedtdr125 speedtdr126 speedtdr127 ...
    speedtdr128 speedtdr129 speedtdr130];

% Calculate false positives
flagtd=0;
for ii=1:30,
    if Ztdr(ii) > pd(1)*Xt(ii)^2+pd(2)*Xt(ii)+pd(3)+thresh*std,
        flagtd=flagtd+1;
    elseif Ztdr(ii) < pd(1)*Xt(ii)^2+pd(2)*Xt(ii)+pd(3)-thresh*std,
        flagtd=flagtd+1;
    end
end
NoFPtdr1=flagtd;

% Calculate false positives
flagtd=0;
for ii=1:30,
    if Ztdrp(ii) > pp(1)*Xt(ii)^2+pp(2)*Xt(ii)+pp(3)+thresh*stdp,
        flagtd=flagtd+1;
    elseif Ztdrp(ii) < pp(1)*Xt(ii)^2+pp(2)*Xt(ii)+pp(3)-thresh*stdp,
        flagtd=flagtd+1;
    end
end
NoFPtdr2=flagtd;

```

```
% Calculate false negatives
flagtd=0;
for ii=1:30,
    if Ztdrr(ii) > pdr(1)*Xt(ii)^2+pdr(2)*Xt(ii)+pdr(3)+thresh*stddr,
        flagtd=flagtd+1;
    elseif Ztdrr(ii) < pdr(1)*Xt(ii)^2+pdr(2)*Xt(ii)+pdr(3)-
thresh*stddr,
        flagtd=flagtd+1;
    end
end
NoFNtdr=30-flagtd;

% Calculate false positives
flagtd=0;
for ii=1:30,
    if Ztdrpr(ii) > ppr(1)*Xt(ii)^2+ppr(2)*Xt(ii)+ppr(3)+thresh*stdpr,
        flagtd=flagtd+1;
    elseif Ztdrpr(ii) < ppr(1)*Xt(ii)^2+ppr(2)*Xt(ii)+ppr(3)-
thresh*stdpr,
        flagtd=flagtd+1;
    end
end
NoFPtdr3=flagtd;

% Define damage indices for passenger rear tire fault
Ztpr=[sum(abs(tirepr11sf(frng))) sum(abs(tirepr12sf(frng)))
sum(abs(tirepr13sf(frng))) ...
sum(abs(tirepr14sf(frng))) sum(abs(tirepr15sf(frng)))
sum(abs(tirepr16sf(frng))) sum(abs(tirepr17sf(frng))) ...
sum(abs(tirepr18sf(frng))) sum(abs(tirepr19sf(frng)))
sum(abs(tirepr110sf(frng))) sum(abs(tirepr111sf(frng))) ...
sum(abs(tirepr112sf(frng))) sum(abs(tirepr113sf(frng)))
sum(abs(tirepr114sf(frng))) sum(abs(tirepr115sf(frng))) ...
sum(abs(tirepr116sf(frng))) sum(abs(tirepr117sf(frng)))
sum(abs(tirepr118sf(frng))) sum(abs(tirepr119sf(frng))) ...
sum(abs(tirepr120sf(frng))) sum(abs(tirepr121sf(frng)))
sum(abs(tirepr122sf(frng))) sum(abs(tirepr123sf(frng))) ...
sum(abs(tirepr124sf(frng))) sum(abs(tirepr125sf(frng)))
sum(abs(tirepr126sf(frng))) sum(abs(tirepr127sf(frng))) ...
sum(abs(tirepr128sf(frng))) sum(abs(tirepr129sf(frng)))
sum(abs(tirepr130sf(frng))];

Ztprp=[sum(abs(tirepr11sfp(frng))) sum(abs(tirepr12sfp(frng)))
sum(abs(tirepr13sfp(frng))) ...
sum(abs(tirepr14sfp(frng))) sum(abs(tirepr15sfp(frng)))
sum(abs(tirepr16sfp(frng))) sum(abs(tirepr17sfp(frng))) ...
sum(abs(tirepr18sfp(frng))) sum(abs(tirepr19sfp(frng)))
sum(abs(tirepr110sfp(frng))) sum(abs(tirepr111sfp(frng))) ...
sum(abs(tirepr112sfp(frng))) sum(abs(tirepr113sfp(frng)))
sum(abs(tirepr114sfp(frng))) sum(abs(tirepr115sfp(frng))) ...
sum(abs(tirepr116sfp(frng))) sum(abs(tirepr117sfp(frng)))
sum(abs(tirepr118sfp(frng))) sum(abs(tirepr119sfp(frng))) ...
sum(abs(tirepr120sfp(frng))) sum(abs(tirepr121sfp(frng)))
sum(abs(tirepr122sfp(frng))) sum(abs(tirepr123sfp(frng))) ...
sum(abs(tirepr124sfp(frng))) sum(abs(tirepr125sfp(frng)))
```

```

sum(abs(tirepr126sfp(frng))) sum(abs(tirepr127sfp(frng))) ...
    sum(abs(tirepr128sfp(frng))) sum(abs(tirepr129sfp(frng)))
sum(abs(tirepr130sfp(frng))];

Ztprr=[sum(abs(tirepr11sr(frng))) sum(abs(tirepr12sr(frng)))
sum(abs(tirepr13sr(frng))) ...
    sum(abs(tirepr14sr(frng))) sum(abs(tirepr15sr(frng)))
sum(abs(tirepr16sr(frng))) sum(abs(tirepr17sr(frng))) ...
    sum(abs(tirepr18sr(frng))) sum(abs(tirepr19sr(frng)))
sum(abs(tirepr110sr(frng))) sum(abs(tirepr111sr(frng))) ...
    sum(abs(tirepr112sr(frng))) sum(abs(tirepr113sr(frng)))
sum(abs(tirepr114sr(frng))) sum(abs(tirepr115sr(frng))) ...
    sum(abs(tirepr116sr(frng))) sum(abs(tirepr117sr(frng)))
sum(abs(tirepr118sr(frng))) sum(abs(tirepr119sr(frng))) ...
    sum(abs(tirepr120sr(frng))) sum(abs(tirepr121sr(frng)))
sum(abs(tirepr122sr(frng))) sum(abs(tirepr123sr(frng))) ...
    sum(abs(tirepr124sr(frng))) sum(abs(tirepr125sr(frng)))
sum(abs(tirepr126sr(frng))) sum(abs(tirepr127sr(frng))) ...
    sum(abs(tirepr128sr(frng))) sum(abs(tirepr129sr(frng)))
sum(abs(tirepr130sr(frng))];

Ztprpr=[sum(abs(tirepr11srp(frng))) sum(abs(tirepr12srp(frng)))
sum(abs(tirepr13srp(frng))) ...
    sum(abs(tirepr14srp(frng))) sum(abs(tirepr15srp(frng)))
sum(abs(tirepr16srp(frng))) sum(abs(tirepr17srp(frng))) ...
    sum(abs(tirepr18srp(frng))) sum(abs(tirepr19srp(frng)))
sum(abs(tirepr110srp(frng))) sum(abs(tirepr111srp(frng))) ...
    sum(abs(tirepr112srp(frng))) sum(abs(tirepr113srp(frng)))
sum(abs(tirepr114srp(frng))) sum(abs(tirepr115srp(frng))) ...
    sum(abs(tirepr116srp(frng))) sum(abs(tirepr117srp(frng)))
sum(abs(tirepr118srp(frng))) sum(abs(tirepr119srp(frng))) ...
    sum(abs(tirepr120srp(frng))) sum(abs(tirepr121srp(frng)))
sum(abs(tirepr122srp(frng))) sum(abs(tirepr123srp(frng))) ...
    sum(abs(tirepr124srp(frng))) sum(abs(tirepr125srp(frng)))
sum(abs(tirepr126srp(frng))) sum(abs(tirepr127srp(frng))) ...
    sum(abs(tirepr128srp(frng))) sum(abs(tirepr129srp(frng)))
sum(abs(tirepr130srp(frng))];

Xtp=[speedtp11 speedtp12 speedtp13 speedtp14 speedtp15 speedtp16
speedtp17 speedtp18 speedtp19 ...
    speedtp10 speedtp11 speedtp12 speedtp13 speedtp14
speedtp15 speedtp16 speedtp17 speedtp18 ...
    speedtp19 speedtp120 speedtp121 speedtp122 speedtp123
speedtp124 speedtp125 speedtp126 speedtp127 ...
    speedtp128 speedtp129 speedtp130];

% Calculate false positives
flagtd=0;
for ii=1:30,
    if Ztp(ii) > pd(1)*Xtp(ii)^2+pd(2)*Xtp(ii)+pd(3)+thresh*stdd,
        flagtd=flagtd+1;
    elseif Ztp(ii) < pd(1)*Xtp(ii)^2+pd(2)*Xtp(ii)+pd(3)-thresh*stdd,
        flagtd=flagtd+1;
    end
end
NoFPtp1=flagtd;

```

```

% Calculate false positives
flagtd=0;
for ii=1:30,
    if Ztprp(ii) > pp(1)*Xtp(ii)^2+pp(2)*Xtp(ii)+pp(3)+thresh*stdp,
        flagtd=flagtd+1;
    elseif Ztprp(ii) < pp(1)*Xtp(ii)^2+pp(2)*Xtp(ii)+pp(3)-thresh*stdp,
        flagtd=flagtd+1;
    end
end
NoFPptr2=flagtd;

% Calculate false positives
flagtd=0;
for ii=1:30,
    if Ztprr(ii) > pdr(1)*Xtp(ii)^2+pdr(2)*Xtp(ii)+pdr(3)+thresh*stddr,
        flagtd=flagtd+1;
    elseif Ztprr(ii) < pdr(1)*Xtp(ii)^2+pdr(2)*Xtp(ii)+pdr(3)-
thresh*stddr,
        flagtd=flagtd+1;
    end
end
NoFPptr3=flagtd;

% Calculate false negatives
flagtd=0;
for ii=1:30,
    if Ztprpr(ii) >
ppr(1)*Xtp(ii)^2+ppr(2)*Xtp(ii)+ppr(3)+thresh*stdpr,
        flagtd=flagtd+1;
    elseif Ztprpr(ii) < ppr(1)*Xtp(ii)^2+ppr(2)*Xtp(ii)+ppr(3)-
thresh*stdpr,
        flagtd=flagtd+1;
    end
end
NoFNptr=30-flagtd;

roc(1:5,1:4,kk)=[NoFPd NoFPp NoFPdr NoFPpr; % Baseline
                  NoFNtd NoFPtd1 NoFPtd2 NoFPtd3; % Driver front
tire fault
                  NoFPtp1 NoFNtp NoFPtp2 NoFPtp3; % Passenger front
tire fault
                  NoFPtdr1 NoFPtdr2 NoFNtdr NoFPtdr3; % Driver rear
tire fault
                  NoFPptr1 NoFPptr2 NoFPptr3 NoFNptr]; % Passenger rear
tire fault

end

figure(1);
%plot(squeeze(roc(2,2,:))/90+squeeze(roc(2,3,:))/90+squeeze(roc(2,4,:))
/90,squeeze(roc(2,1,:))/30,'-v',...
%
squeeze(roc(3,1,:))/90+squeeze(roc(3,3,:))/90+squeeze(roc(3,4,:))/90,sq
ueeze(roc(3,2,:))/30,'-^');
plot(squeeze(roc(1,1,:))/164+squeeze(roc(1,2,:))/164+squeeze(roc(1,3,:))

```

```

)/164+squeeze(roc(1,4,:))/164+...
squeeze(roc(2,2,:))/164+squeeze(roc(2,3,:))/164+squeeze(roc(2,4,:))/164
,squeeze(roc(2,1,:))/30,'-v',...
squeeze(roc(1,1,:))/164+squeeze(roc(1,2,:))/164+squeeze(roc(1,3,:))/164
+squeeze(roc(1,4,:))/164+...
squeeze(roc(3,1,:))/164+squeeze(roc(3,3,:))/164+squeeze(roc(3,4,:))/164
,squeeze(roc(3,2,:))/30,'-^',...
squeeze(roc(1,1,:))/164+squeeze(roc(1,2,:))/164+squeeze(roc(1,3,:))/164
+squeeze(roc(1,4,:))/164+...
squeeze(roc(4,1,:))/164+squeeze(roc(4,2,:))/164+squeeze(roc(4,4,:))/164
,squeeze(roc(4,3,:))/30,'-<',...
squeeze(roc(1,1,:))/164+squeeze(roc(1,2,:))/164+squeeze(roc(1,3,:))/164
+squeeze(roc(1,4,:))/164+...
squeeze(roc(5,1,:))/164+squeeze(roc(5,2,:))/164+squeeze(roc(5,3,:))/164
,squeeze(roc(5,4,:))/30,'->');
xlabel('False Positive rate (healthy tires flagged as flat)');
ylabel('False Negative rate (flat tires flagged as healthy)');
axis([0 1 0 1]);

% Plot detection results/driver front tire
figure(2);
plot([speedb11 speedb12 speedb13 speedb14 speedb15 speedb16 speedb17
speedb18 speedb19 ...
speedb10 speedb11 speedb12 speedb13 speedb14 speedb15
speedb16 speedb17 speedb18 ...
speedb19 speedb20 speedb21 speedb22 speedb23 speedb24
speedb25 speedb26 speedb27 ...
speedb28 speedb29 speedb30],fibd,'bx',[speedb21 speedb22
speedb23 speedb24 speedb25 speedb26 ...
speedb27 speedb28 speedb29 speedb210
speedb211],fib2d,'bs',[speedb31 speedb32 speedb33 speedb34 speedb35
speedb36 ...
speedb37 speedb38 speedb39 speedb310
speedb311],fib3d,'bd',[speedb41 speedb42 speedb43 speedb44 speedb45
speedb46 ...
speedb47 speedb48 speedb49 speedb410
speedb411],fib4d,'bv',[speedb51 speedb52 speedb53 speedb54 speedb55
speedb56 ...
speedb57 speedb58 speedb59 speedb510 speedb511],fib5d,'b^');
xlabel('Speed [mph]');
ylabel('Fault index driver');
hold on;
plot(X,(pd(1)*X.^2+pd(2)*X+pd(3))+3*std, 'k.', X, (pd(1)*X.^2+pd(2)*X+pd(3))-3*std, 'k.', Xt, Ztdf, 'rx');
hold off;

% Plot false positive results/passenger front tire
figure(3);
plot([speedb11 speedb12 speedb13 speedb14 speedb15 speedb16 speedb17

```

```

speedb18 speedb19 ...
    speedb10 speedb11 speedb12 speedb13 speedb14 speedb15
speedb16 speedb17 speedb18 ...
    speedb19 speedb20 speedb21 speedb22 speedb23 speedb24
speedb25 speedb26 speedb27 ...
    speedb28 speedb29 speedb210
speedb211],fibp,'bx',[speedb21 speedb22
speedb23 speedb24 speedb25 speedb26 ...
    speedb27 speedb28 speedb29 speedb210
speedb211],fib2p,'bs',[speedb31 speedb32 speedb33 speedb34 speedb35
speedb36 ...
    speedb37 speedb38 speedb39 speedb310
speedb311],fib3p,'bd',[speedb41 speedb42 speedb43 speedb44 speedb45
speedb46 ...
    speedb47 speedb48 speedb49 speedb410
speedb411],fib4p,'bv',[speedb51 speedb52 speedb53 speedb54 speedb55
speedb56 ...
    speedb57 speedb58 speedb59 speedb510 speedb511],fib5p,'b^');
xlabel('Speed [mph]');
ylabel('Fault index passenger');
hold on;
plot(X,(pp(1)*X.^2+pp(2)*X+pp(3))+3*stdp,'k.',X,(pp(1)*X.^2+pp(2)*X+pp(3))-3*stdp,'k.',Xt,Ztdfp,'rx');
hold off;

% Plot false positive results/driver rear tire
figure(4);
plot([speedb11 speedb12 speedb13 speedb14 speedb15 speedb16 speedb17
speedb18 speedb19 ...
    speedb10 speedb11 speedb12 speedb13 speedb14 speedb15
speedb16 speedb17 speedb18 ...
    speedb19 speedb20 speedb21 speedb22 speedb23 speedb24
speedb25 speedb26 speedb27 ...
    speedb28 speedb29 speedb210
speedb211],fibdr,'bx',[speedb21 speedb22
speedb23 speedb24 speedb25 speedb26 ...
    speedb27 speedb28 speedb29 speedb210
speedb211],fib2dr,'bs',[speedb31 speedb32 speedb33 speedb34 speedb35
speedb36 ...
    speedb37 speedb38 speedb39 speedb310
speedb311],fib3dr,'bd',[speedb41 speedb42 speedb43 speedb44 speedb45
speedb46 ...
    speedb47 speedb48 speedb49 speedb410
speedb411],fib4dr,'bv',[speedb51 speedb52 speedb53 speedb54 speedb55
speedb56 ...
    speedb57 speedb58 speedb59 speedb510 speedb511],fib5dr,'b^');
xlabel('Speed [mph]');
ylabel('Fault index driver rear');
hold on;
plot(X,(pdr(1)*X.^2+pdr(2)*X+pdr(3))+3*stddr,'k.',X,(pdr(1)*X.^2+pdr(2)
*X+pdr(3))-3*stddr,'k.',Xt,Ztdfr,'rx');
hold off;

% Plot false positive results/passenger rear tire
figure(5);
plot([speedb11 speedb12 speedb13 speedb14 speedb15 speedb16 speedb17
speedb18 speedb19 ...
    speedb10 speedb11 speedb12 speedb13 speedb14 speedb115
speedb16 speedb17 speedb18 ...
    speedb19 speedb20 speedb21 speedb22 speedb23 speedb24
speedb25 speedb26 speedb27 ...
    speedb28 speedb29 speedb210
speedb211],fibp,'bx',[speedb21 speedb22
speedb23 speedb24 speedb25 speedb26 ...
    speedb27 speedb28 speedb29 speedb210
speedb211],fib2p,'bs',[speedb31 speedb32 speedb33 speedb34 speedb35
speedb36 ...
    speedb37 speedb38 speedb39 speedb310
speedb311],fib3p,'bd',[speedb41 speedb42 speedb43 speedb44 speedb45
speedb46 ...
    speedb47 speedb48 speedb49 speedb410
speedb411],fib4p,'bv',[speedb51 speedb52 speedb53 speedb54 speedb55
speedb56 ...
    speedb57 speedb58 speedb59 speedb510 speedb511],fib5p,'b^');
xlabel('Speed [mph]');
ylabel('Fault index passenger');
hold on;
plot(X,(pp(1)*X.^2+pp(2)*X+pp(3))+3*stdp,'k.',X,(pp(1)*X.^2+pp(2)
*X+pp(3))-3*stdp,'k.',Xt,Ztdfp,'rx');
hold off;

```

```

speedb116 speedb117 speedb118 ...
    speedb119 speedb120 speedb121 speedb122 speedb123 speedb124
speedb125 speedb126 speedb127 ...
    speedb128 speedb129 speedb130],fibpr,'bx',[speedb21 speedb22
speedb23 speedb24 speedb25 speedb26 ...
    speedb27 speedb28 speedb29 speedb210
speedb211],fib2pr,'bs',[speedb31 speedb32 speedb33 speedb34 speedb35
speedb36 ...
    speedb37 speedb38 speedb39 speedb310
speedb311],fib3pr,'bd',[speedb41 speedb42 speedb43 speedb44 speedb45
speedb46 ...
    speedb47 speedb48 speedb49 speedb410
speedb411],fib4pr,'bv',[speedb51 speedb52 speedb53 speedb54 speedb55
speedb56 ...
    speedb57 speedb58 speedb59 speedb510 speedb511],fib5pr,'b^');
xlabel('Speed [mph]');
ylabel('Fault index passenger rear');
hold on;
plot(X,(ppr(1)*X.^2+ppr(2)*X+ppr(3))+3*stdpr,'k.',X,(ppr(1)*X.^2+ppr(2)
*X+ppr(3))-3*stdpr,'k.',Xt,Ztdfpr,'rx');
hold off;

% Plot driver front false positives
figure(6);
plot([speedb11 speedb12 speedb13 speedb14 speedb15 speedb16 speedb17
speedb18 speedb19 ...
    speedb110 speedb111 speedb112 speedb113 speedb114 speedb115
speedb116 speedb117 speedb118 ...
    speedb119 speedb120 speedb121 speedb122 speedb123 speedb124
speedb125 speedb126 speedb127 ...
    speedb128 speedb129 speedb130],fibd,'bx',[speedb21 speedb22
speedb23 speedb24 speedb25 speedb26 ...
    speedb27 speedb28 speedb29 speedb210
speedb211],fib2d,'bs',[speedb31 speedb32 speedb33 speedb34 speedb35
speedb36 ...
    speedb37 speedb38 speedb39 speedb310
speedb311],fib3d,'bd',[speedb41 speedb42 speedb43 speedb44 speedb45
speedb46 ...
    speedb47 speedb48 speedb49 speedb410
speedb411],fib4d,'bv',[speedb51 speedb52 speedb53 speedb54 speedb55
speedb56 ...
    speedb57 speedb58 speedb59 speedb510 speedb511],fib5d,'b^');
xlabel('Speed [mph]');
ylabel('Fault index driver');
hold on;
plot(X,(pd(1)*X.^2+pd(2)*X+pd(3))+3*stdd,'k.',X,(pd(1)*X.^2+pd(2)*X+pd
(3))-3*stdd,'k.',Xtp,Ztpf,'rx');
hold off;

% Plot passenger front tire fault correct indications
figure(7);
plot([speedb11 speedb12 speedb13 speedb14 speedb15 speedb16 speedb17
speedb18 speedb19 ...
    speedb110 speedb111 speedb112 speedb113 speedb114 speedb115
speedb116 speedb117 speedb118 ...
    speedb119 speedb120 speedb121 speedb122 speedb123 speedb124

```

```

speedb125 speedb126 speedb127 ...
    speedb128 speedb129 speedb130],fibp,'bx',[speedb21 speedb22
speedb23 speedb24 speedb25 speedb26 ...
    speedb27 speedb28 speedb29 speedb210
speedb211],fib2p,'bs',[speedb31 speedb32 speedb33 speedb34 speedb35
speedb36 ...
    speedb37 speedb38 speedb39 speedb310
speedb311],fib3p,'bd',[speedb41 speedb42 speedb43 speedb44 speedb45
speedb46 ...
    speedb47 speedb48 speedb49 speedb410
speedb411],fib4p,'bv',[speedb51 speedb52 speedb53 speedb54 speedb55
speedb56 ...
    speedb57 speedb58 speedb59 speedb510 speedb511],fib5p,'b^');
xlabel('Speed [mph]');
ylabel('Fault index passenger');
hold on;
plot(X,(pp(1)*X.^2+pp(2)*X+pp(3))+3*stdp,'k.',X,(pp(1)*X.^2+pp(2)*X+pp(3))-3*stdp,'k.',Xtp,Ztpfp,'rx');
hold off;

% Plot driver rear false positives
figure(8);
plot([speedb11 speedb12 speedb13 speedb14 speedb15 speedb16 speedb17
speedb18 speedb19 ...
    speedb110 speedb111 speedb112 speedb113 speedb114 speedb115
speedb116 speedb117 speedb118 ...
    speedb119 speedb120 speedb121 speedb122 speedb123 speedb124
speedb125 speedb126 speedb127 ...
    speedb128 speedb129 speedb130],fibdr,'bx',[speedb21 speedb22
speedb23 speedb24 speedb25 speedb26 ...
    speedb27 speedb28 speedb29 speedb210
speedb211],fib2dr,'bs',[speedb31 speedb32 speedb33 speedb34 speedb35
speedb36 ...
    speedb37 speedb38 speedb39 speedb310
speedb311],fib3dr,'bd',[speedb41 speedb42 speedb43 speedb44 speedb45
speedb46 ...
    speedb47 speedb48 speedb49 speedb410
speedb411],fib4dr,'bv',[speedb51 speedb52 speedb53 speedb54 speedb55
speedb56 ...
    speedb57 speedb58 speedb59 speedb510 speedb511],fib5dr,'b^');
xlabel('Speed [mph]');
ylabel('Fault index driver rear');
hold on;
plot(X,(pdr(1)*X.^2+pdr(2)*X+pdr(3))+3*stddr,'k.',X,(pdr(1)*X.^2+pdr(2)*X+pdr(3))-3*stddr,'k.',Xtp,Ztpfr,'rx');
hold off;

% Plot passenger rear tire false positives
figure(9);
plot([speedb11 speedb12 speedb13 speedb14 speedb15 speedb16 speedb17
speedb18 speedb19 ...
    speedb110 speedb111 speedb112 speedb113 speedb114 speedb115
speedb116 speedb117 speedb118 ...
    speedb119 speedb120 speedb121 speedb122 speedb123 speedb124
speedb125 speedb126 speedb127 ...
    speedb128 speedb129 speedb130],fibpr,'bx',[speedb21 speedb22

```

```

speedb23 speedb24 speedb25 speedb26 ...
    speedb27 speedb28 speedb29 speedb210
speedb211],fib2pr,'bs',[speedb31 speedb32 speedb33 speedb34 speedb35
speedb36 ...
    speedb37 speedb38 speedb39 speedb310
speedb311],fib3pr,'bd',[speedb41 speedb42 speedb43 speedb44 speedb45
speedb46 ...
    speedb47 speedb48 speedb49 speedb410
speedb411],fib4pr,'bv',[speedb51 speedb52 speedb53 speedb54 speedb55
speedb56 ...
    speedb57 speedb58 speedb59 speedb510 speedb511],fib5pr,'b^');
xlabel('Speed [mph]');
ylabel('Fault index passenger');
hold on;
plot(X,(ppr(1)*X.^2+ppr(2)*X+ppr(3))+3*stdpr,'k.',X,(ppr(1)*X.^2+ppr(2)
*X+ppr(3))-3*stdpr,'k.',Xtp,Ztpfpr,'rx');
hold off;

% Plot changes in response spectra for driver front tire fault
figure(10);
plot(f,mean([abs(base11sf) abs(base12sf) abs(base13sf) abs(base14sf)
abs(base15sf) abs(base16sf) abs(base17sf) ...
    abs(base18sf) abs(base19sf) abs(base110sf) abs(base111sf)
abs(base112sf) abs(base113sf) abs(base114sf) abs(base115sf) ...
    abs(base116sf) abs(base117sf) abs(base118sf) abs(base119sf)
abs(base120sf) abs(base121sf) abs(base122sf) abs(base123sf) ...
    abs(base124sf) abs(base125sf) abs(base126sf) abs(base127sf)
abs(base128sf) abs(base129sf) abs(base130sf)],2),'b'); hold on;
plot(f,mean([abs(base21sf) abs(base22sf) abs(base23sf) abs(base24sf)
abs(base25sf) abs(base26sf) abs(base27sf) ...
    abs(base28sf) abs(base29sf) abs(base210sf) abs(base211sf)],2),'g');
plot(f,mean([abs(base31sf) abs(base32sf) abs(base33sf) abs(base34sf)
abs(base35sf) abs(base36sf) abs(base37sf) ...
    abs(base38sf) abs(base39sf) abs(base310sf) abs(base311sf)],2),'r');
plot(f,mean([abs(base41sf) abs(base42sf) abs(base43sf) abs(base44sf)
abs(base45sf) abs(base46sf) abs(base47sf) ...
    abs(base48sf) abs(base49sf) abs(base410sf) abs(base411sf)],2),'c');
plot(f,mean([abs(base51sf) abs(base52sf) abs(base53sf) abs(base54sf)
abs(base55sf) abs(base56sf) abs(base57sf) ...
    abs(base58sf) abs(base59sf) abs(base510sf) abs(base511sf)],2),'m');
plot(f,mean([abs(tiredf11sf) abs(tiredf12sf) abs(tiredf13sf)
abs(tiredf14sf) abs(tiredf15sf) abs(tiredf16sf) abs(tiredf17sf) ...
    abs(tiredf18sf) abs(tiredf19sf) abs(tiredf110sf) abs(tiredf111sf)
abs(tiredf112sf) abs(tiredf113sf) abs(tiredf114sf) abs(tiredf115sf) ...
    abs(tiredf116sf) abs(tiredf117sf) abs(tiredf118sf) abs(tiredf119sf)
abs(tiredf120sf) abs(tiredf121sf) abs(tiredf122sf) abs(tiredf123sf) ...
    abs(tiredf124sf) abs(tiredf125sf) abs(tiredf126sf) abs(tiredf127sf)
abs(tiredf128sf) abs(tiredf129sf) abs(tiredf130sf)],2),'k'); hold off;
xlabel('Frequency [Hz]');
ylabel('Magnitude \mu Accel [g]');
axis([0 200 0 3e-3]);

% Plot changes in response spectra for passenger front tire fault
figure(11);
plot(f,mean([abs(base11sfp) abs(base12sfp) abs(base13sfp)
abs(base14sfp) abs(base15sfp) abs(base16sfp) abs(base17sfp) ...

```

```

    abs(base18sfp) abs(base19sfp) abs(base110sfp) abs(base111sfp)
abs(base112sfp) abs(base113sfp) abs(base114sfp) abs(base115sfp) ...
    abs(base116sfp) abs(base117sfp) abs(base118sfp) abs(base119sfp)
abs(base120sfp) abs(base121sfp) abs(base122sfp) abs(base123sfp) ...
    abs(base124sfp) abs(base125sfp) abs(base126sfp) abs(base127sfp)
abs(base128sfp) abs(base129sfp) abs(base130sfp)],2), 'b'); hold on;
plot(f,mean([abs(base21sfp) abs(base22sfp) abs(base23sfp)
abs(base24sfp) abs(base25sfp) abs(base26sfp) abs(base27sfp) ...
    abs(base28sfp) abs(base29sfp) abs(base210sfp)
abs(base211sfp)],2), 'g');
plot(f,mean([abs(base31sfp) abs(base32sfp) abs(base33sfp)
abs(base34sfp) abs(base35sfp) abs(base36sfp) abs(base37sfp) ...
    abs(base38sfp) abs(base39sfp) abs(base310sfp)
abs(base311sfp)],2), 'r');
plot(f,mean([abs(base41sfp) abs(base42sfp) abs(base43sfp)
abs(base44sfp) abs(base45sfp) abs(base46sfp) abs(base47sfp) ...
    abs(base48sfp) abs(base49sfp) abs(base410sfp)
abs(base411sfp)],2), 'c');
plot(f,mean([abs(base51sfp) abs(base52sfp) abs(base53sfp)
abs(base54sfp) abs(base55sfp) abs(base56sfp) abs(base57sfp) ...
    abs(base58sfp) abs(base59sfp) abs(base510sfp)
abs(base511sfp)],2), 'm');
plot(f,mean([abs(tirepf11sfp) abs(tirepf12sfp) abs(tirepf13sfp)
abs(tirepf14sfp) abs(tirepf15sfp) abs(tirepf16sfp) abs(tirepf17sfp) ...
    abs(tirepf18sfp) abs(tirepf19sfp) abs(tirepf110sfp)
abs(tirepf111sfp) abs(tirepf112sfp) abs(tirepf113sfp) abs(tirepf114sfp)
abs(tirepf115sfp) ...
    abs(tirepf116sfp) abs(tirepf117sfp) abs(tirepf118sfp)
abs(tirepf119sfp) abs(tirepf120sfp) abs(tirepf121sfp) abs(tirepf122sfp)
abs(tirepf123sfp) ...
    abs(tirepf124sfp) abs(tirepf125sfp) abs(tirepf126sfp)
abs(tirepf127sfp) abs(tirepf128sfp) abs(tirepf129sfp)
abs(tirepf130sfp)],2), 'k'); hold off;
xlabel('Frequency [Hz]');
ylabel('Magnitude \mu Accel [g]');
axis([0 200 0 2e-1]);

% Plot changes in response spectra for driver rear tire fault
figure(12);
plot(f,mean([abs(base11sr) abs(base12sr) abs(base13sr) abs(base14sr)
abs(base15sr) abs(base16sr) abs(base17sr) ...
    abs(base18sr) abs(base19sr) abs(base110sr) abs(base111sr)
abs(base112sr) abs(base113sr) abs(base114sr) abs(base115sr) ...
    abs(base116sr) abs(base117sr) abs(base118sr) abs(base119sr)
abs(base120sr) abs(base121sr) abs(base122sr) abs(base123sr) ...
    abs(base124sr) abs(base125sr) abs(base126sr) abs(base127sr)
abs(base128sr) abs(base129sr) abs(base130sr)],2), 'b'); hold on;
plot(f,mean([abs(base21sr) abs(base22sr) abs(base23sr) abs(base24sr)
abs(base25sr) abs(base26sr) abs(base27sr) ...
    abs(base28sr) abs(base29sr) abs(base210sr) abs(base211sr)],2), 'g');
plot(f,mean([abs(base31sr) abs(base32sr) abs(base33sr) abs(base34sr)
abs(base35sr) abs(base36sr) abs(base37sr) ...
    abs(base38sr) abs(base39sr) abs(base310sr) abs(base311sr)],2), 'r');
plot(f,mean([abs(base41sr) abs(base42sr) abs(base43sr) abs(base44sr)
abs(base45sr) abs(base46sr) abs(base47sr) ...
    abs(base48sr) abs(base49sr) abs(base410sr) abs(base411sr)],2), 'c');
plot(f,mean([abs(base51sr) abs(base52sr) abs(base53sr) abs(base54sr)

```

```

abs(base55sr) abs(base56sr) abs(base57sr) ...
abs(base58sr) abs(base59sr) abs(base510sr) abs(base511sr)],2), 'm');
plot(f,mean([abs(tiredr11sr) abs(tiredr12sr) abs(tiredr13sr)
abs(tiredr14sr) abs(tiredr15sr) abs(tiredr16sr) abs(tiredr17sr) ...
abs(tiredr18sr) abs(tiredr19sr) abs(tiredr110sr) abs(tiredr111sr)
abs(tiredr112sr) abs(tiredr113sr) abs(tiredr114sr) abs(tiredr115sr) ...
abs(tiredr116sr) abs(tiredr117sr) abs(tiredr118sr) abs(tiredr119sr)
abs(tiredr120sr) abs(tiredr121sr) abs(tiredr122sr) abs(tiredr123sr) ...
abs(tiredr124sr) abs(tiredr125sr) abs(tiredr126sr) abs(tiredr127sr)
abs(tiredr128sr) abs(tiredr129sr) abs(tiredr130sr)],2), 'k'); hold off;
xlabel('Frequency [Hz]');
ylabel('Magnitude \mu Accel [g]');
axis([0 200 0 3e-3]);

% Plot changes in response spectra for passenger rear tire fault
figure(13);
plot(f,mean([abs(base11srp) abs(base12srp) abs(base13srp)
abs(base14srp) abs(base15srp) abs(base16srp) abs(base17srp) ...
abs(base18srp) abs(base19srp) abs(base110srp) abs(base111srp)
abs(base112srp) abs(base113srp) abs(base114srp) abs(base115srp) ...
abs(base116srp) abs(base117srp) abs(base118srp) abs(base119srp)
abs(base120srp) abs(base121srp) abs(base122srp) abs(base123srp) ...
abs(base124srp) abs(base125srp) abs(base126srp) abs(base127srp)
abs(base128srp) abs(base129srp) abs(base130srp)],2), 'b'); hold on;
plot(f,mean([abs(base21srp) abs(base22srp) abs(base23srp)
abs(base24srp) abs(base25srp) abs(base26srp) abs(base27srp) ...
abs(base28srp) abs(base29srp) abs(base210srp)
abs(base211srp)],2), 'g');
plot(f,mean([abs(base31srp) abs(base32srp) abs(base33srp)
abs(base34srp) abs(base35srp) abs(base36srp) abs(base37srp) ...
abs(base38srp) abs(base39srp) abs(base310srp)
abs(base311srp)],2), 'r');
plot(f,mean([abs(base41srp) abs(base42srp) abs(base43srp)
abs(base44srp) abs(base45srp) abs(base46srp) abs(base47srp) ...
abs(base48srp) abs(base49srp) abs(base410srp)
abs(base411srp)],2), 'c');
plot(f,mean([abs(base51srp) abs(base52srp) abs(base53srp)
abs(base54srp) abs(base55srp) abs(base56srp) abs(base57srp) ...
abs(base58srp) abs(base59srp) abs(base510srp)
abs(base511srp)],2), 'm');
plot(f,mean([abs(tirepr11srp) abs(tirepr12srp) abs(tirepr13srp)
abs(tirepr14srp) abs(tirepr15srp) abs(tirepr16srp) abs(tirepr17srp) ...
abs(tirepr18srp) abs(tirepr19srp) abs(tirepr110srp)
abs(tirepr111srp) abs(tirepr112srp) abs(tirepr113srp) abs(tirepr114srp)
abs(tirepr115srp) ...
abs(tirepr116srp) abs(tirepr117srp) abs(tirepr118srp)
abs(tirepr119srp) abs(tirepr120srp) abs(tirepr121srp) abs(tirepr122srp)
abs(tirepr123srp) ...
abs(tirepr124srp) abs(tirepr125srp) abs(tirepr126srp)
abs(tirepr127srp) abs(tirepr128srp) abs(tirepr129srp)
abs(tirepr130srp)],2), 'k'); hold off;
xlabel('Frequency [Hz]');
ylabel('Magnitude \mu Accel [g]');
axis([0 200 0 2e-1]);

```

```
% Modal analysis of extended diagnostic cleat
load Workspace

% Plot driving point frequency response functions on two plates
figure(1);
semilogy(f,abs(squeeze(DriverInner(:,13,[3 6]))));
xlabel('Freq [Hz]');
ylabel('Mag. H [g/lb], Coh');
axis([0 200 1e-6 1e0]);

figure(2);
semilogy(f,abs(squeeze(PassengerOuter(:,13,[3 6]))));
xlabel('Freq [Hz]');
ylabel('Mag. H [g/lb], Coh');
axis([0 200 1e-6 1e0]);

% Define plate geometry
X=[(0:1:17)'; (0:1:17)'; (0:1:17)'];
Y=[ones(18,1)*0; ones(18,1)*1; ones(18,1)*2];
Z=[ones(18,1)*0; ones(18,1)*0; ones(18,1)*0];

% Plot FRFs
figure(3);
subplot(131);
semilogy(f,abs(squeeze(DriverInner(:,1:18,[3]))),'-');
xlabel('Freq [Hz]');
ylabel('Mag. H [g/lb]');
axis([0 200 1e-6 1e0]);
subplot(132);
semilogy(f,abs(squeeze(DriverCenter(:,1:18,[3]))),'-');
xlabel('Freq [Hz]');
ylabel('Mag. H [g/lb]');
axis([0 200 1e-6 1e0]);
subplot(133);
semilogy(f,abs(squeeze(DriverOuter(:,1:18,[3]))),'-');
xlabel('Freq [Hz]');
ylabel('Mag. H [g/lb]');
axis([0 200 1e-6 1e0]);

figure(4);
subplot(131);
semilogy(f,abs(squeeze(PassengerOuter(:,1:18,[3]))),'-');
xlabel('Freq [Hz]');
ylabel('Mag. H [g/lb]');
axis([0 200 1e-6 1e0]);
subplot(132);
semilogy(f,abs(squeeze(PassengerCenter(:,1:18,[3]))),'-');
xlabel('Freq [Hz]');
ylabel('Mag. H [g/lb]');
axis([0 200 1e-6 1e0]);
subplot(133);
semilogy(f,abs(squeeze(PassengerInner(:,1:18,[3]))),'-');
xlabel('Freq [Hz]');
```

```

ylabel('Mag. H [g/lb]');
axis([0 200 1e-6 1e0]);

% Find amplitudes and frequencies
% Driver side 18.5 Hz, 35 Hz, 57 Hz, 75 Hz, 102 Hz, 146 Hz
% Passenger side 21 Hz, 35 Hz, 86 Hz, 105 Hz, 127 Hz

drivmd1=[conj(DriverInner(round(18.5/f(2)),1:18,3))';
conj(DriverCenter(round(18.5/f(2)),1:18,3))';
conj(DriverOuter(round(18.5/f(2)),1:18,3))'];
drivmd2=[conj(DriverInner(round(35/f(2)),1:18,3))';
conj(DriverCenter(round(35/f(2)),1:18,3))';
conj(DriverOuter(round(35/f(2)),1:18,3))'];
drivmd3=[conj(DriverInner(round(57/f(2)),1:18,3))';
conj(DriverCenter(round(57/f(2)),1:18,3))';
conj(DriverOuter(round(57/f(2)),1:18,3))'];
drivmd4=[conj(DriverInner(round(75/f(2)),1:18,3))';
conj(DriverCenter(round(75/f(2)),1:18,3))';
conj(DriverOuter(round(75/f(2)),1:18,3))'];
drivmd5=[conj(DriverInner(round(102/f(2)),1:18,3))';
conj(DriverCenter(round(102/f(2)),1:18,3))';
conj(DriverOuter(round(102/f(2)),1:18,3))'];
drivmd6=[conj(DriverInner(round(146/f(2)),1:18,3))';
conj(DriverCenter(round(146/f(2)),1:18,3))';
conj(DriverOuter(round(146/f(2)),1:18,3))];

passmd1=[conj(PassengerOuter(round(21/f(2)),1:18,3))';
conj(PassengerCenter(round(21/f(2)),1:18,3))';
conj(PassengerInner(round(21/f(2)),1:18,3))'];
passmd2=[conj(PassengerOuter(round(35/f(2)),1:18,3))';
conj(PassengerCenter(round(35/f(2)),1:18,3))';
conj(PassengerInner(round(35/f(2)),1:18,3))'];
passmd3=[conj(PassengerOuter(round(86/f(2)),1:18,3))';
conj(PassengerCenter(round(86/f(2)),1:18,3))';
conj(PassengerInner(round(86/f(2)),1:18,3))'];
passmd4=[conj(PassengerOuter(round(105/f(2)),1:18,3))';
conj(PassengerCenter(round(105/f(2)),1:18,3))';
conj(PassengerInner(round(105/f(2)),1:18,3))'];
passmd5=[conj(PassengerOuter(round(127/f(2)),1:18,3))';
conj(PassengerCenter(round(127/f(2)),1:18,3))';
conj(PassengerInner(round(127/f(2)),1:18,3))];

% Plot shapes
figure(5);
plot3(X(1:18),Y(1:18),Z(1:18), 'b.-'
',X(1+18:18+18),Y(1+18:18+18),Z(1+18:18+18), 'b.-'
',X(1+36:18+36),Y(1+36:18+36),Z(1+36:18+36), 'b.-'); hold on;
plot3(X([1 19 37]),Y([1 19 37]),Z([1 19 37]), 'b.-',X([1 19 37]+1),Y([1 19 37]+1),Z([1 19 37]+1), 'b.-',X([1 19 37]+2),Y([1 19 37]+2),Z([1 19 37]+2), 'b.-',...
X([1 19 37]+3),Y([1 19 37]+3),Z([1 19 37]+3), 'b.-',X([1 19 37]+4),Y([1 19 37]+4),Z([1 19 37]+4), 'b.-',X([1 19 37]+5),Y([1 19 37]+5),Z([1 19 37]+5), 'b.-',...
X([1 19 37]+6),Y([1 19 37]+6),Z([1 19 37]+6), 'b.-',X([1 19 37]+7),Y([1 19 37]+7),Z([1 19 37]+7), 'b.-',X([1 19 37]+8),Y([1 19 37]+8),Z([1 19 37]+8), 'b.-',...

```

```

X([1 19 37]+9),Y([1 19 37]+9),Z([1 19 37]+9),'b.-',X([1 19
37]+10),Y([1 19 37]+10),Z([1 19 37]+10),'b.-',X([1 19 37]+11),Y([1 19
37]+11),Z([1 19 37]+11),'b.-',...
    X([1 19 37]+12),Y([1 19 37]+12),Z([1 19 37]+12),'b.-',X([1 19
37]+13),Y([1 19 37]+13),Z([1 19 37]+13),'b.-',X([1 19 37]+14),Y([1 19
37]+14),Z([1 19 37]+14),'b.-',...
    X([1 19 37]+15),Y([1 19 37]+15),Z([1 19 37]+15),'b.-',X([1 19
37]+16),Y([1 19 37]+16),Z([1 19 37]+16),'b.-',X([1 19 37]+17),Y([1 19
37]+17),Z([1 19 37]+17),'b.-';
Z=abs(drivmd5).*sin(angle(drivmd5));
plot3(X(1:18),Y(1:18),Z(1:18),'r.-
',X(1+18:18+18),Y(1+18:18+18),Z(1+18:18+18),'r.-
',X(1+36:18+36),Y(1+36:18+36),Z(1+36:18+36),'r.-'); hold on;
plot3(X([1 19 37]),Y([1 19 37]),Z([1 19 37]),'r.-',X([1 19 37]+1),Y([1
19 37]+1),Z([1 19 37]+1),'r.-',X([1 19 37]+2),Y([1 19 37]+2),Z([1 19
37]+2),'r.-',...
    X([1 19 37]+3),Y([1 19 37]+3),Z([1 19 37]+3),'r.-',X([1 19
37]+4),Y([1 19 37]+4),Z([1 19 37]+4),'r.-',X([1 19 37]+5),Y([1 19
37]+5),Z([1 19 37]+5),'r.-',...
    X([1 19 37]+6),Y([1 19 37]+6),Z([1 19 37]+6),'r.-',X([1 19
37]+7),Y([1 19 37]+7),Z([1 19 37]+7),'r.-',X([1 19 37]+8),Y([1 19
37]+8),Z([1 19 37]+8),'r.-',...
    X([1 19 37]+9),Y([1 19 37]+9),Z([1 19 37]+9),'r.-',X([1 19
37]+10),Y([1 19 37]+10),Z([1 19 37]+10),'r.-',X([1 19 37]+11),Y([1 19
37]+11),Z([1 19 37]+11),'r.-',...
    X([1 19 37]+12),Y([1 19 37]+12),Z([1 19 37]+12),'r.-',X([1 19
37]+13),Y([1 19 37]+13),Z([1 19 37]+13),'r.-',X([1 19 37]+14),Y([1 19
37]+14),Z([1 19 37]+14),'r.-',...
    X([1 19 37]+15),Y([1 19 37]+15),Z([1 19 37]+15),'r.-',X([1 19
37]+16),Y([1 19 37]+16),Z([1 19 37]+16),'r.-',X([1 19 37]+17),Y([1 19
37]+17),Z([1 19 37]+17),'r.-');
view(-5.5,16);
Z=[ones(18,1)*0; ones(18,1)*0; ones(18,1)*0];
xlabel('Length of plate');
ylabel('Width of plate');
zlabel('Operational deflection');

figure(6);
plot3(X(1:18),Y(1:18),Z(1:18),'b.-
',X(1+18:18+18),Y(1+18:18+18),Z(1+18:18+18),'b.-
',X(1+36:18+36),Y(1+36:18+36),Z(1+36:18+36),'b.-'); hold on;
plot3(X([1 19 37]),Y([1 19 37]),Z([1 19 37]),'b.-',X([1 19 37]+1),Y([1
19 37]+1),Z([1 19 37]+1),'b.-',X([1 19 37]+2),Y([1 19 37]+2),Z([1 19
37]+2),'b.-',...
    X([1 19 37]+3),Y([1 19 37]+3),Z([1 19 37]+3),'b.-',X([1 19
37]+4),Y([1 19 37]+4),Z([1 19 37]+4),'b.-',X([1 19 37]+5),Y([1 19
37]+5),Z([1 19 37]+5),'b.-',...
    X([1 19 37]+6),Y([1 19 37]+6),Z([1 19 37]+6),'b.-',X([1 19
37]+7),Y([1 19 37]+7),Z([1 19 37]+7),'b.-',X([1 19 37]+8),Y([1 19
37]+8),Z([1 19 37]+8),'b.-',...
    X([1 19 37]+9),Y([1 19 37]+9),Z([1 19 37]+9),'b.-',X([1 19
37]+10),Y([1 19 37]+10),Z([1 19 37]+10),'b.-',X([1 19 37]+11),Y([1 19
37]+11),Z([1 19 37]+11),'b.-',...
    X([1 19 37]+12),Y([1 19 37]+12),Z([1 19 37]+12),'b.-',X([1 19
37]+13),Y([1 19 37]+13),Z([1 19 37]+13),'b.-',X([1 19 37]+14),Y([1 19
37]+14),Z([1 19 37]+14),'b.-',...
    X([1 19 37]+15),Y([1 19 37]+15),Z([1 19 37]+15),'b.-',X([1 19
37]+16),Y([1 19 37]+16),Z([1 19 37]+16),'b.-',X([1 19 37]+17),Y([1 19
37]+17),Z([1 19 37]+17),'b.-');

```

```

37]+16),Y([1 19 37]+16),Z([1 19 37]+16),'b.-',X([1 19 37]+17),Y([1 19
37]+17),Z([1 19 37]+17),'b.-');
Z=abs(passmd4).*sin(angle(passmd4));
plot3(X(1:18),Y(1:18),Z(1:18),'r.-
',X(1+18:18+18),Y(1+18:18+18),Z(1+18:18+18),'r.-
',X(1+36:18+36),Y(1+36:18+36),Z(1+36:18+36),'r.-'); hold on;
plot3(X([1 19 37]),Y([1 19 37]),Z([1 19 37]),'r.-',X([1 19 37]+1),Y([1
19 37]+1),Z([1 19 37]+1),'r.-',X([1 19 37]+2),Y([1 19 37]+2),Z([1 19
37]+2),'r.-',...
    X([1 19 37]+3),Y([1 19 37]+3),Z([1 19 37]+3),'r.-',X([1 19
37]+4),Y([1 19 37]+4),Z([1 19 37]+4),'r.-',X([1 19 37]+5),Y([1 19
37]+5),Z([1 19 37]+5),'r.-',...
        X([1 19 37]+6),Y([1 19 37]+6),Z([1 19 37]+6),'r.-',X([1 19
37]+7),Y([1 19 37]+7),Z([1 19 37]+7),'r.-',X([1 19 37]+8),Y([1 19
37]+8),Z([1 19 37]+8),'r.-',...
            X([1 19 37]+9),Y([1 19 37]+9),Z([1 19 37]+9),'r.-',X([1 19
37]+10),Y([1 19 37]+10),Z([1 19 37]+10),'r.-',X([1 19 37]+11),Y([1 19
37]+11),Z([1 19 37]+11),'r.-',...
                X([1 19 37]+12),Y([1 19 37]+12),Z([1 19 37]+12),'r.-',X([1 19
37]+13),Y([1 19 37]+13),Z([1 19 37]+13),'r.-',X([1 19 37]+14),Y([1 19
37]+14),Z([1 19 37]+14),'r.-',...
                    X([1 19 37]+15),Y([1 19 37]+15),Z([1 19 37]+15),'r.-',X([1 19
37]+16),Y([1 19 37]+16),Z([1 19 37]+16),'r.-',X([1 19 37]+17),Y([1 19
37]+17),Z([1 19 37]+17),'r.-');
view(-5.5,16);
Z=[ones(18,1)*0; ones(18,1)*0; ones(18,1)*0];
xlabel('Length of plate');
ylabel('Width of plate');
zlabel('Operational deflection');

% Extended diagnostic cleat model
% D. E. Adams
% February 20, 2011

cd('c:\documents and settings\deadams\my documents\purd10_11');

clear all;
%close all;

% Define element parameters
Ms=400;
Mu=Ms/8;
Ks=60000*1.00;
Ku=Ks*5*1.00;
Mp=58/40; % Mass of plate in kg with density 7850 kg/m^3
7850*(5*12*0.0254*2.5*12*0.0254*0.25*0.0254)
Kp=4.8e4; %
(3*2e11*(2.5*12*0.0254*(0.25*0.0254)^3/12))/(2.5/5*12*0.0254)^3
Kb=0.0001*Kp;
Cu=0.003*Ku*1.00;
Cs=0.003*Ks*1.00;

% State equations for quarter car model
% Ms*xsddot = +Cs*(xudot-xsdot)+Ks*(xu-xs)
% Mu*xuddot = +Cu*(xcdot-xudot)+Ku*(xc-xu)-Cs*(xudot-xsdot)-Ks*(xu-xs)

```

```
% q = [xu xs xudot xsdot]
Ac=[0 0 1 0;0 0 0 1; -(Ku+Ks)/Mu Ks/Mu -(Cu+Cs)/Mu Cs/Mu; Ks/Ms -Ks/Ms
Cs/Ms -Cs/Ms];
Bc=[0 0;0 0; Ku/Mu Cu/Mu;0 0]; % Inputs in displacement and velocity of
tire base over the cleat
Cc=[Ku 0 Cu 0]; % Force output in tire for zero road deflection after
the tire rolls over cleat
Dc=zeros(1,2);

% Define mass and stiffness matrices for extended cleat plate
Nw=5;
Nl=8;
M=diag(ones(Nw*Nl,1)*Mp);
K=0*M;
K(1,1)=Kp+Kp+Kp;
K(1,2)=-Kp; K(1,9)=-Kp; K(1,10)=-Kp; K(1,3:8)=0; K(1,11:40)=0;
K(2,2)=Kp+Kp+Kp+Kp+Kp;
K(2,3)=-Kp; K(2,9)=-Kp; K(2,10)=-Kp; K(2,11)=-Kp; K(2,4:8)=0;
K(2,12:40)=0;
K(3,3)=Kp+Kp+Kp+Kp+Kp;
K(3,4)=-Kp; K(3,10)=-Kp; K(3,11)=-Kp; K(3,12)=-Kp; K(3,5:9)=0;
K(3,13:40)=0;
K(4,4)=Kp+Kp+Kp+Kp+Kp;
K(4,5)=-Kp; K(4,11)=-Kp; K(4,12)=-Kp; K(4,13)=-Kp; K(4,6:10)=0;
K(4,14:40)=0;
K(5,5)=Kp+Kp+Kp+Kp+Kp;
K(5,6)=-Kp; K(5,12)=-Kp; K(5,13)=-Kp; K(5,14)=-Kp; K(5,7:11)=0;
K(5,15:40)=0;
K(6,6)=Kp+Kp+Kp+Kp+Kp;
K(6,7)=-Kp; K(6,13)=-Kp; K(6,14)=-Kp; K(6,15)=-Kp; K(6,8:12)=0;
K(6,16:40)=0;
K(7,7)=Kp+Kp+Kp+Kp+Kp;
K(7,8)=-Kp; K(7,14)=-Kp; K(7,15)=-Kp; K(7,16)=-Kp; K(7,9:13)=0;
K(7,17:40)=0;
K(8,8)=Kp+Kp+Kp;
K(8,15)=-Kp; K(8,16)=-Kp; K(8,9:14)=0; K(8,17:40)=0;

K(9,9)=Kp+Kp+Kp+Kp+Kp;
K(9,10)=-Kp; K(9,17)=-Kp; K(9,18)=-Kp; K(9,11:16)=0; K(9,19:40)=0;
K(10,10)=Kp+Kp+Kp+Kp+Kp+Kp+Kp;
K(10,11)=-Kp; K(10,17)=-Kp; K(10,18)=-Kp; K(10,19)=-Kp; K(10,12:16)=0;
K(10,20:40)=0;
K(11,11)=Kp+Kp+Kp+Kp+Kp+Kp+Kp;
K(11,12)=-Kp; K(11,18)=-Kp; K(11,19)=-Kp; K(11,20)=-Kp; K(11,13:17)=0;
K(11,21:40)=0;
K(12,12)=Kp+Kp+Kp+Kp+Kp+Kp+Kp;
K(12,13)=-Kp; K(12,19)=-Kp; K(12,20)=-Kp; K(12,21)=-Kp; K(12,14:18)=0;
K(12,22:40)=0;
K(13,13)=Kp+Kp+Kp+Kp+Kp+Kp+Kp;
K(13,14)=-Kp; K(13,20)=-Kp; K(13,21)=-Kp; K(13,22)=-Kp; K(13,15:19)=0;
K(13,23:40)=0;
K(14,14)=Kp+Kp+Kp+Kp+Kp+Kp+Kp;
K(14,15)=-Kp; K(14,21)=-Kp; K(14,22)=-Kp; K(14,23)=-Kp; K(14,16:20)=0;
K(14,24:40)=0;
K(15,15)=Kp+Kp+Kp+Kp+Kp+Kp+Kp;
K(15,16)=-Kp; K(15,22)=-Kp; K(15,23)=-Kp; K(15,24)=-Kp; K(15,17:21)=0;
```

$K(15, 25: 40) = 0;$
 $K(16, 16) = K_p + K_p + K_p + K_p + K_p;$
 $K(16, 23) = -K_p; \quad K(16, 24) = -K_p; \quad K(16, 17: 22) = 0; \quad K(16, 25: 40) = 0;$

 $K(17, 17) = K_p + K_p + K_p + K_p + K_p;$
 $K(17, 18) = -K_p; \quad K(17, 25) = -K_p; \quad K(17, 26) = -K_p; \quad K(17, 19: 24) = 0; \quad K(17, 27: 40) = 0;$
 $K(18, 18) = K_p + K_p + K_p + K_p + K_p + K_p + K_p;$
 $K(18, 19) = -K_p; \quad K(18, 25) = -K_p; \quad K(18, 26) = -K_p; \quad K(18, 27) = -K_p; \quad K(18, 20: 24) = 0;$
 $K(18, 28: 40) = 0;$
 $K(19, 19) = K_p + K_p + K_p + K_p + K_p + K_p + K_p;$
 $K(19, 20) = -K_p; \quad K(19, 26) = -K_p; \quad K(19, 27) = -K_p; \quad K(19, 28) = -K_p; \quad K(19, 21: 25) = 0;$
 $K(19, 29: 40) = 0;$
 $K(20, 20) = K_p + K_p + K_p + K_p + K_p + K_p + K_p;$
 $K(20, 21) = -K_p; \quad K(20, 27) = -K_p; \quad K(20, 28) = -K_p; \quad K(20, 29) = -K_p; \quad K(20, 22: 26) = 0;$
 $K(20, 30: 40) = 0;$
 $K(21, 21) = K_p + K_p + K_p + K_p + K_p + K_p + K_p;$
 $K(21, 22) = -K_p; \quad K(21, 28) = -K_p; \quad K(21, 29) = -K_p; \quad K(21, 30) = -K_p; \quad K(21, 23: 27) = 0;$
 $K(21, 31: 40) = 0;$
 $K(22, 22) = K_p + K_p + K_p + K_p + K_p + K_p + K_p;$
 $K(22, 23) = -K_p; \quad K(22, 29) = -K_p; \quad K(22, 30) = -K_p; \quad K(22, 31) = -K_p; \quad K(22, 24: 28) = 0;$
 $K(22, 32: 40) = 0;$
 $K(23, 23) = K_p + K_p + K_p + K_p + K_p + K_p + K_p;$
 $K(23, 24) = -K_p; \quad K(23, 30) = -K_p; \quad K(23, 31) = -K_p; \quad K(23, 32) = -K_p; \quad K(23, 25: 29) = 0;$
 $K(23, 33: 40) = 0;$
 $K(24, 24) = K_p + K_p + K_p + K_p + K_p;$
 $K(24, 31) = -K_p; \quad K(24, 32) = -K_p; \quad K(24, 25: 30) = 0; \quad K(24, 33: 40) = 0;$

 $K(25, 25) = K_p + K_p + K_p + K_p + K_p;$
 $K(25, 26) = -K_p; \quad K(25, 33) = -K_p; \quad K(25, 34) = -K_p; \quad K(25, 27: 32) = 0; \quad K(25, 35: 40) = 0;$
 $K(26, 26) = K_p + K_p + K_p + K_p + K_p + K_p + K_p;$
 $K(26, 27) = -K_p; \quad K(26, 33) = -K_p; \quad K(26, 34) = -K_p; \quad K(26, 35) = -K_p; \quad K(26, 28: 32) = 0;$
 $K(26, 36: 40) = 0;$
 $K(27, 27) = K_p + K_p + K_p + K_p + K_p + K_p + K_p;$
 $K(27, 28) = -K_p; \quad K(27, 34) = -K_p; \quad K(27, 35) = -K_p; \quad K(27, 36) = -K_p; \quad K(27, 29: 33) = 0;$
 $K(27, 37: 40) = 0;$
 $K(28, 28) = K_p + K_p + K_p + K_p + K_p + K_p + K_p;$
 $K(28, 29) = -K_p; \quad K(28, 35) = -K_p; \quad K(28, 36) = -K_p; \quad K(28, 37) = -K_p; \quad K(28, 30: 34) = 0;$
 $K(28, 38: 40) = 0;$
 $K(29, 29) = K_p + K_p + K_p + K_p + K_p + K_p + K_p;$
 $K(29, 30) = -K_p; \quad K(29, 36) = -K_p; \quad K(29, 37) = -K_p; \quad K(29, 38) = -K_p; \quad K(29, 31: 35) = 0;$
 $K(29, 39: 40) = 0;$
 $K(30, 30) = K_p + K_p + K_p + K_p + K_p + K_p + K_p;$
 $K(30, 31) = -K_p; \quad K(30, 37) = -K_p; \quad K(30, 38) = -K_p; \quad K(30, 39) = -K_p; \quad K(30, 32: 36) = 0;$
 $K(30, 40) = 0;$
 $K(31, 31) = K_p + K_p + K_p + K_p + K_p + K_p + K_p;$
 $K(31, 32) = -K_p; \quad K(31, 38) = -K_p; \quad K(31, 39) = -K_p; \quad K(31, 40) = -K_p; \quad K(31, 33: 37) = 0;$
 $K(32, 32) = K_p + K_p + K_p + K_p + K_p;$
 $K(32, 39) = -K_p; \quad K(32, 40) = -K_p; \quad K(32, 33: 38) = 0;$

 $K(33, 33) = K_p + K_p + K_p;$
 $K(33, 34) = -K_p; \quad K(33, 35: 40) = 0;$
 $K(34, 34) = K_p + K_p + K_p + K_p + K_p;$
 $K(34, 35) = -K_p; \quad K(34, 36: 40) = 0;$
 $K(35, 35) = K_p + K_p + K_p + K_p + K_p;$
 $K(35, 36) = -K_p; \quad K(35, 37: 40) = 0;$
 $K(36, 36) = K_p + K_p + K_p + K_p + K_p;$

```

K(36,37)=-Kp; K(36,38:40)=0;
K(37,37)=Kp+Kp+Kp+Kp;
K(37,38)=-Kp; K(37,39:40)=0;
K(38,38)=Kp+Kp+Kp+Kp;
K(38,39)=-Kp; K(38,40)=0;
K(39,39)=Kp+Kp+Kp+Kp;
K(39,40)=-Kp;
K(40,40)=Kp+Kp+Kp;

% Complete symmetry
temp=K;
for ii=1:40,
    temp(ii,ii)=0;
end
K=K+temp';

% Add in elastic foundation of rubber support
for ii=1:40,
    K(ii,ii)=K(ii,ii)+Kb;
end

% Create damping matrix
C=0.003*K;

% Create state variable matrix for extended cleat plates
Ap=zeros(max(size(K))); eye(max(size(K))); -inv(M)*K -inv(M)*C];
Bp=zeros(2*max(size(K)),8);
Bp(1:2*max(size(K)),1)=[zeros(max(size(K)),1); zeros(16,1); 1;
zeros(7,1); zeros(16,1)]; % Inputs along centerline of plate
Bp(1:2*max(size(K)),2)=[zeros(max(size(K)),1); zeros(17,1); 1;
zeros(6,1); zeros(16,1)];
Bp(1:2*max(size(K)),3)=[zeros(max(size(K)),1); zeros(18,1); 1;
zeros(5,1); zeros(16,1)];
Bp(1:2*max(size(K)),4)=[zeros(max(size(K)),1); zeros(19,1); 1;
zeros(4,1); zeros(16,1)];
Bp(1:2*max(size(K)),5)=[zeros(max(size(K)),1); zeros(20,1); 1;
zeros(3,1); zeros(16,1)];
Bp(1:2*max(size(K)),6)=[zeros(max(size(K)),1); zeros(21,1); 1;
zeros(2,1); zeros(16,1)];
Bp(1:2*max(size(K)),7)=[zeros(max(size(K)),1); zeros(22,1); 1;
zeros(1,1); zeros(16,1)];
Bp(1:2*max(size(K)),8)=[zeros(max(size(K)),1); zeros(23,1); 1;
zeros(16,1)];

% Bp(1:2*max(size(K)),1)=[zeros(max(size(K)),1); zeros(8,1); 1;
zeros(7,1); zeros(24,1)]; % Inputs along line left of center of plate
% Bp(1:2*max(size(K)),2)=[zeros(max(size(K)),1); zeros(9,1); 1;
zeros(6,1); zeros(24,1)];
% Bp(1:2*max(size(K)),3)=[zeros(max(size(K)),1); zeros(10,1); 1;
zeros(5,1); zeros(24,1)];
% Bp(1:2*max(size(K)),4)=[zeros(max(size(K)),1); zeros(11,1); 1;
zeros(4,1); zeros(24,1)];
% Bp(1:2*max(size(K)),5)=[zeros(max(size(K)),1); zeros(12,1); 1;
zeros(3,1); zeros(24,1)];
% Bp(1:2*max(size(K)),6)=[zeros(max(size(K)),1); zeros(13,1); 1;
zeros(2,1); zeros(24,1)];

```

```

% Bp(1:2*max(size(K)),7)=[zeros(max(size(K)),1); zeros(14,1); 1;
zeros(1,1); zeros(24,1)];
% Bp(1:2*max(size(K)),8)=[zeros(max(size(K)),1); zeros(15,1); 1;
zeros(24,1)];
%
% Bp(1:2*max(size(K)),1)=[zeros(max(size(K)),1); 1; zeros(7,1);
zeros(32,1)]; % Inputs along line left on left edge of plate
% Bp(1:2*max(size(K)),2)=[zeros(max(size(K)),1); zeros(1,1); 1;
zeros(6,1); zeros(32,1)];
% Bp(1:2*max(size(K)),3)=[zeros(max(size(K)),1); zeros(2,1); 1;
zeros(5,1); zeros(32,1)];
% Bp(1:2*max(size(K)),4)=[zeros(max(size(K)),1); zeros(3,1); 1;
zeros(4,1); zeros(32,1)];
% Bp(1:2*max(size(K)),5)=[zeros(max(size(K)),1); zeros(4,1); 1;
zeros(3,1); zeros(32,1)];
% Bp(1:2*max(size(K)),6)=[zeros(max(size(K)),1); zeros(5,1); 1;
zeros(2,1); zeros(32,1)];
% Bp(1:2*max(size(K)),7)=[zeros(max(size(K)),1); zeros(6,1); 1;
zeros(1,1); zeros(32,1)];
% Bp(1:2*max(size(K)),8)=[zeros(max(size(K)),1); zeros(7,1); 1;
zeros(32,1)];
%
% Bp(1:2*max(size(K)),1)=[zeros(max(size(K)),1); zeros(24,1); 1;
zeros(7,1); zeros(8,1)]; % Inputs along line right of center of plate
% Bp(1:2*max(size(K)),2)=[zeros(max(size(K)),1); zeros(25,1); 1;
zeros(6,1); zeros(8,1)];
% Bp(1:2*max(size(K)),3)=[zeros(max(size(K)),1); zeros(26,1); 1;
zeros(5,1); zeros(8,1)];
% Bp(1:2*max(size(K)),4)=[zeros(max(size(K)),1); zeros(27,1); 1;
zeros(4,1); zeros(8,1)];
% Bp(1:2*max(size(K)),5)=[zeros(max(size(K)),1); zeros(28,1); 1;
zeros(3,1); zeros(8,1)];
% Bp(1:2*max(size(K)),6)=[zeros(max(size(K)),1); zeros(29,1); 1;
zeros(2,1); zeros(8,1)];
% Bp(1:2*max(size(K)),7)=[zeros(max(size(K)),1); zeros(30,1); 1;
zeros(1,1); zeros(8,1)];
% Bp(1:2*max(size(K)),8)=[zeros(max(size(K)),1); zeros(31,1); 1;
zeros(8,1)];
%
% Bp(1:2*max(size(K)),1)=[zeros(max(size(K)),1); zeros(32,1); 1;
zeros(7,1)]; % Inputs along line on right edge of plate
% Bp(1:2*max(size(K)),2)=[zeros(max(size(K)),1); zeros(33,1); 1;
zeros(6,1)];
% Bp(1:2*max(size(K)),3)=[zeros(max(size(K)),1); zeros(34,1); 1;
zeros(5,1)];
% Bp(1:2*max(size(K)),4)=[zeros(max(size(K)),1); zeros(35,1); 1;
zeros(4,1)];
% Bp(1:2*max(size(K)),5)=[zeros(max(size(K)),1); zeros(36,1); 1;
zeros(3,1)];
% Bp(1:2*max(size(K)),6)=[zeros(max(size(K)),1); zeros(37,1); 1;
zeros(2,1)];
% Bp(1:2*max(size(K)),7)=[zeros(max(size(K)),1); zeros(38,1); 1;
zeros(1,1)];
% Bp(1:2*max(size(K)),8)=[zeros(max(size(K)),1); zeros(39,1); 1];

Bp(41:80,:)=inv(M)*Bp(41:80,:);
Cp=[eye(2*max(size(K)))];

```

```

Dp=zeros(2*max(size(K)),8);

% Generate frequency response functions
w=0:1:400;
for ii=1:max(size(w)),
    H(:,:,:,ii)=-w(ii)^2*inv(K-M*w(ii)^2+j*w(ii)*C);
end

% Plot frequency response functions
figure(1);
subplot(311);
semilogy(w/2/pi,abs(squeeze(H(4,17:19,:)))/9.81);
xlabel('Frequency [Hz]');
ylabel('Mag. H_{p,4} [g/N]');
axis([0 60 5e-4 5e-2]);
subplot(312);
semilogy(w/2/pi,abs(squeeze(H(4,20:21,:)))/9.81);
xlabel('Frequency [Hz]');
ylabel('Mag. H_{p,4} [g/N]');
axis([0 60 5e-4 5e-2]);
subplot(313);
semilogy(w/2/pi,abs(squeeze(H(4,22:24,:)))/9.81);
xlabel('Frequency [Hz]');
ylabel('Mag. H_{p,4} [g/N]');
axis([0 60 5e-4 5e-2]);

figure(2);
subplot(311);
semilogy(w/2/pi,abs(squeeze(H(4,17:19,:)))/9.81,'--'); hold on;
semilogy(w/2/pi,abs(squeeze(H(4,33:35,:)))/9.81); hold off
xlabel('Frequency [Hz]');
ylabel('Mag. H_{p,4} [g/N]');
axis([0 60 5e-4 5e-2]);
subplot(312);
semilogy(w/2/pi,abs(squeeze(H(4,20:21,:)))/9.81,'--'); hold on;
semilogy(w/2/pi,abs(squeeze(H(4,36:37,:)))/9.81); hold off
xlabel('Frequency [Hz]');
ylabel('Mag. H_{p,4} [g/N]');
axis([0 60 5e-4 5e-2]);
subplot(313);
semilogy(w/2/pi,abs(squeeze(H(4,22:24,:)))/9.81,'--'); hold on;
semilogy(w/2/pi,abs(squeeze(H(4,38:40,:)))/9.81); hold off
xlabel('Frequency [Hz]');
ylabel('Mag. H_{p,4} [g/N]');
axis([0 60 5e-4 5e-2]);

% Calculate natural frequencies
[v,d]=eig((-inv(M)*K));
wn=imag(sqrt(diag(d)))/2/pi;

% Establish static geometry for plate
x=[0 1 2 3 4 5 6 7 0 1 2 3 4 5 6 7 0 1 2 3 4 5 6 7 0 1
2 3 4 5 6 7];
y=[zeros(1,8) ones(1,8) ones(1,8)*2 ones(1,8)*3 ones(1,8)*4];
z=zeros(1,40);

```

```
% Plot mode shape for plate
figure(3);
plot3(x,y,z,'.');
hold on;
plot3(x(1:8),y(1:8),z(1:8),'b',x(9:16),y(9:16),z(9:16),'b',x(17:24),y(17:24),z(17:24),'b',x(25:32),y(25:32),z(25:32),'b',x(33:40),y(33:40),z(33:40),'b');
plot3(x([1 9 17 25 33]),y([1 9 17 25 33]),z([1 9 17 25 33]),'b',x([1 9 17 25 33]+1),y([1 9 17 25 33]+1),z([1 9 17 25 33]+1),'b',x([1 9 17 25 33]+2),y([1 9 17 25 33]+2),z([1 9 17 25 33]+2),'b',x([1 9 17 25 33]+3),y([1 9 17 25 33]+3),z([1 9 17 25 33]+3),'b',x([1 9 17 25 33]+4),y([1 9 17 25 33]+4),z([1 9 17 25 33]+4),'b',x([1 9 17 25 33]+5),y([1 9 17 25 33]+5),z([1 9 17 25 33]+5),'b',x([1 9 17 25 33]+6),y([1 9 17 25 33]+6),z([1 9 17 25 33]+6),'b',x([1 9 17 25 33]+7),y([1 9 17 25 33]+7),z([1 9 17 25 33]+7),'b');
%shp=imag(squeeze(H(4,:,:round(17*2*pi/w(2))))));
shp=v(:,36)/max((v(:,36)));
shp=shp';
plot3(x,y,z+shp,'.');
hold on;
plot3(x(1:8),y(1:8),z(1:8)+shp(1:8),'r',x(9:16),y(9:16),z(9:16)+shp(9:16),'r',x(17:24),y(17:24),z(17:24)+shp(17:24),'r',x(25:32),y(25:32),z(25:32)+shp(25:32),'r',x(33:40),y(33:40),z(33:40)+shp(33:40),'r');
plot3(x([1 9 17 25 33]),y([1 9 17 25 33]),z([1 9 17 25 33])+shp([1 9 17 25 33]),'r',x([1 9 17 25 33]+1),y([1 9 17 25 33]+1),z([1 9 17 25 33]+1)+shp([1 9 17 25 33]+1),'r',x([1 9 17 25 33]+2),y([1 9 17 25 33]+2),z([1 9 17 25 33]+2)+shp([1 9 17 25 33]+2),'r',x([1 9 17 25 33]+3),y([1 9 17 25 33]+3),z([1 9 17 25 33]+3)+shp([1 9 17 25 33]+3),'r',x([1 9 17 25 33]+4),y([1 9 17 25 33]+4),z([1 9 17 25 33]+4)+shp([1 9 17 25 33]+4),'r',x([1 9 17 25 33]+5),y([1 9 17 25 33]+5),z([1 9 17 25 33]+5)+shp([1 9 17 25 33]+5),'r',x([1 9 17 25 33]+6),y([1 9 17 25 33]+6),z([1 9 17 25 33]+6)+shp([1 9 17 25 33]+6),'r',x([1 9 17 25 33]+7),y([1 9 17 25 33]+7),z([1 9 17 25 33]+7),'r');
xlabel('Length');
ylabel('Width');
zlabel('Deflection');

% Setup time domain simulation
Fs=1000*(max(wn)/2/pi);
wc=9/12; % width of cleat (feet)
hc=3*2.54e-2; % height (meters)
wp=5; % length of plate (feet)
vs=5*5280*1/3600; % feet/sec
Tc=wc/vs; % time on cleat
Tp=wp/vs; % time on plate
Nc=round(Tc/(1/Fs));
Np=round(Tp/(1/Fs));
Nt=Np+Nc;
tc=0:1/Fs:(Nc-1)/Fs;
tp=0:1/Fs:(Np-1)/Fs;
uc=hc*(1-cos(2*pi*tc/Tc));
vc=hc*(2*pi/Tc*sin(2*pi*tc/Tc));
t=0:1/Fs:(Nt-1)/Fs;

delta=max(size(t))-max(size(tc));

% Run simulation with quarter car on cleat
```

```

yc=lsim(ss(Ac,Bc,Cc,Dc),[uc' vc'; zeros(delta,2)],t);
yp=yc(Nc+1:Nt);

% Split force from tire into 8 segments to apply to
% lumped parameter degrees of freedom
dTp=Tp/8;
dNp=round(dTp/t(2));
%w=hanning(dNp);
w=ones(dNp,1);
%w2=hanning(dNp-3);
w2=ones(dNp-3,1);
u17=zeros(Np,1);
u17(1:dNp,1)=yp(1:dNp).*w;
u18=zeros(Np,1);
u18(1+dNp:2*dNp,1)=yp(dNp+1:2*dNp).*w;
u19=zeros(Np,1);
u19(1+2*dNp:3*dNp,1)=yp(2*dNp+1:3*dNp).*w;
u20=zeros(Np,1);
u20(1+3*dNp:4*dNp,1)=yp(3*dNp+1:4*dNp).*w;
u21=zeros(Np,1);
u21(1+4*dNp:5*dNp,1)=yp(4*dNp+1:5*dNp).*w;
u22=zeros(Np,1);
u22(1+5*dNp:6*dNp,1)=yp(5*dNp+1:6*dNp).*w;
u23=zeros(Np,1);
u23(1+6*dNp:7*dNp,1)=yp(6*dNp+1:7*dNp).*w;
u24=zeros(Np,1);
u24(1+7*dNp:8*dNp-3,1)=yp(7*dNp+1:8*dNp-3).*w2;

figure(4);
plot(tp,[u17 u18 u19 u20 u21 u22 u23 u24]); hold on;
plot(tp,[yp],'k--'); hold off;
xlabel('Time [sec]');
ylabel('Force [N]');

figure(5);
semilogy(0:1/tp(max(size(tp))):((max(size(tp))-1)/tp(max(size(tp)))),abs(fft([u17 u18 u19 u20 u21 u22 u23 u24]))/max(size(tp))^2); hold on;
semilogy(0:1/tp(max(size(tp))):((max(size(tp))-1)/tp(max(size(tp)))),abs(fft([yp]))/max(size(tp))^2,'k--'); hold off;
xlabel('Freq [Hz]');
ylabel('Force [N]');

% Run simulation with quarter car on plate
y=lsim(ss(Ap,Bp,Cp,Dp),[u17 u18 u19 u20 u21 u22 u23 u24],tp);
figure(6);
plot(tp,y(:,4),tp,yp/1000,tp(1:max(size(y))-2),diff(diff(y(:,4)))/tp(2)/tp(2)/9.81,'--');
legend('x_4','force in tire','a_4');
xlabel('Time [sec]');
ylabel('Displ [m], Accel [g], Force [N]');

figure(7);
subplot(211);
plot(0:1/tp(max(size(tp))):((max(size(tp))-1)/tp(max(size(tp)))),abs(fft(yp/1000))/max(size(yp))^2,'c'); hold on;

```

```
%legend('x_4','force in tire','a_4');
xlabel('Freq [Hz]');
ylabel('Force [N]');
axis([0 60 0 8]);
subplot(212);
plot(0:1/tp(max(size(tp(1:max(size(y))-2)))):(max(size(tp(1:max(size(y))-2)))-1)/tp(max(size(tp(1:max(size(y))-2))))),abs(fft(diff(diff(y(:,4)))/tp(2)/tp(2)/9.81))/max(size(yp))*2,'c');
hold on;
xlabel('Freq [Hz]');
ylabel('Accel [g]');
axis([0 60 0 8]);
%plot(0:1/tp(max(size(tp))):((max(size(tp))-1)/tp(max(size(tp))),abs(fft(y(:,4))),0:1/tp(max(size(tp))):((max(size(tp))-1)/tp(max(size(tp))),abs(fft(yp/1000)),0:1/tp(max(size(tp(1:max(size(y))-2)))):(max(size(tp(1:max(size(y))-2)))-1)/tp(max(size(tp(1:max(size(y))-2))))),abs(fft(diff(diff(y(:,4)))/tp(2)/tp(2)/9.81)), '--');

f=0:1/tp(max(size(tp(1:max(size(y))-2)))):(max(size(tp(1:max(size(y))-2))-1)/tp(max(size(tp(1:max(size(y))-2)))));

figure(8);
plot(0:1/tp(max(size(tp(1:max(size(y))-2))):((max(size(tp(1:max(size(y))-2)))-1)/tp(max(size(tp(1:max(size(y))-2))))),abs(fft(diff(diff(y(:,4)))/tp(2)/tp(2)/9.81))/max(size(yp))*2,'k');
hold on;
xlabel('Freq [Hz]');
ylabel('Accel [g]');
axis([0 20 0 8]);

% Calculate fault indices
SP=abs(fft(diff(diff(y(:,4)))/tp(2)/tp(2)/9.81))/max(size(yp))*2;
fs=1; % 0 Hz
fe=12; % 16.1 Hz

sum(abs(SP(fs:fe)))

indx=[36.1209 33.2444 32.4544 39.4622 41.6257;
      41.0779 37.6804 36.7044 44.8242 47.2310;
      39.4749 36.3807 35.4099 42.8990 45.0970;
      37.9682 34.8426 34.0394 41.6106 43.9602;
      47.7581 43.3696 43.4246 52.9929 56.3130];

figure(9);
plot(indx'-[indx(1,:); indx(1,:); indx(1,:); indx(1,:); indx(1,:)],'--x');
xlabel('Crossing location');
ylabel('Spectral energy from 0-16 Hz');
```

Instrumented Diagnostic Cleat for Condition-Based Maintenance of Wheeled Ground Vehicles

June 21, 2011

Douglas Adams, Raymond Bond
David Arseneau, Tiffany DiPetta, David Koester
Purdue Center for Systems Integrity

DISTRIBUTION STATEMENT A. Approved for public release; distribution is unlimited.

Disclaimer: Reference herein to any specific commercial company, product, process, or service by trade name, trademark, manufacturer, or otherwise, does not necessarily constitute or imply its endorsement, recommendation, or favoring by the United States Government or the Department of the Army (DoA). The opinions of the authors expressed herein do not necessarily state or reflect those of the United States Government or the DoA, and shall not be used for advertising or product endorsement purposes.



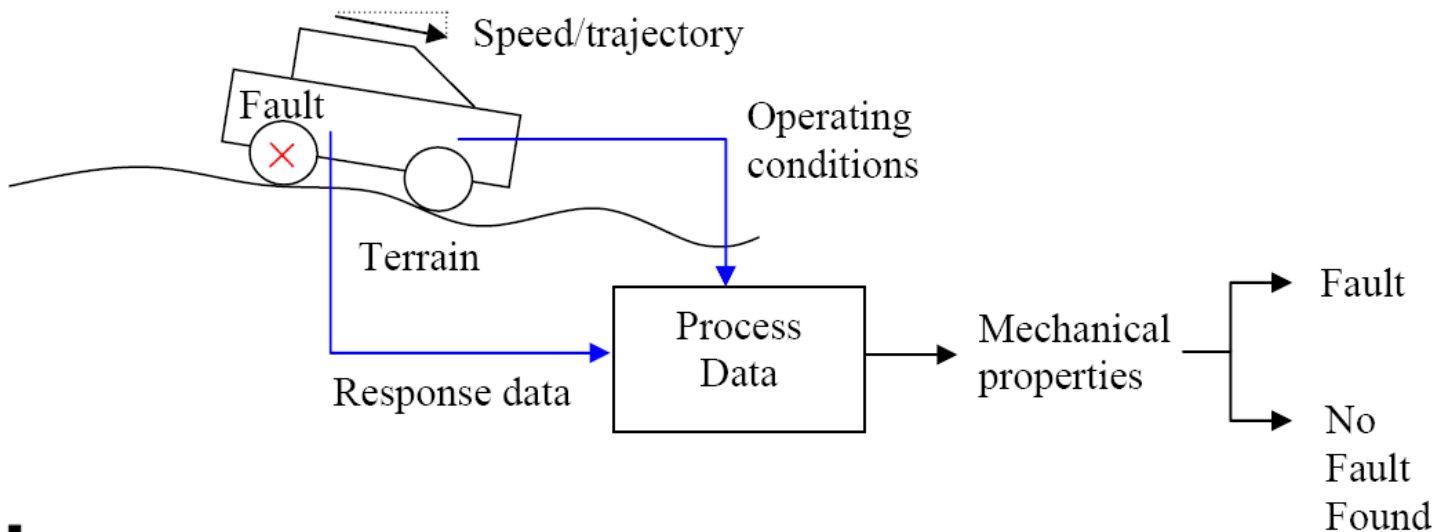
Technical Need

- **Supportability of ground vehicles:**
 - 3/5th of the DoD budget for O&S (Gorsich, 2007).
 - Maintenance based on reliability of a population.
 - Run to failure (find and fix)
 - Preventative (service when convenient)

Technical Issues

- **Condition monitoring of vehicles:**

- Widely varying terrains introduce variability that makes condition assessment difficult.
- Curse of dimensionality: M terrains with N sensors yields M^N datasets (Bishop, 1990), e.g., 6 sensors, 10 terrains, $1e6$ datasets, 11 years at 240 sets/day.



Cost

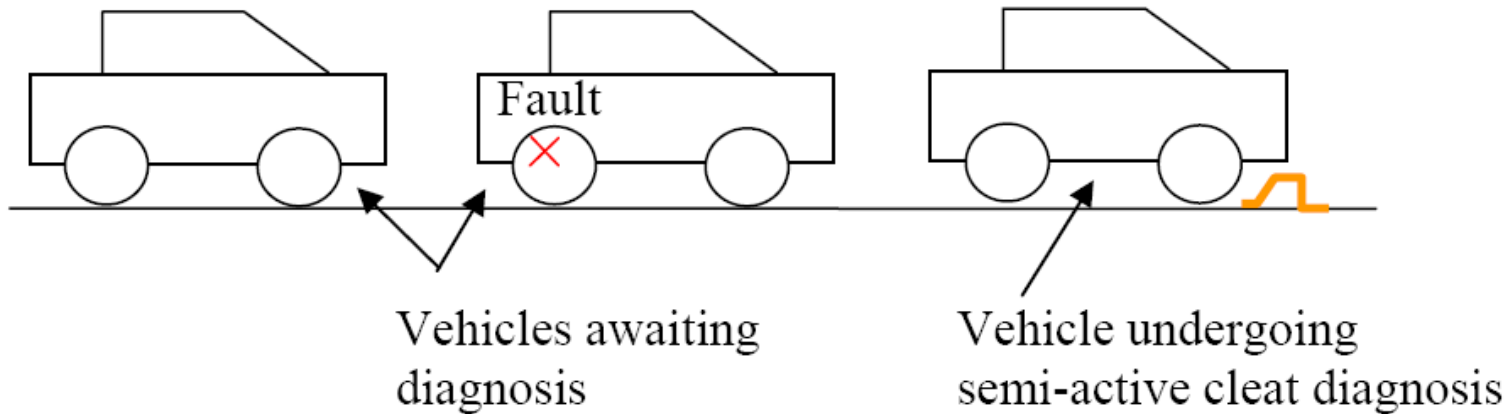
- **Cost of on-board measurement systems:**
 - HMMWV
 - 140,000 U.S. Army
 - 35,000 U.S. Marine Corps
 - Ground vehicles are a fraction of the cost of aircraft, so cost per vehicle must be lower.

Technical Solution

- To address the issue of variability in terrain, the condition monitoring system must somehow control the input loading.
- To address the issue of cost per vehicle, the technical solution must somehow distribute the cost of the condition monitoring system over the fleet of vehicles.

Instrumented Diagnostic Cleat

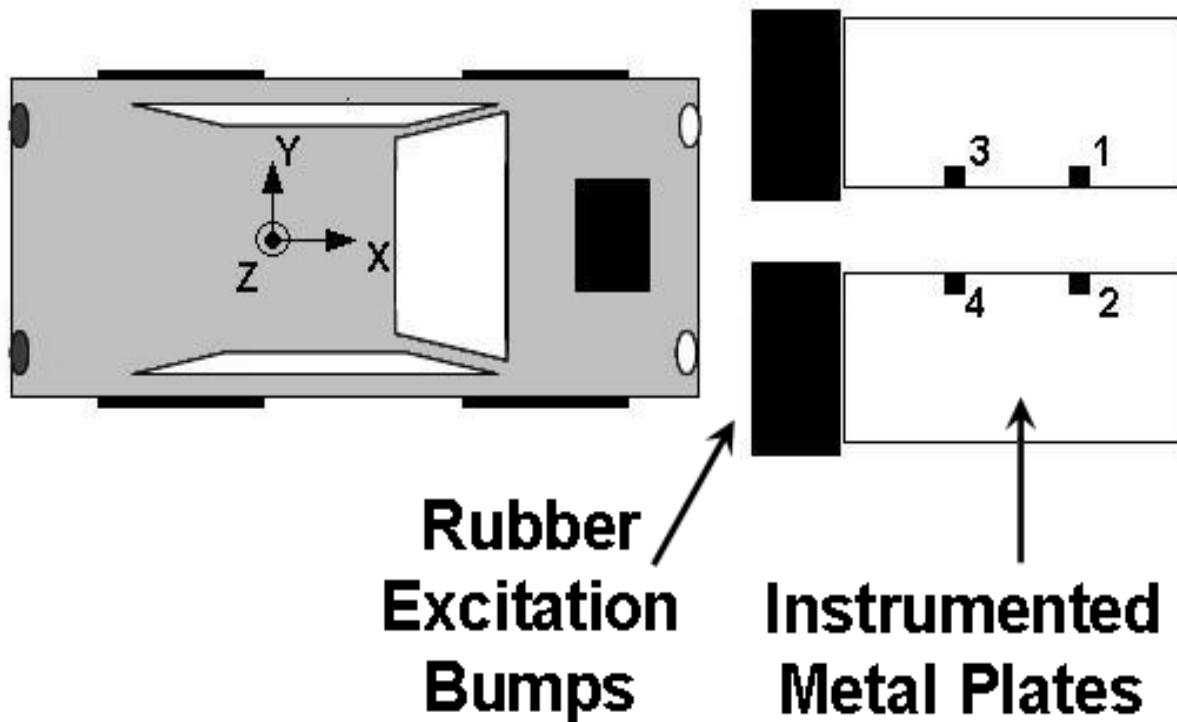
- The instrumented diagnostic cleat is a completely off board system that measures the response of the vehicle after it passes over the cleat.
- Faults can be identified (detected, located, quantified) by (a) comparing the measured response to a reference signature or (b) detecting asymmetries in the response.



Instrumented Cleat Test

Test Procedure:

- A vehicle is driven over the instrumented cleat at ~5 mph.
- Acceleration data from the instrumented plates is acquired.
- Data is analyzed to detect, locate, and quantify faults.









POLICE
SCHOOL

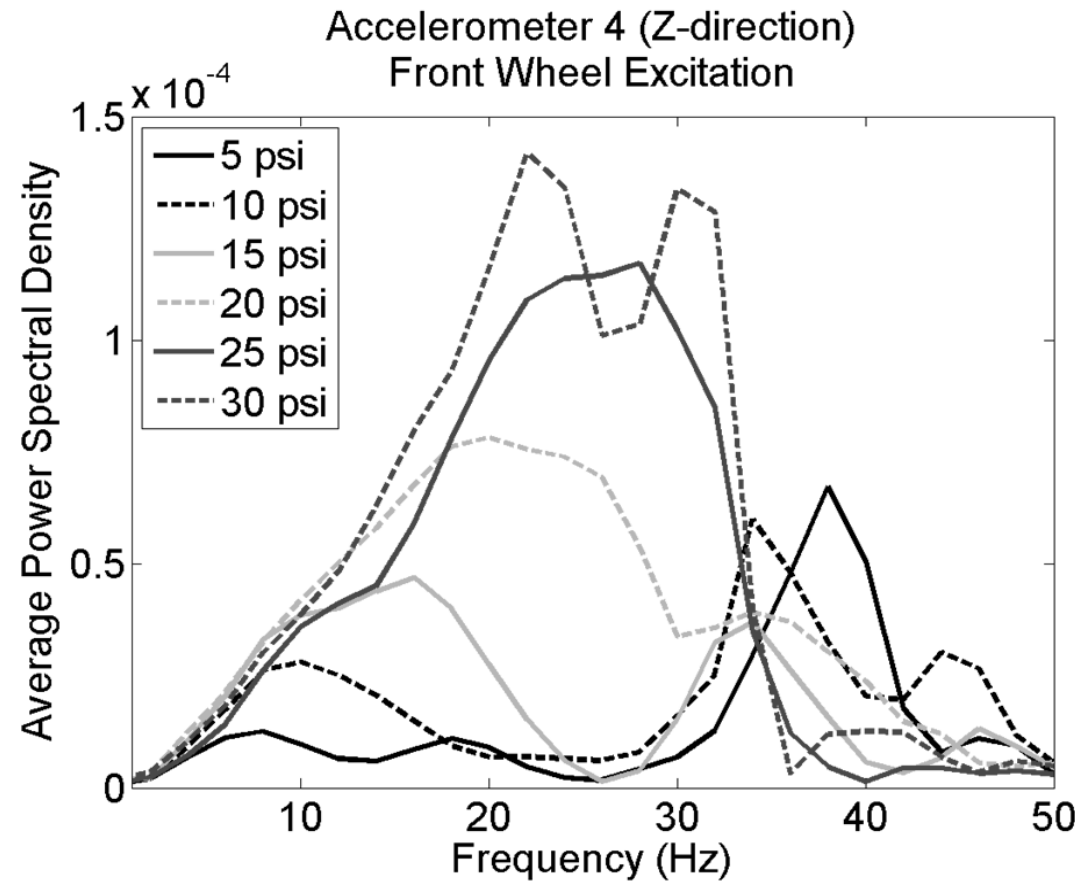
83



Fault Tests: Tire Pressure

Test Procedure:

- Nominal tire pressures in all tires except passenger front.



Identifying Faults: Method #1

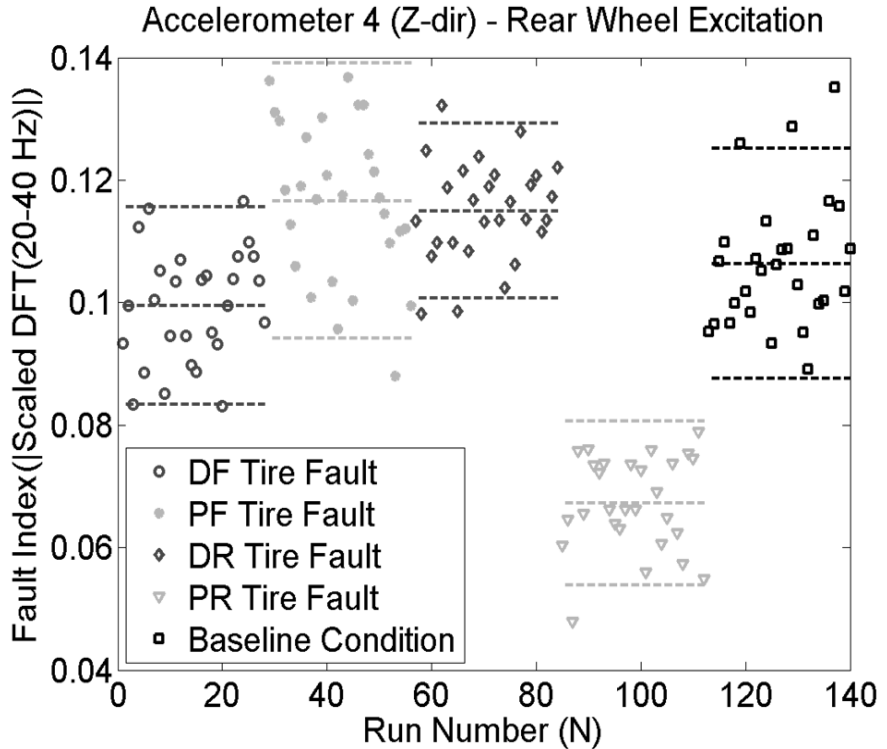
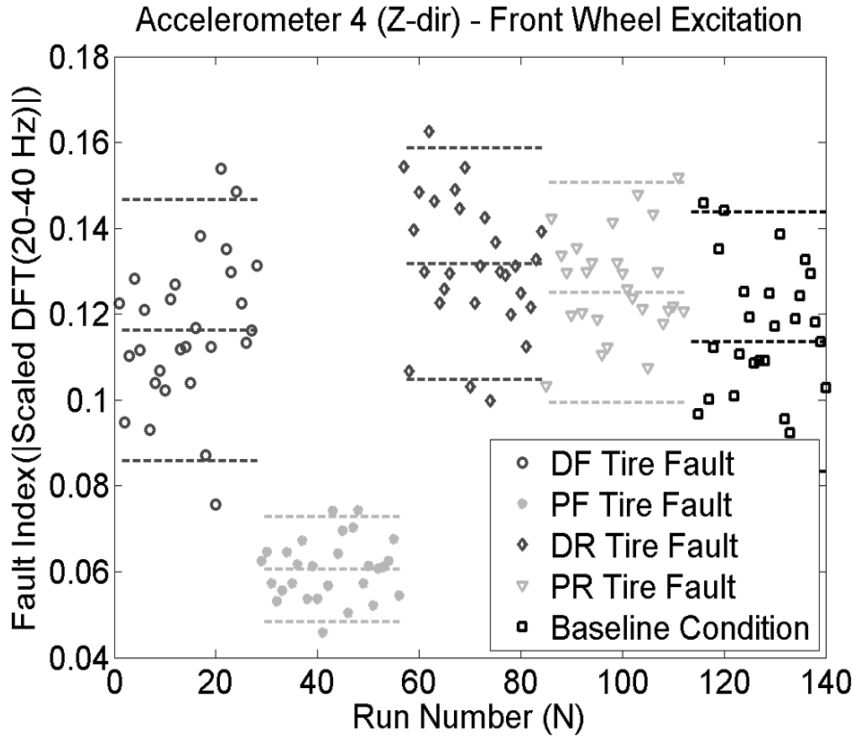
Fault Index for Reference-Based Method:

- Simple fault index was calculated using the area under the Discrete Fourier Transform magnitude curve:

$$\text{Fault index} = \sum_{n=a}^{n=b} \|DFT(n)\| \Delta f$$

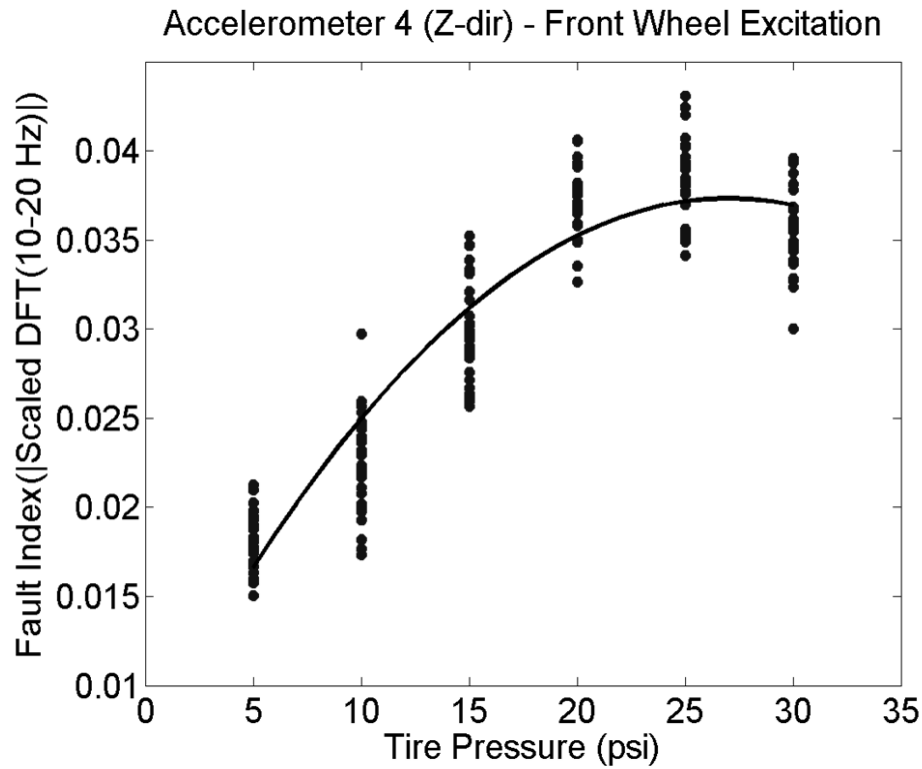
- This approach is not as sensitive nor robust as other possible algorithms.

Tire Pressure: Locate

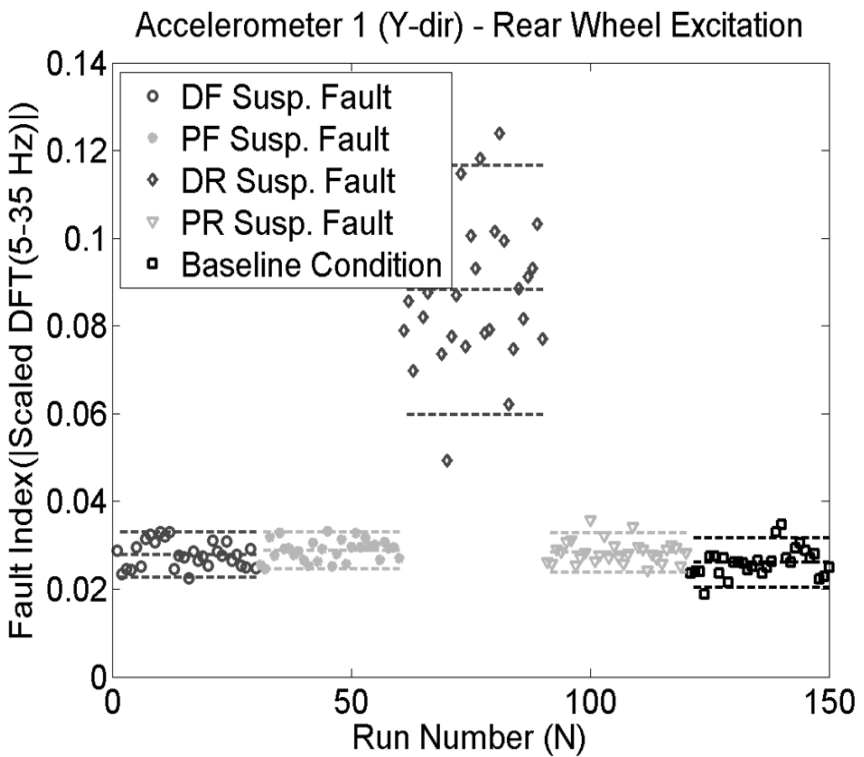
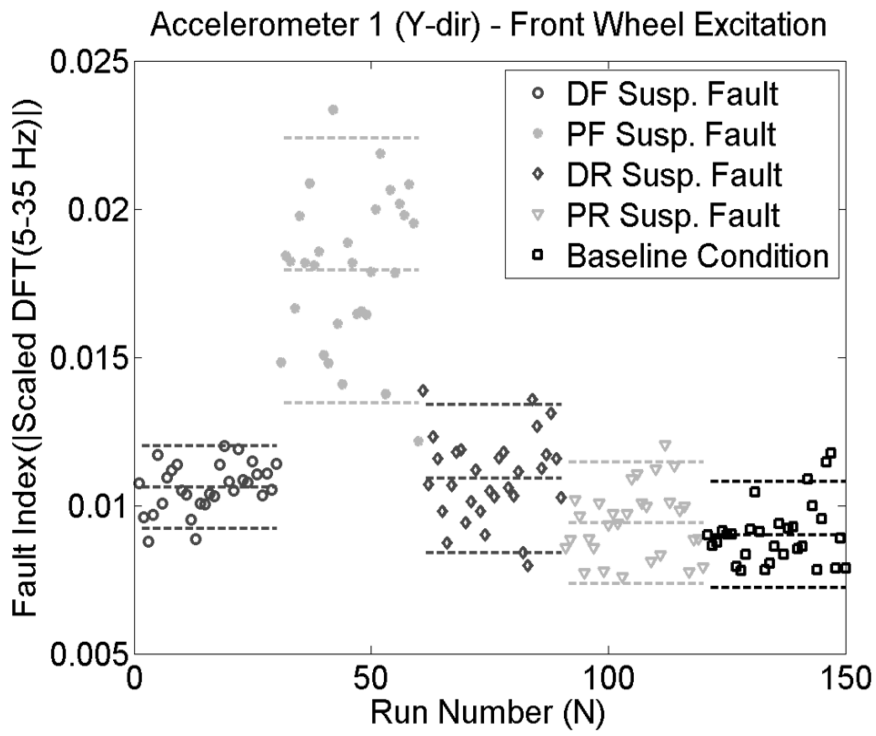


Detected with 90% confidence

Tire Pressure: Quantify



Suspension Fault: Locate



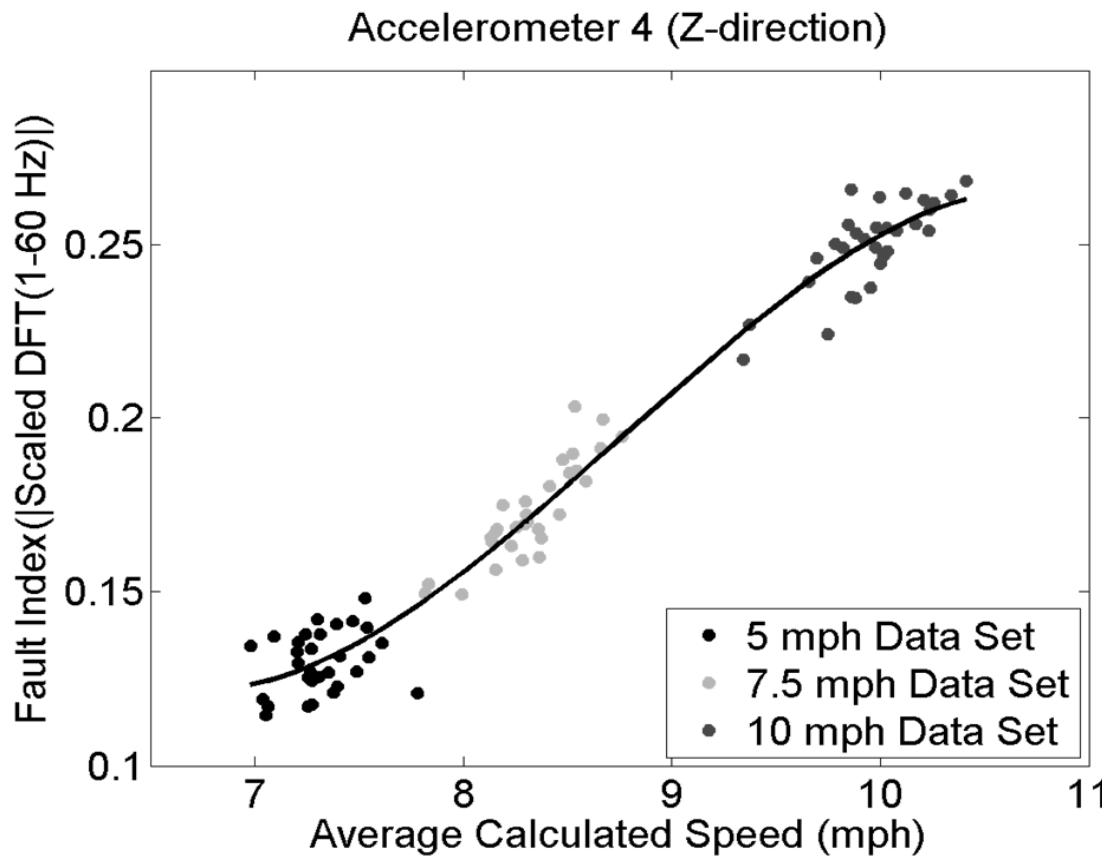
Detected with 90% confidence

Variability

- Work has focused on identifying and compensating for sources of variability in the diagnostic cleat measurement.
- Primary sources of variability that were investigated included:
 - Driver factors:
 - Vehicle approach speed.
 - Vehicle crossing location.
 - Vehicle angle of approach.
 - Environmental factors.

Compensating for Speed

- Speed errors were reduced by estimating the speed (using wheelbase / time between wheel crossings) and modifying fault index as a function of the calibration shown below.

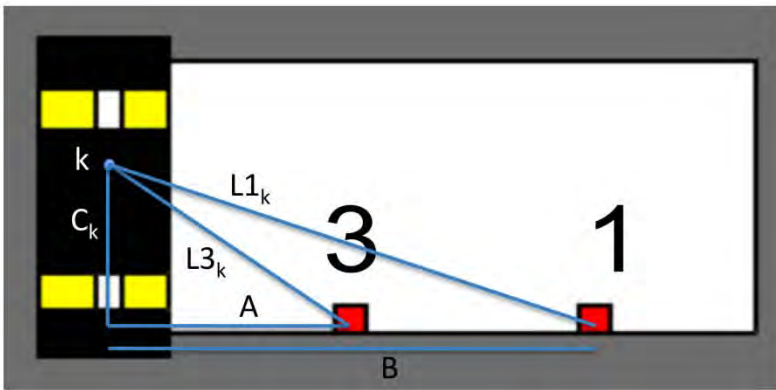


Crossing Location

- Errors due to crossing location were reduced by placing the instrumented plates such that the wheels tend to cross on the outer half of the plates to avoid the possibility of the wheels being on either side of the center node line of the plate.

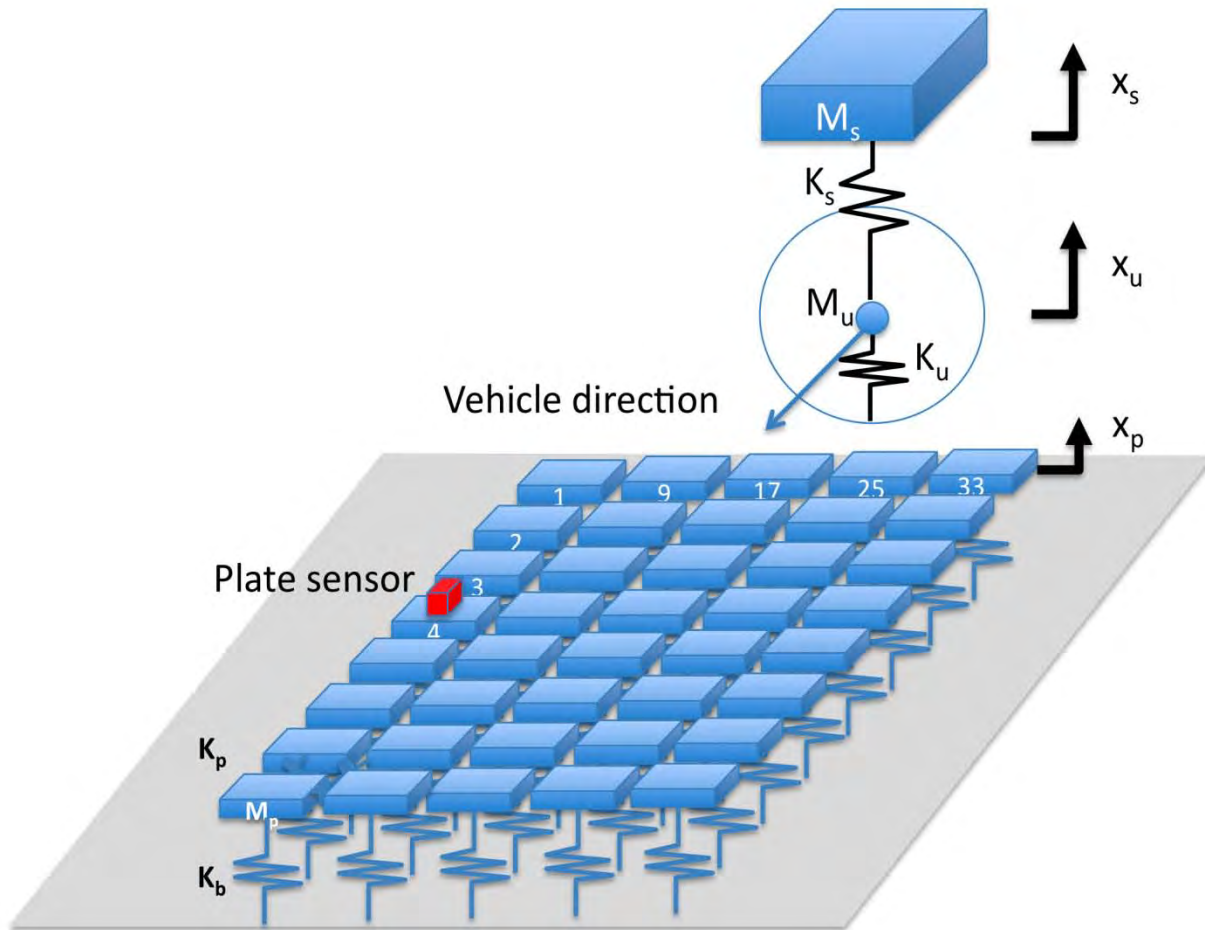
$$L3_k = \sqrt{A^2 + C_k^2}$$

$$L1_k = \sqrt{B^2 + C_k^2}$$



Analytical Model

- An analytical model was also developed and used to verify the experimental findings.



Identifying Faults: Method #2

Fault Index for Reference-Free Method:

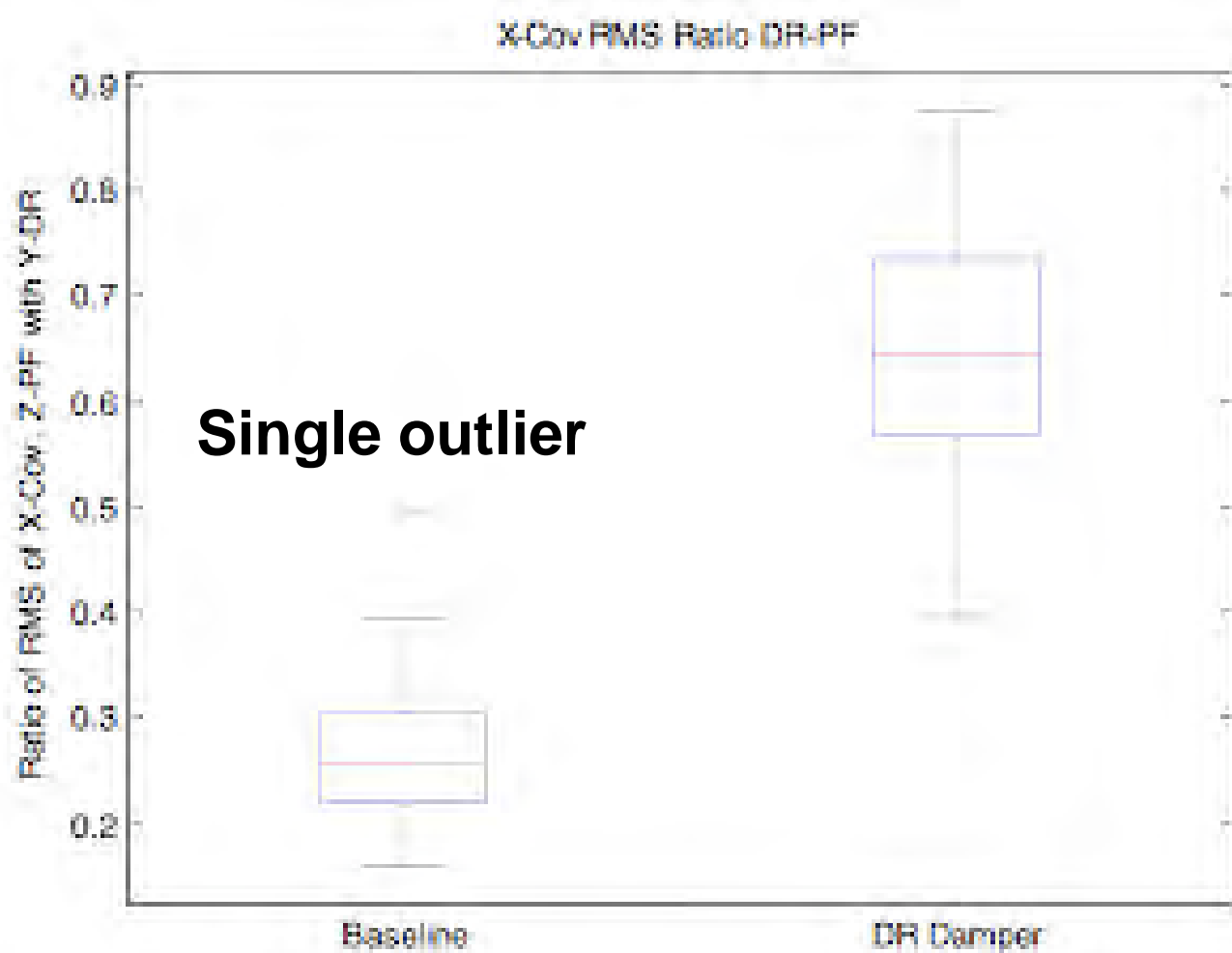
- Fault index was calculated based on the cross correlation function between Z and Y measurements on opposite wheels:

$$\frac{Fault}{index} = RMS[R_{zy}(\tau)]$$

where $R_{zy}(\tau) = E[z(t)y(t + \tau)]$

- This approach eliminates the need for a historical baseline by detecting “limping.”

Method #2



Overview of Demo

- Commercial H1 used for demonstration:
 - Tire faults introduced by adjusting pressure (next slide).
 - Suspension faults introduced by adjusting passively tunable dampers (next slide).
- 5 mph and 10 mph to demonstrate compensation for speed.
- Aluminum plates utilized for lighter weight to increase portability of the diagnostic cleat, along with 1000 mV/g triaxial accelerometers and National Instruments data acquisition system and custom software.

Tire and Suspension Faults

- H1 is fitted with tunable dampers with 9 settings from 0 to 8.

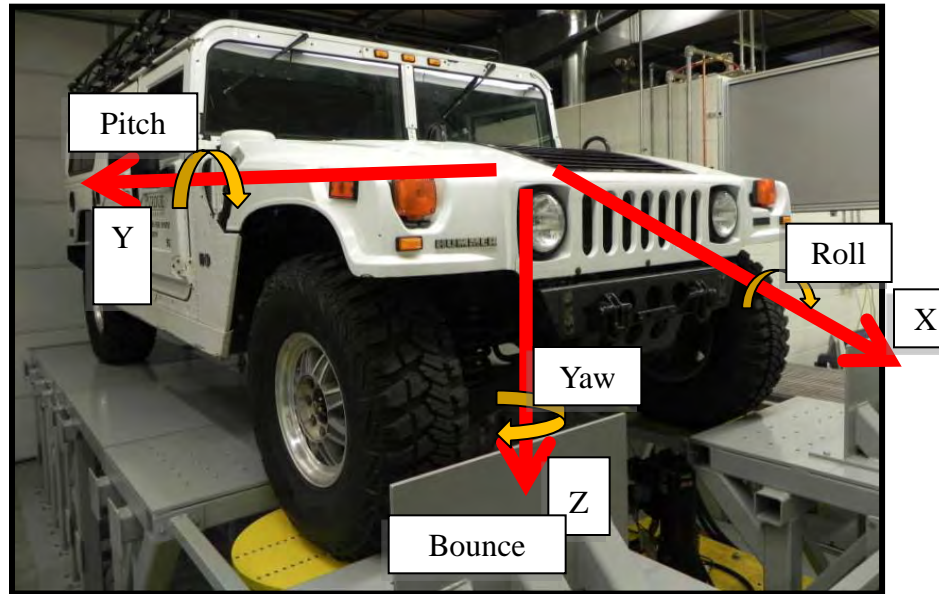


- H1 equipped with central tire inflation system that is used to inflate and deflate tires to desired pressure.



Vehicle Properties

Two-post shaker testing	
Vehicle mode	Frequency (Hz)
Roll	1.8
Bounce	2
Pitch	4.1
Wheel hop	9
Beaming	11.4
Torsional shake	11.9

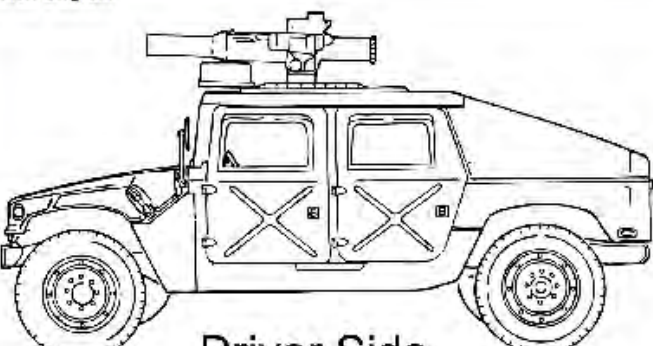


Screen Shots for Demo

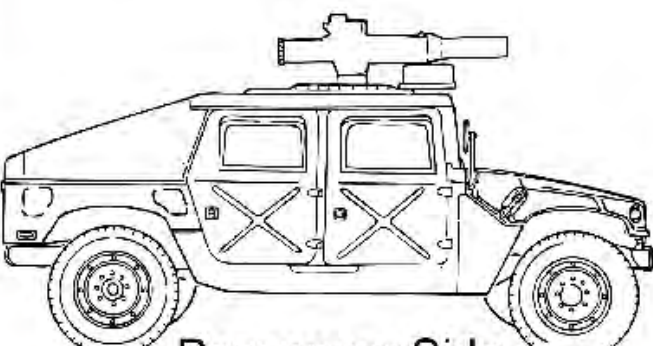
diagnosticCleatDemo2011

PURDUE Instrumented Diagnostic Cleat Demonstration

Vehicle Diagram:



Driver Side



Passenger Side

Vehicle Diagnosis:

- Green
- Warning
- Red

Press 'Start' to Begin

Start

Vehicle Response:

Driver Front Response

$A(t), g's$

Passenger Front Response

Driver Rear Response

$A(t), g's$

Passenger Rear Response

Screen Shots for Demo

diagnosticCleatDemo2011

PURDUE UNIVERSITY Instrumented Diagnostic Cleat Demonstration

Vehicle Diagram

Driver Side

Passenger Side

Vehicle Diagnosis

- Normal
- Warning
- Error

Waiting for Trigger...

Start

Vehicle Response

Driver Front Response

Passenger Front Response

Driver Rear Response

Passenger Rear Response

$A(t), g's$

The application interface for the "Instrumented Diagnostic Cleat Demonstration" software. It features a title bar with the university logo and window controls. The main area is divided into sections: "Vehicle Diagram" with two views of a vehicle; "Vehicle Diagnosis" showing three status levels; a central message area "Waiting for Trigger..." with a "Start" button; and "Vehicle Response" with four graphs showing force over time. The graphs are labeled "Driver Front Response", "Passenger Front Response", "Driver Rear Response", and "Passenger Rear Response". Each graph has an x-axis from 0 to 1 and a y-axis labeled " $A(t), g's$ " ranging from 0 to 1.

Screen Shots for Demo

diagnosticCleatDemo2011

PURDUE UNIVERSITY Instrumented Diagnostic Cleat Demonstration

Vehicle Diagram

Driver Side

Passenger Side

Vehicle Diagnosis

- Normal
- Warning
- Emergency

Triggered!
Acquiring Data

Start

Vehicle Response

Driver Front Response

$A(t), g's$

Passenger Front Response

Driver Rear Response

$A(t), g's$

Passenger Rear Response

The application window displays a vehicle diagram at the top left, followed by three sections: Vehicle Diagnosis, Vehicle Response, and a large area for data acquisition. The Vehicle Diagnosis section shows three colored bars: green for 'Normal', yellow for 'Warning', and red for 'Emergency'. The Vehicle Response section contains three graphs for 'Driver Front Response', 'Driver Rear Response', and 'Passenger Rear Response', each plotting Acceleration ($A(t)$) in g's against time. A central message 'Triggered! Acquiring Data' is displayed above a blue 'Start' button.

Screen Shots for Demo

diagnosticCleatDemo2011

PURDUE UNIVERSITY Instrumented Diagnostic Cleat Demonstration

Vehicle Diagram

Driver Side

Passenger Side

Vehicle Diagnosis

- Normal
- Warning
- Error

Data Acquired, Processing...

Start

Vehicle Response

Driver Front Response

Passenger Front Response

Driver Rear Response

Passenger Rear Response

A(t), g's

A(t), g's

A(t), g's

A(t), g's

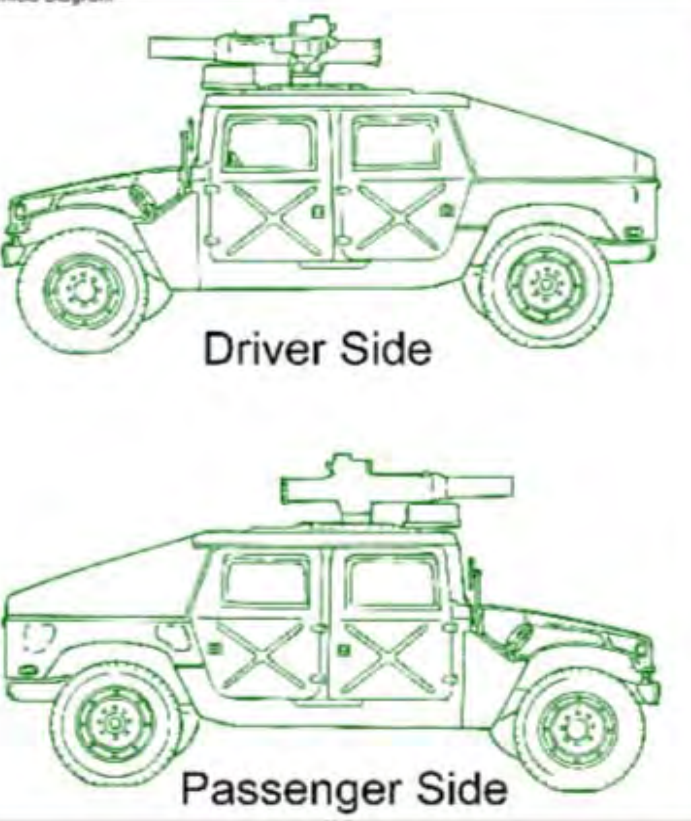
Screen Shots for Demo

diagnosticCleatDemo2011

PURDUE UNIVERSITY

Instrumented Diagnostic Cleat Demonstration

Vehicle Diagram:



Driver Side

Passenger Side

Vehicle Diagnosis:

- Healthy
- Warning
- Critical

Vehicle Response:

Driver Front Response

Passenger Front Response

Driver Rear Response

Passenger Rear Response

$A(t), g/\text{s}$

Analysis Complete.
Press 'Start' to Reset

Start

The software interface displays four time-series plots showing Acceleration ($A(t)$) in g/s over time from 0 to 1.4 seconds. Each plot shows a sharp initial peak followed by a steady state. The plots are labeled: Driver Front Response, Passenger Front Response, Driver Rear Response, and Passenger Rear Response. The y-axis ranges from -5 to 5 g/s . The x-axis ranges from 0 to 1.4 seconds.

Screen Shots for Demo

diagnosticCleatDemo2011

PURDUE UNIVERSITY

Instrumented Diagnostic Cleat Demonstration

Vehicle Diagram -



Driver Side



Passenger Side

Vehicle Diagnosis

- Green Bar: **Normal**
- Green Bar: **Warning**
- Red Bar: **Fault Detected**

Fault Detected!
Inspect
Passenger
Front Damper

Analysis Complete.
Press 'Start' to Reset

Start

Vehicle Response

Driver Front Response

$A(t), g/\text{s}$

Passenger Front Response

0 0.2 0.4 0.6 0.8 1 1.2 1.4 1.6

Driver Rear Response

$A(t), g/\text{s}$

Passenger Rear Response

0 0.2 0.4 0.6 0.8 1 1.2 1.4 1.6

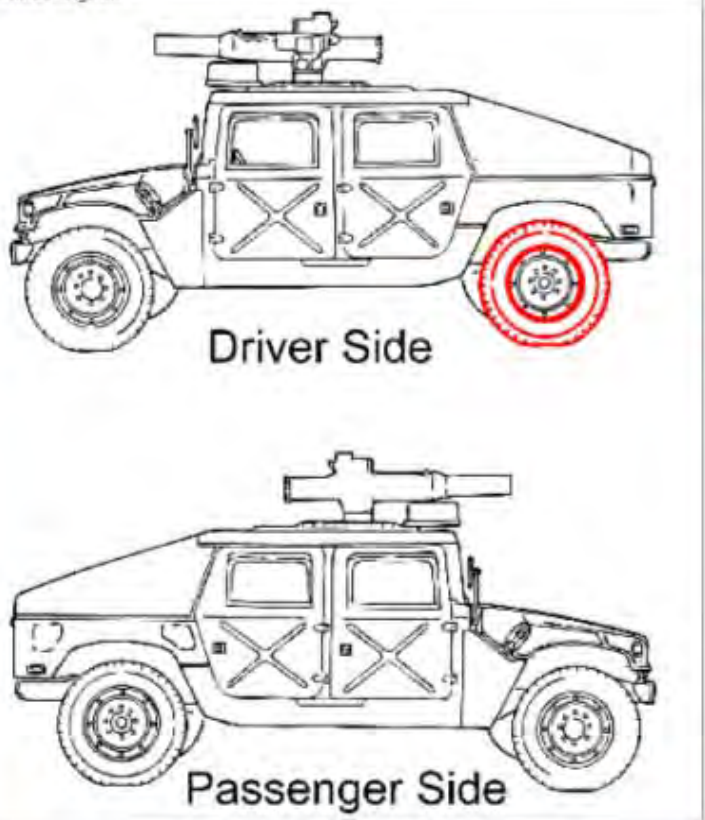
0 0.2 0.4 0.6 0.8 1 1.2 1.4 1.6

Screen Shots for Demo

diagnosticCleatDemo2011

PURDUE UNIVERSITY Instrumented Diagnostic Cleat Demonstration

Vehicle Diagram



Driver Side

Passenger Side

Vehicle Diagnosis

- Normal
- Warning
- Fault Detected

**Fault Detected!
Inspect Driver
Rear Tire**

Analysis Complete.
Press 'Start' to Reset

Start

Vehicle Response

Driver Front Response

$A(t, g/s)$

Passenger Front Response

Driver Rear Response

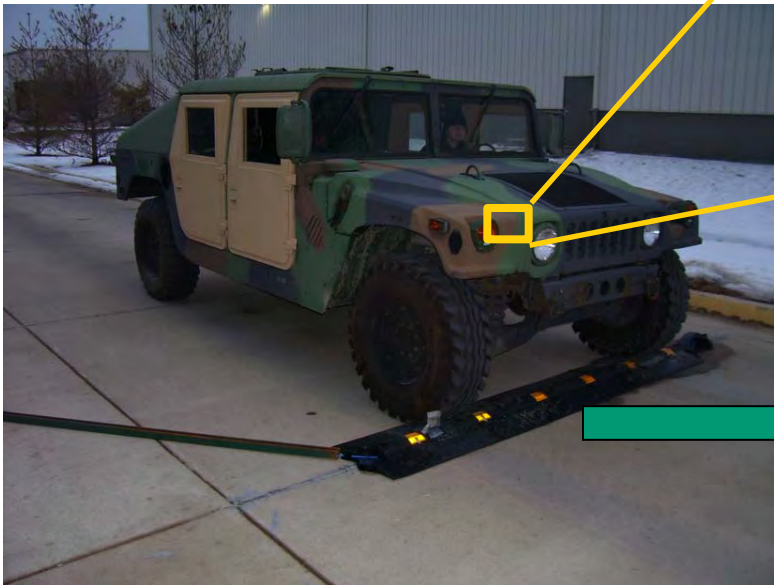
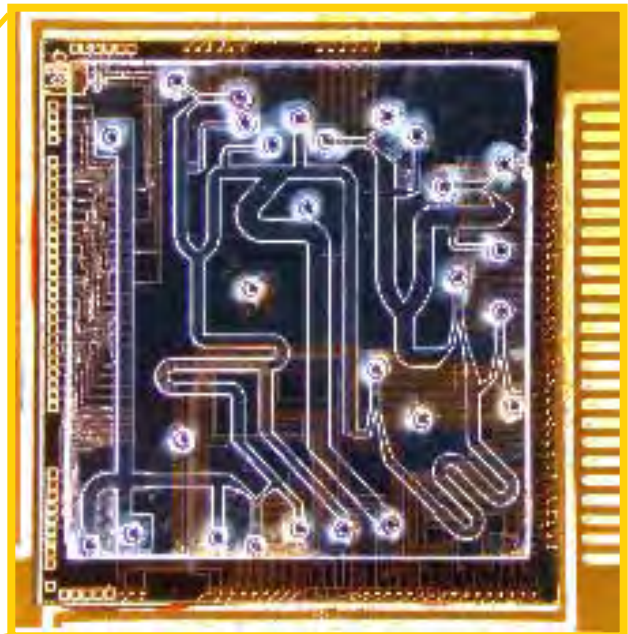
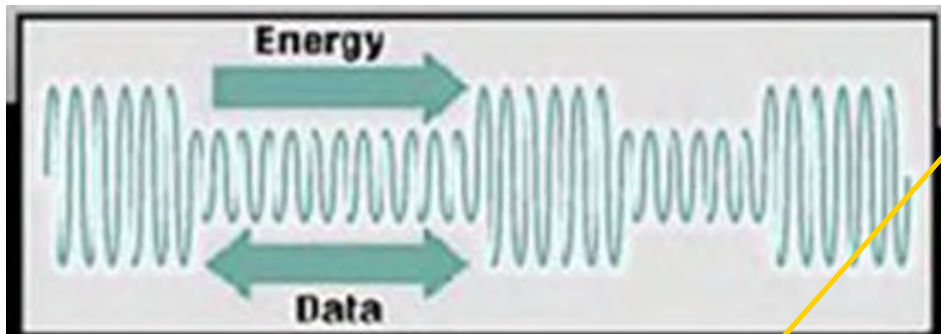
$A(t, g/s)$

Passenger Rear Response

$A(t, g/s)$

Detailed description: This screenshot shows a diagnostic software interface for a vehicle's rear tire monitoring system. It features a top-down diagram of a four-door vehicle. The driver's side rear tire is highlighted with a red circle, signifying a fault. Two other vehicle diagrams below show the front and passenger sides. A central 'Vehicle Diagnosis' section displays three buttons: 'Normal' (green), 'Warning' (yellow), and 'Fault Detected' (red). Below this, a large red warning message reads 'Fault Detected! Inspect Driver Rear Tire'. A note at the bottom says 'Analysis Complete. Press \'Start\' to Reset'. On the right, four time-series plots show 'Driver Front Response', 'Passenger Front Response', 'Driver Rear Response', and 'Passenger Rear Response'. Each plot has an x-axis from 0 to 1.4 and a y-axis from -5 to 5. Red spikes are visible on the initial segments of the plots.

Sensored Inventory Point Vision



Peer Reviewed Publications

- Adams, D. E., Gothamy, J., Decker, P., and Lamb, D., "Analysis of Passive Vibration Measurement and Data Interrogation Issues in Health Monitoring of a HMMWV Using a Dynamic Simulation Model," 2008, *Society for Automotive Engineers Transactions Journal of Materials & Manufacturing*, Vol. 1, No. 1, pp. 235-242.
- DiPetta, T., Adams, D. E., Koester, D., Gothamy, J., Decker, P., and Lamb, D., "Health Monitoring for Condition-Based Maintenance of a HMMWV using an Instrumented Diagnostic Cleat," 2009, *Proceedings of the 2009 Congress of the Society for Automotive Engineers*.
- DiPetta, T., Adams, D., E., Koester, D., Gothamy, J., Lamb, D., Decker, P., Gorsich, D., Bechtel, J., and Wright, G., and Gordon, G., "Enhancing HMMWV Operational Availability through the use of an Instrumented Diagnostic Cleat," 2009, *Proceedings of the International Workshop on Structural Health Monitoring*, Stanford, CA.
- DiPetta, T., Adams, D. E., Koester, D., Fischer, K., and Doherty, P., "Study of an Instrumented Diagnostic Cleat for Diagnosing Vehicle Mechanical Faults using Off-Board Dynamic Response Measurements", 2011, *Journal of Condition Monitoring and Diagnostic Engineering*, submitted for review.

Instrumented Diagnostic Cleat for Condition-Based Maintenance of Wheeled Ground Vehicles

June 21, 2011

**Douglas Adams, Raymond Bond
David Arseneau, Tiffany DiPetta, David Koester
Purdue Center for Systems Integrity**

